Universidad de Oviedo

Programa de Doctorado en Ingeniería de Producción, Minero–Ambiental y de Proyectos

TESIS DOCTORAL

Metodología para la optimización de biolubricantes derivados de microalgas

---

Presentada por:

Claudia Sanjurjo Muñiz

Gijón, xx de Octubre de 2024

Universidad de Oviedo

Programa de Doctorado en Ingeniería de Producción, Minero–Ambiental y de Proyectos

TESIS DOCTORAL

Metodología para la optimización de biolubricantes derivados de microalgas

---

Presentada por:

Claudia Sanjurjo Muñiz

En cumplimiento de los requisitos para la obtención del Grado de Doctor

Directores de Tesis:

Dr. D. Antolin Esteban Hernández Battez

Dr. D. Eduardo Rodríguez Ordóñez

Gijón, xx de octubre de 2024

Universidad de Oviedo

RESUMEN DEL CONTENIDO DE TESIS DOCTORAL

1.- Título de la Tesis	
Español/Otro Idioma: Metodología para la optimización de biolubricantes derivados de microalgas	Inglés: Methodology for the optimization of microalgae-derived biolubricants

2.- Autor	
Nombre: Claudia Sanjurjo Muñiz	
Programa de Doctorado: Ingeniería de Producción, Minero-Ambiental y de Proyectos	
Órgano responsable: Centro Internacional de Postgrado	

RESUMEN (en español)

La incorporación de fuentes biológicas en los procesos industriales significa un cambio revolucionario hacia prácticas más sostenibles y conscientes del medio ambiente. Al utilizar materiales biológicos como las microalgas, la industria puede reducir su dependencia de fuentes fósiles, minimizar las emisiones de gases de efecto invernadero e incentivar una economía circular. Este enfoque sirve para mitigar el impacto ambiental al mismo tiempo que estimula la innovación dentro de los sectores energético y químico. La adopción de fuentes biológicas es imperativa para lograr la sostenibilidad a largo plazo, mejorar la eficiencia de los recursos y estimular el crecimiento económico, garantizando al mismo tiempo la protección del planeta para las generaciones futuras. Las microalgas se han convertido en una fuente prometedora para la producción industrial, ofreciendo diversidad de ventajas sobre las materias primas tradicionales como los aceites vegetales y las grasas animales. Estas incluyen un mayor contenido lipídico, rápidas tasas de crecimiento, uso de tierras no cultivables, mayor captura de CO_2, escalabilidad y potencial, y una gran versatilidad de subproductos cuando se aplican en el contexto de la economía circular. La presente tesis doctoral se centra en la producción de ésteres metílicos de ácidos grasos (FAMEs) a partir de aceites derivados de las microalgas *Nannochloropsis gaditana* y *Haematococcus pluvialis*, así como de su caracterización fisicoquímica y tribológica, y su aplicación como aditivos lubricantes.

Para este fin, inicialmente se optimizó la reacción de transesterificación en medio básico del aceite obtenido, tanto de la microalga *N. gaditana* como de la *H. pluvialis*, mediante el empleo de la metodología de superficie de respuesta (RSM). Los FAMEs resultantes fueron identificados mediante una caracterización de sus estructuras moleculares. Además, fueron determinadas sus propiedades fisicoquímicas tales como la densidad, viscosidad, punto de inflamación, punto de congelación, humedad, acidez, poder calorífico superior e inferior, y estabilidad térmica. A continuación, se realizó la caracterización tribológica donde se determinó el coeficiente de fricción y los regímenes de lubricación a diferentes temperaturas a través de ensayos de deslizamiento alternativo y ensayos de rodadura/deslizamiento. Esta caracterización tribológica fue complementada con un análisis de la huella de desgaste generada durante los ensayos de deslizamiento alternativo mediante el uso de microscopia confocal e interferómetro, así como el análisis del mecanismo de desgaste con microscopia electrónica de barrido (SEM).

Una vez evaluadas las propiedades tribológicas de ambos FAMEs, se decidió continuar la investigación con la microalga *H. pluvialis* ya que presentó los mejores resultados de estabilidad, desgaste y fricción. La mezcla de FAMEs obtenida a partir de la *H. pluvialis* fue purificada con bentonita para la eliminación del pigmento característico de la microalga. Posteriormente, esta mezcla de FAMEs fue usada como aditivo a diferentes concentraciones en un diésel estándar. Tanto el diésel y la mezcla de FAMEs puros como las mezclas diésel – FAMEs se caracterizaron fisicoquímica y tribológicamente. El test tribológico seleccionado fue el método de prueba estándar para la evaluación de la lubricidad de combustibles diésel mediante movimiento alternativo de alta frecuencia (HFRR). La finalidad de este estudio es evaluar la habilidad del aceite modificado de *H. pluvialis* como potencial aditivo reductor de la fricción y el desgaste en combustibles.

Adicionalmente, se realizó un análisis preliminar técnico–económico de la producción de FAMEs a partir de desechos de la microalga *H. pluvialis* del sector cosmético/nutricional. Mediante el uso de las condiciones de laboratorio previamente obtenidas y el empleo del simulador de procesos SuperPro Designer v.9, se evaluaron cuatro posibles escenarios a escala industrial. Parámetros como la producción anual de FAMEs, el coste unitario de producción, o el análisis de rentabilidad, fueron importantes para la selección del escenario con la máxima valorización de residuos y viabilidad de los procesos a medio y largo plazo, gracias a la implantación de estrategias de economía circular.

RESUMEN (en inglés)

The incorporation of biological sources in industrial processes signifies a revolutionary shift towards more sustainable and environmentally conscious practices. By exploiting biological materials such as microalgae, industries can diminish their reliance on fossil sources, minimize greenhouse gas emissions, and incentivize a circular economy. This approach serves to mitigate environmental impact while simultaneously stimulating innovation within the energy and chemical sectors. The adoption of bio-based sources is imperative for the realization of long-term sustainability, enhanced resource efficiency, and the stimulation of economic growth, while ensuring the protection of the planet for future generations. Microalgae have emerged as a promising and sustainable source to produce industrial products, offering several advantages over traditional raw materials such as vegetable oils and animal fats. These advantages include a higher lipid content, rapid growth rates, the use of non-arable land, greater CO_2 fixation, scalability and potential, and great versatility of byproducts when applied within the context of the circular economy. The objective of this dissertation is to study the production of fatty acid methyl esters (FAME) derived from the microalgae *Nannochloropsis gaditana* and *Haematococcus pluvialis*, and to evaluate their tribological and physicochemical characteristics and their application as additives.

For this purpose, the basic transesterification reaction of the microalgae *N. gaditana* and *H. pluvialis* bio-oils were first optimized using the Response Surface Methodology (RSM). The resulting FAMEs were identified through a characterization of their molecular structures. In addition, physicochemical properties such as density, viscosity, flash point, pour point, moisture, acidity, lower and higher heating value, and thermal stability were determined. A tribological study was then carried out to evaluate the coefficient of friction and the regime of lubrication at different temperatures through reciprocating sliding tests and rolling/sliding tests. This tribological characterization was complemented by an analysis of the wear volume generated during the reciprocating sliding tests using confocal microscopy and interferometry, as well as an analysis of the wear mechanism using scanning electron microscopy (SEM).

After evaluating the tribological properties of both FAMEs, it was decided to continue the research with the microalgae *H. pluvialis*, since it showed the best results in terms of stability, wear and friction. The FAME produced from *H. pluvialis* was purified with bentonite to remove the characteristic pigment of the microalgae. The FAME was then used as an additive in different concentrations in a standard diesel fuel. The pure diesel and FAMEs, and their mixtures were characterized physicochemically and tribologically. The tribological test selected was the standard high frequency reciprocating rig (HFRR) test method for evaluating the lubricity of diesel fuel. The purpose of this study is to evaluate the ability of the *H. pluvialis* bio-oil derived FAME as a potential friction and wear reducing additive in fuels.

In addition, a preliminary techno–economic analysis of the production of FAME from *H. pluvialis* microalgae waste from the cosmetic/nutritional sector was carried out. Using the previously obtained laboratory scale conditions and the SuperPro Designer v.9 process simulator, four possible industrial scale scenarios were evaluated. Parameters such as the annual production of FAME, the unit cost of production or the profitability analysis were critical for the selection of the scenario with the maximum valorizations of waste and profitability of the processes in the medium and long term, by implementing circular economy strategies.

SR. PRESIDENTE DE LA COMISIÓN ACADÉMICA DEL PROGRAMA DE DOCTORADO EN INGENIERÍA DE PRODUCCIÓN, MINERO-AMBIENTAL Y DE PROYECTOS

Los humanos no están en armonía con la naturaleza, sino que se esfuerzan por conquistarla constantemente. Necesitamos volver a equilibrar esa relación.

Hayao Miyazaki

Ella y yo al final siempre nos encontramos.

Agradecimientos

Quisiera expresar mi más profundo agradecimiento a todas las personas que han formado parte de esta etapa de mi vida:

En primer lugar, a mis directores de tesis, los Doctores Antolin Hernández Battez y Eduardo Rodríguez Ordoñez. Gracias por vuestra orientación y apoyo durante estos años. Vuestra experiencia y guía me han ayudado a iniciarme y crecer como investigadora (y persona), siendo así los pilares fundamentales en mi formación. Pero, sobre todo, gracias por la paciencia y confianza que habéis depositado en mí. Me habéis enseñado que todo esfuerzo tiene su recompensa y que los sacrificios tarde o temprano dan sus frutos. Que lo importante es **seguir remando**. Por todo ello, gracias, no podría haber realizado esta tesis sin vosotros.

A todos los doctores colaboradores de esta tesis. José Luis Viesca Rodríguez, Paula Oulego Blanco, Marlene Bartolomé Sáez, Rubén González Rodríguez y Noelia Rivera Rellán, gracias por vuestra ayuda y apoyo durante el proceso. Me gustaría resaltar especialmente mi agradecimiento a Rubén y Noelia por abrirme las puertas del grupo LuSuTec en 2022. También al doctor Alejandro García Tuero, que me ha escuchado, apoyado y guiado a lo largo de todo el proceso.

A mi familia que me ha acompañado en los buenos y malos momentos. Gracias por creer en mí. Elena y Eric, gracias por estar siempre orgullosos de mí, hasta en los momentos que ni yo misma lo estaba.

A mi marido Jose, que ha sido mi Viento del Oeste a lo largo de esta etapa. Por la paciencia, apoyo y comprensión, gracias.

Por último, quisiera agradecer a los proyectos gracias a los cuales fue posible la financiación de esta investigación: Proyecto LubeMicroAlgae MCINN-23-PID2022-136656NB-100 (Ministerio de Ciencia e Innovación), SV-PA-21-AYUD/2021/50987 (Fundación para la Investigación Científica y Técnica FICYT), y los proyectos CARALGALUB/SV-22-Gijón-1-25 y OPTRANSESTERAL/SV-23-GIJON-1-05 (Instituto Universitario de Tecnología Industrial de Asturias).

Contenido

Índice de Figuras

Índice de Tablas

Abreviaturas

CH_3COCl	Cloruro de acetilo
CH_3ONa	Metóxido de sodio
COF	Coeficiente de fricción
FAAE	Éster alquílico de ácido graso
FAEE	Éster etílico de ácido graso
FAME	Éster metílico de ácido graso
FFA	Ácido graso libre
FP	Punto de inflamación
H_2SO_4	Ácido sulfúrico
HCl	Ácido clorhídrico
HHV	Poder calorífico superior
KOH	Hidróxido de potasio
LHV	Poder calorífico inferior
MUFA	Ácido graso monoinsaturado
NaOH	Hidróxido de sodio
NPI	Índice de no polaridad
PP	Punto de fluidez
PUFA	Ácido graso poliinsaturado
SFA	Ácido graso saturado
SRR	Relación rodadura – deslizamiento
TAN	Índice de acidez total
UPC	Coste unitario de producción
VAN	Valor actual neto
VD	Volumen de desgaste

CAPÍTULO 1

1 Introducción

Los gases de efecto invernadero (GEI) han sido fundamentales para mantener un clima habitable en la superficie de la Tierra durante millones de años. Sin embargo, el aumento desmedido de sus emisiones está poniendo en riesgo la vida tal como se conoce. En la actualidad, los niveles de CO_2 en la atmósfera son los más altos jamás registrados y siguen en aumento, alcanzando un total de 40,5 toneladas de emisiones en 2022 [1].

Los GEI tienen un impacto significativo en el entorno y en la salud de las personas. Son responsables del cambio climático y están relacionados con problemas de salud, como las enfermedades respiratorias provocadas por el esmog y la contaminación del aire. El cambio climático no solo se refiere al aumento de las temperaturas medias de la Tierra, sino que también incluye fenómenos meteorológicos extremos, alteraciones en las poblaciones y hábitats de la fauna y flora, aumento del nivel del mar, cambios en la disponibilidad de alimentos y un incremento en la frecuencia de incendios forestales, entre otros.

El CO_2 es el GEI más peligroso y prevalente, y es responsable de aproximadamente el 75% de las emisiones totales. La industria petrolera se ha establecido como la principal fuente de emisiones, atribuyéndose a esta el 90,47% de las emisiones totales. Dentro de este contexto, se estima que el 25% de dichas emisiones proviene de pérdidas energéticas [1].

La tribología es una de las ciencias clave para afrontar los desafíos globales ambientales. La reducción de la fricción y el desgaste a través del uso de lubricantes adecuados para cada aplicación implicaría la disminución y/o eliminación de factores como el ruido ambiental, generación de residuos, pérdidas de energía y de materiales, entre otros. Esta práctica, implicaría importantes ahorros económicos y reducciones en las emisiones de CO_2.

Sin embargo, la mayoría de los aceites base empleados en la formulación de lubricantes son producidos durante el procesamiento del petróleo crudo. Los aceites minerales se caracterizan por tener una composición diversificada que puede incluir hidrocarburos alifáticos y alicíclicos de cadena ramificada, hidrocarburos aromáticos, principalmente derivados del benceno, pero también

bifenilo, difenilmetano, trifenilmetano, naftaleno, antraceno, fenantreno y derivados del criseno [2].

Para cumplir con su función, los lubricantes necesitan satisfacer una serie de requerimientos mínimos dentro de las cuales se encuentran [3]: a) reducir las pérdidas de energía; b) proteger las superficies del desgaste por fricción; c) proteger contra la corrosión; d) reducir los efectos de la oxidación; e) enfriar las superficies; f) disminuir las pérdidas de calor por contacto entre superficies; g) aumentar la hermeticidad y evitar fugas de contaminantes y sedimentos. Además de ciertos requerimientos dependiendo de la aplicación.

La constante lucha contra el cambio climático, así como el aumento del precio del crudo y el agotamiento de las reservas, han fomentado el interés en el desarrollo y uso de nuevos materiales biodegradables y más sostenibles con el medio ambiente, buscando sustitutos de origen vegetal y/o animal para el desarrollo de biolubricantes.

1.1. Biolubricantes

Se entiende por biolubricante todo aquel lubricante considerado bueno para el medio ambiente, con la capacidad para degradarse en un cierto periodo de tiempo a través de procesos de descomposición natural [4]. Como lubricantes, estos materiales deben cumplir con las propiedades generales descritas anteriormente. Sin embargo, los biolubricantes presentan importantes ventajas atractivas tales como [5]: a) alta biodegradabilidad; b) baja toxicidad; c) naturaleza sostenible (respetuoso con el medio ambiente); d) mayor seguridad laboral; e) vida útil de maquinaria mejorada; f) menores costes laborales; g) menores consumos energéticos; h) mayor lubricidad; i) índices de viscosidad mayores; j) puntos de ebullición más altos; k) y menor volatilidad. Sin embargo, su carácter biodegradable hace de ellos propensos a la degradación (menor vida útil) resultado de una mala estabilidad hidrolítica, térmica y oxidativa, así como baja inhibición a la corrosión y puntos de fluidez altos.

1.1.1. Clasificación de los biolubricantes

Un aspecto importante de los biolubricantes es el origen de la materia prima empleada para su producción. En función de esto, los biolubricantes pueden ser clasificados en cuatro grandes generaciones ilustradas en la Figura 1 [6]. Estas cuatro generaciones siguen el esquema existente para la clasificación de biodiesel. Dentro de la primera generación se encuentran todas aquellas materias primas procedentes de cultivos comestibles, como el girasol, la oliva o la soja. Estas fuentes se caracterizan por tener una baja producción de aceite y fomentar la deforestación y la destrucción de ecosistemas para su cultivo [7]. Además, el uso de cultivos comestibles para una aplicación industrial compite con la producción

de alimento y aumenta los costes finales de los comestibles, lo que es contraproducente en el contexto de la escasez de alimentos a nivel mundial.

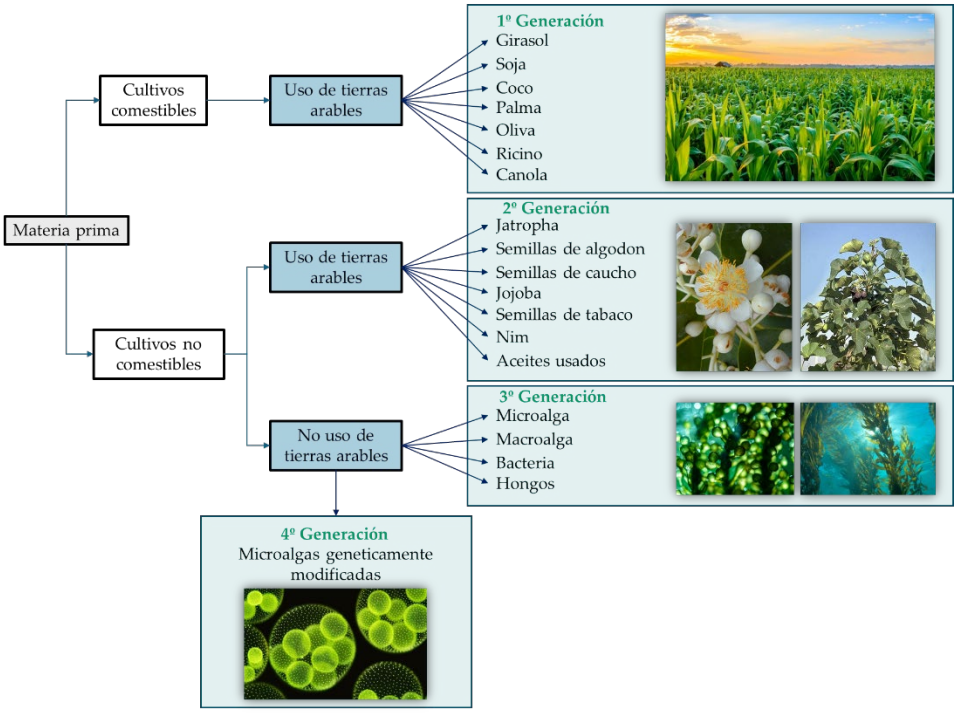

Figura 1. Generaciones de biolubricantes.

La segunda generación de biolubricantes incluiría materias primas de origen no comestible que necesitan de tierras de cultivo para su crecimiento. Por ejemplo, las semillas de algodón, *jatropha* y jojoba [7,8]. Además, en esta categoría, varios autores incluyen también los aceites de cocina usados [9]. Estos cultivos están más disponibles que los de primera generación, pero el uso de terrenos de cultivo para su crecimiento implica una disputa con los cultivos comestibles por las tierras.

En la tercera generación se encuentran todos aquellos biolubricantes derivados de microorganismos como hongos, bacterias, macroalgas y microalgas [7]. Estas últimas están generando gran expectación por sus innumerables ventajas frente a los cultivos de primera y segunda generación.

Las microalgas son microorganismos capaces de realizar la fotosíntesis tanto en agua dulces /saladas como en aguas contaminadas, por lo que no necesitan tierras de cultivo para su crecimiento. Estos microorganismos se caracterizan por la influencia que tienen las condiciones de cultivo en su desarrollo, ya que son organismos fácilmente maleables cuando se cambian parámetros de cultivo. Entre

sus ventajas destacan [5]: a) alta tasa de crecimiento; b) alta producción de biomasa; c) alta producción de aceite; d) cultivables todo el año; e) mayor captación de CO_2 durante la fotosíntesis; f) y eliminación efectiva de fosfatos y nitratos en aguas residuales (biorremediación).

Por último, puede considerarse una cuarta generación procedente de biomasa de microalgas genéticamente modificadas. La posibilidad de manipular el genoma de estos microorganismos podría servir para resolver problemas relacionados con estructuras moleculares no deseadas.

1.2. Producción de biolubricantes a partir de microalgas

De forma general, el proceso de producción de biolubricantes se compone principalmente de cuatro etapas destinadas a la obtención del bioaceite (Figura 2): cultivo de la cepa seleccionada, recolección de la biomasa, secado de la biomasa (opcional) y extracción del bioaceite.

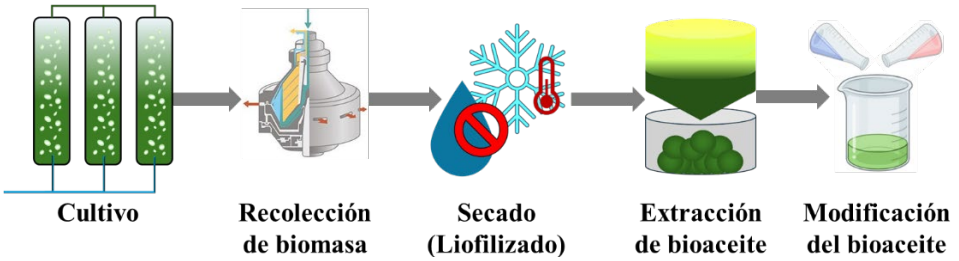

Figura 2. Etapas del proceso de obtención de biolubricantes a partir de microalgas.

La etapa de cultivo es la fase clave del ciclo, ya que será la encargada de definir la composición de la biomasa, así como la estructura molecular de los diferentes activos. Como ya se ha comentado previamente, durante su fase de crecimiento estos microorganismos son muy sensibles a parámetros tales como el tipo de biorreactor (sistemas abiertos, sistemas cerrados o fotobiorreactores), grado de agitación, concentración de O_2, temperatura, intensidad de la luz, CO_2 disuelto, ciclos luz/oscuridad y disponibilidad de nutrientes (C, N, P, entre otros) [5]. Una característica ya destacada de las microalgas es su capacidad de crecer en diversidad de medios siendo posible su cultivo en agua dulce, agua salda o aguas contaminadas.

Una vez finalizado la fase de crecimiento, la biomasa es separada del medio mediante un proceso de recolección. Debido al pequeño tamaño real de las células (3–30 µm) esta etapa se define como de alto coste, adjudicándose el 90% de los costes de instrumentación en el ciclo de producción de biomasa [10]. De forma general, se pueden encontrar métodos de recolección físicos (centrifugación, sedimentación, filtración o flotación), químicos (floculación), biológicos

(biofloculación/autofloculación) y/o separación electromagnética, que pueden ser combinados entre ellos para obtener mejores resultados.

Una vez separada la biomasa, es habitual aplicar un proceso de secado para la obtención de biomasa seca. Esta etapa suele ser necesaria cuando se pretende realizar algún tipo de reacción química aguas abajo que sea sensible o se vea afectada de alguna forma por la presencia de humedad. Destaca la técnica de liofilización, la cual permite eliminar el agua a través de un proceso de congelación y posterior sublimación del hielo. Se caracteriza por ser una técnica no invasiva que no altera la estructura de la muestra.

La extracción del bioaceite es otra etapa de gran importancia que busca substraer la mayor cantidad de lípidos posible. Dentro de los lípidos se contemplan estructuras como los fosfolípidos, esteroles o triglicéridos, siendo este último el de mayor interés en la producción de biolubricantes. En el caso de las microalgas, que presentan unas matrices complejas, suele requerirse un pretratamiento de disrupción celular previo a la extracción. Técnicas de extracción comunes pueden ser la extracción con solventes orgánicos, el empleo de líquidos iónicos o fluidos supercríticos.

1.2.1. Triglicéridos como biolubricantes

Los triglicéridos son estructuras moleculares formadas por la unión de tres ácidos grasos a través de un glicerol. Los ácidos grasos presentes en bioaceites se caracterizan por una longitud de cadena entre 4 a 26 átomos de carbono, así como la posibilidad de presentar insaturaciones. Cuando el ácido graso no presenta ningún enlace doble, se denomina SFA. En caso de presentar un solo enlace doble, se denominará MUFA, y si presenta dos o más enlaces dobles será PUFA. Los ácidos grasos presentes en los aceites derivados de microalgas se caracterizan por tener mayor contenido de insaturaciones. En esta línea, es común la presencia de PUFAs con 5 y 6 enlaces dobles en su estructura.

Debido a su alto peso molecular, los triglicéridos poseen una alta viscosidad e índice de viscosidad. Aceites vegetales como el derivado de *jatropha* ha sido ampliamente estudiado como aditivo modificador de la viscosidad en aceite base mineral [11,12]. Más recientemente, se verificó la viabilidad del aceite de cocina usado como aditivo antidesgaste y antioxidante [13].

Debido a la naturaleza general de los aceites derivados de microalgas, estos no son empleados como biolubricantes y/o aditivos en esta forma. Los aceites derivados de microalgas se caracterizan por una fuerte pigmentación y un estado a temperatura ambiente semisólido y no homogéneo, como se muestra en la Figura 3. Este aspecto se debe a que, a diferencia de los aceites vegetales convencionales (90 – 100% triglicéridos), los aceites de microalgas presentan entre un 15% – 60%

en peso de triglicéridos [14]. El resto de la materia estaría compuesta por otros activos como por ejemplo pigmentos que aportan un color característico a cada microalga. Es por ello que, en el caso de las microalgas, es necesaria una cuarta fase para la ruptura del triglicérido y la disminución del peso molecular.

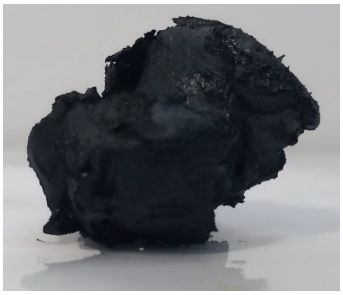

Figura 3. Aceite derivado de la microalga de *N. gaditana*.

1.2.2. Aceites modificados como biolubricantes

La transesterificación es la técnica más empleada en la ruptura del triglicérido y obtención de los ácidos grasos constituyentes (Figura 4). Esta vía se basa en la reacción del triglicérido con un alcohol (normalmente metanol o etanol) en presencia de un catalizador y bajo condiciones de calor, para dar como resultado FAME (o FAEE si se emplea etanol) y glicerol [6]. La producción de FAME mediante transesterificación es la técnica por excelencia en la obtención de biodiesel a nivel industrial. Es por ello por lo que se trata de una vía ampliamente estudiada en el campo de los biocombustibles derivados de fuentes vegetales de primera y segunda generación. En cuanto al catalizador, su naturaleza puede ser ácida, básica o enzimática, así como homogénea o heterogénea.

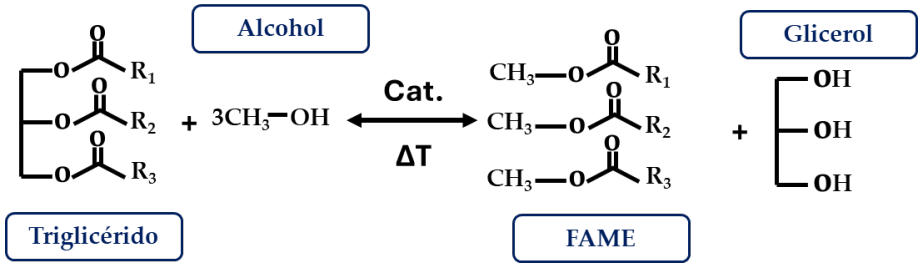

Figura 4. Reacción de transesterificación.

Esta reacción es sensible a la presencia de humedad y FFA, los cuales fomentan el desarrollo de reacciones secundarias como la saponificación. De acuerdo con esto, es común el empleo de catalizadores ácidos cuando el TAN supera los 2 – 4 mg KOH/g muestra [15].

El grupo de Investigación de Ingeniería Química y Química–Física de la Universidad de Extremadura, ha estudiado en profundidad en los últimos años la producción de biodiesel y biolubricantes a partir de aceites vegetales como el girasol, el cardo o el aceite de ricino, empleando esta técnica de transesterificación [16–20]. De sus investigaciones, se ha observado que para este tipo de aceites las condiciones de ensayo más efectivas se encontrarían en un ratio molar bioaceite:alcohol de 1:6 (0,35 mL/g muestra aproximadamente), durante 60 – 150 min (dependiendo de las características del aceite), y bajo una temperatura de 60 – 65 ºC. Siempre empleando CH_3ONa como catalizador básico a una concentración entre 0,5 – 1,5%.

Buscando ir un paso más allá, la investigación en la producción de biolubricantes a partir de fuentes vegetales ha intentado en los últimos años modificar la estructura molecular de los FAME para dar solución a problemas relacionados con la presencia de enlaces dobles y/o mejorar sus propiedades fisicoquímicas y tribológicas. Como se muestra en la Figura 5, en esta línea se encontrarían las técnicas de doble transesterificación con alcoholes complejos para la formación de FAAE, o técnicas de epoxidación para la eliminación de los dobles enlaces y mejora de la estabilidad del compuesto.

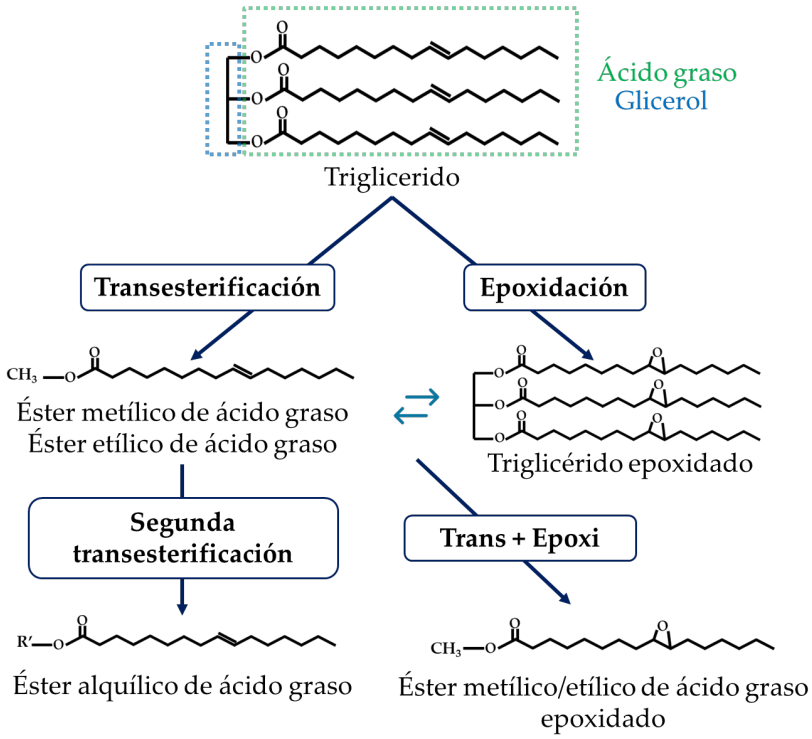

Figura 5. Principales rutas para la producción de biolubricantes a partir de aceites vegetales.

El grupo de investigación extremeño es uno de los pioneros en la aplicación de las técnicas de doble transesterificación en aceites vegetales tradicionales. La doble transesterificación se basa en hacer reaccionar el FAME con un alcohol complejo (mayor longitud de cadena y/o presencia de ramificaciones) para dar como producto FAAE y metanol. La ventaja de este modelo de refinería es la diversidad de productos principales (biodiesel, biolubricantes) y el ahorro económico y energético con la recuperación de productos secundarios como el glicerol o el metanol.

Por otro lado, la neutralización de los enlaces dobles mediante técnicas de epoxidación se basa en propiciar la interacción de los alquenos de la muestra con un peroxiácido para formar lo que se conoce como epóxido (compuesto de éter cíclico). Esta modificación ha sido verificada como una vía alternativa para la mejora de las propiedades anticorrosivas y de lubricidad, así como un gran aliado en la lucha contra las malas propiedades oxidativas de estos materiales [21,22]. Una de las mayores ventajas de esta reacción es la posibilidad de ser aplicada tanto en triglicéridos (antes de la reacción de transesterificación) como en FAME o derivados (después de la reacción de transesterificación o similares).

Sin embargo, la aplicación de materias primas novedosas como las microalgas en este campo supone una novedad desafiante, ya que los aceites derivados de estos microorganismos presentan unas propiedades totalmente diferentes a los aceites vegetales convencionales estudiados hasta la fecha.

Casi la totalidad de estudios existentes en el campo de la transesterificación de aceites derivados de microalgas basan sus investigaciones en la producción y caracterización de biodiesel, no contemplando por ende su potencial como biolubricante. *C. protothecoides*, *C. vulgaris*, *S. limacinum* o *N. gaditana*, son algunas de las cepas más estudiadas en la producción de biocombustibles [23–26].

Las dificultades a la hora de manipular los aceites derivados de microalgas resultaron en el estudio de nuevas variantes a la reacción de transesterificación. De esta forma nació la modalidad de transesterificación directa o in situ, la cual combina la extracción del bioaceite y la reacción de transesterificación en un único proceso. Estas reacciones necesitan ser catalizadas en medio ácido, por lo que el contenido de agua deja de ser un parámetro crítico, ya que favorece la estabilidad hidrolítica de los compuestos. Sin embargo, la aplicación de esta tecnología requiere de configuración de ensayo complejas. Esto implica condiciones supercríticas con mayores tiempos de reacción, elevadas temperaturas e incluso condiciones de vació. En la Tabla 1 se resumen algunas de las configuraciones más usadas en esta línea. Como se puede observar, debido a la baja homogeneidad de los aceites y al bajo contenido en triglicéridos, la cantidad de alcohol pasa a expresarse en mL de metanol por g de muestra. Esta cantidad es bastante más

elevada que las usadas con aceites convencionales. Las temperaturas y tiempos de reacción también se ven fuertemente afectados, llegando a alcanzar en algunos casos los 300 ºC y 360 min.

Tabla 1. Configuraciones de ensayos realizadas en estudios sobre la transesterificación directa de microalgas.

	Cantidad de alcohol	Tipo de catalizador	Temperatura	Tiempo	Ref.
	2,5 – 9,3 mL/g	CH_3COCl	80	105	[27]
	9,1 mL/g	H_2SO_4	100	120	[28]
NG	30 – 120 mL/g	HCl	60 – 90	30 – 150	[29]
	6 – 12 mL/g	–	245 – 290	10 – 50	[30]
	2,5 – 9,3 mL/g	H_2SO_4	100	105	[31]
	1:56 molar	H_2SO_4	30	240	[32]
CP	1:56 molar	H_2SO_4	50	300	[23]
	79,4 mL/g	CH_3COCl	100	120	[33]
SL	6,8 – 8,5 mL/g	H_2SO_4	40	90	[26]
DS	1:180 molar	$H_3PMo_{12}O_{40}/Nb_2O_5$	250	360	[34]
SP	4 – 12 mL/g	–	200 – 300	10 – 50	[35]

**NG: Nannochloropsis gaditana; CP: Chlorella protothecoides; SL: Schizochytrium limacinum; DS: Dunaliella salina; SP: Spirulina platensis*

Es importante destacar que el uso de estos microorganismos en el campo de la tribología vagamente ha sido estudiado. Escasos artículos se pueden encontrar sobre la transesterificación para la producción de biolubricantes, pero menos aún sobre la caracterización desde el punto de vista tribológico. Estudios como el de Savienne [34] o Da Silva [36] evaluaron el potencial de especies como *D. salina* en la producción de FAME para su uso como biolubricante, pero sin caracterización tribológica. Sin embargo, pueden encontrarse algunos estudios como el de Cheah [37] donde se investigó la producción de FAME y el perfil lipídico del aceite derivado de *Chlorella sp*., así como su aplicación a bajas concentraciones en un aceite lubricante sintético PAO. Este estudio evaluó el comportamiento tribológico a través de ensayos de deslizamiento alternativo a alta frecuencia (HFRR). Finalmente se pudo demostrar las capacidades antifricción y antidesgaste de los aceites modificados de microalgas a bajas contracciones.

Más recientemente en 2024, Khan [38] evaluó el potencial de ocho cepas en la producción de biolubricantes. *Coelastrella sp., Chlorocystis sp., Ceatocerous sp., Neochloris sp., Picochlorum sp., Tisochrysis sp., Tetraselmis sp.* y *Synechococcus sp.,* fueron las seleccionadas. Sin embargo, solo la *Colaestrella sp.* pasó el corte para la síntesis de biolubricantes. Este estudio es el primero en aplicar las dobles transesterificaciones en bioaceites derivados de microalgas. En él

realizan una transesterificación ácida con H_2SO_4 y metanol para la neutralización de los FFA y producción de FAME. A continuación, someten al FAME a una segunda reacción con trimetilpropano a 100 ºC durante 120 min. A pesar de que esta tecnología es novedosa en el campo de las microalgas, sería aún necesario completar esta investigación con una caracterización tribológica en profundidad que verifique las propiedades del producto.

1.3. *Nannochloropsis gaditana* y *Haematococcus pluvialis*

Nannochloropsis gaditana es un alga unicelular miembro de la clase *Eustigmatophyceae*, derivada de un evento endosimbiótico secundario, lo que la hace estar más relacionada con algas pardas y las diatomeas que con las algas verdes [39]. Sin embargo, se caracteriza por tener tonalidades que van desde el amarillo al verde como se observa en la Figura 6 (derecha).

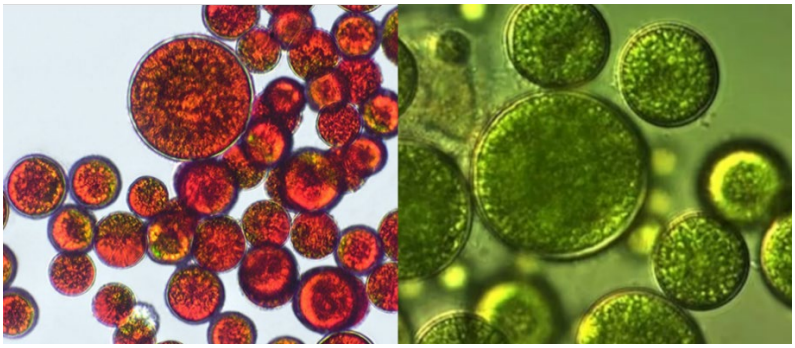

Figura 6. Cepa de *H. pluvialis* (Algatex Biotechnology), izquierda; y cepa de *N. gaditana*, derecha.

En la última década, esta microalga ha suscitado cierto interés en el sector energético por su alto contenido de lípidos, el cual varía entre el 25% y el 45%. Se trata de una fuente rica en omega 3, principalmente en forma de EPA (ácido graso eicosapentaenoico, C20:5) [40]. Además, ha sido demostrado que sometida a las condiciones de cultivo adecuadas, esta cepa es capaz de aumentar su contenido lipídico hasta en un 75% (mayoritariamente lípidos neutros – triglicéridos) [41].

Como ya se ha discutido en la Tabla 1, esta microalga ha sido ampliamente estudiada en la producción de biodiesel a través de transesterificaciones directas. Estas reacciones, aún eliminando la etapa de extracción del bioaceite, requieren de condiciones de ensayo complejas. Sería de interés la optimización de la reacción de transesterificación a partir de su bioaceite, intentando implementar configuraciones de ensayo más asequibles que no impliquen tener que llegar a condiciones supercríticas.

La segunda cepa de interés sería la *Haematococcus pluvialis*, siendo esta una de las especies más cultivadas en la industria junto con la *Spirulina, Chlorella* y *Dunaliella*. Se trata de un alga verde unicelular perteneciente a la familia de las *Haematococcaceae* [42]. Es la fuente por excelencia del antioxidante natural astaxantina, causante de la pigmentación rojiza característica de esta microalga (Figura 6, izquierda). Este microorganismo tiene la capacidad de acumular hasta un 5% en peso de astaxantina, siendo esta su principal explotación en la industria [43]. A pesar de que existen numerosos estudios destacando el potencial de esta microalga en el campo de los biocombustibles, vagamente ha sido estudiada en la producción de biodiesel [43–45]. Se trata de una gran candidata tanto en la producción de biodiesel como en la de biolubricante, debido al alto contenido lipídico de su bioaceite. Además, la combinación de estos procesos junto con la extracción de astaxantina a nivel industrial supondría un gran avance en la valorización de residuos, así como una reducción en los costes de producción gracias a la implantación de estrategias de economía circular.

CAPÍTULO 2

2 Objetivos

En base a lo expuesto en la introducción, el **objetivo general** de la presente tesis doctoral es estudiar la factibilidad del uso de bioaceites modificados de tercera generación, derivados de microalgas, como mejoradores de la lubricidad en un combustible diésel. Para este propósito se seleccionaron las cepas de microalgas de *Nannochloropsis gaditana* y *Haematococcus pluvialis*.

Para conseguir el objetivo general antes planteado, se definieron los siguientes **objetivos específicos**:

1) Optimizar las reacciones de transesterificación de los bioaceites derivados de *N. gaditana y H. pluvialis* con la finalidad de obtener el mayor rendimiento en la obtención de FAMEs.
2) Caracterizar desde el punto de vista fisicoquímico los FAMEs derivados de *N. gaditana* y *H. pluvialis*.
3) Caracterizar desde el punto de vista tribológico los FAMEs derivados de *N. gaditana* y *H. pluvialis*, así como las mezclas de esta última con un combustible diésel.
4) Determinar la necesidad de optimización e implantación de un proceso de purificación de la mezcla de FAMEs derivada de la *H. pluvialis* para su aplicación como aditivo.
5) Estudiar la factibilidad técnico-económica de la producción de FAMEs a partir de la microalga de *H. pluvialis* a escala industrial.

CAPÍTULO

3

3 Optimización de la reacción de transesterificación de *N. gaditana* y *H. pluvialis*

En este capítulo se exponen los resultados obtenidos durante el proceso de optimización de la reacción de transesterificación para la producción de FAMEs a partir de los bioaceites derivados de las microalgas *N. gaditana* y *H. pluvialis*, publicados en los artículos científicos:

- **Claudia Sanjurjo**, Oulego P, Rodríguez E, Battez AH. Biodiesel production from the microalgae Nannochloropsis gaditana: Optimization of the transesterification reaction and physicochemical characterization. Biomass and Bioenergy 2024;185:107240. https://doi.org/10.1016/j.biombioe.2024.107240.

- **Claudia Sanjurjo**, Rodríguez E, Bartolomé M, González R, Hernández A. Optimizing the Conversion of Bio-Oil from Haematococcus pluvialis to Fatty Acid Methyl Esters. BioEnergy Research 2024. https://doi.org/10.1007/s12155-024-10794-9.

3.1. Caracterización del bioaceite y obtención del perfil lipídico de *N. gaditana* y *H. pluvialis*

Los bioaceites fueron sometidos a un análisis del contenido en agua y TAN para evaluar la necesidad de implantación de un proceso previo de esterificación con catalizador ácido y/o secado. Los resultados de *N. gaditana* fueron 1583,7 ppm de humedad y 1,11 mg KOH/g, mientras que para *H. pluvialis* fueron 1826,4 ppm y 0 mg KOH/g. A la vista de estos resultados, se verificó que no era necesario ningún pretratamiento.

Para la obtención del contenido de lípidos saponificables totales y del perfil lipídico, se sometió a ambas muestras a una reacción de transesterificación con metanol en presencia del catalizador ácido CH_3COCl. Tras este proceso se concluyó que el contenido de lípidos saponificables era del 35% y 50% para *N. gaditana* y *H. pluvialis*, respectivamente.

En cuanto a la distribución de ácidos grasos, en la Figura 7 se muestras los cromatogramas correspondientes al perfil lipídico de cada uno de los bioaceites

derivados de microalgas. *N. gaditana* presentó tres ácidos grasos predominantes: C16:0 (ácido palmítico), C16:1 (ácido palmitoleico) y C20:5 (ácido eicosapentanoico). Como ya se comentó en el *Capítulo 1*, esta cepa de microalga es famosa por su alto contenido en C20:5 (EPA), de gran valor en la industria farmacéutica. Los picos mayoritarios en el caso de *H. pluvialis* fueron el C16:0, C18:1 (ácido oleico) y C18:2 (ácido linolénico). La composición completa de ácidos grasos se muestra en la Tabla 2.

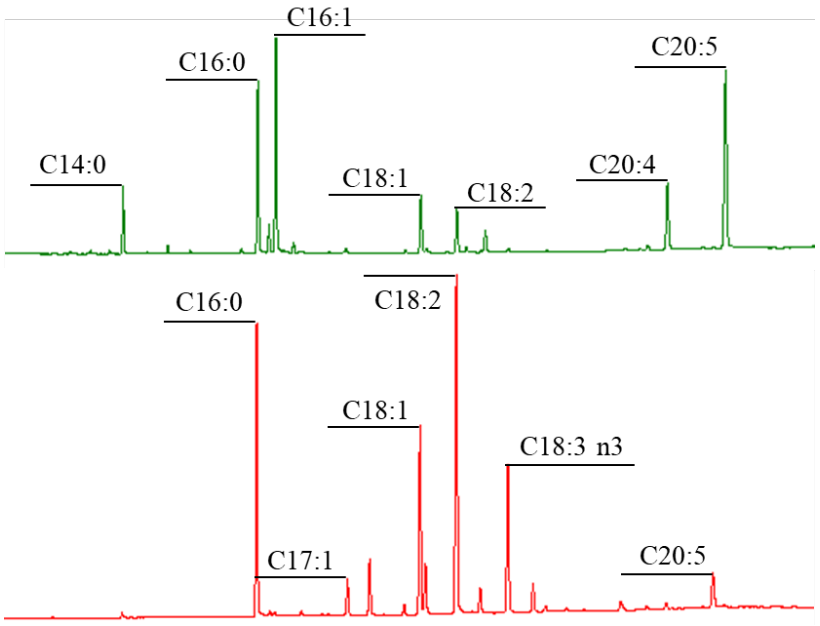

Figura 7. Cromatograma del perfil lipídico de *N. gaditana* (arriba) y *H. pluvialis* (abajo).

Tabla 2. Composición de ácidos grasos de *N. gaditana* y *H. pluvialis*.

Ácido graso	***N. gaditana***	***H. pluvialis***
C14:0	5,35	–
C16:0	25,2	20,38
C16:1	24,5	–
C17:1	–	2,92
C18:1	5,88	15,89
C18:2	2,79	29,92
C18:3	1,17	15,21
C20:4	3,84	–
C20:5	28,5	3,52

*Los ácidos grasos con concentraciones por debajo de 1% no han sido incluidos en la tabla.

N. gaditana exhibió una distribución equitativa entre SFA, MUFAs y PUFAs, con porcentajes del 30,55%, 31,91% y 37,54%, respectivamente. El bioaceite de *H. pluviales* se caracterizó por un contenido de PUFAs del 59,96%. Es importante recordar que la presencia de ácidos grasos insaturados, especialmente PUFAs, tienden a favorecer la oxidación del material y, por ende, este tipo de estructuras no son deseadas.

Con el propósito de confirmar los resultados del GC-FID y observar las colecciones de enlaces presentes antes y después de la reacción de transesterificación, las muestras fueron sometidas a un análisis por FTIR. Los resultados de estos análisis están representados en la Figura 8.

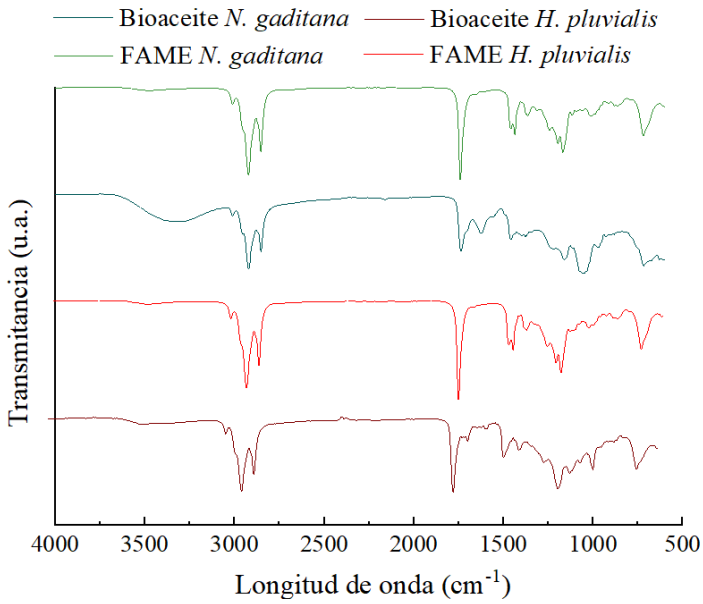

Figura 8. Espectros FTIR de los bioaceites y los FAMEs derivados de las microalgas *N. gaditana* y *H. pluvialis.*

El aumento en todas las muestras de FAME de las bandas características a 2921,63 cm^{-1} y 2852,2 cm^{-1} corresponde al incremento de alcanos ($-CH_3$), resultado de la ruptura de los triglicéridos en sus constituyentes ácidos grasos, verificando así la formación de FAME durante la reacción. La disminución, tras la reacción de transesterificación, de las bandas a 715 cm^{-1} y 725 cm^{-1} se debe a la pérdida de alcanos ($-CH_2$) presentes en el triglicérido.

Puede apreciarse en las muestras una banda constante a 3012,27 cm^{-1} atribuida a dobles enlaces (-C=C-). Además, los ésteres (-C=O) a 1739,48 cm^{-1}, los compuestos de acetato de metilo ((CO)-O-C) a 1434,78 cm-1 y otros compuestos de metilo (-C-C(O)-C) a 1166,72 cm^{-1}, están presentes de forma

constante antes y después de la reacción. De forma puntual, se aprecia una amplia banda a 3342,03 cm^{-1} en el bioaceite derivado de *H. pluvialis*, indicando la presencia de compuestos de alcohol (-OH), correspondientes a restos de etanol utilizados en el proceso de extracción del bioaceite.

3.2. Diseño de experimentos

Para proceder con el diseño de experimentos, se empleó la misma metodología de superficie de respuesta en ambos bioaceites. Para ello, fue necesario definir las variables independientes de entrada, la variable de salida, así como los niveles de ensayo (Tabla 3).

Tabla 3. Variables de entrada, variable de salida y niveles para la optimización de la reacción de transesterificación.

Variables Independientes	**Factor**	**Niveles**				
		-2 (-α)	**-1**	**0**	**1**	**+2 (+α)**
Ratio bioaceite:alcohol (g)	A	1:3	1:6	1:9	1:12	1:15
Temperatura de reacción (ºC)	B	30	50	70	90	110
Tiempo de reacción (min)	C	30	67,5	105	142,5	180
Variable de salida	Y	Conversión de FAME (%)				

En la Tabla 4 se muestran los resultados obtenidos para *N. gaditana* y *H. pluvialis*. El análisis de estos resultados con el software Design Expert v.9 se resumió en la generación de un modelo empírico que correlaciona las diferentes variables de entrada con la variable de salida a través de un modelo de regresión cuadrática. Para el caso de *N. gaditana*, el modelo se ajustó de acuerdo con la Ecuación 1, mientras que para *H. pluvialis* se ajustó a la Ecuación 2.

$$Y = 78{,}90 + 8{,}11A - 7{,}44B + 1{,}17C + 0{,}9217AB - 6{,}77AC + 4{,}39BC - 6{,}31A^2 - 2{,}40B^2 - 5{,}94C^2 \quad (1)$$

$$Y = 55{,}77 - 6{,}94A + 2{,}70B - 3{,}90C + 0{,}8588AB + 2{,}45AC - 2{,}73BC + 6{,}96A^2 + 6{,}88B^2 + 0{,}5278C^2 \quad (2)$$

Tabla 4. Diseño de experimento y resultados para la producción de FAME a partir de *N. gaditana* y *H. pluvialis*.

Orden std.	Nº test	Variable entrada			Respuesta (%)					
					N. gaditana			*H. pluvialis*		
		A	B	C	Real	Modelo		Real	Modelo	
					Y	Y	Error	Y	Y	Error
11	1	0	–2	0	81,81	84,18	2,90	80,48	77,89	3,21
18	2	0	0	0	78,52	78,90	0,49	56,89	55,77	1,96
2	3	1	–1	–1	86,99	88,87	2,16	57,65	58,37	1,25
6	4	1	–1	1	72,69	68,89	5,24	60,94	60,91	0,04
10	5	2	0	0	70,35	69,88	0,67	67,84	69,73	2,78
4	6	1	1	–1	70,37	67,05	4,72	74,01	70,93	4,16
9	7	–2	0	0	33,44	37,44	11,95	97,23	97,49	0,27
13	8	0	0	–2	50,90	52,80	3,74	65,23	65,69	0,71
3	9	0	0	0	35,21	35,45	0,66	49,12	55,77	13,55
8	10	–1	1	–1	62,08	64,63	4,11	90,12	88,00	2,36
1	11	1	1	1	67,09	60,95	9,15	66,12	62,57	5,37
7	12	–1	–1	–1	65,57	60,11	8,33	77,47	78,87	1,81
14	13	0	0	0	55,80	57,48	3,02	56,93	55,77	2,03
12	14	–1	1	1	53,22	54,42	2,25	72,71	69,84	3,95
5	15	0	0	2	68,31	68,05	0,37	48,39	50,08	3,48
15	16	0	2	0	77,44	78,90	1,88	83,94	88,68	5,64
17	17	–1	–1	1	77,72	78,90	1,52	70,69	71,62	1,31
16	18	0	0	0	78,35	78,90	0,70	55,36	55,77	0,75
19	19	0	0	0	–	–	–	58,42	55,77	4,53

Observando ambas ecuaciones, se puede percibir una diferencia de comportamiento entre los bioaceites. La reacción de transesterificación de *H. pluvialis* se ve beneficiada por ratios bioaceite:alcohol y tiempos de reacción menores, mientras que la reacción con *N. gaditana* se ve potenciada por un aumento en ambos parámetros. Para el caso de la temperatura, también parecen tener comportamientos opuestos, siendo la respuesta Y en *H. pluvialis* directamente proporcional al aumento da la temperatura.

Los resultados de los análisis finales de ANOVA para la evaluación del ajuste demostraron en ambos casos que los modelos son adecuados para su aplicación con estos bioaceites. En la Tabla 5 se muestra un resumen de dichos resultados, los cuales pueden ser consultados en su totalidad en las publicaciones correspondientes.

Tabla 5. Análisis de ANOVA para la adecuación de los modelos matemáticos.

Parámetro	*N. gaditana*		*H. pluvialis*	
	Valor F	**Valor *p***	**Valor F**	**Valor *p***
Modelo	24,28	< 0,0001	24,95	< 0,0001
A	61,52	< 0,0001	54,19	< 0,0001
B	51,75	0,2891	8,17	0,0188
C	1,29	0,5461	17,15	0,0025
AB	0,3973	0,0017	0,4148	0,5355
AC	21,44	< 0,0001	3,37	0,0995
BC	9,02	0,0170	4,18	0,0712
A^2	50,70	< 0,0001	80,62	< 0,0001
B^2	7,35	0,0266	78,75	< 0,0001
C^2	45,03	0,0002	0,4637	0,5130
Resumen del modelo	**R_2**	0,9647	**R^2**	0,9614
	R^2_{adj}	0,9250	**R^2_{adj}**	0,9228
	R^2_{pred}	0,7366	**R^2_{pred}**	0,7884

Los valores de F y *p* representan la significancia de los modelos, considerando los parámetros significativos para valores de $p < 0,05$. Los modelos presentaron un valor de $p < 0.0001$, siendo estos significativos. Sin embargo, *N. gaditana* exhibió un mejor ajuste de los parámetros individuales. Este hecho se ve reflejado en un mayor coeficiente de determinación R^2 de 0,9647 frente al 0,9614 de *H. pluvialis*.

En la Figura 9a se muestra la comparación de los valores predichos mediante la aplicación de las Ecuaciones 1 y 2, frente a los valores reales experimentales. Las diferencias entre los valores generados y los actuales resultaron menores del 10% para todos ensayos a excepción de la presencia de dos valores atípicos. El primero se encontró en la prueba nº7 para *N. gaditana* con un error del 11,95% (Tabla 4), mientras que el segundo correspondió a la prueba nº9 de *H. pluvialis* con un error del 13,55%. La exclusión de estos valores atípicos permitiría alcanzar un error medio de predicción de los modelos del 2,8%.

Otro diagnóstico de interés es el análisis de los residuos estudentizados frente a los valores predichos, que se muestra en la Figura 9b. Esta representación tiene como finalidad comprobar la adecuación de los modelos para su aplicación, y verificar si es necesaria la modificación de dichos modelos para la reducción de la dispersión. Los resultados de ambos análisis presentaron una distribución aleatoria de puntos dentro de los límites establecidos de ± 5, lo que indica una discrepancia constante y que, en los dos casos a estudiar, no es necesario reducir la dispersión para su aplicación.

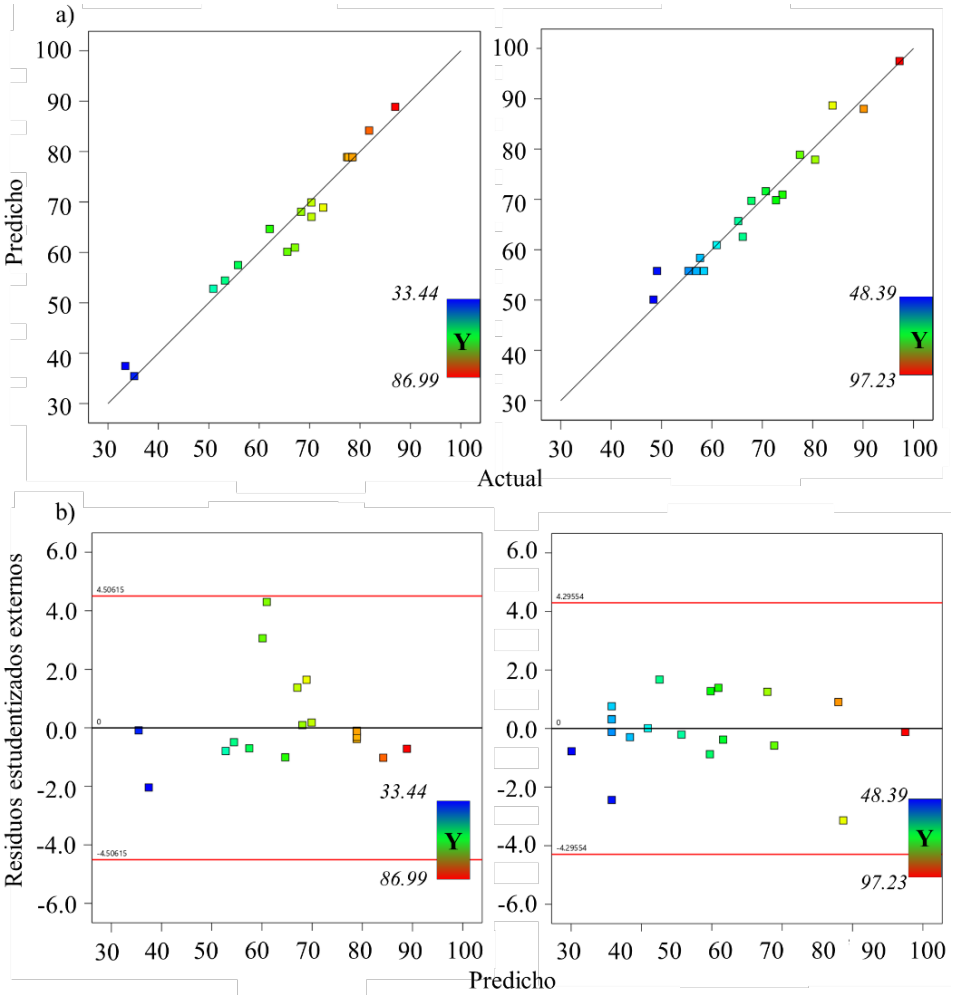

Figura 9. Resultados *N. gaditana* (izquierda) y *H. pluvialis* (derecha): a) Comparación de los valores predichos frente a los actuales; b) Valores residuales frente a los predichos.

La interacción entre las diferentes variables independientes (A, B y C) y la respuesta (Y) se examinó mediante un análisis de gráficos de superficie 3D proporcionados en la Figura 10. Como ya se observó en la Tabla 5 del análisis de ANOVA, el factor determinante en la reacción de transesterificación con *N. gaditana* es el ratio bioaceite:alcohol. La conversión de FAME tiende a aumentar con el incremento del ratio de forma general, comportamiento apreciable en las Figuras 10a y 10b. Por otro lado, se ve negativamente afectada por el aumento de la temperatura. El tiempo de reacción no guarda una relación directa con la conversión, sino que se encuentra fuertemente influenciada por las otras dos variables de entrada.

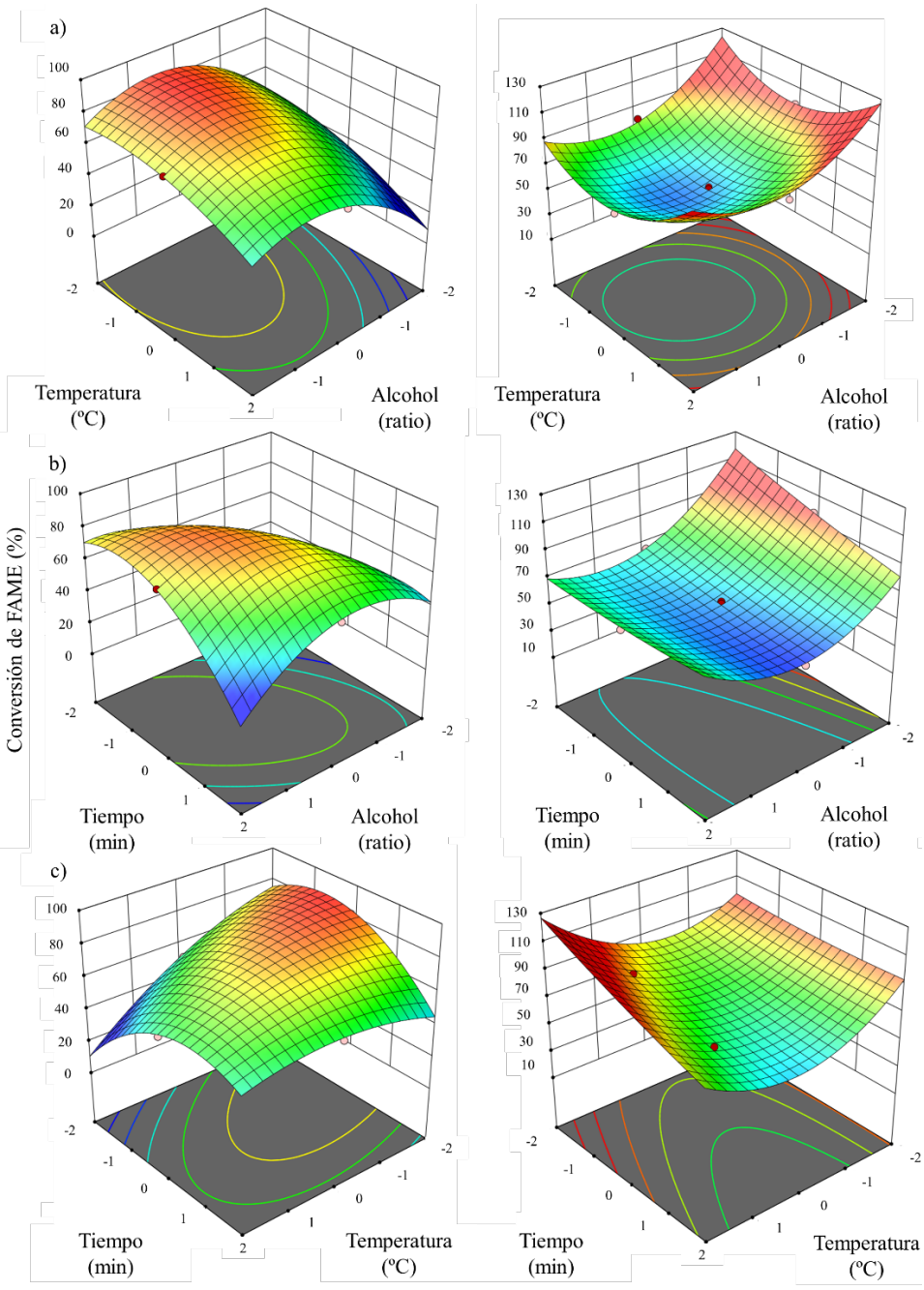

Figura 10. Interacción entre las variables independientes y la respuesta Y. Resultados *N. gaditana* (izquierda) y *H. pluvialis* (derecha): a) Interacción entre la temperatura y el ratio bioaceite:alcohol; b) Interacción entre el tiempo de reacción y el ratio bioaceite:alcohol; c) Interacción entre el tiempo de reacción y la temperatura.

En la Figura 10b el rendimiento más alto de conversión de FAME se encuentra para tiempos de reacción bajos siempre y cuando el ratio bioaceite:alcohol sea alto. En la Figura 10c este punto de conversión máxima se desplaza a tiempos de reacción mayores debido a la interacción temperatura–tiempo (desplazamiento del punto de equilibrio).

La conversión de FAME a partir de *H. pluviales* presentó un comportamiento opuesto al caso anterior. La variable de entrada más definida sería el tiempo de reacción, ya que a menores tiempos de reacción se obtienen las máximas conversiones de FAME, independientemente de la configuración del resto de variables (Figura 10b y 10c). Esta afirmación respalda los resultados del análisis de ANOVA presentados en la Tabla 5, donde los factores AC y BC presentaron valores de *p* mayor de 0,05 y, por ende, no son factores significativos. Por el contrario, la relación entre el ratio bioaceite:alcohol y la temperatura (Figura 10a) indica un punto estacionario mínimo entorno al [0, 0], presentando valores de conversión máximos en los extremos.

3.3. Condiciones óptimas de ensayo

Los modelos validados por el análisis de ANOVA se emplearon en la determinación de las condiciones óptimas de reacción para la obtención de la máxima conversión de FAME (Tabla 6).

Tabla 6. Valores codificados y reales de para la obtención de conversiones de FAME máximas con *N. gaditana* y *H. pluvialis*.

Variable de entrada	**Valor codificado**		**Valor real**
N. gaditana			
Ratio bioaceite:metanol	0,99		1:12
Temperatura (ºC)	–1		50
Tiempo (min)	–0,84		75
Respuesta, Y	**Teórico**	**Real**	**Error (%)**
Conversión de FAME (%)	89,02	87,25	2,00
H. pluvialis			
Ratio bioaceite:metanol	–1,61		1:4,17
Temperatura (ºC)	0,53		80
Tiempo (min)	–1,54		47
Respuesta, Y	**Teórico**	**Real**	**Error (%)**
Conversión de FAME (%)	103,32	98,44	2,26

Los límites establecidos para encontrar el punto óptimo fueron: variables de entrada dentro del rango de estudio [-2, 2] y variable de salida maximizada al 100%. En consonancia con todo lo descrito anteriormente, las configuraciones óptimas de ensayo difirieron en gran medida de un aceite de microalga a otro. El

aceite de *N. gaditana* resultó tener un punto óptimo de ensayo a un ratio bioaceite: metanol de 1:12, durante 75 min y bajo una temperatura de 50 ºC. Por otro lado, para *H. pluvialis* se encontró la configuración óptima a un ratio de 1:4,17, durante un tiempo de 47 min y bajo una temperatura de 80 ºC. Además, la conversión de FAME máxima exhibida por *H. pluvialis* resultó en más de un 10% superior al de *N. gaditana*.

Estas condiciones de ensayo demuestran que la implantación de metodologías para la optimización de la reacción de transesterificación en aceites derivados de microalgas permite alcanzar condiciones de ensayo comparables a las empleadas con los aceites vegetales tradicionales, sin tener que llegar a condiciones supercríticas como en la técnica de transesterificación directa.

CAPÍTULO 4

4 Caracterización fisicoquímica de los aceites modificados de microalga (FAME)

En este capítulo se exponen los resultados obtenidos durante la caracterización fisicoquímica llevada a cabo a los FAME derivados de las microalgas *N. gaditana* y *H. pluvialis*, publicados en los artículos científicos:

- **Claudia Sanjurjo**, Oulego P, Rodríguez E, Battez AH. Biodiesel production from the microalgae Nannochloropsis gaditana: Optimization of the transesterification reaction and physicochemical characterization. Biomass and Bioenergy 2024;185:107240. https://doi.org/10.1016/j.biombioe.2024.107240.

- **Claudia Sanjurjo**, Rodríguez E, Bartolomé M, González R, Hernández A. Optimizing the Conversion of Bio-Oil from Haematococcus pluvialis to Fatty Acid Methyl Esters. BioEnergy Research 2024. https://doi.org/10.1007/s12155-024-10794-9.

Propiedades tales como humedad, TAN, densidad, viscosidad, PP, FP, y estabilidad térmica, fueron las seleccionadas para caracterizar los FAME.

Las mediciones de humedad y TAN de las muestras de FAME demostraron una reducción del contenido en agua y FFA de las muestras tras el proceso completo de síntesis (reacción de transesterificación + limpieza), con valores inferiores a los 1.000 ppm y 0,45 mg KOH/g en ambos casos, respectivamente.

Los resultados de densidad y viscosidad se muestran en la Figura 11. Como se puede observar, la muestra de *H. pluvialis* presentó unos valores de densidad superiores a *N. gaditana*, llegando a alcanzar los 900 kg/m^3 a 20 ºC. Este valor es notablemente superior al reportado para FAME derivado de aceites vegetales como el aceite de palma o *S. oleosa* con valores de densidad de 879 kg/m^3 [46,47]. En términos de viscosidad, *N. gaditana* exhibió unos valores a temperatura ambiente muy elevados, por encima de los 20 mm^2/s. Sin embargo, disminuye rápidamente con el aumento de la temperatura alcanzando valores inferiores a *H. pluvialis* una vez sobrepasados los 50 ºC. Este suceso sugiere que la viscosidad se ve más influenciada por el peso molecular con el aumento de la temperatura. Longitudes de cadena más largas propician mayores grados de interacciones

intermoleculares y, en este caso, *H. pluvialis* exhibió la longitud de cadena media de ácidos grasos mayor, con predominio de cadenas de 18 átomos de carbono [48]. Además, esta propiedad también se ve afectada por la presencia de insaturaciones. Concretamente, la presencia de MUFAs favorece el aumento de la viscosidad, mientras que los PUFAs tienden a disminuirla. De forma general, ambas muestras de microalga presentan valores de viscosidad también notablemente elevados en comparación con los derivados de aceites de primera y segunda generación. Por ejemplo, para 40 ºC, las viscosidades reportadas son inferiores a 5 mm^2/s [47]. Estas diferencias de densidad y viscosidad se deben principalmente a las diferencias en las estructuras moleculares entre unas materias primas y otras.

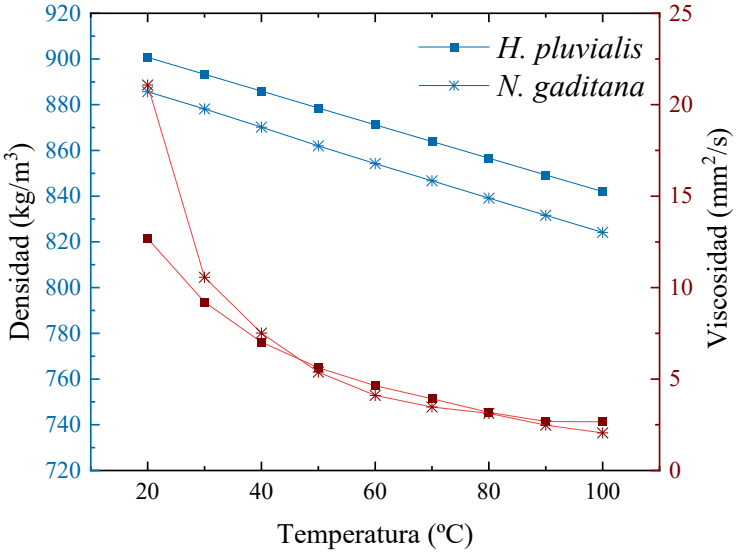

Figura 11. Variación de la densidad y la viscosidad con la temperatura de los FAME derivados de *N. gaditana* y *H. pluvialis*.

Durante la determinación del PP ambos bioaceites presentaron bandas de congelación exotérmicas sin ningún pico definido. Por otro lado, las muestras de FAME si exhibieron picos perfectamente definidos mostrados en la Figura 12 (izquierda). Los valores del PP fueron de –7,2 y –5,1 para *N. gaditana* y *H. pluvialis*. Los FAME derivados de primera y segunda generación tienden a presentar valores del PP por encima de 0 ºC [46,47]. La reducción del PP en los derivados de microalgas se atribuye al mayor contenido de PUFAs, ya que la presencia de enlaces dobles cis en compuestos insaturados dificulta el empaquetamiento de los cristales, lo que da como resultado valores del PP más bajo [49]. El ácido graso C20:5 en *N. gaditana* es un claro ejemplo de enlaces dobles cis, aportándole al fluido un PP menor que el exhibido por *H. pluvialis*.

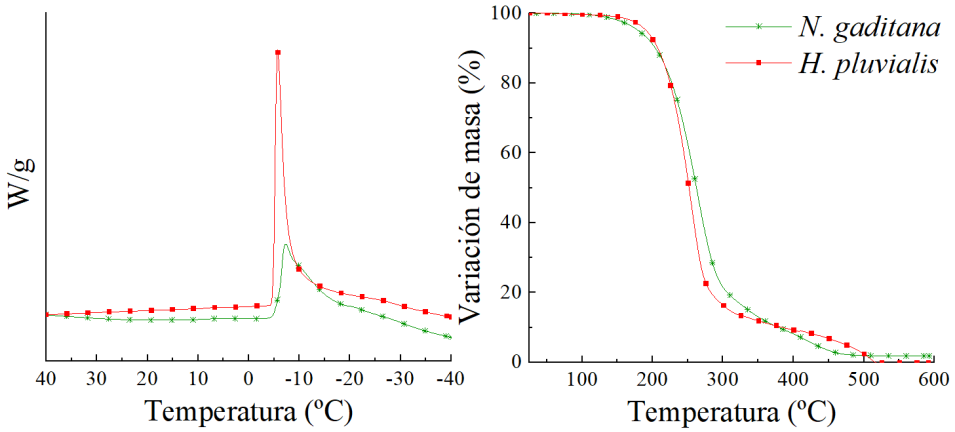

Figura 12. Curvas de DSC para la estimación del PP de los FAME (izquierda) y curvas de TGA para el estudio de la estabilidad térmica de los FAME (derecha).

Las curvas de TGA para el estudio de la estabilidad térmica se presentan de nuevo en la Figura 12 (derecha). Las medidas fueron realizadas bajo una atmósfera de N_2, por lo tanto, no pueden ser empleados en discusiones en términos de estabilidad oxidativa. Si pueden ser utilizadas para conocer el comportamiento de estos FAME cuando están sometidos a variaciones de temperatura. La muestra de *H. pluvialis* presentó una temperatura de inicio de degradación más temprana, a 211 ºC frente a los 244,8 ºC de la muestra de *N. gaditana*. Además, *H. pluvialis* exhibió una pérdida de masa más acelerada a partir de los 220 ºC, así como una degradación completa a 515 ºC. *N. gaditana* consiguió degradarse en un 98,12% a la temperatura máxima de la prueba.

Comparando los resultados con pruebas realizadas en otros estudios bajo las mismas condiciones, puede concluirse que la estabilidad térmica de los FAME derivados de *N. gaditana* y *H. pluviales* son favorablemente superiores a los FAME derivados de vegetales como la colza o *jatropha* [50,51].

En cuanto a las medidas del FP, la muestra de *N. gaditana* no presentó ninguna anomalía durante la prueba, exhibiendo un valor del FP entre 140 – 150 ºC. Sin embargo, la muestra de *H. pluvialis* presentó una formación de espuma al alcanzar los 100 ºC durante la prueba. Este suceso puede deberse a presencia de pequeños contaminantes, como otra clase de lípidos (pigmento), que se descomponen a esa temperatura y tienden a formar una fina capa de espuma en presencia de aire [52]. La presencia de espuma en la superficie dificulta la dispersión de los gases de combustión, provocando la expansión de la muestra. Finalmente, alcanzó su FP a 150 ºC.

CAPÍTULO 5

5 Caracterización tribológica de los aceites modificados de microalgas (FAME)

En este capítulo se exponen los resultados obtenidos durante la caracterización tribológica llevaba a cabo a los FAME derivados de las microalgas *N. gaditana* y *H. pluvialis*, publicado en el artículo científico:

- **Claudia Sanjurjo**, Rivera N, Rodríguez E, Fernández-González A, Battez AH. Biodiesel derived from the microalgae Nannochloropsis gaditana and Haematococcus pluvialis: Physicochemical and tribological properties. Journal of Molecular Liquids 2024;408:125391. https://doi.org/10.1016/j.molliq.2024.125391.

5.1. Ensayo rodadura/deslizamiento

Los resultados del ensayo de rodadura/deslizamiento se muestran en la Figura 13.

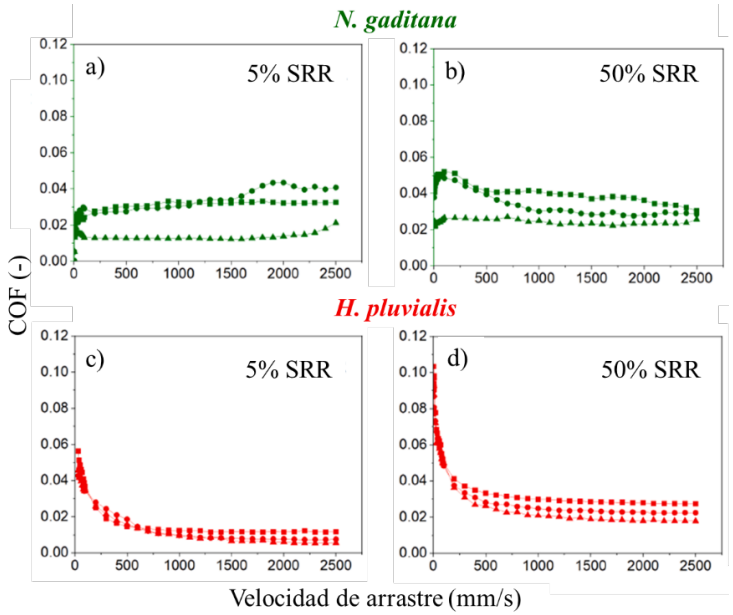

Figura 13. Valores de COF frente a la velocidad de arrastre durante los ensayos rodadura–deslizamiento: a) *N. gaditana* a 5% de SRR; b) *N. gaditana* a 50% de SRR; c) *H. pluvialis* a 5% de SRR; d) *H. pluvialis* a 50% de SRR.

Los coeficientes de fricción se han mantenido generalmente dentro del rango 0,01 – 0,1, valores típicos de la lubricación mixta–EHL (elastohidrodinámica). Los resultados indican que la fricción disminuyó con la temperatura debido a una reducción de la viscosidad por parte de las muestras de FAME.

Por el contrario, se observó un aumento de la fricción con el incremento de la componente deslizante en el contacto bola – disco. Es importante destacar que la muestra derivada de *H. pluvialis* presentó mejores resultados que la de *N. gaditana*. Como ya se observó en el *Capítulo 3*, la longitud de cadena media del FAME derivado de *H. pluvialis* es mayor, resultando en valores del COF más bajos. Esto se debe a la presencia de enlaces moleculares más fuertes y películas de adsorción más gruesas [5].

5.2. Ensayo deslizamiento alternativo

A continuación, se muestran en la Figura 14c los resultados de la variación del COF medio con la temperatura durante los ensayos de deslizamiento alternativo. Además, en la Figura 14a y 14b se encuentra representado la evolución del COF frente al tiempo.

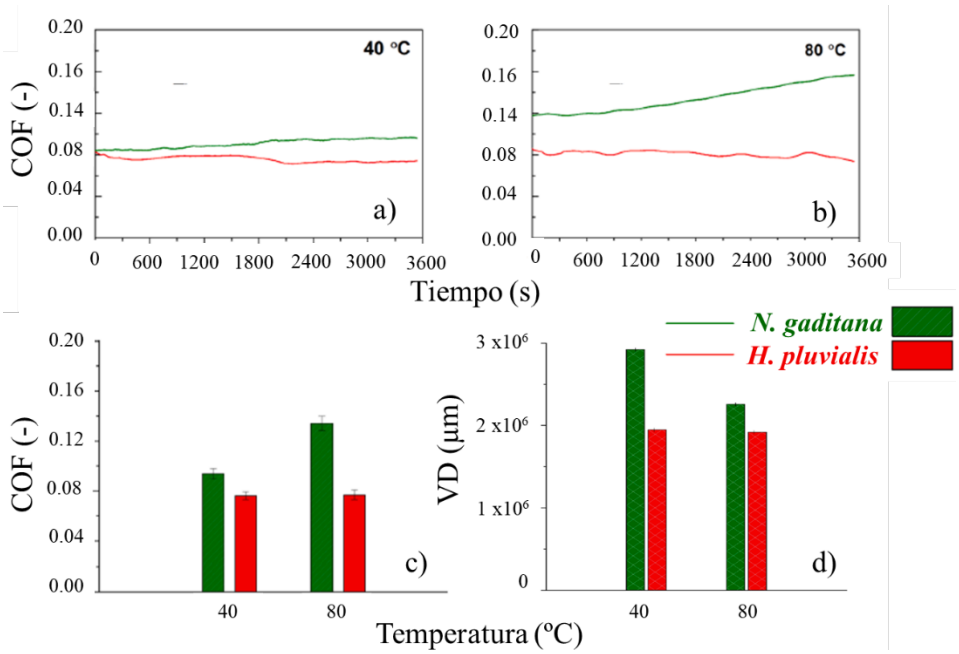

Figura 14. Resultados de COF del ensayo de deslizamiento alternativo: a) 40 ºC; b) 80 ºC; c) COF medio y desviación estándar a 40 ºC y 80 ºC; d) volumen de desgaste en la huella del disco.

Analizando los resultados, se puede observar que los valores exhibidos del COF son típicos del régimen de lubricación mixta, a excepción de la muestra de FAME derivada de *N. gaditana* a 80 ºC que presentó un valor típico del régimen de lubricación límite por encima del 0,1.

Durante los ensayos a 40 ºC la fricción se mantuvo relativamente constante para ambas muestras de FAME. Sin embargo, la muestra derivada de *H. pluvialis* presentó el mejor comportamiento antifricción, así como una mejor estabilidad frente al aumento de la temperatura. En contraste, el FAME derivado de *N. gaditana* exhibió valores de COF más elevados, que se vieron agravados por el aumento de la temperatura. Estos resultados pueden atribuirse a la adsorción de moléculas polares orgánicas en la superficie metálica que reducen la fricción, así como a los enlaces moleculares más fuertes y tribocapas adsorbidas más gruesas por parte de la muestra de *H. pluvialis*. Este tipo de compuestos tienden a tener una fuerte polaridad debido a la presencia de oxígeno en el grupo carbonilo del éster.

En este estudio se determinó la polaridad a través del cálculo del NPI [53]. Los ácidos grasos no identificados no fueron tenidos en cuenta para el cálculo, obteniendo así unos valores para *H. pluvialis* y *N. gaditana* de 49,12 y 50,15. Un NPI bajo indica una alta polaridad (NPI = 50 para ésteres sintéticos), mientras que un NPI alto indica que se trata de una molécula/compuesto no polar (NPI = 300 para polialfaolefinas).

A pesar de que ambas muestras presentaron polaridades similares, sus moléculas pueden estar adsorbiéndose de diferentes formas, ya sea a través de adsorción física (fisisorción) o adsorción química (quimisorción). La primera tiene lugar a temperatura ambiente mediante la formación de enlaces de hidrógeno con los óxidos superficiales de los hidróxidos. Este proceso suele tener una temperatura límite máxima [54,55]. En este caso, el mecanismo de adsorción durante las pruebas a 40 ºC es principalmente de fisisorción, mientras que a 80 ºC es de quimisorción.

Las diferencias en los resultados de la fricción podrían estar relacionados con la fuerza de los enlaces químicos formados por las moléculas de los ácidos grasos con la superficie metálica, ya que ambos compuestos presentan perfiles de ácidos grasos muy diferentes.

Otros autores han reportado que la longitud de cadena, el grado de insaturación y la distribución de dichas insaturaciones a lo largo de la cadena carbonada, pueden afectar a su adsorción en la superficie del metal [56,57]. En base a estos estudios, longitudes de cadena de entre 17–18 átomos de carbono favorecen valores de ΔG_{ads} (energía libre de adsorción) más bajos, resultando en una fuerte adsorción en la superficie metálica. Por otro lado, el aumento del grado

de insaturación genera el efecto inverso, valores de ΔG_{ads} más altos y, por ende, una adsorción más débil. Esto mismo estaría ocurriendo en el caso actual, donde la alta presencia de C20:5 en FAME derivado de *N. gaditana* contribuirían a valores de ΔG_{ads} más altos, y por consiguiente una adsorción más débil y peor comportamiento antifricción.

5.3. Análisis superficial

La Figura 15 muestra las imágenes del SEM de la superficie de desgaste del disco después de los ensayos de deslizamiento alternativo. Se apreciaron mecanismos de desgaste por adhesión y deformación plástica en ambos casos. Se encontraron picaduras, particularmente en las probetas de los ensayos a 40 ºC con el FAME derivado *N. gaditana*, lo que explica el mayor volumen de desgaste en la Figura 14d.

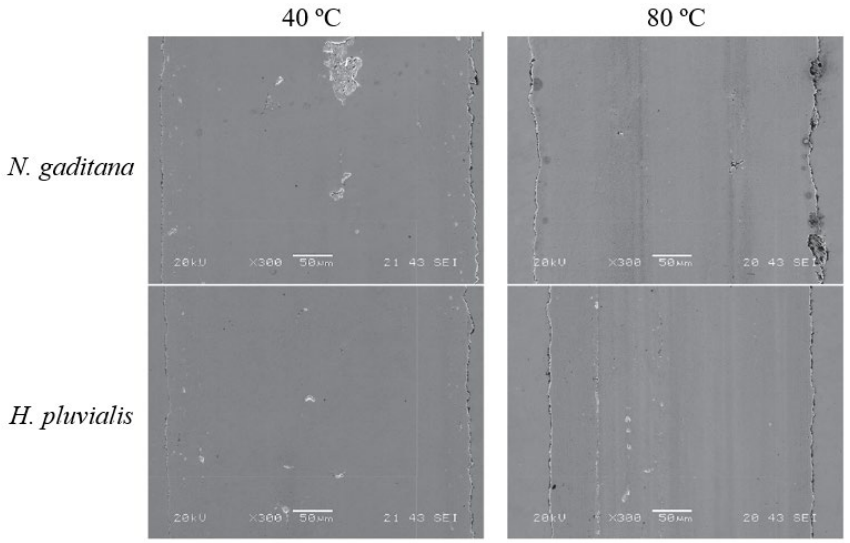

Figura 15. Imágenes del SEM de las superficies del disco tras los ensayos de deslizamiento alternativo para el FAME derivado de *N. gaditana* y *H. pluvialis*.

En la Figura 16 se muestra el ajuste de curva tentativo para el espectro Fe 2p3/2, que emplea cuatro curvas distintas asociadas a Fe (0). Las formas de curva seleccionadas se basaron en el trabajo de Mangolini [58]. Los resultados muestran la formación de una tribocapa de óxido, aunque las diferencias entre las muestras de *N. gaditana* y *H. pluvialis* son sutiles, siendo no significativas.

El ajuste de C1 es un desafío, en particular con muestras orgánicas complejas como es el caso de las microalgas. Sin embargo, parece evidente que *N. gaditana* a 40 ºC exhibe un mayor pico con la energía de enlace más baja (Figura 17), lo que es particularmente destacable ya que esta muestra presentó los

comportamientos de fricción y desgaste más desfavorables. Estas posiciones bajas son asociadas a compuestos con bajo grado de oxidación. En cuanto a las posibles asignaciones de las posiciones ajustadas, coinciden con las que se asignan habitualmente a C – C (284,9 eV), C = O (287,6 eV), $–CO_2H$ (288,7 eV) y carburos metálicos (283,0 eV) [59,60].

Los espectros O1s de las cuatro muestras (Figura 18) no mostraron diferencias apreciables, con una combinación de tres curvas a 530,3 eV, 531,9 eV y 533,0 eV, con una relación de área aproximada de 10:5:2. Estas características se atribuyen habitualmente a óxidos metálicos, C – O y C = O [61].

Por último, los espectros de N1s (Figura 19) exhiben un valor de pico entre 399,5–399,9 eV.

La Tabla 7 presenta la relación molar de Fe, O, C y N en las diferentes muestras. Se observa una mayor cantidad de materia orgánica (C) en la superficie en las muestras de *N. gaditana*. Esto concuerda con el mayor desgaste observado en la Figura 14d. De igual forma la cantidad de materia orgánica presente en las muestras de *H. pluvialis* coincide con los resultados de desgaste, al presentar cantidades de C similares a 40 ºC y 80 ºC.

Tabla 7. Ratios molares en el análisis superficial XPS.

		Fe	C	O	N
40 ºC	*H. pluvialis*	1	27,3	12,2	0,4
	H. pluvialis	1	24,8	10,3	0,5
80 ºC	*N. gaditana*	1	41,1	10,6	0,8
	N. gaditana	1	19,9	10,1	0,4

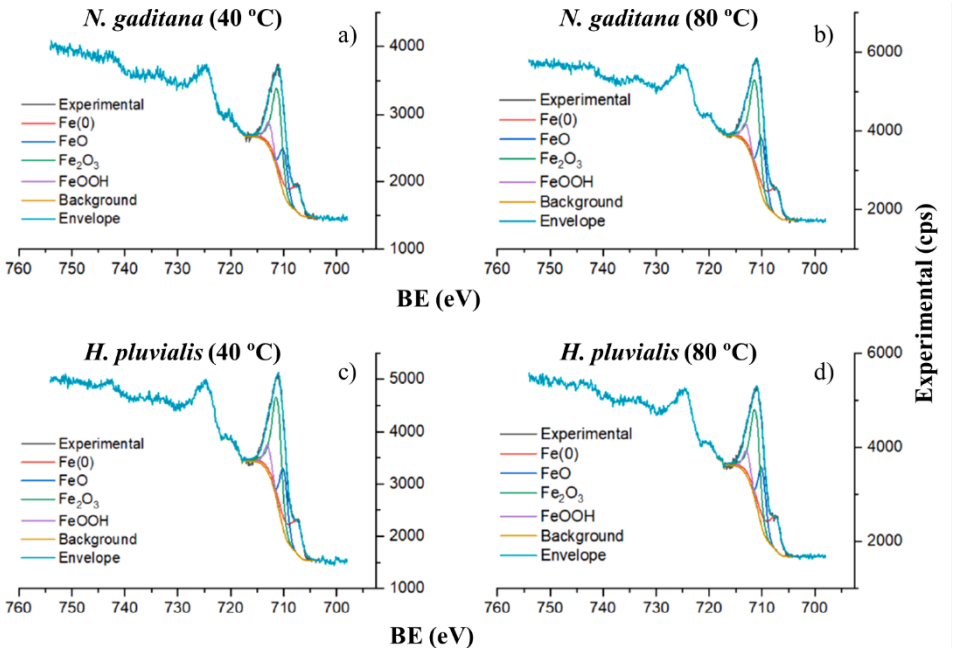

Figura 16. Ajuste de curvas para espectros de alta resolución de Fe 2p3/2 para las muestras: a) *N. gaditana* a 40 ºC; b) *N. gaditana* a 80 ºC; c) *H. pluvialis* a 40 ºC; d) *H. pluvialis* a 80 ºC.

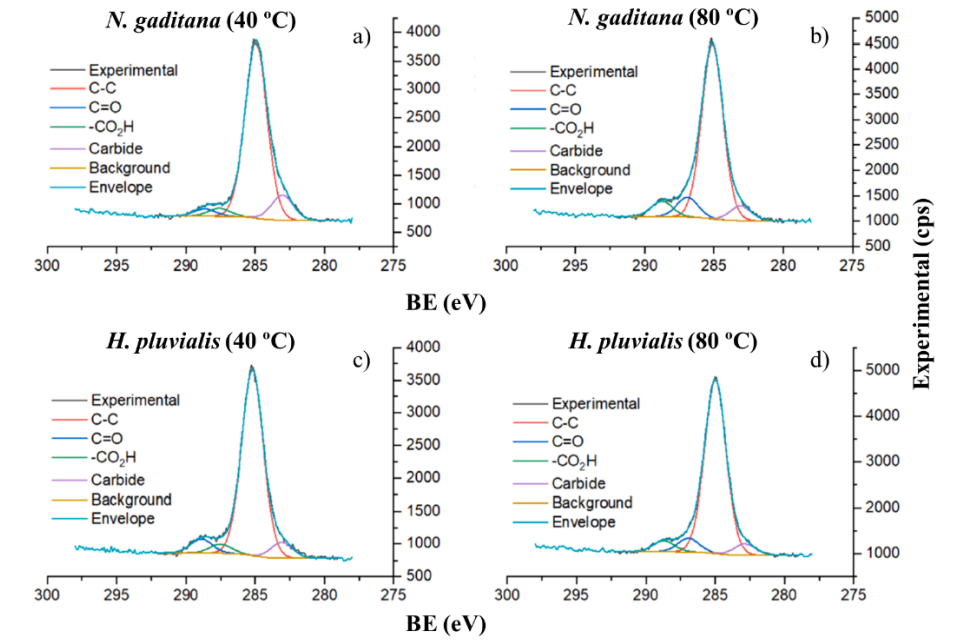

Figura 17. Ajuste de curvas para espectros de alta resolución de C1s para las muestras: a) *N. gaditana* a 40 ºC; b) *N. gaditana* a 80 ºC; c) *H. pluvialis* a 40 ºC; d) *H. pluvialis* a 80 ºC

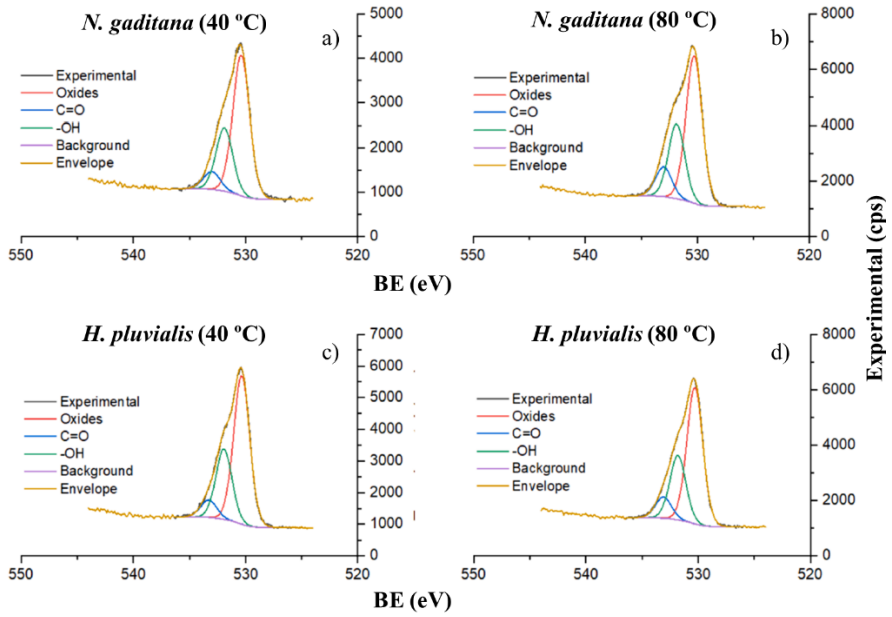

Figura 18. Ajuste de curvas para espectros de alta resolución de O1s para las muestras: a) *N. gaditana* a 40 ºC; b) *N. gaditana* a 80 ºC; c) *H. pluvialis* a 40 ºC; d) *H. pluvialis* a 80 ºC

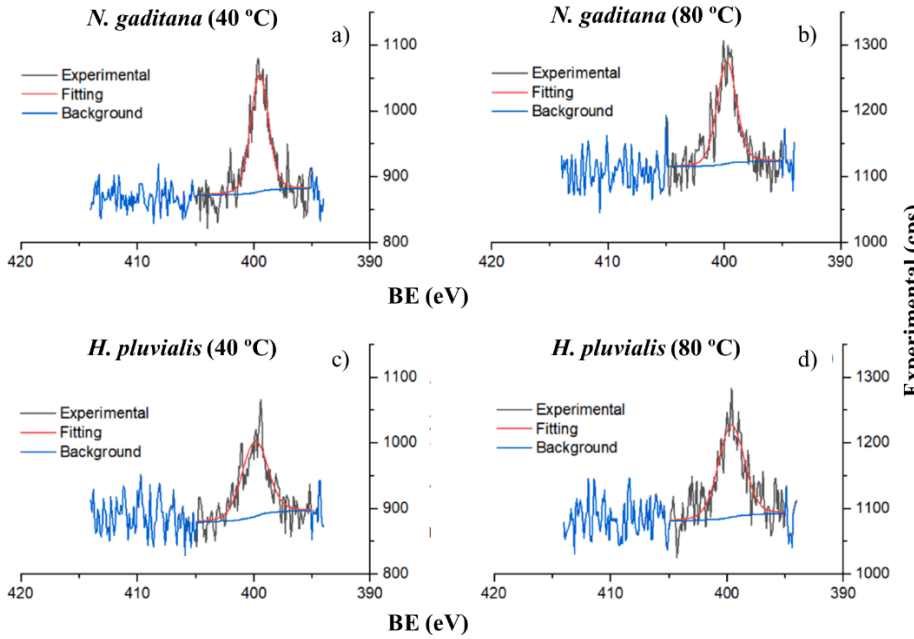

Figura 19. Ajuste de curvas para espectros de alta resolución de N1s para las muestras: a) *N. gaditana* a 40 ºC; b) *N. gaditana* a 80 ºC; c) *H. pluvialis* a 40 ºC; d) *H. pluvialis* a 80 ºC.

CAPÍTULO

6

6 Purificación de FAME derivado de *H. pluvialis* y su uso como aditivo lubricante en diésel

En base a los resultados obtenidos en los capítulos anteriores, se tomó la decisión de continuar la investigación solo con la muestra de FAME derivada de la microalga de *H. pluvialis*. Esta cepa de microalga presentó ventajas destacadas tales como:

- Mayor contenido de triglicéridos en la muestra del bioaceite de partida.
- Mejor comportamiento frente a la fricción y el desgaste.
- Propiedades tribológicas más estables con la temperatura.

6.1. Purificación de FAME con bentonitas

Para continuar con la investigación y emplear los FAME como aditivo lubricante en un combustible diésel, era necesario realizar un proceso de purificación con la finalidad de reducir la pigmentación de la muestra. La técnica seleccionada fue la adsorción con bentonitas, ya que se trata de un método óptimo para el tratamiento de pigmentos, que ya había sido empleada con anterioridad por otros autores en el tratamiento de aceites vegetales y derivados de microalgas [27,62]. El uso de bentonitas presenta una serie de ventajas donde se incluyen un bajo coste, alta eficiencia, de fácil manejo y alta estabilidad del adsorbente [63].

En la Figura 20 se muestra una composición de imágenes donde se puede apreciar la intensidad del pigmento en la muestra inicial de FAME debido al alto contenido de astaxantina. Además, se incluyen instantáneas de los diferentes resultados y como las muestras van clareando con el aumento de la concentración de bentonitas.

Para llevar a cabo este proceso, se mezcló 1 g de muestra con 10 mL de hexano y la concentración correspondiente de bentonitas. Las mezclas se agitaron a 250 rpm durante 24 horas [27]. Finalizado el tiempo de mezcla, la fase de hexano–FAME se separó de la fase bentonita–pigmento mediante centrifugación a 7.000 rpm durante 10 min. A continuación, la fase hexano–FAME se llevó a un evaporador rotativo para la eliminación del hexano a 50 ºC y 150 mbar durante 20 min.

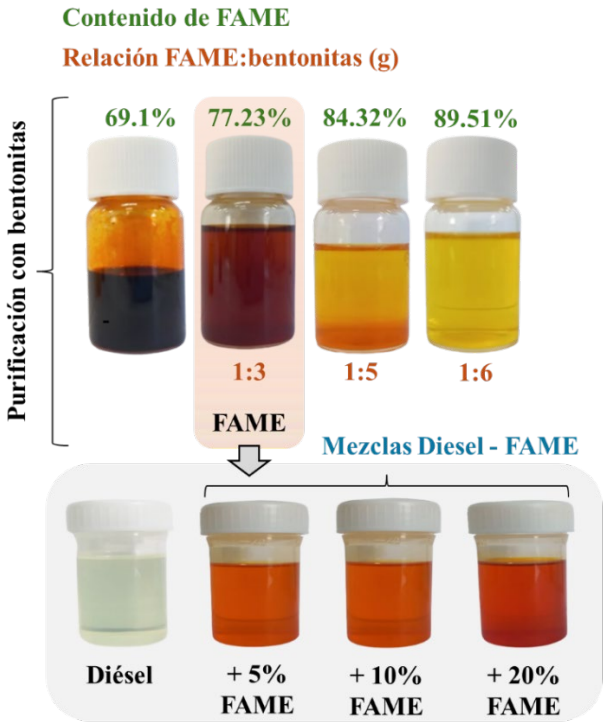

Figura 20. Muestras de FAME tras el proceso de purificación con bentonitas y mezclas con un combustible diésel.

El proceso de purificación con bentonitas demostró ser una técnica eficiente en la eliminación de astaxantina. Como se puede observar en la Tabla 8, se alcanzó una contracción de FAME de 89,51% para la relación de bentonitas 1:6, lo que supone una reducción de impurezas del 29,54%. Sin embargo, además de adsorber pigmento la bentonita arrastraba gran parte del FAME. Se verificó que un aumento en la concentración de bentonitas producía un aumento en las pérdidas de FAME. Para la relación 1:6, la pérdida de FAME ascendía al 30% de la muestra, un 10% mayor que la exhibida por la relación 1:3.

Tabla 8. Caracterización fisicoquímica del proceso de purificación con bentonitas.

Propiedad	**Relación FAME: bentonitas (g)**			
	1:0	**1:3**	**1:5**	**1:6**
Contenido de FAME (%)	69,10	77,23	84,32	89,51
PP (ºC)	– 5,1	– 4,3	– 4,93	– 5,15
T_{onset} (ºC)	211	232,42	233,74	289,16
T_{offset} (ºC)	286	325	321	322

*T_{onset}: temperatura de inicio de degradación; T_{offset}: temperatura final de degradación

El análisis de FTIR de las cuatro muestras se puede ver en la Figura 21. A primera vista, no se observaron diferencias discernibles entre las muestras. Esto se debe al hecho de que la estructura molecular de la astaxantina también está compuesta principalmente de largas cadenas carbonadas con dobles enlaces y ésteres en su estructura. Los picos presentes a 3006 cm^{-1}, 2923 cm^{-1} y 2854 cm^{-1} corresponderían a las vibraciones de tensión de los grupos funcionales de (-CH), ($-CH_2$) y ($-CH_3$). El pico característico de la vibración de tensión del grupo carbonilo (-C=O) se encontró a 1739 cm^{-1}, mientras que el grupo funcional C(C=O)-O- fue identificado a 1168 cm^{-1}.

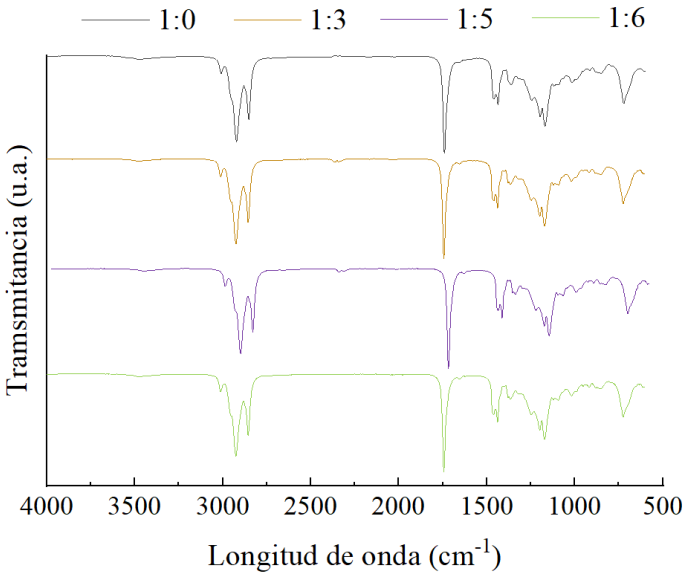

Figura 21. Espectros FTIR de las muestras de FAME purificadas con bentonitas.

En lo referente a la estabilidad térmica de las muestras, se han presentado en la Figura 22 (derecha) las curvas de TGA representativas. Las muestras tratadas con bentonitas exhibieron unas temperaturas de inicio y fin de degradación notablemente más elevadas en comparación con la muestra de FAME sin tratar (Tabla 8). Sin embargo, entre las diferentes muestras tratadas con bentonitas no se apreciaron diferencias destacables.

Por otro lado, en la Figura 22 (izquierda) se ha representado la curva de DSC para la estimación del PP. De forma general, el aumento de la pureza se asocia con una leve mejora en los valores del PP. El mejor resultado fue el presentado por la muestra con relación FAME:bentonitas de 1:6.

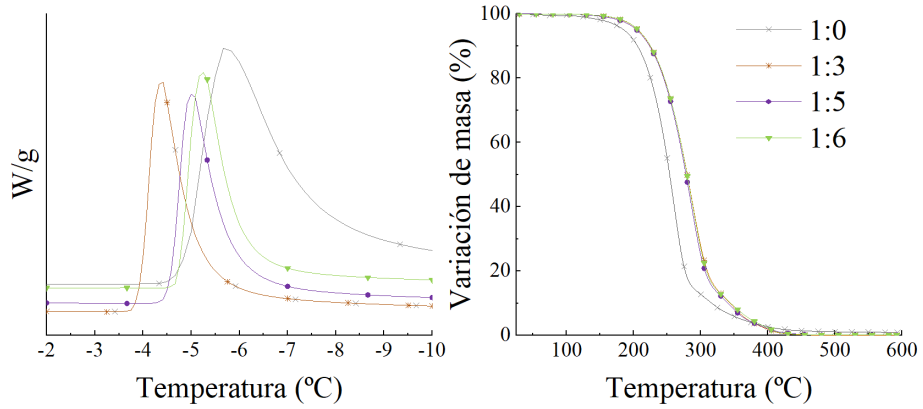

Figura 22. Curvas de DSC para la estimación del PP (izquierda); Curva de TGA para el estudio de la estabilidad térmica (derecha) de las muestras de FAME purificadas con bentonitas.

A la luz de las consideraciones antes mencionadas, se concluyó que la muestra purificada con la relación de FAME:bentonitas de 1:3 representaba la mejor opción para su aplicación como aditivo en un combustible diésel. La decisión se tomó en base a las mínimas diferencias observadas entre las propiedades fisicoquímicas de las muestras tratadas. Además, se optó por la opción más sostenible, que implicaba un menor consumo de bentonitas y menor pérdida de FAME durante el proceso.

6.2. Mezclas FAME – diésel

La muestra seleccionada de FAME purificado de *H. pluvialis* se empleó a tres concentraciones diferentes como aditivo en un combustible diésel. Estas mezclas se prepararon teniendo en cuenta las concentraciones empleadas en estudios previos FAME–diésel [64,65]. En la Figura 20 se muestran las diferentes concentraciones estudiadas, así como imágenes de las mezclas.

6.2.1. Caracterización fisicoquímica de las mezclas FAME–diésel

Tanto las mezclas como los compuestos puros fueron sometidas a una caracterización fisicoquímica, incluyendo las principales propiedades incluidas en la norma para mezclas biodiesel–diésel [66].

Los cambios en la densidad/viscosidad con la temperatura de las mezclas FAME–diésel y los compuestos puros se muestran en la Figura 23. Como se puede observar, la muestra de FAME presentó valores de densidad y viscosidad muy por encima del diésel. Este fenómeno se atribuye a las diferencias en las estructuras moleculares de ambos compuestos. Las cadenas de los ácidos grasos modificados en el derivado de *H. pluvialis* aparecen como largas cadenas lineales de átomos

de carbono con un éster. Esta estructura se caracteriza por tener un peso molecular más alto que el del diésel, lo que tiende a duplicar su viscosidad cinemática [67].

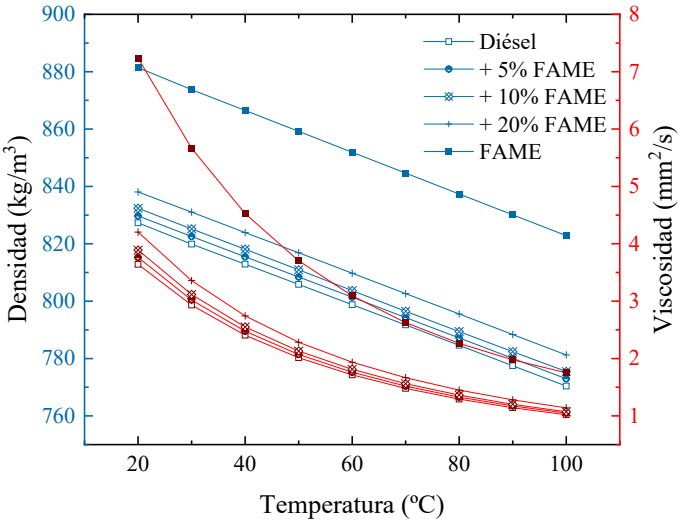

Figura 23. Variación de la densidad y la viscosidad con la temperatura de las mezclas FAME–diésel.

Volviendo a los valores de la Figura 11 del FAME derivado de *H. pluvialis* sin purificar, se observa que tanto la densidad como la viscosidad disminuyeron tras purificar la muestra con bentonitas. La densidad varió de 900 kg/m^3 a 881,4 kg/m^3 a 20 ºC, mientras que la viscosidad de 7,02 mm^2/s a 4,53 mm^2/s. Esto es debido de nuevo a las diferencias en las estructuras moleculares, ya que la astaxantina presenta un peso molecular muy superior al de los FAME.

En la Tabla 9 se presenta un resumen de la caracterización fisicoquímica realizada, donde se incluyen propiedades de interés para el diésel Los valores observados para dichas propiedades cumplieron con la normativa ASTD D7467 para diésel y mezclas biodiesel–diésel (viscosidad entre 1,9 – 4,1 mm^2/s; FP > 52 ºC) [66]. Los valores de LHV y HHV de la muestra de FAME pura resultaron en un 12,28% y 12,45% inferiores a las del diésel. Este hecho se atribuye a un menor contenido de moléculas de hidrógeno y carbono en el FAME, lo que deriva en un menor contenido energético [67]. Las mayores diferencias se encontraron en las medidas del PP, donde la muestra de FAME mostró valor 19 ºC por encima del diésel. En cuanto a la estabilidad térmica, esta se vio beneficiada por el aumento de la concentración de FAME. Por el contrario, las medidas de FP mostraron un comportamiento anómalo. El aumento de la concertación de FAME resultó inicialmente en una reducción del FP, estabilizándose con las adicciones de FAME sucesivas. Esto implica que el FP no se comporta como una propiedad aditiva, y que lideran las características del diésel.

Tabla 9. Propiedades fisicoquímicas de las mezclas FAME–diésel.

Propiedad	Diésel	Porcentaje de FAME			FAME
		+ 5%	+ 10%	+ 20%	
Densidad 20 ºC (kg/m^3)	827,31	829,7	832,4	838,1	881,4
Viscosidad 40 ºC (mm^2/s)	2,407	2,477	2,551	2,743	4,526
FP (ºC)	98	90	83-87	87	180-190
PP (ºC)	–23,35	–22,36	–21,76	–18,44	– 4,30
LHV (MJ/kg)	43,44	43,20	42,72	42,45	38,03
HHV (ºC)	46,03	45,66	45,31	44,83	40,38
T_{onset} (ºC)	114	128	132	138	231
T_{offset} (ºC)	229	257	263	276	325
Lubricidad HFRR 60 ºC (µm)	453	251	239	240	276

6.2.2. Caracterización tribológica de las mezclas FAME–diésel

Las propiedades tribológicas de los compuestos puros y las mezclas se evaluaron mediante el ensayo HFRR. La configuración del ensayo se estableció de acuerdo con las condiciones de la norma para combustible diésel ASTM D6079, mostradas en la Tabla 10 [68].

Tabla 10. Condiciones de ensayo para HFRR según la norma ASTM D6079.

Configuración	
Volumen de muestra (mL)	2 ± 0,2
Longitud de carrera (mm)	1 ± 0,02
Frecuencia (Hz)	50 ± 1
Temperatura (ºC)	60 ± 2
Humedad relativa (%)	30 – 85
Carga (g)	200 ± 1
Duración (min)	75 ± 0,1

Los resultados obtenidos mostrados en la Tabla 9 demuestran que todas las muestras cumplen con el requisito de la norma de lubricidad (WSD < 520 µm). En la Figura 24 se muestran las imágenes de la huella de desgaste generada tanto en la bola como en el disco tras los ensayos. La Figura 25a muestra la variación del COF con la adición de FAME, donde se puede apreciar una reducción del 50% del COF en la muestra + 5% FAME respecto del diésel puro. El valor del COF de la muestra de diésel es típico de un régimen de lubricación límite, mientras que el resto de las muestras presentan valores de lubricación mixta. Un fenómeno similar se observa en el volumen de desgaste del disco en la Figura 25c. La adición del FAME como aditivo a bajas concentraciones provoca una reducción considerable

del desgaste, mostrando la eficacia del FAME derivado de *H. pluvialis* como un excelente aditivo antifricción y antidesgaste.

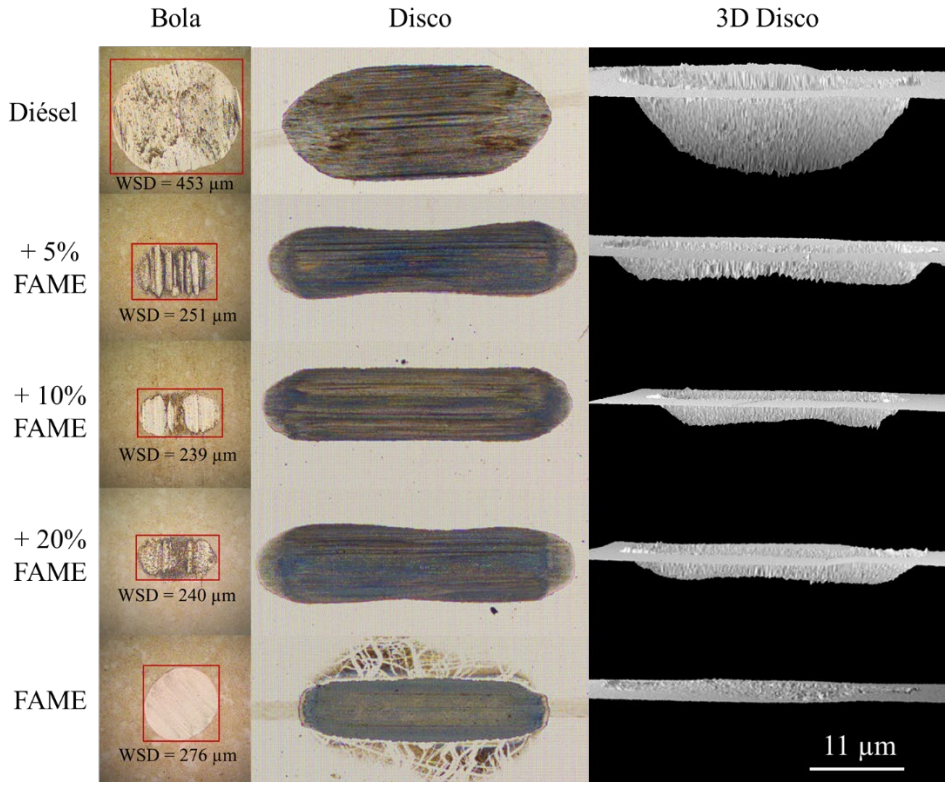

Figura 24. Imágenes de la huella en bola y disco (2D y 3D) de los ensayos tribológicos.

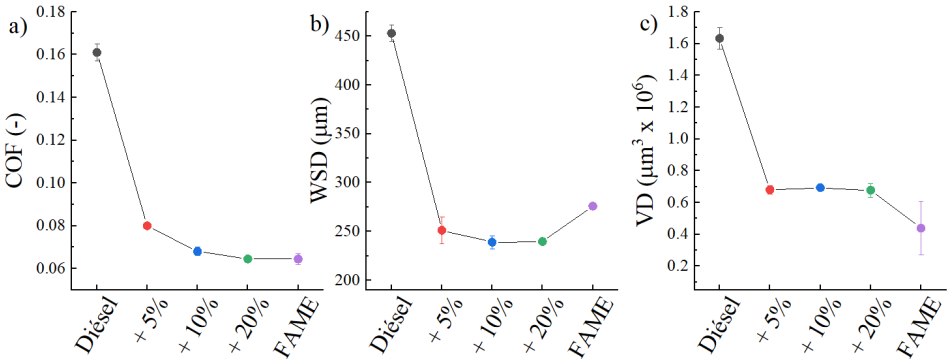

Figura 25. Efecto de la adición de FAME derivado de *H. pluvialis* en un diésel puro en el: a) COF medio; b) desgaste en la bola WSD; c) volumen de desgaste en el disco VD.

La muestra de 5% FAME exhibió una gran reducción del WSD frente al diésel, manteniendo después los valores de WSD constantes para el resto de las mezclas. Este gran comportamiento antidesgaste es atribuible a la presencia de

ácidos grasos de cadena larga y grupos polares que exhiben un comportamiento anfifílico y una excelente relación película/fuerza [69]. Los ésteres metílicos presentes en los aceites modificados son compuestos activos que tienden a concentrarse en la superficie metálica formando finas capas que son adsorbidas. Su adición en el diésel se traduce en un aumento de las moléculas de oxígeno en la mezcla, lo que a su vez facilita los procesos triboquímicos y los cambios en la composición química. Este proceso resulta en la formación de óxidos metálicos en la superficie [70]. Bajas concentraciones de oxígeno facilitan la formación de películas delgadas de óxidos antiadherentes que sirven para reducir el desgaste y la fricción. Sin embargo, concentraciones elevadas pueden resultar en el efecto opuesto, promoviendo una oxidación excesiva y un mayor desgaste [71]. Este fenómeno podría dar explicación al aumento del WSD para el FAME puro.

Tras los ensayos tribológicos las superficies de los discos fueron analizadas mediante SEM/EDX. Los resultados (Figura 26) mostraron una deformación plástica en la marca de desgaste de los discos, que disminuyó con el aumento de la concentración de FAME. El análisis de EDX de la Tabla 11 también indicó que las muestras con FAME presentaban mayor concentración de oxígeno en las superficies. Estos resultados apoyan la teoría de formación de películas de óxido, ayudando a la reducción de la fricción y el desgaste.

Tabla 11. Resultados del análisis de EDX sobre las huellas de desgaste de los discos.

Muestra	Localización	C	O	Cr	Mn	Fe
Diésel	Spectrum 1	5,0	5,4	2,5	0,5	86,5
	Spectrum 2	7,0	6,3	2,1	0,7	83,9
+ 5% FAME	Spectrum 1	5,5	7,2	2,3	0,8	84,2
	Spectrum 2	11,9	9,4	2,2	0,6	75,9
+ 10% FAME	Spectrum 1	6,5	6,6	2,7	0,7	83,5
	Spectrum 2	20,1	6,1	2,6	0,5	70,7
+ 20% FAME	Spectrum 1	7,1	7,3	2,9	0,6	82,1
	Spectrum 2	6,2	5,4	3,1	0,5	84,8
FAME	Spectrum 1	5,1	7,2	2,1	0,6	85,0
	Spectrum 2	7,2	7,5	2,0	0,6	82,7

En base a todos los resultados expuestos, la adición de FAME al diésel supuso una notable mejora en términos de fricción para todas las mezclas. Sin embargo, la muestra con 10% FAME exhibió el mejor comportamiento frente al desgaste. Superada esta concentración aumenta el desgaste en la bola (Figura 24) y las deposiciones en el disco (Figura 26).

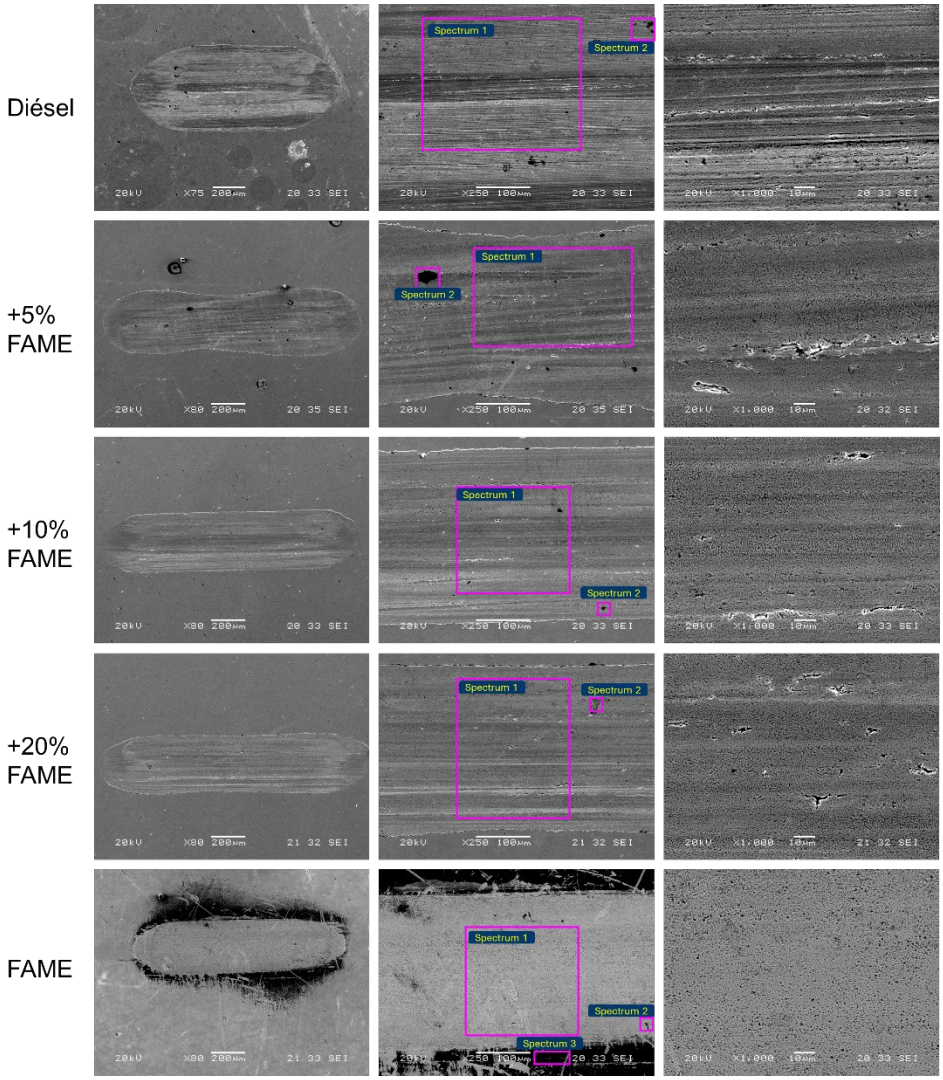

Figura 26. Imágenes del SEM sobre las huellas de desgaste de los discos.

CAPÍTULO 7

7 Análisis técnico-económico del uso de aceites modificados de microalgas

En capítulos anteriores ha sido demostrado el potencial del aceite derivado de *H. pluvialis* como materia prima para la producción de FAME. También han sido verificadas sus propiedades antifricción y antidesgaste tanto puro como en forma de aditivo en mezcla con un combustible diésel. En este capítulo, se evaluará la factibilidad de producir FAME derivado de *H. pluvialis* a escala industrial.

El estudio se basa en un análisis preliminar técnico–económico mediante el empleo del software SuperPro Designer v.9, tomando como referencia las condiciones de ensayo óptimas verificadas en el *Capítulo 3*.

7.1. Descripción del proceso

En la Figura 27 se muestra el diagrama de flujo diseñado para llevar a cabo el análisis. La base de cálculo empleada fue de 30.000 toneladas/año de biomasa residual, procedente del proceso de extracción de astaxantina de *H. pluvialis,* como materia prima.

El proceso se dividió en tres bloques principales: 1) extracción de los lípidos presentes en la biomasa de entrada; 2) producción de FAME de acuerdo con las condiciones óptimas descritas en el *Capítulo 3*; 3) purificación del flujo de glicerol resultante de la reacción de transesterificación como producto secundario. Además, fueron evaluados cuatro escenarios posibles, descritos en la Tabla 12.

Tabla 12. Escenarios evaluados en el estudio técnico–económico.

	Descripción	**Abrev.**
Escenario 1	Producción de FAME y purificación de glicerol empleando centrifugación en las etapas de separación	GPC
Escenario 2	Producción de FAME y purificación de glicerol empleando decantación en las etapas de separación	GPD
Escenario 3	Producción de FAME sin purificación de glicerol, empleando centrifugación en las etapas de separación	NGPC
Escenario 4	Producción de FAME sin purificación de glicerol, empleando decantación en las etapas de separación	NGPD

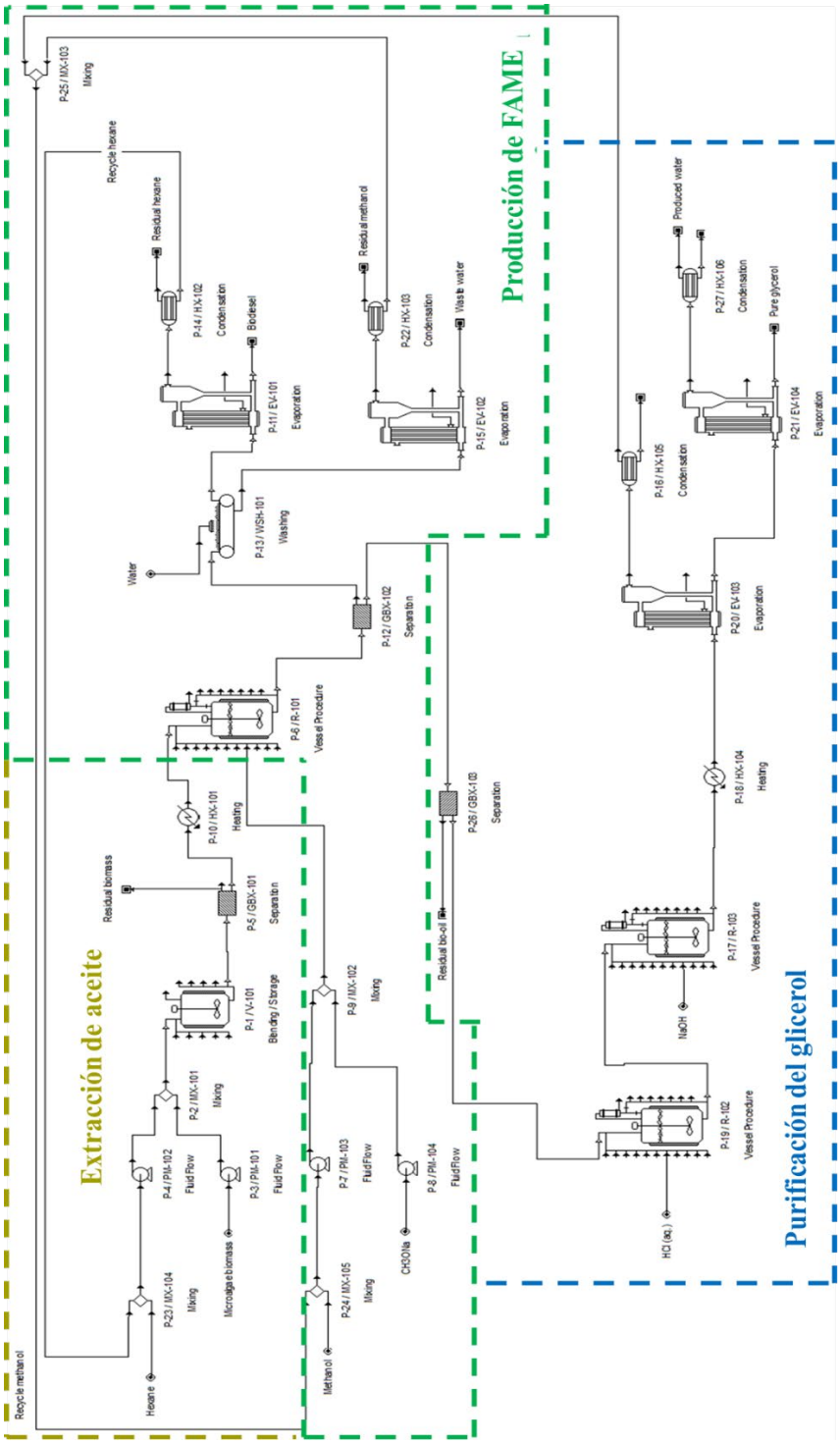

Figura 27. Diagrama de flujo de producción de FAME a partir de residuos de *H. pluvialis* y posterior purificación de glicerol.

Para la extracción del aceite de la biomasa de entrada se seleccionó la extracción con hexano, ya que ha sido reportado como un solvente eficiente en la extracción de lípidos a escala industrial en biomasa derivada de la microalga *Tetraselmis sp.* [72]. Además, se trata de una vía más sostenible en comparación con las extracciones tradicionales con cloroformo.

A continuación, la fase hexano–aceite es separada del resto de la biomasa por diferencia de densidad, y dirigida al tanque de reacción para proceder con la reacción de transesterificación.

Una vez transcurrido el tiempo de reacción, los productos resultantes se separan por diferencia de densidad. El flujo principal (FAME, metanol en exceso, hexano y trazas de catalizador) se deriva a un tanque de lavado donde será lavado con agua hasta alcanzar un pH neutro. Esta etapa elimina los restos de metanol y trazas de catalizador. Finalmente, el hexano será eliminado en una etapa de evaporación.

Por otro lado, la corriente de glicerol residual es purificada en varias etapas: 1) separación de restos de aceite; 2) acidificación con HCl (aq.); 3) neutralización con NaOH; 4) eliminación de agua y metanol por evaporación.

Las principales configuraciones de los procesos y reacciones se encuentran resumidos en la Tabla 13.

Tabla 13. Configuración de los equipos de operación de los procesos incluidos en el diagrama de flujo.

Extracción de aceite	
Extracción con hexano	1,5% (w/v), 2 h
Producción de FAME	
Reacción de transesterificación	$TRI + 3MeOH \leftrightarrow 3FAME + Glicerol$ 80 ºC, 47 min, CH_3ONa 1,5% (w/w)
Purificación de FAME	
Lavado con agua	Hasta pH neutro
Evaporación hexano	Capacidad 0,275 ton/h
Purificación glicerol	
Acidificación	$CH_3ONa + HCl\ (aq) \rightarrow\ MeOH + NaCl$ HCl (35% wt.)
Neutralización	$HCl + NaOH \rightarrow\ NaCl + H_2O$
Evaporación metanol	Capacidad 0,131 kg/h
Evaporación agua	Capacidad 0,338 kg/h

7.2. Simulación y análisis preliminar económico

Para la simulación del proceso se empleó el software SuperPro Designer v.9. Se establecieron las siguientes suposiciones: 1) la materia prima del proceso será biomasa residual del proceso de obtención de astaxantina de *H. pluvialis*; 2) la concentración de aceite en la biomasa de entrada será del 85%; 3) la concentración de triglicéridos en el aceite extraído será del 50%; 4) el 90% de los efluentes de hexano y metanol se recircularán para su reincorporación y reutilización en el proceso; 5) el agua producida durante el proceso de purificación del glicerol será recuperada y reutilizada en el lavado de la corriente de FAME; 6) el producto principal del proceso será el FAME y el producto secundario el glicerol purificado (precio de venta del glicerol puro 1,11 €/kg) [73].

Los flujos anuales y precios empleados para las materias primas del proceso se muestran en la Tabla 14.

Tabla 14. Flujos anuales y precios de las materias primas estipulados en el Mercado Asiático [74].

Material	Precio (€/kg)	Flujo (ton/año)	Material	Precio (€/kg)	Flujo (ton/año)
Hexano	0,56	45.000,00	NaOH	0,26	5,50
Metanol	0,17	3.975,60	Electricidad	0,07 €/kWh	–
Agua	0,185	–	Vapor	8,406 €/Mt	–
CH_3ONa	0,56	60,54	Agua fría	0,28 €/Mt	–
HCl	0,123	45,86			

Los resultados del balance de masa mostraron que la producción anual de FAME fue relativamente consistente en los cuatro escenarios, con una producción anual de 12.810 toneladas/año. Sin embargo, la producción de glicerol si se vio afectada por los procesos de separación. El escenario GPC obtuvo una producción anual de glicerol de 1.420,49 toneladas/año para una pureza del 96,45%, mientras que para GPD fue de 1.443,63 toneladas/año para una pureza del 94,90%. En ausencia de etapas de purificación del glicerol (NGPC y NGPD) se generó una corriente residual con un contenido en glicerol inferior al 50%.

Para el cálculo del UPC, se empleó la Ecuación 3.

$$UPC\ (€/kg) = \frac{Coste\ de\ producción\ anual\ (€/kg)}{Producción\ anual\ de\ FAME\ (kg/año)} \quad (3)$$

Los parámetros económicos más relevantes se presentan en la Tabla 15. Los valores de UPC resultaron entre 0,63 – 0,48 €/kg. Los cuatro casos mostraron valores de UPC competitivos, por debajo de los precios reportados en estudios de índole similar para FAME derivado de aceites de primera y segunda generación que oscilan entre 0,83 – 1,22 €/kg [75–77].

Tabla 15. Resumen del análisis preliminar económico de los cuatro escenarios.

	GPC	GPD	NGPC	NGPD
FCI (€)	7.702.000	8.180.000	4.180.000	3.834.000
UPC (€/kg)	0,63	0,55	0,49	0,48
UPR (€/kg)	0,75	0,67	0,49	0,48
TCI (€)	49.058.000	52.108.000	26.746.000	24.459.000
Coste operativo (€/año)	7.282.000	6.448.000	5.700.000	5.590.000
Ingresos princ. (€/año)	7.321.000	6.392.000	5.694.000	5.578.000
Otros ingresos (€/año)	1.417.514	1.440.598	-	-
Ingresos totales (€/año)	8.739.000	7.832.000	5.694.000	5.578.000
Margen bruto (%)	16,67	17,67	–0,09	–0,22
Rentabilidad de inversión (%)	11,30	11,34	8,85	8,81
Amortización (años)	8,85	8,82	11,30	11,34
TIR (después de impuestos %)	11,64	10,39	7,11	8,05

*FCI: coste de capital fijo; UPR: ingresos unitarios de producción; TCI: inversión de capital total; TIR: tasa interna de retorno.

El uso de decantación en vez de centrifugación como tecnología de separación favoreció la reducción del UPC, siendo este efecto más pronunciado en los escenarios GPC y GPD debido al mayor número de fases de separación al incluir la purificación del glicerol en el proceso (Figura 28).

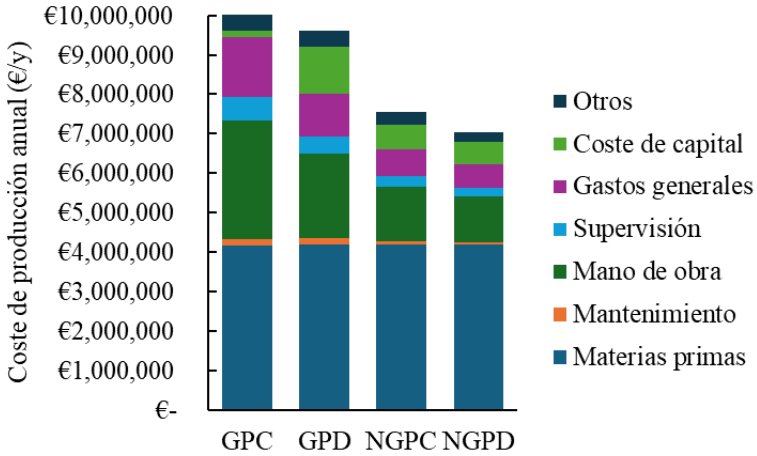

Figura 28. Distribución del coste de producción anual para cada escenario.

A la hora de seleccionar estas tecnologías habría que tener en cuenta las prioridades industriales, ya que la centrifugación permite trabajar con tiempos de separación menores.

La exclusión del proceso de purificación del glicerol implicó un ahorro económico en términos de compra y mantenimiento de equipos, mano de obra, supervisión y consumos energéticos. Sin embargo, se pierde los ingresos correspondientes a la venta del glicerol.

7.3. Análisis de rentabilidad

Para el análisis de rentabilidad se fijó el año de construcción en 2024, con un período de construcción de 30 meses, 3 meses de puesta en marcha y una vida útil de proyecto de 30 años. La tasa de inflación se estableció en el 4%, siendo los valores del VAN bajo, medio y alto del 7%, 9% y 11%, respectivamente. Para los costes financiados se estableció un plazo de préstamo de 10 años con tipo de interés al 5%. La distribución del desembolso del flujo de fondos descontados fue: 30% el primer año, 40% el segundo año y 30% el tercer año. El plazo de préstamos para el capital de explotación, I+D y regalías, se fijó a 6 años, con tipos de interés del 12%, 10% y 10%, respectivamente.

La Figura 29 muestra el análisis de rentabilidad utilizando el diagrama de flujo de caja acumulado durante los 30 años de vida de la planta.

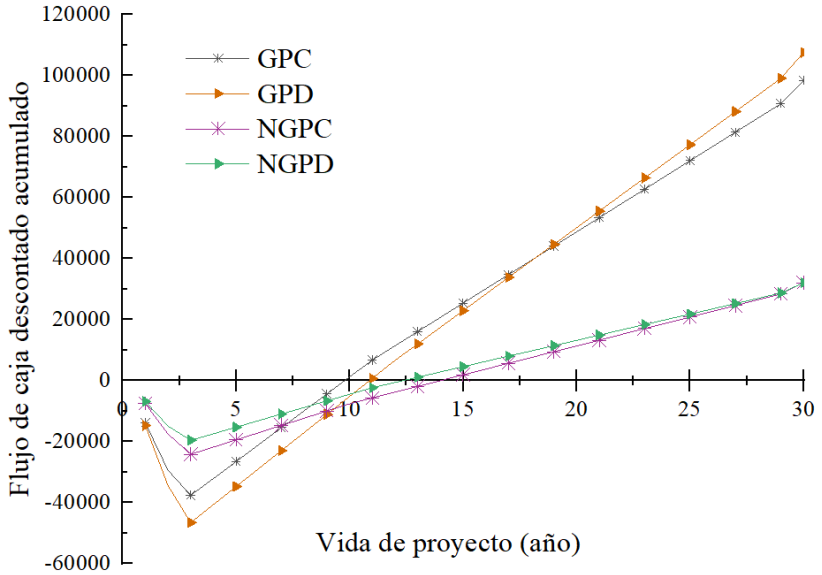

Figura 29. Análisis de rentabilidad del coste de producción de FAME mediante diagrama de flujo de caja acumulado.

Los escenarios GPC y GPD presentan los valores de flujo de caja acumulado más bajos en los primeros 5 años, especialmente GPD. Esto se debe a la mayor inversión inicial necesaria por la implantación del proceso de purificación de glicerol. Sin embargo, los valores de UPR asociados a las ventas del glicerol purificado producen un rápido crecimiento a largo plazo y tiempos recuperación de la inversión significativamente más cortos en comparación con NGPC y NGPD (Tabla 15).

Los escenarios sin purificación de glicerol experimentan una caída inicial leve, pero depender únicamente de los ingresos procedentes de la venta de FAME deriva en un lento crecimiento a largo plazo. Esto se traduce en un flujo de caja acumulado a final de la vida del proyecto hasta un 50% menor que GPC y GPD. Este hecho resalta el potencial de la valorización de productos segundarios y/o desechos en los procesos industriales

En cuanto a las diferencias entre las técnicas de separación, el uso de centrifugación en vez de decantación reduce el tiempo de recuperación de inversión. Este suceso es más visible en GPC por el mayor número de etapas de separación en el proceso. Sin embargo, con el paso de los años el flujo de caja de GPD sobrepasa ligeramente los de GPC. Este hecho solo es relevante para proyectos con periodos de vida largos. Como se comentaba anteriormente, la selección de una tecnología u otra dependerá de los intereses de cada industria.

CAPÍTULO 8

8 Conclusiones y líneas futuras

8.1. Conclusiones

En la presente tesis doctoral se han obtenido dos biolubricantes (mezclas de FAMEs) derivados de las microalgas *N. gaditana* y *H. pluvialis*. Estos biolubricantes han sido caracterizados fisicoquímica y tribológicamente. Tras analizar los resultados de estos estudios, se decidió continuar la investigación solo con el biolubricante derivado de *H. pluvialis*. Este fue purificado mediante el uso de bentonitas y aplicado como aditivo en un combustible diésel. Finalmente, se realizó un estudio técnico–económico para evaluar la rentabilidad de la producción del biolubricante derivado de *H. pluvialis* a escala industrial. Atendiendo a los distintos apartados de la investigación, ha sido posible llegar a las siguientes conclusiones:

En el marco del trabajo desarrollado en los *Capítulos 3* y *4* referente a la optimización de la reacción de transesterificación para la obtención del máximo contenido de FAME y su caracterización fisicoquímica, se han obtenido las siguientes conclusiones:

- Los aceites derivados de las microalgas *N. gaditana* y *H. pluvialis* presentaron perfiles lipídicos muy diferentes. Dichos perfiles influenciaron de forma directa en las condiciones óptimas de la reacción de transesterificación.
- La reacción de transesterificación del aceite de la microalga de *N. gaditana* resultó dominada por el ratio bioaceite:alcohol, favorecida a valores altos. Sin embargo, la reacción de transesterificación del aceite de microalga de *H. pluvialis* resultó dominada por el tiempo de reacción, favorecida por tiempos cortos.
- La optimización de las reacciones de transesterificación con *N. gaditana* y *H. pluvialis* han demostrado que no es necesario el uso de condiciones supercríticas para la eficiente producción de FAME en microalgas.
- Los **FAMEs de microalgas estudiados** resultaron en **propiedades fisicoquímicas mejoradas** (estabilidad térmica, PP y FP) en comparación con aceites de primera y segunda generación. Esto se debe **longitud de cadena más largas** y **mayor grado de insaturación**, especialmente en PP.

- No se apreciaron diferencias significativas entre las propiedades fisicoquímicas de ambas mezclas de FAMEs.

Del estudio de las propiedades tribológicas de las muestras de FAME descrito en el *Capítulo 5* se pudo concluir lo siguiente:

- La mezcla de FAMEs derivada de ***H. pluvialis*** presentó un **mejor comportamiento antifricción y antidesgaste** en comparación con la de *N. gaditana*, así como una **mejor estabilidad** con la **variación de la temperatura**.
- La lubricación con ambas mezclas de FAMEs resultó en mecanismos de desgaste por adhesión y deformación plástica.
- La longitud de cadena media y el alto contenido de C20:5 en la muestra de *N. gaditana* promovieron un peor comportamiento tribológico.
- Se detectó la formación de tribocapas de óxidos metálicos generadas por la reacción entre las superficies metálicas y la fase polar de los FAMEs (ésteres).
- Las tribocapas generadas por las muestras de *H. pluvialis* presentaron **mayor concentración de oxígeno**, con un mayor espesor de película y **mejor comportamiento frente a la fricción y el desgaste**.

Evaluando los resultados obtenidos de la purificación de la mezcla de FAMEs derivada de *H. pluvialis* y su aplicación como aditivo a bajas concentración en un combustible diésel en el *Capítulo 6*, las principales conclusiones son:

- La purificación con bentonitas alcanzó una reducción de impurezas del 20% en los FAMEs derivados de *H. pluvialis*.
- La **eliminación de astaxantina permitió reducir la densidad** del FAME de 900 kg/m^3 a 881,4 kg/m^3, y la viscosidad de 7,02 mm^2/s a 4,53 mm^2/s.
- No se apreciaron diferencias destacables en las propiedades fisicoquímicas entre las diferentes muestras de FAME purificadas con bentonitas.
- El **FAME purificado de *H. pluvialis*** demostró un **excelente comportamiento antifricción y antidesgaste como aditivo** en el combustible diésel.
- Todas las mezclas cumplieron con las limitaciones establecidas por la normativa para mezclas biodiesel–diésel.
- La mezcla + 5% FAME consiguió reducir el desgaste y la fricción en un 44,6% y 50%, respectivamente.
- La **mezcla + 10% FAME** exhibió las **mejores propiedades tribológicas**.

Finalmente, el análisis preliminar técnico–económico realizado en el *Capítulo 7* para evaluar la viabilidad a escala industrial de producción de biolubricante a partir de *H. pluvialis* aportó las siguientes conclusiones:

- Los **costes unitarios de producción** de FAME pudieron reducirse hasta **0,48 €/kg** con la venta de glicerol como producto secundario.
- La **explotación de *H. pluvialis*** para la producción de FAME presentó ser una **alternativa viable en la revalorización de residuos** generados en la industria de microalgas.
- La clave en la **viabilidad del proyecto** residió en la implantación de **estrategias de economía circular** para la revalorización de residuos.
- La venta del glicerol purificado implicó un aumento de los ingresos anuales del 53,5%.

8.2. Líneas futuras

Una vez analizados los resultados obtenidos a lo largo de la presente tesis, se propone abordar las siguientes líneas fututas de trabajo:

- Utilizar nuevas cepas de microalgas que presenten contenido de triglicéridos superiores. Esto permitirá obtener productos más puros tras la reacción de transesterificación, así como mejores rentabilidades a escala industrial.
- Analizar la estabilidad oxidativa de los biolubricantes derivados de microalgas. En función de los resultados, implantar la técnica de epoxidación para la obtención de biolubricantes mejorados.
- Explorar la aplicación de estos biolubricantes en distintas aplicaciones.
- Explorar la posibilidad de realizar dobles transesterificaciones en aceites derivados de microalga.
- Evaluar los aspectos medioambientales a través de un análisis de emisiones de CO_2 equivalente.

Bibliografía

[1] Global Carbon Project (GCP). Available online: https://www.globalcarbonproject.org/ (accessed on 19 January 2023).

[2] Nowak P, Kucharska K, Kamiński M. Ecological and health effects of lubricant oils emitted into the environment. Int J Environ Res Public Health 2019;16:3002. https://doi.org/10.3390/ijerph16163002.

[3] Torbacke, M.; Rudolphi, Å.K.; Kassfeldt, E. Lubricants: Introduction to Properties and Performance, 1st ed.; John Wiley and Sons: Hoboken, NJ, USA, 2014; ISBN 978-1-118-79974-1.

[4] UNE-EN 16807:2017; Liquid Petroleum Products—Bio-Lubricants—Criteria and Requirements of Bio-Lubricants and Bio-Based Lubricants. UNE: Madrid, Spain, 2017.

[5] Farfan-Cabrera LI, Franco-Morgado M, González-Sánchez A, Pérez-González J, Marín-Santibáñez BM. Microalgae Biomass as a New Potential Source of Sustainable Green Lubricants. Molecules 2022;27:1205. https://doi.org/10.3390/molecules27041205.

[6] Sanjurjo C, Rodríguez E, Viesca JL, Battez AH. Influence of Molecular Structure on the Physicochemical and Tribological Properties of Biolubricants: A Review. Lubricants 2023;11:380. https://doi.org/10.3390/lubricants11090380.

[7] Shaah MAH, Hossain MS, Allafi FAS, Alsaedi A, Ismail N, Kadir MOA, et al. A review on non-edible oil as a potential feedstock for biodiesel: physicochemical properties and production technologies. RSC Adv 2021;11:25018–37. https://doi.org/10.1039/d1ra04311k.

[8] Brahma S, Nath B, Basumatary B, Das B, Saikia P, Patir K, et al. Biodiesel production from mixed oils: A sustainable approach towards industrial biofuel production. Chemical Engineering Journal Advances 2022;10:100284. https://doi.org/10.1016/j.ceja.2022.100284.

[9] Aron NSM, Khoo KS, Chew KW, Show PL, Chen WH, Nguyen THP. Sustainability of the four generations of biofuels – A review. Int J Energy Res 2020;44:9266–82. https://doi.org/10.1002/er.5557.

[10] Mathimani T, Mallick N. A comprehensive review on harvesting of microalgae for biodiesel - Key challenges and future directions.

Renewable and Sustainable Energy Reviews 2018;91:1103–20. https://doi.org/10.1016/j.rser.2018.04.083.

[11] Contreras-Gallegos E, Domínguez-Pacheco FA, Hernández-Aguilar C, Bedoya A, Alvarado S, Marín E, et al. Study of Mineral-Based oils with Jatropha curcas L. as Bio-Additive Through Thermal and Kinematic Viscosity Properties. Int J Thermophys 2022;43. https://doi.org/10.1007/s10765-021-02932-8.

[12] Gallardo-Hernández EA, Lara-Hernández G, Nieto-Camacho F, Domínguez-Pacheco A, Cruz-Orea A, Hernández-Aguilar C, et al. Thermal and Tribological Properties of Jatropha Oil as Additive in Commercial Oil. Int J Thermophys 2017;38. https://doi.org/10.1007/s10765-017-2185-y.

[13] Singh N, Agarwal P, Porwal SK. Natural Antioxidant Extracted Waste Cooking Oil as Sustainable Biolubricant Formulation in Tribological and Rheological Applications. Waste Biomass Valorization 2022;13:3127–37. https://doi.org/10.1007/s12649-022-01745-6.

[14] Sanjurjo C, Rivera N, Rodríguez E, Fernández A, Hernández A. Biodiesel derived from the microalgae *Nannochloropsis gaditana* and *Haematococcus pluvialis*: Physicochemical and tribological properties. J Mol Liq 2024;408:125391. https://doi.org/10.1016/j.molliq.2024.125391.

[15] Azad AK, Sharma SC, Saul MG. Clean Energy for Sustainable Development : Comparisons and Contrasts of New Approaches. Academic Press: Cambridge, MA, USA, 2016; ISBN 9780128054239

[16] Nogales-Delgado S, Martín JME. Cardoon biolubricant through double transesterification: Assessment of its oxidative, thermal and storage stability. Mater Lett 2021;302:130454. https://doi.org/10.1016/j.matlet.2021.130454.

[17] Encinar JM, Nogales S, González JF. Biodiesel and biolubricant production from different vegetable oils through transesterification. Engineering Reports 2020;2:e12190. https://doi.org/10.1002/eng2.12190.

[18] Nogales-Delgado S, Sánchez N, Encinar JM. Valorization of cynara Cardunculus L. Oil as the basis of a biorefinery for biodiesel and biolubricant production. Energies (Basel) 2020;13:5085. https://doi.org/10.3390/en13195085.

[19] Encinar JM, Nogales-Delgado S, Pinilla A. Biolubricant production through double transesterification: Reactor design for the implementation

of a biorefinery based on rapeseed. Processes 2021;9:1224. https://doi.org/10.3390/pr9071224.

[20] Encinar JM, Nogales-Delgado S, Álvez-Medina CM. High oleic safflower biolubricant through double transesterification with methanol and pentaerythritol: Production, characterization, and antioxidant addition. Arabian Journal of Chemistry 2022;15:103796. https://doi.org/10.1016/j.arabjc.2022.103796.

[21] Hoong SS, Arniza MZ, Mariam NMDNS, Armylisas AHN, Yeong SK. Synthesis and physicochemical properties of novel lauric acid capped estolide esters and amides made from oleic acid and their evaluations for biolubricant basestock. Ind Crops Prod 2019;140:111653. https://doi.org/10.1016/j.indcrop.2019.111653.

[22] Singh Y, Abd Rahim E. Michelia Champaca: Sustainable novel non-edible oil as nano based bio-lubricant with tribological investigation. Fuel 2020;282:118830. https://doi.org/10.1016/j.fuel.2020.118830.

[23] Miao X, Wu Q. Biodiesel production from heterotrophic microalgal oil. Bioresour Technol 2006;97:841–6. https://doi.org/10.1016/j.biortech.2005.04.008.

[24] Al-Humairi ST, Lee JGM, Harvey AP. Direct and rapid production of biodiesel from algae foamate using a homogeneous base catalyst as part of an intensified process. Energy Conversion and Management: X 2022;16. https://doi.org/10.1016/j.ecmx.2022.100284.

[25] Al-Humairi ST, Lee JGM, Salihu M, Harvey AP. Biodiesel Production through Acid Catalyst In Situ Reactive Extraction of Chlorella vulgaris Foamate. Energies (Basel) 2022;15:4482. https://doi.org/10.3390/en15124482.

[26] Johnson MB, Wen Z. Production of biodiesel fuel from the microalga schizochytrium limacinum by direct transesterification of algal biomass. Energy and Fuels 2009;23:5179–83. https://doi.org/10.1021/ef900704h.

[27] Macías-Sánchez MD, Robles-Medina A, Hita-Peña E, Jiménez-Callejón MJ, Estéban-Cerdán L, González-Moreno PA, et al. Biodiesel production from wet microalgal biomass by direct transesterification. Fuel 2015;150:14–20. https://doi.org/10.1016/j.fuel.2015.01.106.

[28] Torres S, Acien G, García-Cuadra F, Navia R. Direct transesterification of microalgae biomass and biodiesel refining with vacuum distillation. Algal Res 2017;28:30–8. https://doi.org/10.1016/j.algal.2017.10.001.

[29] Tang Y, Rosenberg JN, Betenbaugh MJ, Wang F. Optimization of one-step in situ transesterification method for accurate quantification of epa in nannochloropsis gaditana. Applied Sciences (Switzerland) 2016;6:343. https://doi.org/10.3390/app6110343.

[30] Jazzar S, Olivares-Carrillo P, de los Ríos AP, Marzouki MN, Acién-Fernández FG, Fernández-Sevilla JM, et al. Direct supercritical methanolysis of wet and dry unwashed marine microalgae (Nannochloropsis gaditana) to biodiesel. Appl Energy 2015;148:210–9. https://doi.org/10.1016/j.apenergy.2015.03.069.

[31] Macías-Sánchez MD, Robles-Medina A, Jiménez-Callejón MJ, Hita-Peña E, Estéban-Cerdán L, González-Moreno PA, et al. Optimization of biodiesel production from wet microalgal biomass by direct transesterification using the surface response methodology. Renew Energy 2018;129:141–9. https://doi.org/10.1016/j.renene.2018.06.001.

[32] Xu H, Miao X, Wu Q. High quality biodiesel production from a microalga Chlorella protothecoides by heterotrophic growth in fermenters. J Biotechnol 2006;126:499–507. https://doi.org/10.1016/j.jbiotec.2006.05.002.

[33] Cerón-García MC, Macías-Sánchez MD, Sánchez-Mirón A, García-Camacho F, Molina-Grima E. A process for biodiesel production involving the heterotrophic fermentation of Chlorella protothecoides with glycerol as the carbon source. Appl Energy 2013;103:341–9. https://doi.org/10.1016/j.apenergy.2012.09.054.

[34] Zorn SMFE, da Silva APT, Bredda EH, Bento HBS, Pedro GA, Carvalho AKF, et al. In Situ Transesterification of Microbial Biomass for Biolubricant Production Catalyzed by Heteropolyacid Supported on Niobium. Energies (Basel) 2022;15:1591. https://doi.org/10.3390/en15041591.

[35] Mohamadzadeh Shirazi H, Karimi-Sabet J, Ghotbi C. Biodiesel production from Spirulina microalgae feedstock using direct transesterification near supercritical methanol condition. Bioresour Technol 2017;239:378–86. https://doi.org/10.1016/j.biortech.2017.04.073.

[36] Da Silva APT, Bredda EH, de Castro HF, Da Rós PCM. Enzymatic catalysis: An environmentally friendly method to enhance the transesterification of microalgal oil with fusel oil for production of fatty acid esters with potential application as biolubricants. Fuel 2020;273:117786. https://doi.org/10.1016/j.fuel.2020.117786.

[37] Cheah MY, Ong HC, Zulkifli NWM, Masjuki HH, Salleh A. Physicochemical and tribological properties of microalgae oil as biolubricant for hydrogen-powered engine. Int J Hydrogen Energy 2020;45:22364–81. https://doi.org/10.1016/j.ijhydene.2019.11.020.

[38] Khan S, Das P, Radwan AB, Thaher M, Abdulquadir M, Faisal M, et al. Biolubricant Synthesis by Additization and Chemical Modification from Lipid-Rich Brackish Coelastrella sp. Using a Biorefinery Approach. ACS Sustain Chem Eng 2024;12:7289–99. https://doi.org/10.1021/acssuschemeng.3c08324.

[39] Chukhutsina VU, Fristedt R, Morosinotto T, Croce R. Photoprotection strategies of the alga Nannochloropsis gaditana. Biochim Biophys Acta Bioenerg 2017;1858:544–52. https://doi.org/10.1016/j.bbabio.2017.05.003.

[40] Castejón N, Marko D. Fatty Acid Composition and Cytotoxic Activity of Lipid Extracts from Nannochloropsis gaditana Produced by Green Technologies. Molecules 2022;27:3710. https://doi.org/10.3390/molecules27123710.

[41] Matos ÂP, Feller R, Moecke EHS, Sant'Anna ES. Biomass, lipid productivities and fatty acids composition of marine Nannochloropsis gaditana cultured in desalination concentrate. Bioresour Technol 2015;197:48–55. https://doi.org/10.1016/j.biortech.2015.08.041.

[42] Mularczyk M, Michalak I, Marycz K. Astaxanthin and other nutrients from haematococcus pluvialis—Multifunctional applications. Mar Drugs 2020;18:459. https://doi.org/10.3390/md18090459.

[43] Nishshanka GKSH, Liyanaarachchi VC, Nimarshana PHV, Ariyadasa TU, Chang JS. Haematococcus pluvialis: A potential feedstock for multiple-product biorefining. J Clean Prod 2022;344:131103. https://doi.org/10.1016/j.jclepro.2022.131103.

[44] Otero P, Saha SK, Gushin JM, Moane S, Barron J, Murray P. Identification of optimum fatty acid extraction methods for two different microalgae Phaeodactylum tricornutum and Haematococcus pluvialis for food and biodiesel applications. Anal Bioanal Chem 2017;409:4659–67. https://doi.org/10.1007/s00216-017-0412-9.

[45] Damiani MC, Popovich CA, Constenla D, Leonardi PI. Lipid analysis in Haematococcus pluvialis to assess its potential use as a biodiesel

feedstock. Bioresour Technol 2010;101:3801–7. https://doi.org/10.1016/j.biortech.2009.12.136.

[46] Foroutan R, Esmaeili H, Mousavi SM, Hashemi SA, Yeganeh G. The physical properties of biodiesel-diesel fuel produced via transesterification process from different oil sources. Physical Chemistry Research 2019;7:415–24. https://doi.org/10.22036/pcr.2019.173224.1600.

[47] Suherman S, Abdullah I, Sabri M, Silitonga AS. Evaluation of Physicochemical Properties Composite Biodiesel from Waste Cooking Oil and Schleichera oleosa Oil. Energies (Basel) 2023;16:5771. https://doi.org/10.3390/en16155771.

[48] Knothe G, Steidley KR. Kinematic viscosity of biodiesel fuel components and related compounds. Influence of compound structure and comparison to petrodiesel fuel components. Fuel 2005;84:1059–65. https://doi.org/10.1016/j.fuel.2005.01.016.

[49] Bahubali C, Gopalan A. Improving biodiesel's properties. Digital Refining Proce 2019:1–5. https://www.digitalrefining.com/article/1002283/improving-biodiesels-properties Accessed 17 July 2024

[50] Jain S, Sharma MP. Application of thermogravimetric analysis for thermal stability of Jatropha curcas biodiesel. Fuel 2012;93:252–7. https://doi.org/10.1016/j.fuel.2011.09.002.

[51] Alves CT, Peters MA, Onwudili JA. Application of thermogravimetric analysis method for the characterisation of products from triglycerides during biodiesel production. J Anal Appl Pyrolysis 2022;168:105766. https://doi.org/10.1016/j.jaap.2022.105766.

[52] Kubar AA, Ali A, Kumar S, Huo S, Ullah MW, Alabbosh KFS, et al. Dynamic Foam Characteristics during Cultivation of Arthrospira platensis. Bioengineering 2022;9:257. https://doi.org/10.3390/bioengineering9060257.

[53] Van der Waal G. The relationship between the chemical structure of ester base fluids and their influence on elastomer seals, and wear characteristics, J. Synth. Lubr. 1984;1:280–301. https://doi.org/10.1002/jsl.3000010404

[54] Wang W, Shen B, Li Y, Ni Q, Zhou L, Du F. Friction reduction mechanism of glycerol monooleate-containing lubricants at elevated

temperature - transition from physisorption to chemisorption. Sci Prog 2021;104:1-15. https://doi.org/10.1177/0036850421998529.

[55] Lubricant Additives Chemistry and Applications Second Edition, CRC, Boca Raton, 2009.

[56] Adhvaryu A, Biresaw G, Sharma BK, Erhan SZ. Friction behavior of some seed oils: Biobased lubricant applications. Ind Eng Chem Res 2006;45:3735–40. https://doi.org/10.1021/ie051259z.

[57] Simič R, Kalin M. Adsorption mechanisms for fatty acids on DLC and steel studied by AFM and tribological experiments. Appl Surf Sci 2013;283:460–70. https://doi.org/10.1016/j.apsusc.2013.06.131.

[58] Mangolini F, Rossi A, Spencer ND. Influence of metallic and oxidized iron/steel on the reactivity of triphenyl phosphorothionate in oil solution. Tribol Int 2011;44:670–83. https://doi.org/10.1016/j.triboint.2010.02.009.

[59] Xu Y, Hu X, Yuan K, Zhu G, Wang W. Friction and wear behaviors of catalytic methylesterified bio-oil. Tribol Int 2014;71:168–74. https://doi.org/10.1016/j.triboint.2013.11.018.

[60] Xu Y, Zheng X, Hu X, Dearn KD, Xu H. Effect of catalytic esterification on the friction and wear performance of bio-oil. Wear 2014;311:93–100. https://doi.org/10.1016/j.wear.2013.12.029.

[61] Das T, Saikia BK, Dekaboruah HP, Bordoloi M, Neog D, Bora JJ, et al. Blue-fluorescent and biocompatible carbon dots derived from abundant low-quality coals. J Photochem Photobiol B 2019;195:1–11. https://doi.org/10.1016/j.jphotobiol.2019.04.004.

[62] Kelechukwu C, Akarante O. Removal of Colorants Using Locally Activated Bentonite Clay: A Review. Journal of Environmental Science 2021;15:1-14. http://doi.org/10.9790/2402-1509030114

[63] Zheng R, Gao H, Ren Z, Cen D, Chen Z. Preparation of activated bentonite and its adsorption behavior on oil-soluble green pigment. Physicochemical Problems of Mineral Processing 2017;53:829–45. https://doi.org/10.5277/ppmp170213.

[64] Alviso D, Saab E, Clevenot P, Romano SD. Flash point, kinematic viscosity and refractive index: variations and correlations of biodiesel–diesel blends. Journal of the Brazilian Society of Mechanical Sciences and Engineering 2020;42:347. https://doi.org/10.1007/s40430-020-02428-w.

[65] Fazal MA, Haseeb ASMA, Masjuki HH. Investigation of friction and wear characteristics of palm biodiesel. Energy Convers Manag 2013;67:251–6. https://doi.org/10.1016/j.enconman.2012.12.002.

[66] ASTM D7467-17. Standard Specification for Diesel Fuel Oil, Biodiesel Blend (B6 to B20), 2017. https://doi.org/10.1520/D7467-17.

[67] Hoekman SK, Broch A, Robbins C, Ceniceros E, Natarajan M. Review of biodiesel composition, properties, and specifications. Renewable and Sustainable Energy Reviews 2012;16:143–69. https://doi.org/10.1016/j.rser.2011.07.143.

[68] ASTM D6079-22. Standard Test Method for Evaluating Lubricity of Diesel Fuels by the High-Frequency Reciprocating Rig (HFRR), 2022.

[69] Zewdie H, Tibba GS, Zeleke DS, Perumal V, Remedios Castañeiras PD. A Review on the Impact of Bio-Additives on Tribological Behavior of Diesel Fuels. Advances in Tribology 2024;2024:15. https://doi.org/10.1155/2024/5530337.

[70] Fathurrahman NA, Auzani AS, Zaelani R, Anggarani R, Aisyah L, Maymuchar, et al. Lubricity Properties of Palm Oil Biodiesel Blends with Petroleum Diesel and Hydrogenated Vegetable Oil. Lubricants 2023;11:176. https://doi.org/10.3390/lubricants11040176.

[71] Kuszewski H, Jaworski A, Ustrzycki A. Lubricity of ethanol–diesel blends – Study with the HFRR method. Fuel 2017;208:491–8. https://doi.org/10.1016/j.fuel.2017.07.046.

[72] Wan Mahmood WMA, Theodoropoulos C, Gonzalez-Miquel M. Enhanced microalgal lipid extraction using bio-based solvents for sustainable biofuel production. Green Chemistry 2017;19:5723–33. https://doi.org/10.1039/c7gc02735d.

[73] Dias da Silva Ruy A, Luíza Freitas Ferreira A, Ésio Bresciani A, Maria de Brito Alves R, Antônio Magalhães Pontes L. Market Prospecting and Assessment of the Economic Potential of Glycerol from Biodiesel. Biotechnological Applications of Biomass, IntechOpen; 2021, p. 1–19. https://doi.org/10.5772/intechopen.93965.

[74] Business Anaytiq. Price index: Affordable market trend data & online tools to create benchmarks and leading indicators. https://businessanalytiq.com/ (accessed March 10, 2024).

[75] Apostolakou AA, Kookos IK, Marazioti C, Angelopoulos KC. Techno-economic analysis of a biodiesel production process from vegetable oils. Fuel Processing Technology 2009;90:1023–31. https://doi.org/10.1016/j.fuproc.2009.04.017.

[76] Cho HJ, Kim JK, Cho HJ, Yeo YK. Techno-economic study of a biodiesel production from palm fatty acid distillate. Ind Eng Chem Res 2013;52:462–8. https://doi.org/10.1021/ie301651b.

[77] Yusuf NNAN, Kamarudin SK. Techno-economic analysis of biodiesel production from Jatropha curcas via a supercritical methanol process. Energy Convers Manag 2013;75:710–7. https://doi.org/10.1016/j.enconman.2013.08.017.

Publicaciones

Factor de impacto

Esta sección presenta la información principal referente a las revistas donde han sido publicados los artículos científicos de la presente tesis doctoral. Las referencias completas de las revistas, las cuales se encuentran indexadas en el *Science Citation Index* (SCI), así como su factor de impacto (IF) y el cuartil donde se ubican según el Journal Citation Reports (JCR) aparecen recogidos en la siguiente tabla.

Publicación	Revista	Editorial	IF	Cuartil y categoría
[I]	Lubricants	MDPI	3.5	Q2 Engineering, Mechanical (47/180)
[II]	Biomass and Bioenergy	Elsevier	5.8	Q1 Biotechnolog& Applied Microbiology (24/174)
[III]	Journal of Molecular Liquids	Elsevier	5.3	Q1 Physics, Atomic, Molecular & Chemical (6/40)
[IV]	BioEnergy Research	Springer	3.1	Q2 Environmental Sciences (167/358)

Todos estos artículos han sido publicados en acceso abierto.

La publicación I cuenta con 6 citas en Scopus. De acuerdo con Dimensions (https://badge.dimensions.ai/details/id/pub.1163930537/categories) estas citas provienen de distintos ámbitos (40% de Ingeniería, 28.57% de Ciencias Químicas, 14.29% de Agricultura, Veterinaria y Ciencias de los Alimentos y 14.29% Ciencias Biológicas), lo que demuestra el interés para distintas áreas de conocimiento. Esta publicación ha sido visualizada en 40 ocasiones en el repositorio de la Universidad de Oviedo (https://digibuo.uniovi.es/dspace/handle/10651/71713), principalmente desde China, USA y España. Por último, esta publicación tiene 23 visualizaciones y 15 descargas en el repositorio generalista Zenodo (https://zenodo.org/records/10657579).

La publicación II cuenta con 2 citas en Scopus, lo cual la sitúa en el percentil 92, lo que significa que se encuentra entre el 8% de los más citados de acuerdo con el año de publicación y su especialidad. Además, su índice FWCI es de 3.62,

lo que significa que ha sido citado casi 4 veces más que la media de su especialidad.

El trabajo realizado en las publicaciones II y IV se alinean con el Objetivo de Desarrollo Sostenible (ODS) 7: Energía asequible y no contaminante. De forma indirecta, el uso de microalgas en las publicaciones II, III e IV, también se relacionan de forma indirecta con los objetivos establecidos en el ODS 2 (Hambre cero), ODS 15 (vida y tierra), ODS 6 (agua limpia y saneamiento) y ODS 13 (acción por el clima).

Publicación I

MDPI 2023

Claudia Sanjurjo, Rodríguez E, Viesca JL, Battez AH. Influence of Molecular Structure on the Physicochemical and Tribological Properties of Biolubricants: A Review. Lubricants 2023;11:380. https://doi.org/10.3390/lubricants11090380.

lubricants

MDPI

Review

Influence of Molecular Structure on the Physicochemical and Tribological Properties of Biolubricants: A Review

Claudia Sanjurjo *, Eduardo Rodríguez, José L. Viesca and A. Hernández Battez *

Department of Construction and Manufacturing Engineering, University of Oviedo, Pedro Puig Adam s/n, 33203 Gijón, Spain; eduardo@uniovi.es (E.R.); viescajose@uniovi.es (J.L.V.)
* Correspondence: sanjurjoclaudia@uniovi.es (C.S.); aehernandez@uniovi.es (A.H.B.)

Abstract: The increase in the price of crude oil, the environmental impact, or the depletion of fossil resources has increased the need for bio-based alternatives. This has led to the search for renewable, biodegradable, and environmentally friendly raw materials to obtain lubricants that meet these characteristics. This review deals with the state of the art of biolubricants along with their most common raw materials and molecular structures, processes of chemical modification of bio-oils, as well as the relationship between their structural features and physicochemical/tribological properties. This review concludes that the production of fatty acid alkyl esters from vegetable oils is the most promising chemical route to produce a wide range of biolubricants through double transesterification reactions. It also highlights the need to explore this route for the production of microalgae-derived biolubricants due to its environmental benefits during cultivation and production processes.

Keywords: biolubricant; molecular structure; tribological properties; physicochemical properties

Citation: Sanjurjo, C.; Rodríguez, E.; Viesca, J.L.; Battez, A.H. Influence of Molecular Structure on the Physicochemical and Tribological Properties of Biolubricants: A Review. *Lubricants* **2023**, *11*, 380. https://doi.org/10.3390/lubricants11090380

Received: 18 July 2023
Revised: 31 August 2023
Accepted: 5 September 2023
Published: 7 September 2023

1. Introduction

Water and food shortages are just some of the direct consequences of global warming caused by the increase in CO_2 emissions in recent decades. According to Lindsey's report [1], global sea levels have risen 24 cm since 1880, triggered by the start of the second industrial revolution. The highest peak emissions in history were recorded last year with 40.5 tons, behind pre-COVID-19 levels of 40.9 tons, with the use of fossil sources being the main emitter of greenhouse gases, leading with 90.47%, of which 25% came from energy losses [2].

Maintaining machinery properly, conserving energy, and finding potential substitutes for petroleum derivatives are necessary to combat accelerating climate change. One of the sciences that can contribute to this purpose is tribology, which is responsible for optimizing lubrication in the interaction between moving surfaces, and which has led to large amounts of energy and money being saved in industry. Jost [3] estimated that GBP 515 million could be saved by improving tribological conditions in the UK industry. In addition, recent research into natural lubricant sources is helping to move society toward more sustainable industries.

To achieve these goals, it is necessary to review the minimum requirements for lubricants, the advantages and disadvantages of natural sources, and the existing techniques for improving these materials to produce potential alternatives to petroleum-based lubricants. The basic functions of lubricants can be summarized as follows: (a) to reduce energy losses; (b) to protect surfaces from wear due to friction; (c) to protect against corrosion; (d) to reduce oxidation effects; (e) to cool down surfaces; (f) to decrease heat losses due to contact between moving surfaces; or (g) to increase tightness and prevent the leakage of contaminants and sediments [4,5], in addition to certain requirements depending on the application.

Lubricants can be classified according to their physical state as solid, liquid, or semi-fluid (greases). The former is used when it is difficult to maintain contact with the fluid,

while the latter is used in situations where liquid lubricants are not applicable. They can be further classified according to their source material as mineral-, synthetic-, animal-, or vegetable-based lubricants (Figure 1). All base fluids directly refined from crude oil are called mineral bases, those refined from natural sources are called vegetable bases, and those synthesized (natural or mineral) are called synthetic bases [6].

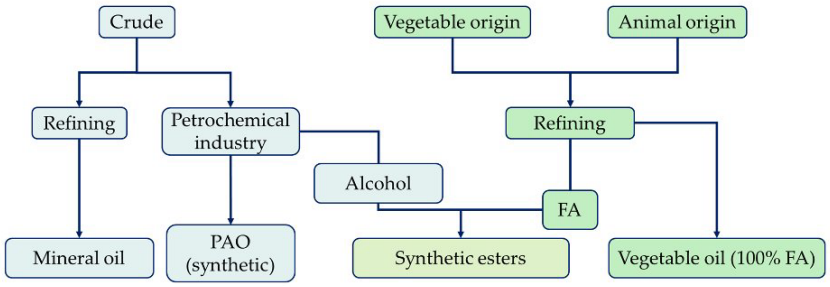

Figure 1. Origin and classification of base fluids.

Environmental concerns about the accelerated development of global warming have led to the promotion of the use of new biodegradable and more environmentally sustainable materials. As part of this movement, new competitive lubricants are being sought from organic materials such as vegetable oils and animal fats to create what are known as biodegradable lubricants or biolubricants. As lubricants, they must fulfill the basic lubricating properties listed above. Thus, biolubricants show important attractive advantages such as high biodegradability, low toxicity, sustainability (eco-friendly), increased worker safety, increased machine life, reduced labor costs, and reduced energy consumption as well as other tribological and physicochemical properties such as increased lubricity, higher viscosity index, higher boiling point, or lower volatility [7,8]. On the contrary, they have certain disadvantages, including poor oxidative, thermal, and hydrolytic stability (leading to shorter shelf life); low corrosion inhibition properties; and poor to bad pour point (PP) [7,9].

According to Verified Market Research [10], the biolubricants market was valued at USD 2.82 billion in 2018 and is expected to reach USD 3.63 billion by 2026, growing at a Compound Annual Growth Rate (CAGR) of 3.2% from 2019 to 2026. Asia and the Americas are also expected to have the highest growth rate in this sector between 2019 and 2024 [11]. These data show the growing industry interest in replacing petroleum-based lubricants with more environmentally friendly ones, and therefore the need to find solutions to concerns about production costs and other more functional aspects, including poor oxidation stability.

This review deals with the state of the art of biolubricants along their most common raw materials and molecular structures, processes of chemical modification of bio-oils, as well as the relationship between their structural features and physicochemical/tribological properties. In addition, due to the close relationship between physicochemical and tribological properties, from the physicochemical characterization of bio-oils, the necessity of using some additives to improve these properties can be considered. The aim of this work is to provide comprehensive information for the selection of bio-oils for the production of biolubricants.

2. Biolubricants

According to the UNE-EN 16807 standard [12], the term "bio" is considered synonymous with good for the environment. Its use in lubricants is linked to its environmental

Lubricants **2023**, *11*, 380

properties; therefore, it is expected that all compounds called bio-lubricants will degrade in the environment. According to this standard, bio-lubricants and bio-based lubricants must fulfill a minimum requirement:

- Biological carbon (C14) content greater than or equal to 25%.
- Biodegradability of oils greater than or equal to 60% (50% for greases).
- Ecotoxicity: not classified as "dangerous for the environment".

Proper Classification for Biolubricants from Feedstock

An important characteristic of biodegradable lubricants is the raw material used to produce them. Therefore, these materials could be classified into first, second, third, and fourth generations based on the feedstock, as shown in Figure 2 [13,14]. The first generation would include all lubricants derived from edible crops like sunflower, rapeseed, soybean, palm, palm kernel, coconut, olive, or castor [15]. These oils are characterized by a low oil production yield and encourage the deforestation and destruction of ecosystems for their cultivation [16]. In addition, the use of arable land competes with food sources, which increases the cost of the final product and is counterproductive in the current context of global food shortages. The second generation comes from non-edible materials such as *Jatropha*, tobacco, or cotton seeds [17]. These materials are more widely available than the previous ones, but they do still require arable lands for their growth and compete with edible crops for land as in the first case. Third-generation biolubricants derived from microalgae are emerging to solve this problem. Also, biolubricants derived from macroalgae, bacteria, and fungi can also be included in this category [16,18].

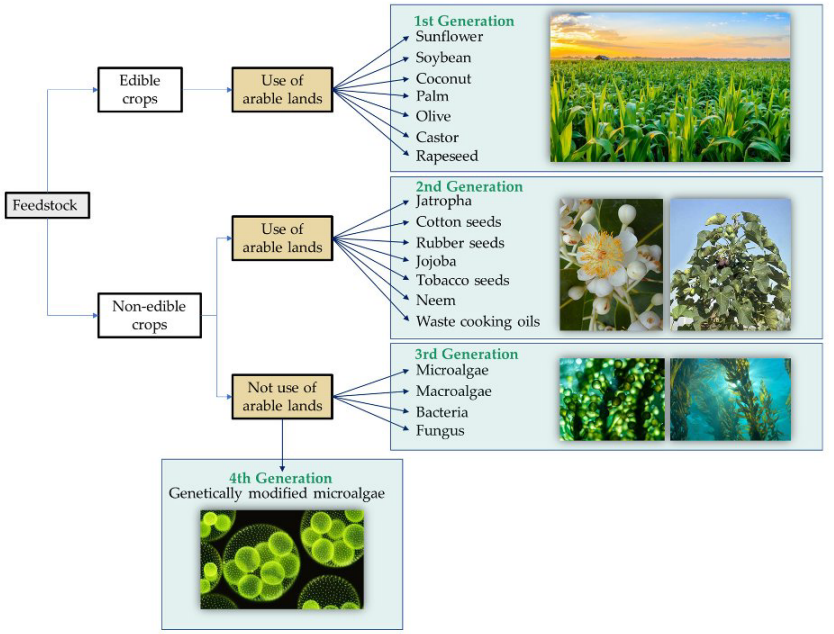

Figure 2. Biolubricant classification according to feedstock.

Microalgae are microorganisms capable of photosynthesis in freshwater, seawater, or wastewater and therefore do not require arable land for their cultivation. Among the requirements for the growth of these microorganisms, the presence of nutrients such as nitrogen, carbon, phosphorus, and potassium makes it possible to use them for wastewater treatment [19,20]. Compared to previous plant sources, they have additional economic and environmental advantages for their application as biolubricants: (a) high growth rate; (b) high biomass production; (c) high lipid content; (d) cultivable all-year-round; (e) higher CO_2 reduction during photosynthesis; and (f) effective removal of phosphates and nitrates in wastewater during cultivation [21,22].

Finally, a fourth generation of biomass derived from genetically modified microalgae is being considered. The possibility of manipulating microalgae through mutagenesis or genetic transformation will open the door to the production of suitable bio-oils for biolubricant formulation without the need to improve them using chemical techniques such as epoxidation or the use of additives [18,23,24].

3. Common Techniques for Biolubricant Production

Obtaining biomass from crops is the first step in the biolubricant production process. Depending on the type of crop, this can involve simple collection and purification processes, for example, using agricultural residues or waste cooking oil [25]. Raw materials such as macro- and microalgae require more elaborate harvesting processes, which can be physical, chemical, or biological (Figure 3). Centrifugation is the most widely used technique in the biomass-derived microalgae industry, usually complemented by drying systems such as lyophilization to efficiently remove moisture [13,22]. Figure 3 shows the bio-oil production chain including harvest, drying, pretreatment (if necessary), and extraction, and identifies the most used techniques at each stage.

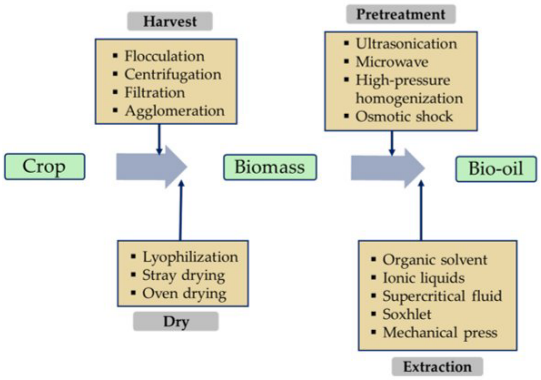

Figure 3. Various techniques to produce bio-oil from plants.

Once the biomass has been obtained, it is subjected to bio-oil production techniques. For materials with simple matrices, such as vegetable oils, more rudimentary methods are used, for example, mechanical or expeller pressing [26,27]. In the case of complex matrices like microalgae, pretreatment for cell disruption is required to facilitate bio-oil extraction. The use of high-pressure homogenization or ultra-high-pressure homogenization as a pretreatment resulted in high lipid extraction yields, reaching an increase of 30% in some cases [28–30]. The disadvantage of these techniques is the high operating cost due to the increased working pressures (supercritical conditions). As a solution, other procedures are being studied, including ultrasound, microwave, or osmotic shock [31–33].

In terms of extraction techniques, organic solvents are the most implemented, which can be alone or supported by complementary pretreatments [27]. If the biomass is semi-solid or solid, solvent extraction would be carried out using a Soxhlet device [34,35]. Ionic liquids with magnetic nanoparticles were also introduced as a potential alternative in 2021 by Egesa and Plucinski [36], where an extraction efficiency of 99% was achieved with a hexane-ionic liquid mixture.

3.1. Bio-Oils (Triglycerides) as Biolubricants

Vegetable oils are mainly composed of triglycerides: three fatty acids (FA) linked by a glycerol. Compared to the long-chain hydrocarbons of mineral oils, which have between 20 and 50 carbon atoms, FAs have shorter chains of between 4 and 26 carbon atoms [37]. They may also contain one or more double bonds and branches. Figure 4 shows the most common FA found in olive oil (mainly oleic acid).

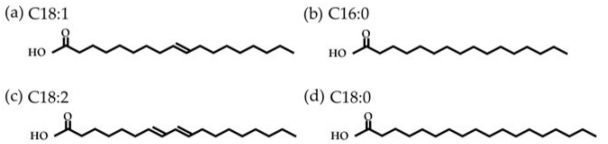

Figure 4. Common fatty acids found in olive oil: (**a**) oleic acid; (**b**) palmitic acid; (**c**) linoleic acid; (**d**) and stearic acid.

The use of these oils as lubricants has usually been studied as additives to improve a specific property, such as viscosity modifiers. Gallardo-Hernández [38] studied the use of *Jatropha* oil as an additive in a mineral oil (SAE40W oil) to evaluate its lubricating and thermal properties. The improvement in the lubricity in terms of friction and the deterioration in the anti-wear properties were observed, both related to the tribosystem created by the blend. A strong influence on the thermal properties was also observed at a content of less than 20%. Later, Contreras-Gallego [37] studied the variation in density and kinematic viscosity when the above bio-oil was added at 10% and 20% in four different mineral oils (SAE 5W-30, SAE 15W-40, SAE 25W-50, and SAE 40), as well as thermal conductivity and specific heat. An improvement in thermal properties associated with the increase in *Jatropha* oil was demonstrated. There was also a reduction in viscosity at higher additive contents, related to the substitution of long-chain hydrocarbons (mineral base oil) by shorter bio-oil ones. Recently, the feasibility of curcumin-extracted soybean waste cooking oil as a 10%, 20%, and 30% additive in N-150 mineral oil was verified by analyzing the tribological and physicochemical properties. In contrast to the previous case, a reduction in wear volume and coefficient of friction (COF) of up to 16% and 32%, respectively, was observed compared to N-150, due to a stronger tribofilm formed by the additive. The function of curcumin as a natural antioxidant to prevent the oxidation of soybean waste cooking oil was also confirmed. Finally, the increase in viscosity index with the molecular weight was confirmed and the decrease in PP from −12 °C (N-150) to −30 °C (10% bio-oil) was attributed to the increase in blend polarity [25].

3.2. Environmentally Friendly Modifications of Vegetable Oils

Despite the advantages offered by biolubricants based on bio-oils, it is inevitable highlight the need for improvement to provide functional storage properties, in addition to modifying psychochemical and tribological properties depending on the final applications. This led to the search for techniques capable of modifying the chemical structure of triglycerides, producing so-called modified esters, as shown in Figure 5.

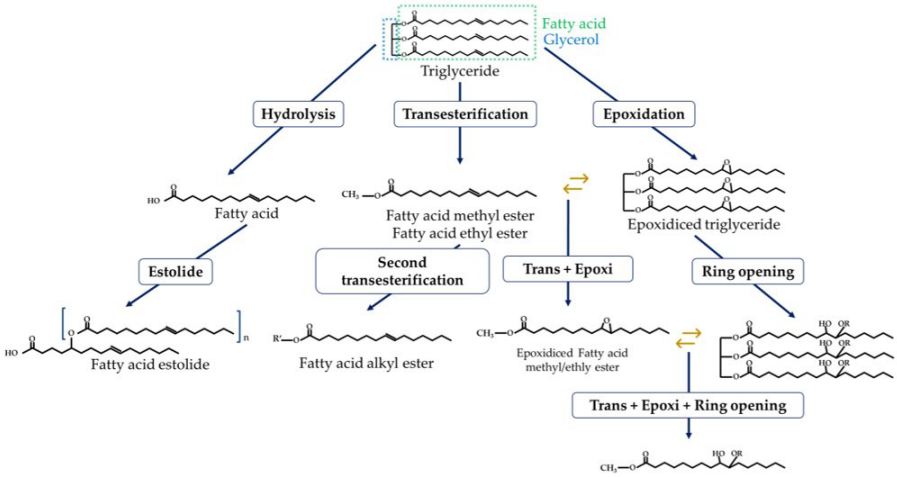

Figure 5. Eco-friendly modifications of oil sources (esters)–palmitoleic acid example.

3.2.1. Hydrolysis

As explained above, bio-oils have poor hydrolytic stability and tend to hydrolyze easily in the presence of water or steam. This leads to the breakdown of their triglycerides and the formation of the corresponding free fatty acids (FFA). This is a spontaneous secondary reaction, promoted by the increase in temperature, which must be prevented [39,40].

3.2.2. Transesterification

Transesterification reactions are the most widely used technique for ester modifications, especially in the biodiesel industry. As shown in Figure 6, it is based on the reaction between a triglyceride and an acyl acceptor (an alcohol) in the presence of a catalyst, and under temperature conditions, to produce fatty acid methyl ester (FAME) as the main product and glycerol as the secondary product. The catalyst function aims to assist the reaction and the deprotonation of the alcohol so that it can join the ester group. These can be acid, basic, or enzymatic catalysts, as well as homogeneous or heterogeneous (depending on the reaction phase) [4,13,41].

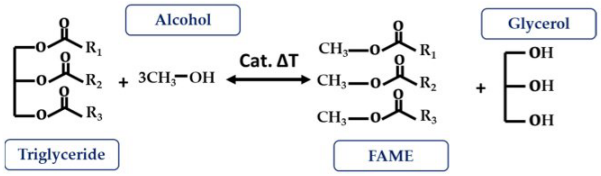

Figure 6. Transesterification reaction.

To avoid secondary reactions such as hydrolysis and thus soap formation at high FFA contents (>2–4 mg KOH/g), it is necessary to neutralize them through an esterification process using an acid catalyst, usually sulfuric acid [42]. It is also necessary to control the humidity of the bio-oil and remove any existing moisture, as this also promotes the saponification reaction.

Lubricants **2023**, *11*, 380

In the last decade, a new modality called direct or in situ transesterification has attracted attention. It combines lipid extraction (bio-oil extraction) and the transesterification reaction into one process, using biomass as a reagent instead of bio-oil, which means energy and economic savings [43]. The water content is also no longer a critical parameter, as it has greater hydrolytic stability. However, it requires more severe temperature conditions and longer reaction times [13]. A notable application is the processing of microalgal biomass. A wide range of species of these organisms develop strong cell walls, which complicates the extraction process and thus requires an efficient prior cell disruption method. As mentioned above, the operating costs of lyophilization or high-pressure homogenization are high, even more so for complex matrices such as microalgae. The ability to skip the cell disruption and extraction steps is advantageous in terms of both operating cost and energy consumption. Table 1 shows the research that has used this technique for FAME (biodiesel) production in recent years, highlighting the presence of microalgae [44–49].

More recently, Encinar et al. [50–54] have worked on the modification of vegetable-oil-derived FA using double transesterification reactions. In the first step (Figure 7), the triglyceride is degraded to the corresponding FAME. The novelty of this process lies in the second step, in which another transesterification reaction is carried out on these FAMEs, this time using a complex alcohol as a reagent, to obtain the so-called fatty acid alkyl [54] esters (FAAEs). According to the researchers, the advantage of this refinery model is the diversity of the main products, starting with the use of bio-oil; the production of biodiesel (FAME) and biolubricants (FAAE); the economic and energy savings with the recovery of materials such as glycerol, as well as the recycling of methanol produced during the second transesterification, which can be reintroduced into the process as a reagent in the first transesterification [55]. So far, only vegetable feedstocks such as safflower, cardoon, rapeseed, soybean, or *Jatropha* oil have been subjected to this technique.

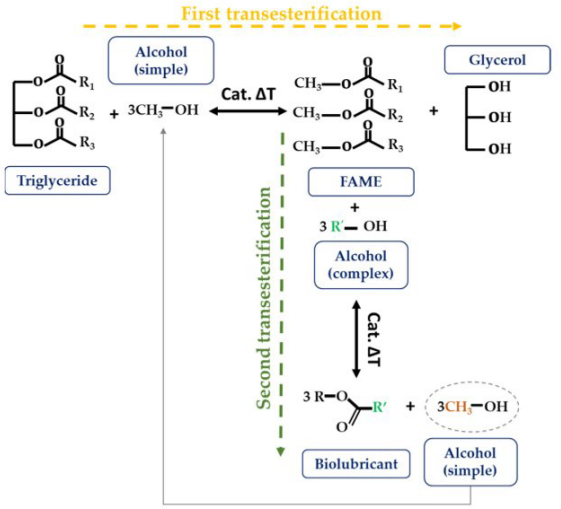

Figure 7. Double transesterification reaction.

3.2.3. Epoxidation/Ring Opening

A significant problem with bio-oils is their poor thermal and oxidative stability due to the effect of double bonds on C-H bond strength. For this reason, the authors recommend raw materials that consist as much as possible of saturated fatty acids (SFAs) because

they do not contain double bonds in their structure [20,56]. One way to neutralize these double bonds is through epoxidation reactions. These are based on the reaction of alkenes with peroxyacids to form a cyclic ether (epoxide) compound [57,58]. Epoxidized compounds have been shown to have superior frictional and anti-corrosive properties and better performance at low temperatures, providing a more economical, sustainable, and environmentally friendly alternative to mineral-based lubricants [58–60].

3.2.4. Estolide Synthesis

Another eco-friendly modification of FFA is the formation of estolides. These are synthetic compounds derived from the linkage of the respective triglycerides or their FFA, which use their hydroxyl groups to form the estolide bonds [59,61]. The advantages of these structures include better oxidative stability, improved PP, and higher flash point (FP). However, this modification does not resolve the hydrolytic stability problems of the compound [62].

Table 1. Environmentally friendly modifications for the production of and improvement in biolubricants. Microalgae species in bold text.

Feedstock	Technique	Molecular Structure	Ref.
High-oleic safflower oil	Double transesterification	FAAE	[52]
Cardoon oil	Double transesterification	FAAE	[50]
Cardoon oil	Double transesterification	FAAE	[53]
Rapeseed oil	Double transesterification	FAAE	[51]
Rapeseed and castor oils	Double transesterification	FAAE	[54]
Indian mustard seed oils	Double transesterification	FAAE	[63]
Rapeseed, seed and frying oils	Double transesterification	FAAE	[55]
Soybean oil	Double transesterification	FAAE	[64]
Jatropha oil	Double transesterification	FAAE	[65]
Coconut oil	Hydrogenation		[66]
Waste cooking oil	Epoxidation + Transesterification	Epoxidized FAME	[60]
Karanja seed oil	Simple transesterification	FAME	[67]
Schlichera oleosa oil	Simple Transesterification	FAME	[68]
Refine bleached palm kernel oil	Simple Transesterification	FAME	[69]
Soybean oil	Epoxidation	Epoxidized triglycerides	[58]
Madhuca indica oil	Epoxidation	Epoxidized triglycerides	[70]
Michelia champaca oil	Epoxidation	Epoxidized triglycerides	[71]
Moringa olifera Lam oil	Epoxidation	Epoxidized triglycerides	[26]
Passiflora edulis oil	Epoxidation	Epoxidized triglycerides	
Crude Palm oil	Hydrolyzation + Esterification	Modified esters	[72]
Crude *Jatropha* oil	Esterification + Transesterification	FAME	[73]
	Esterification + Ultrasound—assisted transesterification		
Waste ayurvedic oil	Ultrasonic irradiation assisted Transesterification	FAME	[74]
Pequi oil	Hydrolyzation + Esterification	FA	[75]
Dunaliella salina	In situ transesterification	FAME	[44]
Chlorella vulgaris foamate	In situ transesterification	FAME	[45]
Chlorella pyrenoidosa	In situ transesterification	FAME	[46]
Chlorella vulgaris	In situ transesterification	FAME	[47]
Rubber seeds	In situ transesterification	FAME	[48]
Botryococcus braunii	In situ transesterification	FAME	[49]
Coccomyxa subellipsoidea	In situ transesterification		

4. Influence of Structural Features on Biolubricant Performance

Among the structural characteristics that determine the physicochemical and tribological properties of a biolubricant, the following stand out: the presence of double bonds or unsaturation; the length of the chains present; or the molecular weight, polarity, and the presence of branches in the structures that make it up. Cecilia [56] and Chan [76] have previously reviewed the influence of these parameters on their performance as bio-lubricants. Table 2 shows in more detail how the different structures can modify some of the main properties of lubricants.

Table 2. Effect of some structural features on the physicochemical and tribological properties of biolubricants.

Property	Unsaturation (Double Bounds)	Chain Length (Molecular Weight)	Polarity	Branching Degree
Pour Point	↓	↑	↑	↓
Flash Point	-	↑	-	-
Viscosity	↓	↑	-	-
Viscosity Index	-	↑	↓	↑
Oxidation stability	↓	↓	↓	↑
Lubricity	↓	↑	↑	↓
Wear protection	↓	↑	↑	↓
Tribofilm thickness	-	↑	↑	-
Tribofilm adhesion strength	↓	-	↑	↓

4.1. Presence of Double Bonds

The molecular structure of these compounds can contain zero (saturated), one (monounsaturated), or multiple C=C double bonds (polyunsaturated). Each FA introduces the double bonds at a specific position in its structure, for example, at the 6, 9, and 12 carbon atom positions [77]. The presence of double bonds promotes oxygen attack on the carbons adjacent to these bonds, as shown in Figure 8. The areas most affected by this phenomenon are the carbons atoms located between two double bonds, so that the oxidative stability of the structure decreases as the areas of oxygen attack increase [57,78,79]. This oxidative stability refers to the ability of lubricants to retain their properties when exposed to environmental oxygen without suffering oxidative degradation [80]. It has also shown an increase in PP and a tendency to increase viscosity and decrease viscosity index (VI) by reducing the content of unsaturated FAs [57,78,81].

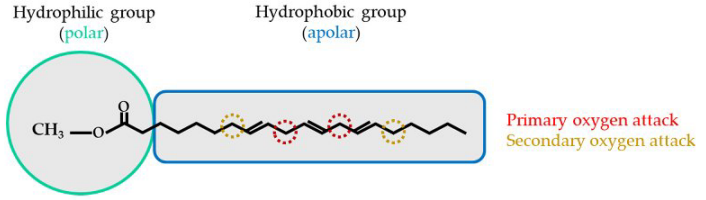

Figure 8. Polarity of the FAME structure and main oxygen attack areas.

4.2. Carbon Chain Length

Chain length and molecular weight are parameters that directly influence important physicochemical properties. Increasing the chain length leads to structures with higher molecular weights, resulting in a higher FP, which is relevant as the FP is an important factor in determining the required safe transport and storage temperatures [79]. In addition, kinematic viscosity increases with the molecular weight and the VI also increases as denser structures help to ensure that the viscosity does not fluctuate significantly with increasing temperature [82].

In terms of tribological properties, it has been found that COF and wear volume decrease with increasing chain length due to the better anti-wear performance of the film formed by the ester groups on the contact surfaces. This is achieved due to the stronger film formed by the biolubricant [25,83].

4.3. Polarity of the Structures

The structures of vegetable oils are linear, unbranched chains with polar end groups, as shown in Figure 8. The polarity of these esters increases the effectiveness of wear reduction by forming an adsorbed protective layer on the contacting metal surfaces, which reduces the surface energy and increases the strength of the formed tribological film due to their high polarity. These tribological films exhibit a low COF at both low and high temperatures [83–85]. This is why the degree of polarity is important when looking at the molecular structure of a lubricant: COOH > CHO > OH > COOCH3 > CO > COC (decreasing polarity degrees) [40]. Parameters such as VI or PP are also strongly influenced by the high polarity of these structures, resulting in higher VI values as the polarity increases, or in a drop in PP due to polar functionality [25,82].

4.4. Branching Degree

The chains that constitute these oils are characterized by the fact that they are formed by linear chains of 4 to 26 carbon atoms, with a natural lack of branches. For this reason, the shorter the chain length, the more the structure tends to clump together, while the longer the chain length, the more linear they are due to the absence of branches. As a result, these chains have higher PP values than branched structures with the same number of carbon atoms, due to the molecular structure, which tend to compact [79,86].

4.5. Selecting Vegetable Oils for Biolubricant Formulation

Based on the evaluation of the influence of the molecular structures of vegetable oils on their physicochemical and tribological properties, the flow chart shown in Figure 9 has been prepared as a guideline for the selection of vegetable oils for the biolubricant formulation. This scheme follows the one proposed by Farfán-Cabrera et al. [20], dedicated to the selection of microalgae species for the production of biolubricants. Critical input variables are considered to be the FFA content or acidity, the degree of unsaturation, and the chain length of the corresponding FAs, which have more influence on the properties of interest of biolubricants, such as hydrolytic, oxidative stability, lubricity, PP, and viscosity. If the balance between these properties does not meet the minimum requirements for a given application, the diagram shows the chemical conversions typically used as a function of the input variable to be improved. Other alternatives may be found in the use of additives or the selection of less demanding applications.

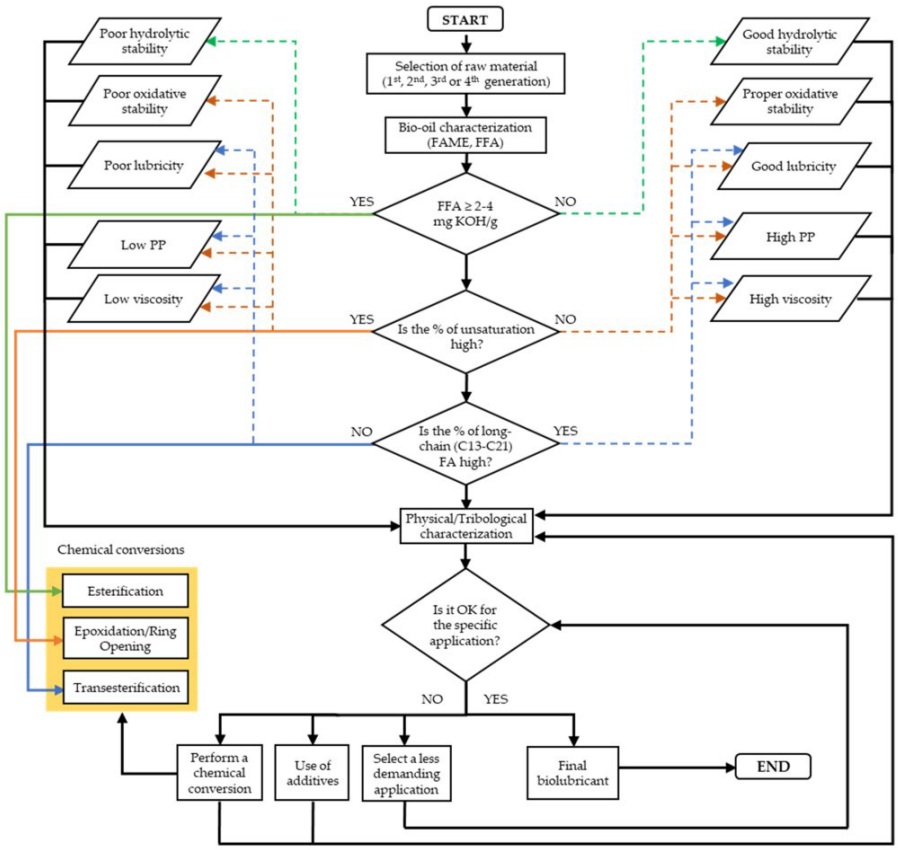

Figure 9. Flow chart for selecting vegetable oils for biolubricant formulation.

5. Tribological Characterization and Performance of Vegetable-Derived Structures

One of the objectives of using vegetable derivatives for the formulation of biolubricants is to reduce the use of elements such as chlorine, sulfur, or phosphorus, as in commercial lubricants formulated from mineral sources, and also to achieve competitive tribological properties. Chan et al. [76] reported the state of the art of tribological tests performed on biolubricants up to 2017. Now, a summary of the publications from 2018 to 2023 in which tribological tests were performed on 1st-, 2nd-, and 3rd-generation biolubricants is shown in Table 3. Table 3 shows the fluids tested, the tribological tests and test conditions used, and the COF and wear results obtained. For studies performed using different additive concentrations and loads, only the results obtained with the highest load and the most representative additive concentrations are included in Table 3.

Table 3. Tribological tests and conditions used for evaluating biolubricants from 2018 to 2022 ([a] 10^{-3} mm^3; [b] mm^3/m; [c] mm^3/Nm; [d] mm; [e] 10^{-7} mm^3/s; [f] g).

Test Fluid	Equipment		Test Conditions	COF	Wear	Ref.
Lithium grease (MVI500/PAO6/DOS)	Ball-on-disc		10–50 Hz, 50 N (1.74 GPa), RT, 30 min	0.16	125×10^{-2} [a]	[87]
Lithium grease (MVI500/PAO6/DOS) + 3% cho-ricinoleic				0.12	5.00×10^{-2} [a]	
Gallate oil ester	Ball-on-disc test	Steel	25 Hz, 100 N (2.19 GPa), RT, 30 min	0.095	0.055 [a]	[80]
		Cooper		0.12	0.045 [a]	
Phe-3Ci8		Steel		0.085	0.045 [a]	
		Cooper		0.069	0.040 [a]	
Auxenochlorella protothecoides	Ball-on-disc test		50 Hz, 77 and 150 N (2 and 2.5 GPa), 25 °C, 60 min	0.065–0.07	0.107–0.175 [a]	[88]
Chlorella sorokiniana				0.07–0.08	0.099–0.148 [a]	
Aurantiochytrium limacinum SR21				0.1–0.14	0.124–0.184 [a]	
Auranti-ochytriumsp. T66				0.09–0.13	0.110–0.169 [a]	
Rhodosporidium toruloides				0.09–0.08	0.139–0.227 [a]	
Cryptococcus curvatus				0.08–0.1	0.128–0.246 [a]	
PEG 200				0.12–0.13	1.140–7.120 [a]	
Jatropha oil (JO)	Ball-on-disc test		0.25 m/s, 50 N (1.2 GPa), 25 °C	0.06	6.00×10^{-4} [b]	[89]
Mineral engine oil (SAE 10W-30)				0.095	1.50×10^{-4} [b]	
Mineral engine oil + 20% JO				0.08	1.50×10^{-4} [b]	
Canola oil (CaO)	Ball-on-disc test		800 rpm, 130 N (2.39 GPa), 25 °C, 15 min	0.125	15.5×10^{-6} [c]	[90]
CaO + 0.05% CuO				0.08	13.0×10^{-6} [c]	
CaO + 0.08% CuO				0.07	9.10×10^{-6} [c]	
CaO + 0.1% CuO				0.05	6.00×10^{-6} [c]	
Codonosis pilosula wax (grease)	Ball-on-disc test		25 Hz, 100 N (2.25 GPa), 150 °C, 20 min	0.148	9×10^{-8} [c]	[91]
Codonosis pilosula wax (base grease) + multilayer graphene				0.145	7×10^{-8} [c]	
Castor oil	Ball-on-three-plates		10 rpm, 20 N, 25 °C, 10 min	0.11	0.47 [d]	[92]
Castor oil + epoxide cellulose pulp (grease)				0.08	0.37 [d]	
Castor oil (CO)	Ball-on-three-plates		20 rpm, 20 N, RT, 30 min	0.084	0.508 [d]	[93]
CO + epoxide-functionalized alkali lignin dispersion grease (EAL-1)				0.09	0.524 [d]	
CO + epoxide-functionalized alkali lignin dispersion grease (EAL-2)				0.07	0.416 [d]	
CO + epoxide-functionalized alkali lignin dispersion grease (EAL-3)				0.09	0.366 [d]	
CO + epoxide-functionalized alkali lignin dispersion grease (EAL-4)				0.08	0.450 [d]	
CO + epoxide-functionalized alkali lignin dispersion grease (EAL-5)				0.22	0.440 [d]	
N-150 mineral oil	Four-ball test		1200 rpm, 392 N, 75 °C, 60 min	0.117	0.685 [d]	[25]
Curcumin-extracted soybean waste cooking oil				0.08	0.573 [d]	
SAE40W + 5% JO	Four-ball test		395, 20 min	0.101	0.950 [d]	[38]
SAE40W + 20% JO				0.113	1.350 [d]	
SAE40W + 50% JO				0.125	1.500 [d]	
SAE 15W40	Four-ball test		1200 rpm, 392 N, 75 °C, 60 min	0.115	2.000 [e]	[94]
Palm oil (PO)				0.08	1.850 [e]	
PO + 0.1% hBN				0.079	1.180 [e]	
PO + 0.5% hBN				0.11	1.100 [e]	

Table 3. *Cont.*

Test Fluid	Equipment	Test Conditions	COF	Wear	Ref.
Soybean oil FAAE Soybean oil FAAE + 5% ZnAl	Four-ball test	1200 rpm, 392 N, 60 min	0.11 0.055	n/a n/a	[64]
Castor oil + seed oil Castor oil + seed oil + 0.25% halloysite clay nanotube Castor oil + seed oil + 0.5% halloysite clay nanotube Castor oil + seed oil + 0.75% halloysite clay nanotube Castor oil + seed oil + 1% halloysite clay nanotube	Four-ball test	1200 rpm, 392 N, 75 °C, 60 min	0.0697 0.0551 0.0527 0.0525 0.0452	0.919 [d] 0.848 [d] 0.845 [d] 0.779 [d] 0.723 [d]	[86]
Pequi oil Mineral oil	Four-ball test	4.95×10^5 µm/s, 55 N, 75 °C, 60 min	0.0588 0.0849	0.371 [d] 0.195 [d]	[75]
Cucurbita pepo L. oil SAE 20W40	Four-ball test	1200 rpm, 392 N, 75 °C, 60 min	0.0506 0.0459	0.333 [d] 0.413 [d]	[95]
Refine bleached palm kernel FAME Engine oil	Four-ball test	1200 rpm, 60, 80, and 100 kg, 75 °C, 60 min	0.07 0.10	2.250 [d] 2.000 [d]	[69]
Sunflower oil Soybean oil	Four-ball test	1200 rpm, 392 N, 75 °C, 60 min	0.06 0.055	0.600 [d] 0.700 [d]	[96]
Karanja FAME	Four-ball test	1200 rpm, 15 and 40 N, 75 °C, 60 min	0.05–0.14	0.300–0.440 [d]	[97]
Rice bran and sunflower oil (RB + SFO) RB + SFO + 0.01% CuO RB + SFO + 0.04% CuO	Four-ball test	1200 rpm, 392 N, 75 °C, 60 min	0.332 0.3298 0.314	0.911 [d] 0.865 [d] 0.830 [d]	[98]
Coconut oil (CO) Mustard oil (MU) SAE20W40 CO + 10% MU CO + 50% MU	Four-ball test	600 rpm, 392 N (1 GPa), 75 °C, 60 min	0.09 0.12 0.103 0.092 0.099	0.587 [d] 0.478 [d] 0.496 [d] 0.585 [d] 0.489 [d]	[99]
Jojoba oil (JJO) Polymerized JJO 1 h (grease) Polymerized JJO 2 h (grease) Polymerized JJO 3 h (grease)	Four-ball test	800 rpm, 492 N, RT, 30 min	0.04 0.015 0.03 0.068	0.422 [d] 0.385 [d] 0.471 [d] 0.420 [d]	[100]
Lithium-based paraffin grease Lithium-based castor oil grease Lithium-based coconut oil grease	Four-ball test	1200 rpm, 392 N, 75 °C, 60 min	0.091 0.07 0.082	0.850 [d] 0.700 [d] 0.930 [d]	[101]
Pailm oil FAME DF-CN48 DF-CN48 + 50% FAME DF-CN51 DF-CN51 + 50% FAME	High-frequency reciprocating test	50 Hz, 200 g, 60 °C, 75 min	0.126 0.15 0.135 0.29 0.13	0.220 [d] 0.290 [d] 0.250 [d] 0.460 [d] 0.300 [d]	[102]
Styrax officinalis oil *Styrax officinalis* FAME	Pin-on-disc test	350 rpm, 35, 70, 105, and 140 N (1.14, 1.43, 1.64, and 1.81 GPa), 125 °C	0.0094 0.0076	0.880 [d] 0.840 [d]	[103]

Table 3. *Cont.*

Test Fluid	Equipment	Test Conditions	COF	Wear	Ref.
Neem oil (NO) NO + 0.15 SiO_2 NO + 0.9 SiO_2	Pin-on-disc test	100 rpm, 40, 60, 80, and 100 N (1.03, 1.17, 1.29, and 1.39 GPa), 150 °C	0.075 0.073 0.94	59 [d] 57 [d] 66 [d]	[104]
Karanja oil Karanja oil + 1% TiO_2 Rice bran oil Rice bran oil + 1% TiO_2	Pin-on-disc test	20, 40, 60, and 80 N (1.28, 1.61, 1.84, and 2.03 GPa)	0.086 0.061 0.056 0.043	4.20×10^{-6} [c] 2.89×10^{-6} [c] 4.70×10^{-6} [c] 3.40×10^{-6} [c]	[105]
Jatropha oil *Jatropha* oil + 0.2% SiO_2 *Jatropha* oil + 1% SiO_2	Pin-on-disc test	120 rpm, 50, 80, 120 N (1.28, 1.5, and 1.72 GPa)	0.085 0.08 0.045	0.890 [f] 0.850 [f] 0.760 [f]	[106]
Waste ayuvedic oil	Pin-on-disc test	300 rpm, 80 N (2.36 GPa), RT, 60 min	0.040	0.800 [d]	[74]
Schlichera oleosa oil *Schlichera oleosa* FAME	Pin-on-disc test	200 rpm, 40, 60, 80, and 100 N (1.03, 1.17, 1.29, and 1.39 GPa), 125 °C	0.0089 0.0065	0.780 [d] 0.720 [d]	[68]
PO PO + 0.5% CuO PO + 0.5% TiO_2 Brassica oil (BO) BO + 0.5% CuO BO + 0.5%v TiO_2	Pin-on-disc test	1000 rpm, 40 N, RT, 20 min	0.045 0.034 0.039 0.047 0.040 0.043	3.60×10^{-8} [c] 1.25×10^{-8} [c] 2.00×10^{-8} [c] 4.00×10^{-8} [c] 1.60×10^{-8} [c] 2.50×10^{-8} [c]	[107]
Michelia champaca oil (MCO) Epoxidized MCO E-MCO + 1.2% CeO_2	Pin-on-disc test	100 rpm, 117 N (1.3 GPa), 75 °C, 60 min	0.084 0.065 0.055	0.1 [f] 0.85 [f] 0.7 [f]	[71]
Vegetable oil (VO) VO + 0.6% GNPs VO + 0.6% hBN VO + 0.6% (GNPs + hBN)	Pin-on-disc test	550 rpm, 18 N (0.98 GPa), RT, 60 min	0.45 0.43 0.42 0.41	8.100 [e] 5.000 [e] 4.500 [e] 3.900 [e]	[108]
Putranjiva oil (PTO) PTO + 1.3 CuO	Pin-on-disc test	500 rpm, 150 N (1.85 GPa), 125 °C	0.66 0.88	1.400 [d] 0.960 [d]	[109]
Crambe abyssinica oil *Crambe abyssinica* FAME	Pin-on-disc test	150 rpm, 30, 60, 90, and 120 N (0.93, 1.17, 1.34, and 1.48 GPa), 125 °C	0.009 0.007	0.780 [d] 0.600 [d]	[110]
Coconut oil Olive oil Rapeseed oil Soybean oil Sunflower seed oil Linseed oil	Reciprocating cylinder-on-disc tests	50 mm/s, 5 N, RT, 10 min	*0.079* 0.071 0.077 0.083 0.075 0.088	n/a	[111]

The tribological performance of vegetable oils depends on their molecular structure, as discussed in Table 2. Having shorter chains than hydrocarbons do would tend to improve lubricity and wear protection, but the presence of double bonds in the structure of vegetable oils has the opposite effect [75,89,95]. Therefore, the higher the degree of unsaturation of these oils, the lower the improvement in friction and wear. It has also been shown that the effect of increased unsaturation on tribological properties is more pronounced at higher

temperatures [112]. Yoshida et al. [111] also investigated the effect of double bonds on the COF of six vegetable oils with different levels of unsaturation in relation to the presence of mono-, di-, and tri-unsaturated FA. The oil with the highest content (%) of triunsaturation showed the highest COF results (linseed oil), followed by the oils with the highest content (%) of monounsaturation (rapeseed and olive oils).

Regarding the modified oils, Singh et al. [68,103,110] carried out comparative tests of three vegetable oils with their corresponding FAME by means of a pin-on-disc test, verifying in all of them the improvement in the anti-friction and anti-wear properties of the FAME compared to the unmodified oil. This could be due to the polarity of these compounds, thanks to the polar COOH groups present in FAME, which are adsorbed on metal surfaces, forming a more resistant film.

Another widely used alternative for improving pure oils is the use of nanoparticles as additives, particularly CuO, TiO_2, and SiO_2. For example, the use of CuO was tested in canola oil and a significant reduction in wear was achieved from 15.5×10^{-6} to 6×10^{-6} mm^3/Nm with 1% of the additive [90]. According to Table 3, at the same maximum contact pressure, pure *Jatropha* oil has lower COF values (0.027) compared to other pure oils such as neem (0.055), karanja (0.08), or rice bran (0.05) [104–106]. Regarding nanoparticle additives, the study using karanja and rice bran combined with TiO_2 showed a higher COF reduction of about 28% at a nanoparticle concentration of 0.5% [105]. In the case of neem, SiO_2 nanoparticles were selected and showed a reduction in friction of 21% at a concentration of 0.33% [93]. In the case of *Jatropha* oil, it was necessary to increase the concentration of SiO_2 nanoparticles to 1% to achieve a friction reduction of 24% [106]. On the other hand, in the case of neem and *Jatropha* oils with SiO_2, the wear was relatively constant [104,106]. On the contrary, a significant reduction in wear was observed when TiO_2 was used as an additive in karanja and rice bran oils [105].

With regard to greases, there is also an increase in the study of obtaining bioalternatives, especially using a vegetable oil as a base oil mixed with an ecological thickener such as natural wax or modified cellulose derived from a vegetable source [92,113–116]. The Chemical Process and Product Technology Research Center (Pro2TecS) of Huelva (Spain) has studied the formulation of bio-greases from castor oil using thickeners such as epoxide-functionalized alkali lignin (EAL) or epoxidized cellulose pulp from *Eucalyptus globulus* as potential substitutes for traditional lithium and calcium greases [92,93]. EALs showed a significant reduction in wear for most of the grease formulations prepared by the authors, while a sharp increase in COF values was found for a high epoxy index (0.79 mol/kg) and a higher thickener content (10%) [93]. In the second case, the COF variation was more significant, with a reduction from 0.11 (castor oil) to 0.08 (grease) and an improvement in wear reduction of 21%, and with the cellulose pulps modified with aromatic epoxides being more efficient in protecting the metal surface [92]. Xie et al. [91] studied the improvement in the tribological properties of a vegetable wax (Codonopsis pilosula)-based grease by using a multilayer graphene as an additive, proving that this material is a good alternative for improving anti-wear properties. Another study by Abbas et al. [100] also compared the tribological performance of polymerized jojoba oil (grease) with the pure oil and found that the polymerized jojoba grade also improved the tribological properties after 1 h of polymerization reaction.

Figure 10 shows the distribution of the different raw materials used in previous papers on the tribological characterization of biolubricants between 2015 and 2023, indicating the raw material generations (1st, 2nd, 3rd, and 4th), the molecular structures (triglyceride, FA, FAME, FAAE), as well as the most used combinations in the formulation of biolubricants. According to Figure 10a, the use of 1st-generation biolubricants derived from vegetable sources (edible plants) dominates with 72% of the references, followed by the 2nd generation with 24% and, to a lesser extent, the 3rd generation with 4%. On the other hand, there are no articles with biolubricants derived from genetically modified (GM) microalgae (4th generation). However, articles with GM oils of the 1st generation have been reported, as in the case of high oleic soybean [23,117,118]. The large number of tribological

studies carried out on biolubricants formulated from pure oils (triglycerides) is shown in Figure 10b, as well as the use of esters modified using the transesterification technique, such as FAME (biodiesel) or FAAE, which have been shown to have better physicochemical and tribological properties [64,68,69,97,102,103]. Finally, Figure 10c highlights the need to use additives when the biolubricant is formulated from pure oil, with the most studied being CuO and TiO_2 nanoparticles. However, it can be observed how those formulated from FAME (better anti-friction and anti-wear properties) are desired as pure base oils or in blends with mineral base oils.

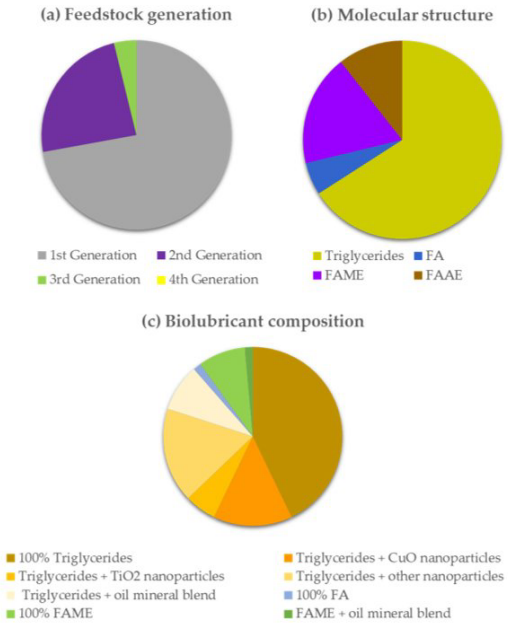

Figure 10. Summary of studies on biolubricant tribology from 2015 up to now.

6. Conclusions

The use of natural feedstocks instead of those derived from petroleum for lubricant production constitutes an alternative in the fight against climate change, but the consumption of edible crops or crops that require arable land is a concern that needs to be overcome. The use of third-generation feedstocks is emerging as an attractive solution. In particular, microalgae have the advantage of being cultured in a wide variety of systems, including wastewater, which offers the possibility of exploiting the growth cycle of these microorganisms in wastewater bioremediation.

Considering the above facts, some weaknesses of bio-oils such as poor oxidation stability due to the presence of double bonds or poor flow properties at low temperatures should be faced. In order to overcome these problems, it is necessary to select the raw material correctly, and then check its lipid profile and verify that its molecular structure is suitable for the properties that may be required by the future biolubricant. Many additives based on nanoparticles have also been tested to improve the tribological performance of biolubricants, with remarkable results at concentrations below 1%.

The double transesterification technique developed for the production of FAAE biolubricants appears to be a promising route for the synthesis of these materials, with the ability to manipulate the degree of branching and chain length almost indefinitely. However, this technique has only been applied to 1st- and 2nd-generation feedstocks with the associated limitations. It would be interesting to apply this technique to more attractive feedstocks such as 3rd-generation feedstocks. In addition, the need to remove the double bonds can be achieved by using the epoxidation technique. Finally, the combined use of 3rd-generation bio-oils, with their molecular structure modified through transesterification and epoxidation techniques, and nano-additives can be a good solution for formulating biolubricants for multiple applications.

Author Contributions: Conceptualization, C.S., A.H.B. and E.R.; formal analysis, C.S.; investigation, C.S.; project administration, A.H.B. and E.R.; supervision, A.H.B. and E.R.; writing—original draft, C.S.; writing—review and editing, A.H.B., E.R. and J.L.V. All authors have read and agreed to the published version of the manuscript.

Funding: This research was funded by the Ministry of Science, Innovation and Universities (Spain) and the State Investigation Agency, grant number: PID2022-136656NB-100 (LubeMicroAlgae project); and by the Foundation for the Promotion of Applied Scientific Research and Technology in Asturias (Spain), which financed the contract of Claudia Sanjurjo at the University of Oviedo (Spain), grant number: SV-PA-21-AYUD/2021/50987.

Data Availability Statement: No new data were created or analyzed in this study. Data sharing is not applicable to this article.

Conflicts of Interest: The authors declare no conflict of interest.

References

1. Climate Change: Global Sea Level | NOAA Climate.Gov. Available online: https://www.climate.gov/news-features/understanding-climate/climate-change-global-sea-level (accessed on 13 June 2023).
2. Global Carbon Project (GCP). Available online: https://www.globalcarbonproject.org/ (accessed on 19 January 2023).
3. Jost, H.P. Tribology—Origin and Future. *Wear* **1990**, *136*, 1–17. [CrossRef]
4. Panchal, T.M.; Patel, A.; Chauhan, D.D.; Thomas, M.; Patel, J.V. A Methodological Review on Bio-Lubricants from Vegetable Oil Based Resources. *Renew. Sustain. Energy Rev.* **2017**, *70*, 65–70. [CrossRef]
5. Biolubricantes Protegiendo El Medio Ambiente. Total Enery. 2012. Available online: https://docplayer.es/28005864-Biolubricantes-protegiendo-el-medio-ambiente.html (accessed on 19 January 2023).
6. Torbacke, M.; Rudolphi, Å.K.; Kassfeldt, E. *Lubricants: Introduction to Properties and Performance*, 1st ed.; John Wiley and Sons: Hoboken, NJ, USA, 2014; ISBN 978-1-118-79974-1.
7. Perera, M.; Yan, J.; Xu, L.; Yang, M.; Yan, Y. Bioprocess Development for Biolubricant Production Using Non-Edible Oils, Agro-Industrial Byproducts and Wastes. *J. Clean. Prod.* **2022**, *357*, 131956. [CrossRef]
8. Almasi, S.; Ghobadian, B.; Najafi, G.; Soufi, M.D. A Review on Bio-Lubricant Production from Non-Edible Oil-Bearing Biomass Resources in Iran: Recent Progress and Perspectives. *J. Clean. Prod.* **2021**, *290*, 125830. [CrossRef]
9. Sarma, R.N.; Vinu, R. Current Status and Future Prospects of Biolubricants: Properties and Applications. *Lubricants* **2022**, *10*, 70. [CrossRef]
10. Global Biolubricants Market Size by Base Oil Type, by Application, by End-User Industry, by Geographic Scope and Forecast. Available online: https://www.verifiedmarketresearch.com/product/bio-lubricants-market/ (accessed on 19 January 2023).
11. Informe de Mercado de Biolubricantes | Tamaño, Participación, Crecimiento y Tendencias (2022–27). Available online: https://www.mordorintelligence.com/es/industry-reports/bio-lubricants-market (accessed on 15 March 2023).
12. *UNE-EN 16807:2017*; Liquid Petroleum Products—Bio-Lubricants—Criteria and Requirements of Bio-Lubricants and Bio-Based Lubricants. UNE: Madrid, Spain, 2017.
13. Eldiehy, K.S.H.; Bardhan, P.; Borah, D.; Gohain, M.; Ahmad Rather, M.; Deka, D.; Mandal, M.A. Comprehensive Review on Microalgal Biomass Production and Processing for Biodiesel Production. *Fuel* **2022**, *324*, 124773. [CrossRef]
14. Zainal, N.A.; Zulkifli, N.W.M.; Gulzar, M.; Masjuki, H.H. A Review on the Chemistry, Production, and Technological Potential of Bio-Based Lubricants. *Renew. Sustain. Energy Rev.* **2018**, *82*, 80–102. [CrossRef]
15. Brahma, S.; Nath, B.; Basumatary, B.; Das, B.; Saikia, P.; Patir, K.; Basumatary, S. Biodiesel Production from Mixed Oils: A Sustainable Approach towards Industrial Biofuel Production. *Chem. Eng. J. Adv.* **2022**, *10*, 100284. [CrossRef]
16. Abdul Hakim Shaah, M.; Hossain, M.S.; Salem Allafi, F.A.; Alsaedi, A.; Ismail, N.; Ab Kadir, M.O.; Ahmad, M.I. A Review on Non-Edible Oil as a Potential Feedstock for Biodiesel: Physicochemical Properties and Production Technologies. *RSC Adv.* **2021**, *11*, 25018–25037. [CrossRef]

17. Ulakpa, W.C.; Ulakpa, R.O.E.; Egwunyenga, M.C.; Egbosiuba, T.C. Transesterification of Non-Edible Oil and Effects of Process Parameters on Biodiesel Yield. *Clean. Waste Syst.* **2022**, *3*, 100047. [CrossRef]
18. Mat Aron, N.S.; Khoo, K.S.; Chew, K.W.; Show, P.L.; Chen, W.H.; Nguyen, T.H.P. Sustainability of the Four Generations of Biofuels—A Review. *Int. J. Energy Res.* **2020**, *44*, 9266–9282. [CrossRef]
19. Olia, M.S.J.; Azin, M.; Sepahi, A.A.; Moazami, N. Miniaturized Culture Method for the Statistical Study of Growth Rate and Carbohydrate Content of Picochlorum Sp. D8 Isolated from the Persian Gulf. *Renew. Energy* **2020**, *149*, 479–488. [CrossRef]
20. Farfan-Cabrera, L.I.; Franco-Morgado, M.; González-Sánchez, A.; Pérez-González, J.; Marín-Santibáñez, B.M. Microalgae Biomass as a New Potential Source of Sustainable Green Lubricants. *Molecules* **2022**, *27*, 1205. [CrossRef]
21. Sánchez-Bayo, A. Biorrefinería de Microalgas Para La Producción de Biocombustibles. Ph.D. Thesis, Universidad Rey Juan Carlos, Madrid, Spain, 2019.
22. Peng, L.; Fu, D.; Chu, H.; Wang, Z.; Qi, H. Biofuel Production from Microalgae: A Review. *Environ. Chem. Lett.* **2020**, *18*, 285–297. [CrossRef]
23. Reeves, C.J.; Menezes, P.L.; Jen, T.C.; Lovell, M.R. The Influence of Fatty Acids on Tribological and Thermal Properties of Natural Oils as Sustainable Biolubricants. *Tribol. Int.* **2015**, *90*, 123–134. [CrossRef]
24. Vuttipongchaikij, S. Genetic Manipulation of Microalgae for Improvement of Biodiesel Production. *Thai J. Genet.* **2012**, *5*, 130–148. [CrossRef]
25. Singh, N.; Agarwal, P.; Porwal, S.K. Natural Antioxidant Extracted Waste Cooking Oil as Sustainable Biolubricant Formulation in Tribological and Rheological Applications. *Waste Biomass Valorization* **2022**, *13*, 3127–3137. [CrossRef]
26. Silva, M.S.; Foletto, E.L.; Alves, S.M.; de Castro Dantas, T.N.; Dantas Neto, A.A. New Hydraulic Biolubricants Based on Passion Fruit and Moringa Oils and Their Epoxy. *Ind. Crops Prod.* **2015**, *69*, 362–370. [CrossRef]
27. Enamala, M.K.; Enamala, S.; Chavali, M.; Donepudi, J.; Yadavalli, R.; Kolapalli, B.; Aradhyula, T.V.; Velpuri, J.; Kuppam, C. Production of Biofuels from Microalgae—A Review on Cultivation, Harvesting, Lipid Extraction, and Numerous Applications of Microalgae. *Renew. Sustain. Energy Rev.* **2018**, *94*, 49–68. [CrossRef]
28. Imatoukene, N.; Koubaa, M.; Perdrix, E.; Benali, M.; Vorobiev, E. Combination of Cell Disruption Technologies for Lipid Recovery from Dry and Wet Biomass of *Yarrowia lipolytica* and Using Green Solvents. *Process. Biochem.* **2020**, *90*, 139–147. [CrossRef]
29. Onumaegbu, C.; Alaswad, A.; Rodriguez, C.; Olabi, A.G. Optimization of Pre-Treatment Process Parameters to Generate Biodiesel from Microalga. *Energies* **2018**, *11*, 806. [CrossRef]
30. Bernaerts, T.M.M.; Gheysen, L.; Foubert, I.; Hendrickx, M.E.; Van Loey, A.M. Evaluating Microalgal Cell Disruption upon Ultra High Pressure Homogenization. *Algal Res.* **2019**, *42*, 101616. [CrossRef]
31. Onumaegbu, C.; Alaswad, A.; Rodriguez, C.; Olabi, A. Modelling and Optimization of Wet Microalgae *Scenedesmus quadricauda* Lipid Extraction Using Microwave Pre-Treatment Method and Response Surface Methodology. *Renew. Energy* **2019**, *132*, 1323–1331. [CrossRef]
32. Halim, R.; Papachristou, I.; Chen, G.Q.; Deng, H.; Frey, W.; Posten, C.; Silve, A. The Effect of Cell Disruption on the Extraction of Oil and Protein from Concentrated Microalgae Slurries. *Bioresour. Technol.* **2022**, *346*, 126597. [CrossRef] [PubMed]
33. Singh, S.; Meena, P.; Saharan, V.K.; Bhoi, R.; George, S. Enhanced Lipid Recovery from Chlorella Sp. Biomass by Green Approach: A Combination of Ultrasonication and Homogenization Pre-Treatment Techniques (Hybrid Method) Using Aqueous Deep Eutectic Solvents. *Mater. Today Proc.* **2022**, *57*, 179–186. [CrossRef]
34. Alrashidi, M.; Derawi, D.; Salimon, J.; Firdaus Yusoff, M. An Investigation of Physicochemical Properties of *Nigella sativa* L. Seed Oil from Al-Qassim by Different Extraction Methods. *J.King Saud Univ. Sci.* **2020**, *32*, 3337–3342. [CrossRef]
35. Hajinajaf, N.; Rabbani, Y.; Mehrabadi, A.; Tavakoli, O. Experimental and Modeling Assessment of Large-Scale Cultivation of Microalgae Nannochloropsis Sp. PTCC 6016 to Reach High Efficiency Lipid Extraction. *Int. J. Environ. Sci. Technol.* **2022**, *19*, 5511–5528. [CrossRef]
36. Egesa, D.; Plucinski, P. Efficient Extraction of Lipids from Magnetically Separated Microalgae Using Ionic Liquids and Their Transesterification to Biodiesel. *Biomass Convers. Biorefin.* **2022**. [CrossRef]
37. Contreras-Gallegos, E.; Domínguez-Pacheco, F.A.; Hernández-Aguilar, C.; Bedoya, A.; Alvarado, S.; Marín, E.; Cruz-Orea, A. Study of Mineral-Based Oils with *Jatropha curcas* L. as Bio-Additive Through Thermal and Kinematic Viscosity Properties. *Int. J. Thermophys.* **2022**, *43*, 4. [CrossRef]
38. Gallardo-Hernández, E.A.; Lara-Hernández, G.; Nieto-Camacho, F.; Domínguez-Pacheco, A.; Cruz-Orea, A.; Hernández-Aguilar, C.; Contreras-Gallegos, E.; Torres, M.V.; Flores-Cuautle, J.J.A. Thermal and Tribological Properties of Jatropha Oil as Additive in Commercial Oil. *Int. J. Thermophys.* **2017**, *38*, 54. [CrossRef]
39. Ngaosuwan, K.; Lotero, E.; Suwannakarn, K.; Goodwin, J.G.; Praserthdam, P. Hydrolysis of Triglycerides Using Solid Acid Catalysts. *Ind. Eng. Chem. Res.* **2009**, *48*, 4757–4767. [CrossRef]
40. Ho, C.K.; McAuley, K.B.; Peppley, B.A. Biolubricants through Renewable Hydrocarbons: A Perspective for New Opportunities. *Renew. Sustain. Energy Rev.* **2019**, *113*, 109261. [CrossRef]
41. Salaheldeen, M.; Mariod, A.A.; Aroua, M.K.; Rahman, S.M.A.; Soudagar, M.E.M.; Fattah, I.M.R. Current State and Perspectives on Transesterification of Triglycerides for Biodiesel Production. *Catalysts* **2021**, *11*, 1121. [CrossRef]
42. Azad, A.K.; Sharma, S.C.; Rasul, M.G. *Clean Energy for Sustainable Development: Comparisons and Contrasts of New Approaches*; Academic Press: Cambridge, MA, USA, 2016; ISBN 9780128054239.

43. Langseter, A.M.; Dzurendova, S.; Shapaval, V.; Kohler, A.; Ekeberg, D.; Zimmermann, B. Evaluation and Optimisation of Direct Transesterification Methods for the Assessment of Lipid Accumulation in Oleaginous Filamentous Fungi. *Microb. Cell Fact.* **2021**, *20*, 59. [CrossRef] [PubMed]
44. Zorn, S.M.F.E.; da Silva, A.P.T.; Bredda, E.H.; Bento, H.B.S.; Pedro, G.A.; Carvalho, A.K.F.; Silva, M.B.; Da Rós, P.C.M. In Situ Transesterification of Microbial Biomass for Biolubricant Production Catalyzed by Heteropolyacid Supported on Niobium. *Energies* **2022**, *15*, 1591. [CrossRef]
45. Al-Humairi, S.T.; Lee, J.G.M.; Harvey, A.P. Direct and Rapid Production of Biodiesel from Algae Foamate Using a Homogeneous Base Catalyst as Part of an Intensified Process. *Energy Convers. Manag. X* **2022**, *16*, 100284. [CrossRef]
46. Sharma, A.K.; Ghodke, P.; Sharma, P.K.; Manna, S.; Pugazhendhi, A.; Matsakas, L.; Patel, A. Holistic Utilization of *Chlorella pyrenoidosa* Microalgae for Extraction of Renewable Fuels and Value-Added Biochar through in Situ Transesterification and Pyrolysis Reaction Process. *Biomass Convers. Biorefin.* **2022**. [CrossRef]
47. Al-Humairi, S.T.; Lee, J.G.M.; Salihu, M.; Harvey, A.P. Biodiesel Production through Acid Catalyst In Situ Reactive Extraction of Chlorella Vulgaris Foamate. *Energies* **2022**, *15*, 4482. [CrossRef]
48. Tarigan, J.B.; Anggraini, R.; Sembiring, R.P.; Supeno, M.; Tarigan, K.; Ginting, J.; Karo-Karo, J.A.; Sitepu, E.K. Waste Rubber Seeds as a Renewable Energy Source: Direct Biodiesel Production Using a Controlled Crushing Device. *RSC Adv.* **2022**, *12*, 2094–2101. [CrossRef]
49. Chávez-Sandoval, B.E.; Hernández-Salgado, K.F.; Martínez-García, M.; Ávila-Paredes, H.J.; Díaz-álvarez, F.H.; García-Franco, F. Obtaining Biodiesel by Direct Transesterification of *Botryococcus braunii* and *Coccomyxa subellipsoidea*. *J. Mex. Chem. Soc.* **2021**, *65*, 318–330. [CrossRef]
50. Nogales-Delgado, S.; Encinar Martín, J.M. Cardoon Biolubricant through Double Transesterification: Assessment of Its Oxidative, Thermal and Storage Stability. *Mater. Lett.* **2021**, *302*, 130454. [CrossRef]
51. Encinar, J.M.; Nogales-Delgado, S.; Pinilla, A. Biolubricant Production through Double Transesterification: Reactor Design for the Implementation of a Biorefinery Based on Rapeseed. *Processes* **2021**, *9*, 1224. [CrossRef]
52. Encinar, J.M.; Nogales-Delgado, S.; Álvez-Medina, C.M. High Oleic Safflower Biolubricant through Double Transesterification with Methanol and Pentaerythritol: Production, Characterization, and Antioxidant Addition. *Arab. J. Chem.* **2022**, *15*, 103796. [CrossRef]
53. Nogales-Delgado, S.; Sánchez, N.; Encinar, J.M. Valorization of Cynara Cardunculus L. Oil as the Basis of a Biorefinery for Biodiesel and Biolubricant Production. *Energies* **2020**, *13*, 5085. [CrossRef]
54. Encinar, J.M.; Nogales-Delgado, S.; Sánchez, N.; González, J.F. Biolubricants from Rapeseed and Castor Oil Transesterification by Using Titanium Isopropoxide as a Catalyst: Production and Characterization. *Catalysts* **2020**, *10*, 366. [CrossRef]
55. Encinar, J.M.; Nogales, S.; González, J.F. Biodiesel and Biolubricant Production from Different Vegetable Oils through Transesterification. *Eng. Rep.* **2020**, *2*, e12190. [CrossRef]
56. Cecilia, J.A.; Plata, D.B.; Saboya, R.M.A.; de Luna, F.M.T.; Cavalcante, C.L.; Rodríguez-Castellón, E. An Overview of the Biolubricant Production Process: Challenges and Future Perspectives. *Processes* **2020**, *8*, 257. [CrossRef]
57. Do Valle, C.P.; Rodrigues, J.S.; Fechine, L.M.U.D.; Cunha, A.P.; Queiroz Malveira, J.; Luna, F.M.T.; Ricardo, N.M.P.S. Chemical Modification of Tilapia Oil for Biolubricant Applications. *J. Clean. Prod.* **2018**, *191*, 158–166. [CrossRef]
58. Cui, X.; Cao, P.; Guo, J.; Ming, P. Use and Performance of Soybean Oil Based Bio-Lubricant in Reducing Specific Cutting Energy during Biomimetic Machining. *J. Manuf. Process.* **2021**, *62*, 577–590. [CrossRef]
59. Hoong, S.S.; Arniza, M.Z.; Mariam, N.M.D.N.S.; Armylisas, A.H.N.; Yeong, S.K. Synthesis and Physicochemical Properties of Novel Lauric Acid Capped Estolide Esters and Amides Made from Oleic Acid and Their Evaluations for Biolubricant Basestock. *Ind. Crops Prod.* **2019**, *140*, 111653. [CrossRef]
60. Li, W.; Wang, X. Bio-Lubricants Derived from Waste Cooking Oil with Improved Oxidation Stability and Low-Temperature Properties. *J. Oleo Sci.* **2015**, *64*, 367–374. [CrossRef] [PubMed]
61. Cermak, S.C.; Isbell, T.A.; Bredsguard, J.W.; Thompson, T.D. Chapter 14—Estolides: Synthesis and Applications. In *Fatty Acids Chemistry, Synthesis, and Applications*; Ahmad, M.U., Ed.; Elsevier: Amsterdam, The Netherlands, 2017; pp. 431–475. [CrossRef]
62. Salimon, J.; Nallathamby, N.; Salih, N.; Abdullah, B.M. Synthesis and Physical Properties of Estolide Ester Using Saturated Fatty Acid and Ricinoleic Acid. *J. Autom. Methods Manag. Chem.* **2011**, *2011*, 263624. [CrossRef] [PubMed]
63. Chen, J.; Bian, X.; Rapp, G.; Lang, J.; Montoya, A.; Trethowan, R.; Bouyssiere, B.; Portha, J.F.; Jaubert, J.N.; Pratt, P.; et al. From Ethyl Biodiesel to Biolubricants: Options for an Indian Mustard Integrated Biorefinery toward a Green and Circular Economy. *Ind. Crops Prod.* **2019**, *137*, 597–614. [CrossRef]
64. Shrivastava, S.; Prajapati, P.; Virendra; Srivastava, P.; Lodhi, A.P.S.; Kumar, D.; Sharma, V.; Srivastava, S.K.; Agarwal, D.D. Chemical Transesterification of Soybean Oil as a Feedstock for Stable Biodiesel and Biolubricant Production by Using Zn Al Hydrotalcites as a Catalyst and Perform Tribological Assessment. *Ind. Crops Prod.* **2023**, *192*, 116002. [CrossRef]
65. Edla, S.; Krishna, A.; Karthik, G.V.S.; Arif, M.M.; Rani, S. Potential Use of Transesterified Vegetable Oil Blends as Base Stocks for Metalworking Fluids and Cutting Forces Prediction Using Machine Learning Tool. *Biomass Convers. Biorefin.* **2021**, *13*, 10665–10676. [CrossRef]
66. Gasni, D.; Mulyadi, I.H.; Affi, J.; Miswar, A.Y. Investigation of Wear Mechanism in Ball Bearings Lubricated by a Bio-Lubricant. *Int. J. Technol.* **2017**, *8*, 1248–1257. [CrossRef]

67. Amriya Tasneem, H.R.; Ravikumar, K.P.; Ramakrishna, H.V. Performance and Wear Debris Characteristics of Karanja Biodiesel and Biolubricant as a Substitute in a Compression Ignition Engine. *Fuel* **2022**, *319*, 123870. [CrossRef]
68. Singh, Y.; Negi, P.; Yadav, A.; Tripathi, R. Development of Bio Based Lubricant from Schlichera Oleosa with Effect of Load during Tribological Analysis. *Mater. Today Proc.* **2021**, *46*, 10527–10529. [CrossRef]
69. Mohd Salleh, Z.A.; Syahrullail, S.; Norzita, N.; Nurun Najwa, R. Friction Study on Chemically Modified RBD PK Oil as a Potential Renewable Resource. *J. Braz. Soc. Mech. Sci. Eng.* **2021**, *43*, 127. [CrossRef]
70. Singh, Y.; Rahim, E.A.; Singh, N.K.; Sharma, A.; Singla, A.; Palamanit, A. Friction and Wear Characteristics of Chemically Modified Mahua (*Madhuca indica*) Oil Based Lubricant with SiO_2 Nanoparticles as Additives. *Wear* **2022**, *508–509*, 204463. [CrossRef]
71. Singh, Y.; Abd Rahim, E. Michelia Champaca: Sustainable Novel Non-Edible Oil as Nano Based Bio-Lubricant with Tribological Investigation. *Fuel* **2020**, *282*, 118830. [CrossRef]
72. Nor, N.M.; Salih, N.; Salimon, J. Optimization and Lubrication Properties of Malaysian Crude Palm Oil Fatty Acids Based Neopentyl Glycol Diester Green Biolubricant. *Renew. Energy* **2022**, *200*, 942–956. [CrossRef]
73. Arce Saavedra, T.; Bueno-Borges, L.B.; Sangaletti-Gerhard, N.; de Alencar, S.M.; Regitano-d'Arce, M.A.B. Optimized Conventional and Ultrasound-Assisted Ethyl Transesterification of Jatropha (*Jatropha curcas*) and Palm (*Elaeis guineensis*) Oil Mixtures. *Chem. Eng. Commun.* **2022**, *209*, 1482–1495. [CrossRef]
74. Balakumar, R.; Sriram, G.; Arumugam, S. Effect of Engine Oil Dilution by Waste Ayurvedic Oil Biodiesel on Tribological Behavior of Liner-Ring Tribo Pair Material. *Mater. Sci. Eng.* **2020**, *954*, 012042. [CrossRef]
75. Ribeiro Filho, P.R.C.F.; da Silva, S.S.O.; do Nascimento, M.R.; de Aguiar Soares, S.; de Luna, F.M.T.; Cavalcante, C.L. Tribological Properties of Bio-Based Lubricant Basestock Obtained from Pequi Oil (*Caryocar brasiliensis*). *J. Braz. Soc. Mech. Sci. Eng.* **2022**, *44*, 51. [CrossRef]
76. Chan, C.H.; Tang, S.W.; Mohd, N.K.; Lim, W.H.; Yeong, S.K.; Idris, Z. Tribological Behavior of Biolubricant Base Stocks and Additives. *Renew. Sustain. Energy Rev.* **2018**, *93*, 145–157. [CrossRef]
77. Los, D.A.; Murata, N. Structure and Expression of Fatty Acid Desaturases. *Biochim. Biophys. Acta* **1998**, *1394*, 3–15. [CrossRef]
78. Lee, C.T.; Lee, M.B.; Mong, G.R.; Chong, W.W.F. A Bibliometric Analysis on the Tribological and Physicochemical Properties of Vegetable Oil–Based Bio-Lubricants (2010–2021). *Environ. Sci. Pollut. Res.* **2022**, *29*, 56215–56248. [CrossRef]
79. Ahmed, W.A.; Salih, N.; Salimon, J. Synthesis, Characterization, Tribological and Rheological Properties of Di (2-Butyloctyl) Dicarboxylate Esters for Environmentally Friendly Biolubricant Applications. *Biointerface Res. Appl. Chem.* **2023**, *1*, 2783. [CrossRef]
80. Hu, C.; Ai, J.; Ma, L.; Wen, P.; Fan, M.; Zhou, F.; Liu, W. Ester Oils Prepared from Fully Renewable Resources and Their Lubricant Base Oil Properties. *ACS Omega* **2021**, *6*, 16343–16355. [CrossRef]
81. Holmberg, K.; Erdemir, A. Influence of Tribology on Global Energy Consumption, Costs and Emissions. *Friction* **2017**, *5*, 263–284. [CrossRef]
82. Al-Arafi, N.; Salih, N.; Salimon, J. Synthesis, Characterization, Tribological and Rheological Properties of Oleyl Oleate Based Biolubricant. *Egypt. J. Chem.* **2022**, *65*, 419–433. [CrossRef]
83. Salih, N.; Salimon, J.; Abdullah, B.M.; Yousif, E. Thermo-Oxidation, Friction-Reducing and Physicochemical Properties of Ricinoleic Acid Based-Diester Biolubricants. *Arab. J. Chem.* **2017**, *10*, S2273–S2280. [CrossRef]
84. Bahadi, M.; Salimon, J.; Derawi, D. Synthesis of ISO Grade 46 and 68 Biolubricant from Palm Kernel Fatty Acids. *Sains Malays.* **2022**, *51*, 2507–2529. [CrossRef]
85. Cheah, M.Y.; Ong, H.C.; Zulkifli, N.W.M.; Masjuki, H.H.; Salleh, A. Physicochemical and Tribological Properties of Microalgae Oil as Biolubricant for Hydrogen-Powered Engine. *Int. J. Hydrogen Energy* **2020**, *45*, 22364–22381. [CrossRef]
86. Ahmed, M.S.; Nair, K.P.; Tirth, V.; Elkhaleefa, A.; Rehan, M. Tribological Evaluation of Date Seed Oil and Castor Oil Blends with Halloysite Nanotube Additives as Environment Friendly Bio-Lubricants. *Biomass Convers. Biorefin.* **2021**. [CrossRef]
87. Ju, C.; Li, W.; Zhao, Q.; Wang, X. Bio-Additives Derived from Ricinoleic Acid and Choline with Improved Tribological Properties in Lithium Base Grease. *J. Oleo Sci.* **2022**, *71*, 915–925. [CrossRef]
88. Patel, A.; Mu, L.; Shi, Y.; Rova, U.; Christakopoulos, P.; Matsakas, L. Single-Cell Oils from Oleaginous Microorganisms as Green Bio-Lubricants: Studies on Their Tribological Performance. *Energies* **2021**, *14*, 6685. [CrossRef]
89. Farfan-Cabrera, L.I.; Gallardo-Hernández, E.A.; Gómez-Guarneros, M.; Pérez-González, J.; Godínez-Salcedo, J.G. Alteration of Lubricity of Jatropha Oil Used as Bio-Lubricant for Engines Due to Thermal Ageing. *Renew. Energy* **2020**, *149*, 1197–1204. [CrossRef]
90. Kumar, V.; Dhanola, A.; Garg, H.C.; Kumar, G. Improving the Tribological Performance of Canola Oil by Adding CuO Nanoadditives for Steel/Steel Contact. *Mater. Today Proc.* **2020**, *28*, 1392–1396. [CrossRef]
91. Xie, M.; Cheng, J.; Huo, C.; Zhao, G. Improving the Lubricity of a Bio-Lubricating Grease with the Multilayer Graphene Additive. *Tribol. Int.* **2020**, *150*, 106386. [CrossRef]
92. Cortés-Triviño, E.; Valencia, C.; Delgado, M.A.; Franco, J.M. Thermo-Rheological and Tribological Properties of Novel Bio-Lubricating Greases Thickened with Epoxidized Lignocellulosic Materials. *J. Ind. Eng. Chem.* **2019**, *80*, 626–632. [CrossRef]
93. Delgado, M.A.; Cortés-Triviño, E.; Valencia, C.; Franco, J.M. Tribological Study of Epoxide-Functionalized Alkali Lignin-Based Gel-like Biogreases. *Tribol. Int.* **2020**, *146*, 106231. [CrossRef]

94. Abdollah, M.F.B.; Amiruddin, H.; Jamallulil, A.D. Experimental Analysis of Tribological Performance of Palm Oil Blended with Hexagonal Boron Nitride Nanoparticles as an Environment-Friendly Lubricant. *Int. J. Adv. Manuf. Technol.* **2020**, *106*, 4183–4191. [CrossRef]
95. Choudhury, N.D.; Saha, N.; Bhaumik, S.; Kataki, R. Production and Evaluation of Physicochemical, Rheological, and Tribological Properties of *Cucurbita pepo* L. Seed Oil. *Biomass Convers. Biorefin.* **2023**, *13*, 1101–1114. [CrossRef]
96. Kumar, R.; Gautam, R.K. Tribological Investigation of Sunflower and Soybean Oil with Metal Oxide Nanoadditives. *Biomass Convers. Biorefin.* **2022**. [CrossRef]
97. Sharma, U.C.; Sachan, S. Friction and Wear Behavior of Karanja Oil Derived Biolubricant Base Oil. *SN Appl. Sci.* **2019**, *1*, 668. [CrossRef]
98. Sunil Kumar, D.; Garg, H.C.; Kumar, G. Tribological Analysis of Blended Vegetable Oils Containing CuO Nanoparticles as an Additive. *Mater. Today Proc.* **2021**, *51*, 1259–1265. [CrossRef]
99. Sajeeb, A.; Rajendrakumar, P.K. Experimental Studies on Viscosity and Tribological Characteristics of Blends of Vegetable Oils with CuO Nanoparticles as Additive. *Micro Nano Lett.* **2019**, *14*, 1121–1125. [CrossRef]
100. Abbas, D.M.; Shoaib, A.M.; ElKady, M.Y.; Ismail, E.A.; Hussuen, M.F.; El-Adly, R.A. A Study on Preparation and Evaluation of the Thread Greases from Renewable Resources Part 1: Tribological Performance of Prepared Polymerized Jojoba Grades Including Jojoba Oil and Their Optimization. *Egypt. J. Chem.* **2022**, *65*, 411–419. [CrossRef]
101. Rawat, S.S.; Harsha, A.P. The Lubrication Effect of Different Vegetable Oil-Based Greases on Steel-Steel Tribo-Pair. *Biomass Convers. Biorefin.* **2022**. [CrossRef]
102. Fathurrahman, N.A.; Auzani, A.S.; Zaelani, R.; Anggarani, R.; Aisyah, L.; Maymuchar; Wibowo, C.S. Lubricity Properties of Palm Oil Biodiesel Blends with Petroleum Diesel and Hydrogenated Vegetable Oil. *Lubricants* **2023**, *11*, 176. [CrossRef]
103. Singh, Y.; Negi, P.; Yadav, A.; Tripathi, R. Friction and Wear Characterization of Chemically Treated Styrax Officinalis L Vegetable Oil. *Mater. Today Proc.* **2021**, *46*, 10507–10509. [CrossRef]
104. Mahara, M.; Singh, Y. Tribological Analysis of the Neem Oil during the Addition of SiO2 Nanoparticles at Different Loads. *Mater. Today Proc.* **2020**, *28*, 1412–1415. [CrossRef]
105. Rajaganapathy, C.; Rajamurugan, T.V.; Dyson Bruno, A.; Murugapoopathi, S.; Armstrong, M. A Study on Tribological Behavior of Rice Bran and Karanja Oil-Based Tio2 Nano Bio-Fluids. *Mater. Today Proc.* **2022**, *57*, 125–129. [CrossRef]
106. Mohan Rastogi, P.; Kumar, R.; Kumar, N. Effect of SiO2nanoparticles on the Tribological Characteristics of Jatropha Oil. *Mater. Today Proc.* **2021**, *46*, 10109–10112. [CrossRef]
107. Rajaganapathy, C.; Vasudevan, D.; Murugapoopathi, S. Tribological and Rheological Properties of Palm and Brassica Oil with Inclusion of CuO and TiO2 Additives. *Mater. Today Proc.* **2020**, *37*, 207–213. [CrossRef]
108. Şirin, Ş.; Akıncıoğlu, S.; Gupta, M.K.; Kıvak, T.; Khanna, N. A Tribological Performance of Vegetable-Based Oil Combined with GNPs and HBN Nanoparticles on the Friction-Wear Tests of Titanium Grade 2. *Tribol. Int.* **2023**, *181*, 108314. [CrossRef]
109. Singh, D.; Ranganathan, A.; Diddakuntla, G. Tribological Analysis of Putranjiva Oil with Effect of CuO as an Additive. *Mater. Today Proc.* **2021**, *46*, 10634–10637. [CrossRef]
110. Singh, Y.; Negi, P.; Yadav, A. Friction and Wear Analysis of Transesterified Crambe Abyssinica Oil at Different Loads. *Mater. Today Proc.* **2021**, *46*, 10523–10526. [CrossRef]
111. Yoshida, K.; Naganuma, Y.; Kano, M. Effect of Degree of Unsaturation in Vegetable Oils on Friction Properties of Dlc Coatings. *Tribol. Online* **2021**, *16*, 210–215. [CrossRef]
112. Loehlé, S.; Matta, C.; Minfray, C.; Le Mogne, T.; Iovine, R.; Obara, Y.; Miyamoto, A.; Martin, J.M. Mixed Lubrication of Steel by C18 Fatty Acids Revisited. Part II: Influence of Some Key Parameters. *Tribol. Int.* **2016**, *94*, 207–216. [CrossRef]
113. Vafaei, S.; Jopen, M.; Jacobs, G.; König, F.; Weberskirch, R. Synthesis and Tribological Behavior of Bio-Based Lubrication Greases with Bio-Based Polyester Thickener Systems. *J. Clean. Prod.* **2022**, *364*, 132659. [CrossRef]
114. Vafaei, S.; Fischer, D.; Jopen, M.; Jacobs, G.; König, F.; Weberskirch, R. Investigation of Tribological Behavior of Lubricating Greases Composed of Different Bio-Based Polymer Thickeners. *Lubricants* **2021**, *9*, 80. [CrossRef]
115. Zhornik, V.I.; Zapolsky, A.V.; Ivakhnik, A.V. The Structure and Properties of a Biodegradable Grease with a Mixed Dispersion Medium and a Heterogeneous Lithium–Calcium Dispersed Phase. *J. Frict. Wear* **2022**, *43*, 229–235. [CrossRef]
116. Padgurskas, J.; Johns, E.I.; Radulescu, I.; Radulescu, A.V.; Rukuiža, R.; Snitka, V.; Kreivaitis, R.; Kupčinskas, A.; Volskis, D. Tribological Study of Beeswax-Thickened Biogrease and its Modification with Carbon Nanoparticles. *Tribol. Int.* **2023**, *184*, 108465. [CrossRef]
117. Delgado, M.A.; Quinchia, L.A.; Spikes, H.A.; Gallegos, C. Suitability of Ethyl Cellulose as Multifunctional Additive for Blends of Vegetable Oil-Based Lubricants. *J. Clean. Prod.* **2017**, *151*, 1–9. [CrossRef]
118. Quinchia, L.A.; Delgado, M.A.; Reddyhoff, T.; Gallegos, C.; Spikes, H.A. Tribological Studies of Potential Vegetable Oil-Based Lubricants Containing Environmentally Friendly Viscosity Modifiers. *Tribol. Int.* **2014**, *69*, 110–117. [CrossRef]

Publicación II

Elsevier 2024

Claudia Sanjurjo, Oulego P, Rodríguez E, Battez AH. Biodiesel production from the microalgae *Nannochloropsis gaditana*: Optimization of the transesterification reaction and physicochemical characterization. Biomass and Bioenergy 2024;185:107240. https://doi.org/10.1016/j.biombioe.2024.107240.

Biomass and Bioenergy 185 (2024) 107240

Contents lists available at ScienceDirect

Biomass and Bioenergy

journal homepage: www.elsevier.com/locate/biombioe

Biodiesel production from the microalgae *Nannochloropsis gaditana*: Optimization of the transesterification reaction and physicochemical characterization

C. Sanjurjo [a], P. Oulego [b], M. Bartolomé [c], E. Rodríguez [a,*], R. Gonzalez [c], A. Hernández Battez [a]

[a] Department of Construction and Manufacturing Engineering, University of Oviedo, Pedro Puig Adam, s/n, 33203, Gijón, Spain
[b] Department of Chemical and Environmental Engineering, University of Oviedo, C/Julián Clavería s/n, E-33071, Oviedo, Spain
[c] Department of Marine Science and Technology, University of Oviedo, Blasco de Garay, s/n, 33203, Gijón, Spain

ARTICLE INFO

Keywords:
Biodiesel
Microalgae
Transesterification
Optimization
Response surface methodology

ABSTRACT

The current environmental scenario has encouraged the study of renewable and competitive alternative feedstocks for biodiesel production. Microalgae present a significant opportunity as a feedstock that does not require arable land and can be cultivated using wastewater. The paper investigates the optimization of biodiesel production from microalgae *Nannochloropsis gaditana* bio-oil using response surface methodology and also analyzes the main physicochemical properties of the bio-oil. It was confirmed that this methodology is suitable for materials with low homogeneity. The model is also adequate for determining optimal experimental conditions, resulting in a FAME content of 87.25 %. The biodiesel's physicochemical properties were analyzed. It was discovered that the high degree of unsaturation in the microalgae bio-oil's chemical structure resulted in a narrower temperature range for its application compared to other vegetable sources.

1. Introduction

The energy industry has shown clear evidence of the urgent need for change over the past decade due to fuel price inflation and the environmental impact of global warming. As fossil resources become scarcer, attention has turned to more environmentally friendly alternatives, such as natural-based biodiesel. Biodiesel, defined by ASTM D6751 [1], refers to mono-alkyl esters of fatty acids derived from vegetable oils and animal fats. Biofuels offer several advantages over petroleum-based fuels. They are more efficient, have lower sulfur and aromatic content, better lubricity, higher cetane number, higher flash point, and a positive energy balance [2,3]. Furthermore, biofuels are renewable, portable, non-toxic, non-flammable, biodegradable, and reduce most regulated exhaust emissions. Additionally, using vegetable-based sources can help grow rural economies and reduce reliance on petroleum-based fuels, ultimately lowering the cost of the final product [4]. However, biodiesel has limitations due to poor flow properties at low temperatures, inadequate storage performance caused by low oxidative stability, and potential NOx emissions, especially when used in older engines without new emission reduction technologies [2].

The four main categories of biodiesel are based on the feedstock used: 1st generation, which uses edible crops; 2nd generation, which uses non-edible crops that require arable land; 3rd generation, which is derived from microalgae, bacteria, fungi, etc.; and 4th generation, which uses genetically modified microalgae [5]. The 1st generation satisfies over two-thirds of the world's bioenergy needs and comprises all arable crops [4,6]. The use of plant resources for energy production has raised concerns about competition with food sources and water supplies. This highlights the problem of water and food scarcity in today's world [7,8]. Increased production costs and higher food prices have resulted. The 2nd generation of plant-based energy sources was developed to address the limitations of the 1st generation. This group includes animal fats, agricultural waste, and oil waste [3,9]. These products are easy to access and do not require investment in cultivation or harvesting since they are waste primary products. This reduces the overall process cost. However, their availability is not fixed and may be insufficient. Additionally, they require pre-treatment to remove any impurities present in the waste [7]. Third-generation biodiesel uses microalgae-derived biomass, which has the advantage of not requiring arable land. Microorganisms can grow in wastewater and absorb nutrients and impurities, making them useful for purifying polluted water [5,10]. The third generation of microorganisms is becoming more popular due to its advantages over the first and second

* Corresponding author.
E-mail address: eduardo@uniovi.es (E. Rodríguez).

https://doi.org/10.1016/j.biombioe.2024.107240
Received 3 January 2024; Received in revised form 24 April 2024; Accepted 2 May 2024
Available online 6 May 2024

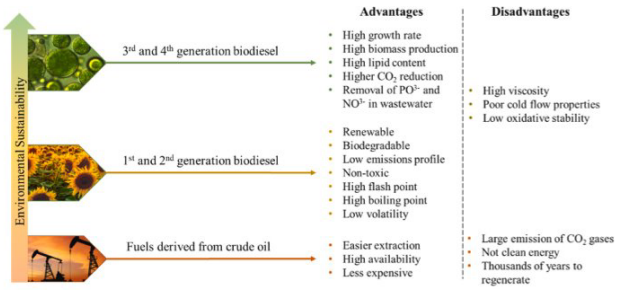

Fig. 1. Advantages and disadvantages of the different feedstocks used in the production of diesel and biodiesel.

Fig. 2. Biodiesel production through transesterification reaction [5].

generations. For example, it does not require arable land and can treat contaminated water. Additionally, it has a high growth rate and high lipid content [11]. The 4th generation is expected to include biomass derived from genetically modified microalgae. This offers the possibility of modifying the molecular structure of the microorganism [12–14]. Fig. 1 summarizes the benefits of vegetable-based fuels and the differences between generations of biodiesel. Microalgae have advantages over vegetable sources, including a high growth rate, high biomass production per culture, higher lipid content, and greater reduction of greenhouse gases (GHG), phosphate, and nitrate compounds [15,16].

In 2016, the European Federation of Transport and Environment evaluated the CO2 emissions of biofuels compared to fossil fuels [17]. The data shows that fossil fuels emit 94.1 g CO2/MJ, while 1st generation biofuels emit over 100 g CO2 eq./MJ due to land-use change emissions. According to 2022 world energy supply ranking, biofuels from edible crops accounted for 9.03 % of the total [18]. Using microalgae could have helped free up land, reduce food costs, and prevent the emission of nearly 9 % of CO_2 eq./MJ caused by land use change.

In the early 1990s, researchers including P. G. Roessler et al. [19] investigated the potential of microalgae for biodiesel production. They found that these microorganisms were capable of accumulating lipids, with a lipid content of up to 60 % relative to the total cell mass. Microalgae can modify their compositionby changing cultivation parameters such as salinity, temperature, light intensity, O2 concentration, agitation, light/dark cycle, or nutrients (carbon, nitrogen, phosphorus …) [20–22]. After selecting the microalgae strain, it must be cultured for optimal growth, harvested and dried to obtain the corresponding biomass. The bio-oil, which is primarily composed of triglycerides, is extracted through solvent-based processes [23–26]. The transesterification reaction is the technique used to convert bio-oil into biodiesel. This reaction involves the reaction of a triglyceride with an alcohol under heat conditions in the presence of a catalyst. The main product of this reaction is modified fatty acids, with glycerol as a secondary product (Fig. 2).

The structure of triglyceride consists of three fatty acids (FA) linked by a glycerol molecule. The transesterification reaction occurs independently for each FA, resulting in a stepwise reaction. Fatty acids with one or more double bonds are less stable against oxidation. Unsaturation promotes hydrolytic degradation and oxidative damage to the carbon atoms adjacent to the bond [27,28]. Vegetable oils have carbon chains ranging from 8 to 20 carbons, while microalgae predominantly have chains of 16–24 carbon atoms. Microalgal FAs usually contain more double bonds than crop oils, with chains having 5 or 6 double bonds [29,30].

For basic transesterifications, simple alcohols like methanol (MeOH) or ethanol (EtOH) are commonly used. This results in fatty acid methyl esters (FAME) and fatty acid ethyl esters (FAEE), respectively [31–33]. The catalyst type can also differ between heterogeneous, homogeneous, or enzymatic, in addition to the acidity (acidic or basic) [34–36]. Industrially, biodiesel (FAME) is obtained by using MeOH in the presence of a basic catalyst such as KOH or CH3ONa [10,31]. If the bio-oil feed has a high free fatty acid (FFA) content, it is necessary to perform esterification before use. This process involves reducing the FFA content through transesterification reaction with an acid catalyst. It is recommended to perform the esterification reaction when the FFA concentration is greater than 2–4 mg KOH/g [37]. Moisture is also a crucial factor to consider during the conversion process. This helps to avoid a secondary saponification reaction that can negatively impact the final product's quality and reduce the conversion yield [2].

To produce high-quality biodiesel from vegetable sources, it is important to optimize the transesterification reaction. Table 1 provides a list of research conducted on optimizing this reaction for biodiesel production.

To optimize the process, it is necessary to select independent input variables such as the bio-oil to alcohol ratio, reaction temperature, reaction time, and catalyst amount. Finally, one or more output variables are selected to analyse the impact of the variation in input parameters. Previous studies on microalgae biodiesel production have used a simple experimental design (TR) [38,39,42,43,45]. This methodology involves changing one variable while keeping the other parameters constant, which requires a large number of experiments. Several microalgae strains, including *C. protothecoides* [38,45], *N. gaditana* [39], and *C. vulgaris* [42,43], have been optimized for biodiesel production using this approach. However, this process is time-consuming and resource-intensive due to the significant number of experiments required.

Response surface methodology (RSM) is mathematical technique that evaluates the effect of each parameter (or input variable) and their interactions with the response (or output parameter). It provides an alternative to reduce the number of runs. RSM has been applied in biodiesel production, mainly focusing on feedstocks with simple and highly homogeneous materials such as 1st and 2nd generation vegetable oils like palm, sunflower, soybean, neem, and waste cooking oils. Recent studies have used this methodology to analyse complex and less

Table 1
Design of experiments for the optimization of biodiesel production from vegetable oils.

Feedstock	Experimental Design	Independent factors	Outputs	Ref.
Chlorella protothecoides	TR	Alcohol ratio (molar), temperature (°C), time (h)	Conversion rate (%)	[38]
Nannochloropsis gaditana	TR	Alcohol ratio (mL/g), temperature (°C), time (h)	Conversion rate (%)	[39]
Palm oil	TR	Catalyst calcination temperature (°C), catalyst (%), alcohol ratio (molar), temperature (°C), stirring speed (rpm)	FAME yield (%)	[40]
Rice bran	TR	Catalyst (g), alcohol ratio (ml)	Conversion rate (%)	[41]
Chlorella vulgaris	TR	Alcohol ratio (mL), temperature (°C), catalyst (%), time (min)	FAME yield (%)	[42]
Chlorella vulgaris	TR	Alcohol ratio (molar); temperature (°C), time (min)	FAME yield (%)	[43]
Waste cooking oil	TR	Alcohol ratio (molar), temperature (°C), time (min)	FAME content (%)	[44]
Chlorella protothecoides	TR	Alcohol ratio (molar), temperature (°C), catalyst (%)	Conversion rate (%)	[45]
Jatropha curcas Elaeis guineensis (palm)	RSM	Alcohol ratio (molar), catalyst (%)	FAME/FAEE content (%)	[46]
Sunflower oil	RSM	Alcohol ratio (molar), temperature (°C), catalyst (g)	Viscosity (cSt)	[47]
Refined soybean oil (RSO)	RSM	Alcohol ratio (molar), temperature (°C), catalyst (%), ultrasound power (W)	Conversion rate (%)	[48]
Pistacia lentiscus	RSM	Alcohol ratio (molar), temperature (°C), catalyst (%)	FAME yield (%)	[49]
Food grade refined palm oil (RPO)	RSM-CCD	Alcohol ratio (molar), temperature (°C) time (h), catalyst (%)	Conversion rate (%)	[36]
Neem oil	RSM-CCD	Alcohol ratio (molar), temperature (°C), time (h), catalyst (%), stirring speed (rpm)	Conversion rate (%)	[9]
Palm oil	RSM-CCD	Alcohol ratio (ml), time (min), catalyst (%)	FAME yield (%)	[50]
Rubber seed oil	RSM-CCD	Alcohol ratio (molar), temperature (°C), time (min), catalyst (%)	Conversion rate (%)	[51]
Chlorella vulgaris + castor oil	RSM-CCD	Alcohol ratio (mL), temperature (°C), catalyst (%)	Conversion rate (%)	[52]
Chlorella protothecoides	RSM-CCD	Alcohol ratio (mol/mol), temperature (°C), residence time (min), pressure (bar), water content (wt%)	FAME yield (%)	[53]
Chlorella variabilis	RSM-CCD	Alcohol ratio (molar), temperature (°C), time (min), catalyst (wt%)	FAME yield (%)	[54]
Spirulina platensis	RSM-CCD	Alcohol ratio (mL/g), temperature (°C), co-solvent ratio (mL/g), time (min), water content (%)	FAME yield (%)	[55]
Brassica campestris	RSM-CCRD	Alcohol ratio (molar), temperature (°C), time (min), catalyst (%)	Conversion rate (%) Viscosity (mm^2/s) Cetane number	[56]
Spirogyra crassa	RSM-CCRD	Alcohol ratio (molar), temperature (°C), time (min), catalyst (%)	FAME yield (%)	[57]
Palm oil	RSM-BBD	EFI (V/cm), time (min)	Conversion rate (%)	[58]
Palm oil	RSM-BBD	Alcohol ratio (molar), temperature (°C), time (min)	FAME yield (%)	[34]
Nannochloropsis gaditana	RSM-BBD	Alcohol ratio (mL/g), catalyst (%), hexane/SL ratio (mL/g)	FAME yield (%)	[59]

homogeneous materials, such as microalgae oils. In most cases, researchers preferred the central composite design (CCD) as the experimental design when dealing with fewer than four independent variables. CCD was used by Nan et al. [53], Nirmala et al. [54], and Mohamadzadeh et al. [55] to optimize the transesterification reaction and achieve the highest FAME yield in microalgae, such as *C. protothecoides*, *C. variabilis*, and *S. platensis*. Beyene et al. [52] used RSM via CCD to optimize the production of biodiesel from a mixture of castor oil and the microalgae *C. vulgaris*.

Macías-Sánchez et al. [59,60] conducted two studies to optimize the FAME yield of direct transesterification of wet *N. gaditana* biomass. In the first study, they optimized temperature and reaction time using a simple experimental design without RSM [60]. Later, they applied RSM-CCD to optimize the catalyst concentration, alcohol, and hexane ratio on the same material, using the optimal conditions of temperature and reaction time obtained in the first study [59].

The aim of this work is to optimize the production of biodiesel from the bio-oil extracted from the microalgae *Nannochloropsis gaditana (N. gaditana)* through transesterification. The study focused solely on microalgae bio-oil, not wet biomass. All independent variables, including alcohol ratio, temperature, and reaction time, were optimized in a single study. A physicochemical characterization was performed to fully understand the resulting product.

Table 2
Input variables and levels for optimizing the MBO transesterification reaction.

Input variables	Factor	Variable levels				
		−2 (−α)	−1	0	+1	+2 (+α)
Bio-oil:methanol ratio	A	1:3	1:6	1:9	1:12	1:15
Reaction temperature (°C)	B	30	50	70	90	110
Reaction time (min)	C	30	67.5	105	142.5	180

Table 3
Design of experiments and responses.

Std. order	Run order	Factorial input variable			Responses, Y		
		A	B	C	Actual	Predicted	
					Y (%)	Y (%)	Error (%)
11	1	0	−2	0	81.81	84.18	2.90
18	2	0	0	0	78.52	78.90	0.49
2	3	1	−1	−1	86.99	88.87	2.16
6	4	1	−1	1	72.69	68.89	5.24
10	5	2	0	0	70.35	69.88	0.67
4	6	1	1	−1	70.37	67.05	4.72
9	7	−2	0	0	33.44	37.44	11.95
13	8	0	0	−2	50.90	52.80	3.74
3	9	−1	1	−1	35.21	35.45	0.66
8	10	1	1	1	62.08	64.63	4.11
1	11	−1	−1	−1	67.09	60.95	9.15
7	12	−1	1	1	65.57	60.11	8.33
14	13	0	0	2	55.80	57.48	3.02
12	14	0	2	0	53.22	54.42	2.25
5	15	−1	−1	1	68.31	68.05	0.37
15	16	0	0	0	77.44	78.90	1.88
17	17	0	0	0	77.72	78.90	1.52
16	18	0	0	0	78.35	78.90	0.70

2. Materials and method

2.1. Bio-oil characterization

N. gaditana was chosen because of its high lipid content, which makes it a promising source for bio-oil production. This strain of microalgae has been reported to accumulate up to 68 % (%wt.) lipid content in the best cases [61]. The bio-oil used in this study (MBO) was provided by Neoalgae (Gijon, Spain).

The MBO's TAN was measured with a Metrohm 848 Tritino PLUS (accuracy ±0.01 mg KOH/g) following ASTM D664 to determine if esterification was necessary. The water content was also measured with a Metrohm 899 Karl Fischer coulometer (accuracy ±0.1 ppm).

The SL was determined using the method outlined by Callejón et al. [39]. The analysis provides the SL content per unit of lyophilized MBO and the lipid profile. This is achieved through a transesterification reaction with a solution of MeOH and acetyl chloride.

The lipid profile was analyzed using gas chromatography with flame ionization detector (GC-FID) following the UNE-EN 14103 standard after the transesterification reaction with acetyl chloride. The equipment used was a Clarus 690 (PerkinElmer) with an Elite-WAX column (30 m × 0.25 mm x 0.25 μm). The oven temperature was programmed in the following sequence: (1) hold at 60 °C for 2 min, (2) heat from 60 °C to 200 °C at 10 °C/min, (3) heat from 200 °C to 240 °C at 5 °C/min, (4) hold at 240 °C for 7 min. Hydrogen was used as the carrier gas, and the detector temperature was set at 250 °C with a flow rate of 2 mL/min. The injector was a split system with a set temperature of 250 °C and a sample volume of 1 μL. The sample was prepared at a concentration of 5 mg biodiesel per mL toluene. The detectable minimum concentration by GC-FID analysis was 1 %.

2.2. Transesterification reaction

2.2.1. Design of Experiments (DOE)

The MBO transesterification reaction was optimized using RSM. Design Expert 13 software was employed with a two-level factorial

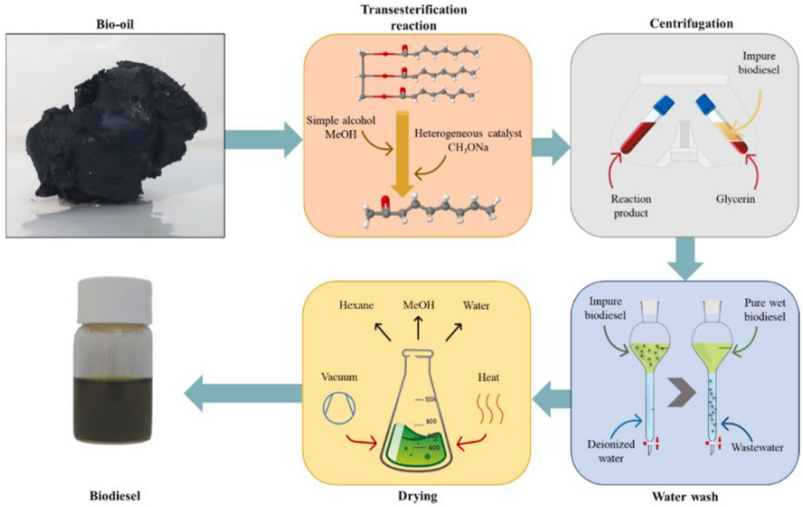

Fig. 3. Biodiesel purification process after transesterification.

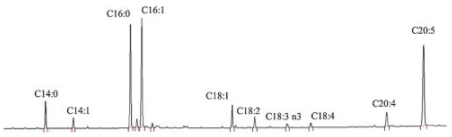

Fig. 4. Lipid profile chromatogram.

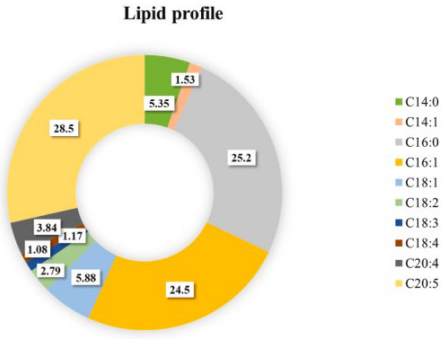

Fig. 5. Distribution of fatty acids in *N. gaditana*.

Table 4
Lipid content and fatty acids distribution of different of *N. gaditana* cultures.

SFA (%)	MUFA (%)	PUFA (%)	Total lipid content (%)	Ref.
30.55	31.91	35.6	35	Current
19	20.5	26.5	10.8	[67]
31.17	30.27	20.79	14	[20]
36.49	18.34	43.41	24.11	[66]
52.47	40.36	7.16	29.73	[68]
24.59	34.41	41	17.82	[69]
29.78	20.49	25.31	–	[70]

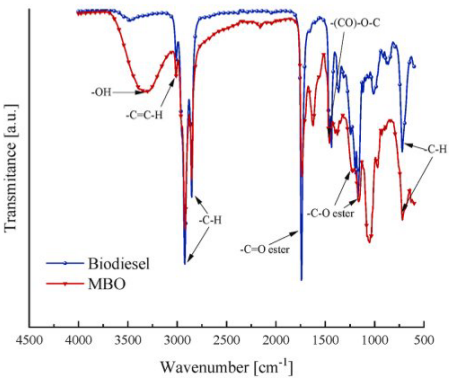

Fig. 6. FTIR spectra of bio-oil and biodiesel.

Table 5
ANOVA analysis of the fitting model for Y.

Source	*df*	*F* value	*p* value	Remark
Model	9	24.28	<0.0001	significant
A - Bio-oil:methanol ratio	1	61.52	<0.0001	
B - Reaction temperature	1	51.75	<0.0001	
C - Reaction time	1	1.29	0.2891	
AB	1	0.3973	0.5461	
AC	1	21.44	0.0017	
BC	1	9.02	0.0170	
A^2	1	50.70	<0.0001	
B^2	1	7.35	0.0266	
C^2	1	45.03	0.0002	
Residual	8			
Lack of Fit	5	105	0.0014	significant
Model summary	R^2	R^2 (adj.)	R^2 (pred.)	Adeq. Precision
	0.9647	0.9250	0.7366	17.3292

approach resulting in CCD [62]. Three numerical factors (input variables) were selected: bio-oil:methanol ratio (A), reaction temperature (B), and reaction time (C). Table 2 shows the values chosen for each input variable. They were chosen after a thorough evaluation of previous studies on biodiesel production from vegetable sources (Table 1). The parameter levels are coded as −1 (minimum), 0 (center), +1 (maximum), and ± α (extreme star points), as shown in Table 2. The distance between α and the center point was set at 2. The study consisted of eighteen runs in total, including eight factorial design runs, six star points, and four replications of the center point, as detailed in Table 3 [63]. The FAME conversion (Y) was evaluated based on to Eq. (1). Optimization runs were conducted using 1 g of MBO as a simple size and 2 mL of hexane in the presence of the basic catalyst CH_3ONa at 1.5 %.

$$Y(FAME\ conversion\ \%) = \frac{Amount\ transformed\ to\ FAME\ (g)}{Total\ SL\ amount\ convertible\ to\ FAME\ (g)} \times 100 \quad \text{Eq.1}$$

2.2.2. Purification process

After completing the transesterification reaction is complete, a purification process is necessary to remove any impurities mixed with the biodiesel. The purification steps used in this study are illustrated in Fig. 3.

After the transesterification reaction, the resulting product was centrifuged at 7000 rpm for 10 min using a Microcen 24 - CE 202 to recover the biodiesel and remove the glycerol formed during the reaction. The liquid was then washed with deionized water until it reached a neutral pH. This step is essential to remove non-reacting MeOH, catalyst residues, and other impurities present in the MBO. Finally, the solution was transferred to a rotary evaporator (Hei-Vap Core, Heidolph) and evaporated at 60 °C and 20 mbar for 20 min to remove any remaining hexane, moisture, and MeOH.

2.3. Biodiesel physicochemical characterization

The GC-FID equipment was used to evaluate the FAME content for all runs. The quantitative analysis was performed according to UNE-EN 14103 using the procedure previously described for the lipid profile, with methyl nonadecanoate as an internal standard.

The density and dynamic viscosity of the samples were determined using a high-precision rotational viscometer (Stabinger SVM 3001) in accordance with the ASTM D7042 guidelines under atmospheric pressure conditions. The density was determined at a temperature of 20 °C, while the viscosity was determined at a temperature of 40 °C.

To determine the pour point (PP), Differential Scanning Calorimetry (DSC Mettler 822e 700) analysis was used, which has a heat flow accuracy of better than ± 2 % and a temperature accuracy of ±1 °C. This

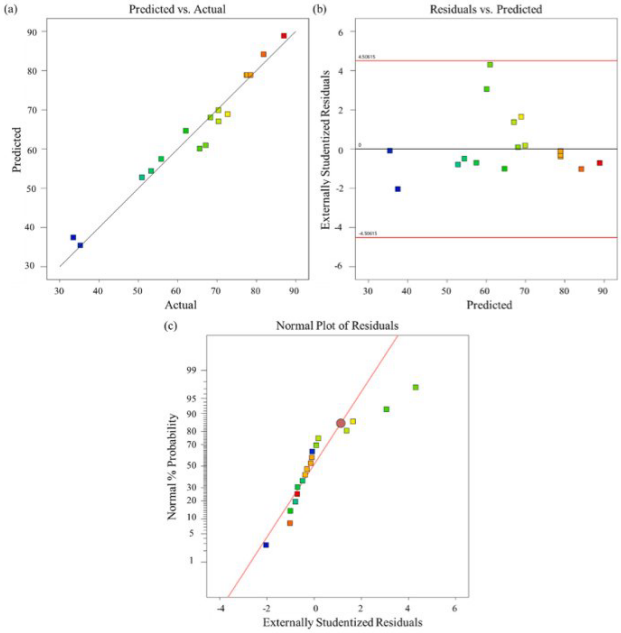

Fig. 7. Statistical analysis of the quadratic model generated for the response Y: (a) Predicted vs. Actuals; (b) Residuals vs. Predicted; (c) Normal plot of Residuals.

technique can provide a direct measurement of the change in enthalpy for a system during cooling, which can be approximated by the sample PP [64]. The procedure involves heating the sample to 50 °C at a steady rate of 10 °C/min and then holding it under isothermal conditions for 10 min. The system is then cooled to −50 °C at a steady rate of 10 °C/min under a nitrogen atmosphere. The PP value can be obtained at the maximum point of the curve by using Heat flow (W/g) versus temperature plots [65]. Additionally, the composition was analyzed using a Fourier Transform Infrared (FTIR) spectrometer (Varian 670-IR) with an accuracy of better than 0.07 cm^{-1}.

Thermal stability (TS) was evaluated using thermogravimetric analysis (TGA). The TA Instruments DSC SDT Q600 TGA & DSC was used for the analysis, which has a temperature accuracy of 0.001 °C (200–1300). The results were analyzed using TA Instruments Universal Analysis 2000 version software. The sample, approximately 6 mg, underwent dynamic scans at a constant heating rate of 20 °C/min from 25 to 600 °C under a nitrogen atmosphere at a flow rate of 50 mL/min. The sample's weight loss was plotted against time to obtain the onset temperature of decomposition.

The modified Cleveland Open Cup Tester, following EN ISO 2592 and ASTM D92 standards, was used to determine the flash point (FP). To determine the FP, 15 mL of biodiesel was gradually heated from room temperature in 5 °C increments until the FP was reached.

3. Results and discussion

3.1. Lipid profile and molecular structure

Fig. 4 displays the chromatogram of the lipid profile of the MBO, while Fig. 5 shows the distribution of FAs. The FAs are evenly balanced between saturated (SFA), monounsaturated (MUFA), and polyunsaturated (PUFA). The GC-FID analysis of the biodiesel sample revealed three major peaks: C16:0 (25.2 %), C16:1 (24.5 %), and C20:5 (28.5 %). Additionally, minor peaks were found between C14:0 to C20:4, which accounted for 21.64 % of the sample. Microalgae oils often contain long-chain fatty acids and numerous double bonds, which are not typical of crop oils. However, a high concentration of double bonds in the molecular structure of fatty acids negatively impacts the material's oxidative stability. The presence of 70 % unsaturated FAs indicates poor resistance to oxidation.

The results are consistent with other cultures of the same species. Callejón et al. [39] and Tang et al. [66] reported a similar lipid profile, as shown in Fig. 4. However, the lipid content of the studied oil is higher than that reported in the literature (Table 4), reaching a lipid content of 35 %. This difference could be attributed to variations in culture and growth stage. Optimizing triglyceride production is essential for biodiesel conversion during these stages.

Fig. 6 shows the FTIR spectrum, highlighting the structural differences between the original bio-oil and the biodiesel. A band at 3342.03 cm^{-1} indicates the presence of alcohol compounds (-OH) used in the bio-oil extraction process. The increase of the characteristic bands at 2921.63 cm^{-1} and 2852.2 cm^{-1} is due to the increase in (-CH_3) alkanes, which result from the breaking of the triglyceride structure. The decrease in bands between 715 and 725 cm^{-1} is due to the loss of alkenes (-CH_2). The constant band at 3012.27 cm^{-1} is attributed to the (-C═C-) bonds. Additionally, esters (-C═O) at 1739.48 cm^{-1}, methyl acetate compounds ((CO)–O–C) at 1434.78 cm^{-1}, and other methyl compounds (-C–C(O)–C) at 1166.72 cm^{-1} are consistently present. The

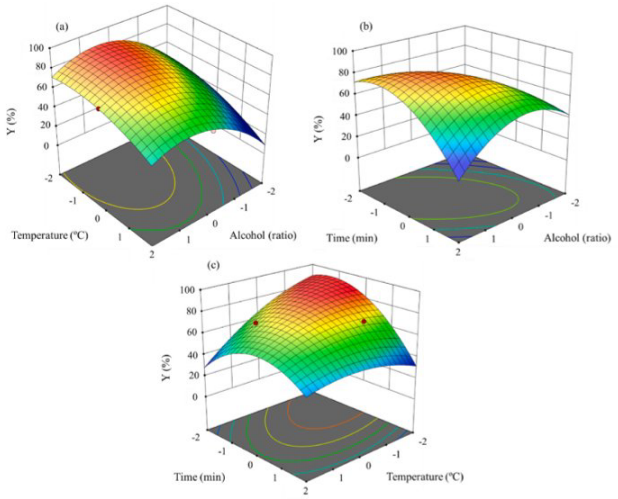

Fig. 8. Interaction between independent variables for response Y. (a) Interaction between temperature and alcohol ratio; (b) Interaction between reaction time and alcohol ratio; (c) Interaction between reaction time and temperature.

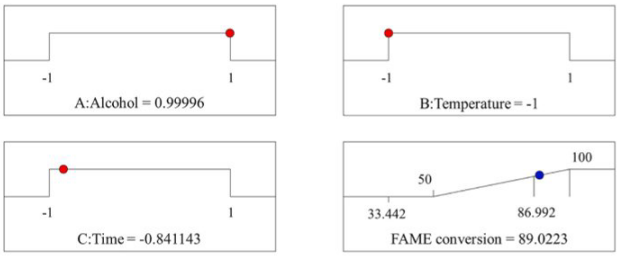

Fig. 9. Optimal conditions designed to produce desired results from independent variables using RSM-CCD.

spectrum of biodiesel obtained from *N. gaditana* agrees with those reported by other authors for the characterization of various vegetable biodiesels [34,51,57].

3.2. Optimization of transesterification reaction by RSM

3.2.1. Model adequacy check

After conducting the 18 tests, the empirical model correlating the input variables (coded) with Y (FAME conversion in %) was generated using a quadratic regression model fitted to Eq. (2):

$$Y = 78.90 + 8.11A - 7.44B + 1.17C + 0.9217AB - 6.77AC + 4.39BC - 6.31A^2 - 2.40B^2 - 5.94C^2 \quad \text{Eq.2}$$

The analysis of variance (ANOVA) was used to determine the interaction between each input variable and the response Y. The final results of the ANOVA analysis are summarized in Table 5.

The F and p values indicates the significance of the model [48]. An F-value of 24.28 and a p-value less than 0.05 indicate that the model terms are significant. A value of R^2 of 0.9647 means that this quadratic regression model can explain over 96.47 % of the changes in the output response. The adjusted R^2 is also consistent with this value at 0.9250. Adequate precision (Adeq. Precision) measures the signal-to-noise ratio. A ratio greater than 4 is desirable. Therefore, a ratio of 17.3293 indicates sufficient signal to allow the model to be used to navigate the design space.

Fig. 7 shows the statistical analysis for the model. In particular, Fig. 7 (a) compares the values predicted by Eq. (2) with the experimental values. The predicted values closely match the actual data, indicating a reasonable correlation between them. The differences between the experimental and predicted values are less than 10 % for all the runs, except for one point (run 7). This result is consistent with the reported R^2, R^2_{adj} and R^2_{pred}. The plot of the studentized residuals against the predicted values is shown in Fig. 7 (b). A random distribution of points is observed within the limit of ±5, indicating a constant discrepancy. This suggests that the models are suitable for their intended application

Table 6
Physicochemical characterization of bio-oil and biodiesel.

		Parameter					Ref.
		TAN	Humidity	PP	FP	TS (T_{onset})	
		mg KOH/g	ppm	°C	°C	°C	
Microalgae bio-oil (MBO)		1.11	1583.7	–	–	208.82	Current
Biodiesel	Microalgae	0.42	850	−7.2, −8.7	140–150	244.8	Current
	Soybean	0.34	–	−2	160	–	[72]
	Sunflower	0.41	–	−6	155	–	
	Corn	0.24	–	−5	140	–	
	Rice bran	0.71	–	−2	180	–	
	Olive	0.60	–	−6	155	–	
	Grape seed	–	–	−9	185	–	
	Edible waste	–	–	15	176	–	[73]
	Palm kernel	–	–	6	171	–	
	Chlorella vulgaris			−4.33	98.67		[74]
	Microalgae (not specified)	0.39		−10	165		[75]
	Chlorella protothecoides	0.224	183		183.9		[76]
	Spirulina platensis	0.75	39	−9	189	330	[77]

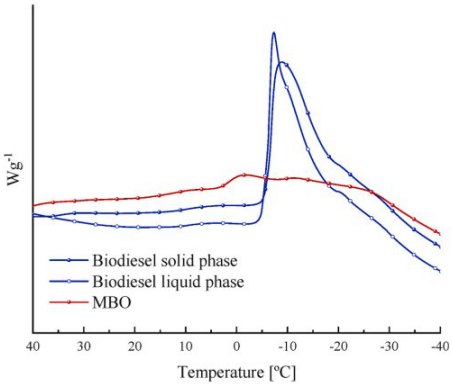

Fig. 10. DSC curve to study the PP of bio-oil and biodiesel.

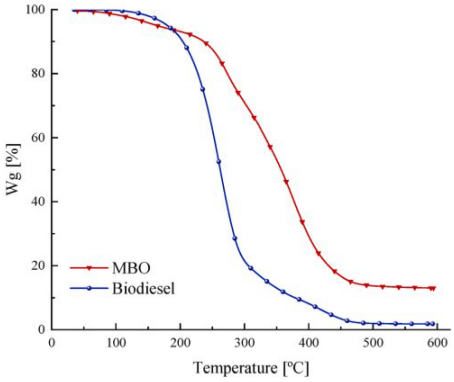

Fig. 11. TGA curve to study the thermal stability of bio-oil and biodiesel.

without requiring modifications to reduce the scatter [71]. Finally, Fig. 7 (c) shows the normalized residuals of Y. The studentized residuals follow a linear distribution that predicts the accuracy of the quadratic model, generally with an S-shape generated by an additional transformation of the response [57]. The lack of precision between the actual and predicted values may be due to the low homogeneity of the sample, as the lipid content is only 35 % of the total of the sample. Additionally, the interference of foreign compounds from the microalgae oils such as liposoluble pigments (astaxanthin or zeaxanthin), may interfere and are difficult to remove during the biodiesel purification stage [67].

The study examines how the independent variables interact with the response using a 3D surface plot (see Fig. 8). The impact of the alcohol ratio is evident in Fig. 8 (a) and (b), where low alcohol ratios consistently lead to low reaction yields. However, an optimal point is reached in relation to the other parameters at a coded value of 1 (ratio 1:12). Fig. 8 (a) and (c) illustrate the relationship between temperature and other variables. Extreme temperatures, both high and low, can negatively affect reaction performance, as can reaction time. However, these variables tend to balance each other out, resulting in optimal performance between 50 and 70 °C and 67.5–105 min.

3.2.2. Optimized conditions of the RSM analysis

The ANOVA-validated model was used to determine the best conditions for producing biodiesel from the chosen microalgae, using Eq. (2). The input variables were limited to the bio-oil:MeOH ratio, reaction temperature, and reaction time within the study range (−1, 1), and the responses were maximized at 100 %. The software provided options with the highest FAME conversion, and the one that required the least amount of time and temperature was chosen. The model suggests that the experimental conditions shown in Fig. 9 are the best for achieving the highest reaction yield.

The transesterification reaction's optimal conditions were determined by decoding the independent variable set values. The reaction time was 75 min, and the temperature was 50 °C, with a bio-oil to alcohol ratio of 1:12. These test conditions resulted in an 87.2549 % FAME conversion, validating the generated model with a 2.20 % error between actual and predicted values.

3.3. Biodiesel physicochemical characterization

Table 6 presents the physicochemical properties of the current biodiesel, MBO, and vegetable and microalgae biodiesels from other

studies. Moreover, the fluid was found to have a density of 885 kg/m^3 and a viscosity of 6.54 mPa s.

The low TAN values of the bio-oil simplified the preparation of the material before the transesterification reaction. A TAN of less than 2 mg KOH/g eliminated the need for a prior esterification due to the low levels of FFAs. The TAN slightly decreases after the reaction, possibly due to FFAs removal during purification or neutralization. Normal moisture levels for both compounds range from 850 to 1590 ppm, depending on ambient humidity. No drying was observed for the of bio-oil.

The working temperature range of the biodiesel was determined through PP and FP measurements. Fig. 10 shows the behavior of both samples during the freezing point test. The bio-oil exhibited a broad exothermic band during the test, and no freezing temperature was defined. In contrast, the biodiesel separated into a liquid and a solid phase. Both phases showed a clear peak. The liquid phase was at −7.2 °C, and the solid phase was at −8.7 °C. These values are slightly lower than those reported for biodiesel from other vegetable sources (see Table 6).

During the biodiesel FP measurements, the sample ignited slightly at 130 °C but remained constant until the temperature range of 140–150 °C was reached. The ASTM D6751 standard [1] states that the FP in biodiesel is never lower than 120 °C, so the sample falls within the acceptable range. However, this value is significantly lower than those reported in Table 6 for biodiesel derived from vegetable sources.

The thermal stability analysis is presented in Fig. 11. The test results indicate that the biodiesel sample degraded completely at the maximum temperature used. The onset of temperature degradation for the biodiesel occurred at 244.8 °C, which was slightly better than the bio-oil that had a T_{onset} at 208.82 °C. Additionally, the biodiesel sample experienced rapid mass loss once it reached 200 °C, while the bio-oil counterpart maintained a constant and lower mass loss until it reached 250 °C. The bio-oil experiences a second phase of degradation at this point, with a steeper slope leading up to 450 °C. The initial loss of mass in the bio-oil may be attributed to the presence of organic solvents or impurities, as its water content was negligible.

Dantas et al. [78] obtained results that agree with ours. They studied the thermal stability variation of corn bio-oil after transesterification for biodiesel production. The degradation curve of the biodiesel showed the same trend as that of the bio-oil, with an onset of mass loss later. Corn oil degradation also proceeded in several phases, similar to our findings. Chand, P. et al. [79] evaluated the variation of the curve obtained from the thermal stability analysis of a soybean bio-oil/biodiesel blend. The trends of the two materials separately were similar to those reported in this study. The authors observed a decrease in thermal stability at higher concentrations of bio-oil. The results showed an improvement in thermal stability when biodiesel (FAME) was used instead of bio-oil (triglycerides).

Mostafa, S. et al. [77] reported higher FP and thermal stability values for a biodiesel derived from S. platensis microalgae compared to the biodiesel studied here (Table 6). This difference can be attributed to the FA distribution, as S. platensis has a higher percentage of PUFAs (2.11 %) which promote better tolerance to biofuel degradation, while the biodiesel studied here has a lower percentage of PUFAs (35.6 %).

4. Conclusions

The study investigated the use of microalgae N. gaditana as a biodiesel feedstock. Optimization of the transesterification reaction by RSM and physicochemical characterization of the biodiesel were carried out. The results showed that RSM is suitable for optimizing the synthesis of biodiesel from low homogeneity materials such as microalgae bio-oil. Using the optimal conditions from the model, the FAME conversion increased to 87.25 %, surpassing previous studies.

However, due to the high presence of double bonds in the fatty acid chains, the final biodiesel's oxidative stability is classified as low and requires their removal. Additionally, the high degree of unsaturation resulted in a lower upper temperature limit, leading to a lower flash point and thermal stability. However, it improved the lower temperature limit by lowering the pour point when compared to first- and second-generation biodiesel.

Future research could explore the removal of double bonds in microalgae fatty acids through epoxidation or the use of antioxidant additives to mitigate their negative effects. Additionally, microalgae biodiesel could be investigated as a pour point depressant additive in diesel.

CRediT authorship contribution statement

C. Sanjurjo: Writing – original draft, Investigation, Conceptualization. **P. Oulego:** Supervision, Conceptualization. **M. Bartolomé:** Formal analysis, Data curation. **E. Rodríguez:** Writing – review & editing, Project administration, Investigation, Funding acquisition. **R. Gonzalez:** Formal analysis, Data curation. **A. Hernández Battez:** Writing – review & editing, Project administration, Investigation, Funding acquisition, Conceptualization.

Data availability

Data will be made available on request.

Acknowledgements

This publication is part of the R&D project PID2022-136656NB-I00, funded by MICIU/AEI/10.13039/501100011033/and by "FEDER/UE". The Foundation for the Promotion of Applied Scientific Research and Technology in Asturias (Spain) is also acknowledged for funding the contract of Claudia Sanjurjo at the University of Oviedo (Spain) [grant number: SV-PA-21-AYUD/2021/50987]. The authors of this work are grateful to the Institute of Industrial Technology of the University of Asturias (IUTA) for the financing of the project "OPTRANSESTERAL" (grant number SV-23-GIJON-1-05).

References

[1] ASTM D6751- 7d, Standard Specification for Biodiesel Fuel Blend Stock (B100) for Middle Distillate Fuels, 2007.
[2] G. Knothe, Biodiesel fuel quality and the ASTM standard, Palmas 31 (2010) 162–171.
[3] M. Kanan, M.S. Habib, A. Shahbaz, A. Hussain, T. Habib, H. Raza, Z. Abusaq, R. Assaf, A grey-fuzzy programming approach towards socio-economic optimization of second-generation biodiesel supply chains, Sustainability 14 (2022) 10169.
[4] D. Neupane, D. Bhattarai, Z. Ahmed, B. Das, S. Pandey, J.K.Q. Solomon, R. Qin, P. Adhikari, Growing jatropha (Jatropha curcas l.) as a potential second-generation biodiesel feedstock, Inventions 6 (2021) 60.
[5] C. Sanjurjo, E. Rodríguez, J.L. Viesca, A.H. Battez, Influence of molecular structure on the physicochemical and tribological properties of biolubricants: a review, Lubricants 11 (2023) 380.
[6] S. Brahma, B. Nath, B. Basumatary, B. Das, P. Saikia, K. Patir, S. Basumatary, Biodiesel production from mixed oils: a sustainable approach towards industrial biofuel production, Chem. Eng. J. Adv. 10 (2022) 100284.
[7] N.S.M. Aron, K.S. Khoo, K.W. Chew, P.L. Show, W.H. Chen, T.H.P. Nguyen, Sustainability of the four generations of biofuels – a review, Int. J. Energy Res. 44 (2020) 9266–9282.
[8] M.A.H. Shaah, M.S. Hossain, F.A.S. Allafi, A. Alsaedi, N. Ismail, M.O.A. Kadir, M. I. Ahmad, A review on non-edible oil as a potential feedstock for biodiesel: physicochemical properties and production technologies, RSC Adv. 11 (2021) 25018–25037.
[9] W.C. Ulakpa, R.O.E. Ulakpa, M.C. Egwunyenga, T.C. Egbosiuba, Transesterification of non-edible oil and effects of process parameters on biodiesel yield, Clean. Waste Syst. 3 (2022) 100047.
[10] K.S.H. Eldiehy, P. Bardhan, D. Borah, M. Gohain, M.A. Rather, D. Deka, M. Mandal, A comprehensive review on microalgal biomass production and processing for biodiesel production, Fuel 324 (2022) 124773.
[11] N.K. Kondrasheva, A. Eremeeva, Production of biodiesel fuel from vegetable raw materials, J. Min. Inst. 260 (2023) 248–256.
[12] S. Vuttipongchaikij, Genetic manipulation of microalgae for improvement of biodiesel production, Genom. Genet. 5 (2012) 130–148.

[13] M. Blanco-Vieites, D. Suárez-Montes, F. Delgado, M. Álvarez-Gil, A.H. Battez, E. Rodríguez, Removal of heavy metals and hydrocarbons by microalgae from wastewater in the steel industry, Algal Res. 64 (2022) 102700.
[14] M. Blanco-Vieites, D. Suárez-Montes, A. Hernández Battez, E. Rodríguez, Enhancement of *Arthrospira* sp. culturing for sulfate removal and mining wastewater bioremediation, Int. J. Phytoremediation 25 (9) (2023) 1116–1126. https://doi.org/10.1080/15226514.2022.2135680.
[15] M.S.J. Olia, M. Azin, A.A. Sepahi, N. Moazami, Miniaturized culture method for the statistical study of growth rate and carbohydrate content of Picochlorum sp. D8 isolated from the Persian Gulf, Renew. Energy 149 (2020) 479–488.
[16] L. Peng, D. Fu, H. Chu, Z. Wang, H. Qi, Biofuel production from microalgae: a review, Environ. Chem. Lett. 18 (2020) 285–297.
[17] European Federation for Transport and Environment, The Basis for Biofuel Policy Post-2020, 2020.
[18] IEA50, Total Biofuel Production by Feedstock, Main Case, 2021-2027, 2022.
[19] P.G. Roessler, L.M. Brown, T.G. Dunahay, D.A. Heacox, E.E. Jarvis, J.C. Schneider, S.G. Talbot, K.G. Zeiler, Genetic Engineering Approaches for Enhanced Production of Biodiesel Fuel from Microalgae, vol. 14, National Renewable Energy Laboratory, 1994, pp. 255–270.
[20] L.I. Farfán-Cabrera, M. Franco-Morgado, A. González-Sánchez, J. Pérez-González, B.M. Marín-Santibáñez, Microalgae biomass as a new potential source of sustainable green lubricants, Molecules 27 (2022) 1205.
[21] T.M.M. Bernaerts, L. Gheysen, I. Foubert, M.E. Hendrickx, A.M. Van Loey, Evaluating microalgal cell disruption upon ultra high pressure homogenization, Algal Res. 42 (2019) 101616.
[22] A. Hernández-Pérez, J.I. Labbé, Microalgae, culture and benefits, Rev. Biol. Mar. Oceanogr. 49 (2014) 157–173.
[23] M.K. Enamala, S. Enamala, M. Chavali, J. Donepudi, R. Yadavalli, B. Kolapalli, T. V. Aradhyula, J. Velpuri, C. Kuppam, Production of biofuels from microalgae - a review on cultivation, harvesting, lipid extraction, and numerous applications of microalgae, Renew. Sustain. Energy Rev. 94 (2018) 49–68.
[24] C. Onumaegbu, A. Alaswad, C. Rodriguez, A.G. Olabi, Optimization of pre-treatment process parameters to generate biodiesel from microalga, Energies 11 (2018) 806.
[25] S. Zhang, L. Zhang, G. Xu, F. Li, X. Li, A review on biodiesel production from microalgae: influencing parameters and recent advanced technologies, Front. Microbiol. 13 (2022) 970028.
[26] P.L. Show, M.S.Y. Tang, D. Nagarajan, T.C. Ling, C.W. Ooi, J.S. Chang, A holistic approach to managing microalgae for biofuel applications, Int. J. Mol. Sci. 18 (2017) 215.
[27] W. Wang, H. Liu, F. Li, H. Wang, X. Ma, J. Li, L. Zhou, Q. Xiao, Effects of unsaturated fatty acid methyl esters on the oxidation stability of biodiesel determined by gas chromatography-mass spectrometry and information entropy methods, Renew. Energy 175 (2021) 880–886.
[28] G.R. Stansell, V.M. Gray, S.D. Sym, Microalgal fatty acid composition: implications for biodiesel quality, J. Appl. Phycol. 24 (2012) 791–801.
[29] N.N. Zulu, K. Zienkiewicz, K. Vollheyde, I. Feussner, Current trends to comprehend lipid metabolism in diatoms, Prog. Lipid Res. 70 (2018) 1–16.
[30] E.G. Giakoumis, A statistical investigation of biodiesel physical and chemical properties, and their correlation with the degree of unsaturation, Renew. Energy 50 (2013) 858–878.
[31] M. Salaheldeen, A.A. Mariod, M.K. Aroua, S.M.A. Rahman, M.E.M. Soudagar, I.M. R. Fattah, Current state and perspectives on transesterification of triglycerides for biodiesel production, Catalysts 11 (2021) 1121.
[32] G.F. Silva, F.L. Camargo, A.L.O. Ferreira, Application of response surface methodology for optimization of biodiesel production by transesterification of soybean oil with ethanol, Fuel Process. Technol. 92 (2011) 407–413.
[33] J.W.Y. Lee, W.Y. Chia, W.J. Ong, W.Y. Cheah, S.S. Lim, K.W. Chew, Advances in catalytic transesterification routes for biodiesel production using microalgae, Sustain. Energy Technol. Assessments 52 (2022) 102336.
[34] C.S. Latchubugata, R.V. Kondapaneni, K.K. Patluri, U. Virendra, S. Vedantam, Kinetics and optimization studies using Response Surface Methodology in biodiesel production using heterogeneous catalyst, Chem. Eng. Res. Des. 135 (2018) 129–139.
[35] V. Singh, L. Belova, B. Singh, Y.C. Sharma, Biodiesel production using a novel heterogeneous catalyst, magnesium zirconate (Mg2Zr5O12): process optimization through response surface methodology (RSM), Energy Convers. Manag. 174 (2018) 198–207.
[36] D.N. Thoai, C. Tongurai, K. Prasertsit, A. Kumar, A novel two-step transesterification process catalyzed by homogeneous base catalyst in the first step and heterogeneous acid catalyst in the second step, Fuel Process. Technol. 168 (2017) 97–104, https://doi.org/10.1016/j.fuproc.2017.08.014.
[37] A.K. Azad, S.C. Sharma, M.G. Rasul, Clean Energy for Sustainable Development: Comparisons and Contrasts of New Approaches, 2017.
[38] X. Li, H. Xu, Q. Wu, Large-scale biodiesel production from microalga Chlorella protothecoides through heterotrophic cultivation in bioreactors, Biotechnol. Bioeng. 98 (2007) 764–771.
[39] M.J.J. Callejón, A.R. Medina, M.D.M. Sánchez, E.H. Peña, L.E. Cerdán, P.A. G. Moreno, E.M. Grima, Extraction of saponifiable lipids from wet microalgal biomass for biodiesel production, Bioresour. Technol. 169 (2014) 198–205.
[40] C. Sronsri, W. Sittipol, K. U-yen, Optimization of biodiesel production using magnesium pyrophosphate, Chem. Eng. Sci. 226 (2020) 115884, https://doi.org/10.1016/j.ces.2020.115884.
[41] A. Prabu, I. Premkumar, A. Pradeep, Production of ricebran biodiesel by the bubble wash method, Int. J. Ambient Energy 42 (2021) 981–984.
[42] N. Hasanudin, N.A. Ghani, A.H.A. Rahim, N.S. Azman, N.A. Rosdi, A.N. Masri, Optimization and kinetic studies on biodiesel conversion from chlorella vulgaris microalgae using pyrrolidinium-based ionic liquids as a catalyst, Catalysts 12 (2022) 277.
[43] S.T. Al-Humairi, J.G.M. Lee, M. Salihu, A.P. Harvey, Biodiesel production through acid catalyst in situ reactive extraction of chlorella vulgaris foamate, Energies 15 (2022) 4482.
[44] O. Paladino, M. Neviani, Sustainable biodiesel production by transesterification of waste cooking oil and recycling of wastewater rich in glycerol as a feed to microalgae, Sustainability 14 (2022) 273.
[45] X. Miao, Q. Wu, Biodiesel production from heterotrophic microalgal oil, Bioresour. Technol. 97 (2006) 841–846.
[46] T.A. Saavedra, L.B. Bueno-Borges, N. Sangaletti-Gerhard, S.M. de Alencar, M.A. B. Regitano-d'Arce, Optimized conventional and ultrasound-assisted ethyl transesterification of jatropha (Jatropha curcas) and palm (Elaeis guineensis) oil mixtures, Chem. Eng. Commun. 209 (2022) 1482–1495.
[47] J. Calero, D. Luna, C. Luna, F.M. Bautista, A.A. Romero, A. Posadillo, R. Estevez, Optimization by response surface methodology of the reaction conditions in 1,3-selective transesterification of sunflower oil, by using CaO as heterogeneous catalyst, Mol. Catal. 484 (2020).
[48] S. Zou, H. Zhang, J. Wang, Ultrasound-assisted pickering interfacial catalysis for transesterification: optimization of biodiesel yield by response surface methodology, J. Oleo Sci. 72 (2023) 233–243.
[49] K. Khiari, L. Tarabet, S. Awad, K. Loubar, R. Mahmoud, M. Tazerout, Optimization of pistacia lentiscus oil transesterification process using central composite design, Waste Biomass Valorization 10 (2019) 2575–2581.
[50] M. Mohamad, N. Ngadi, S.L. Wong, M. Jusoh, N.Y. Yahya, Prediction of biodiesel yield during transesterification process using response surface methodology, Fuel 190 (2017) 104–112.
[51] F.A. Aisien, E.T. Aisien, Modeling and optimization of transesterification of rubber seed oil using sulfonated CaO derived from giant African land snail (Achatina fulica) catalyst by response surface methodology, Renew. Energy 207 (2023) 137–146.
[52] D. Beyene, M. Abdulkadir, A. Befekadu, Production of biodiesel from mixed Castor seed and microalgae oils: optimization of the production and fuel quality assessment, Int. J. Chem. Eng. 2022 (2022) 1–14.
[53] Y. Nan, J. Liu, R. Lin, L.L. Tavlarides, Production of biodiesel from microalgae oil (Chlorella prototheocoides) by non-catalytic transesterification in supercritical methanol and ethanol: process optimization, J. Supercrit. Fluids 97 (2015) 174–182.
[54] N. Nirmala, S.S. Dawn, Optimization of Chlorella variabilis. MK039712.1 lipid transesterification using Response Surface Methodology and analytical characterization of biodiesel, Renew. Energy 179 (2021) 1663–1673.
[55] H. Mohamadzadeh Shirazi, J. Karimi-Sabet, C. Ghotbi, Biodiesel production from Spirulina microalgae feedstock using direct transesterification near supercritical methanol condition, Bioresour. Technol. 239 (2017) 378–386.
[56] H. Ramírez, H. Arteaga, R. Siche, Optimización del proceso de obtención de biodiesel a partir de colza silvestre (Brassica Campestris) Process optimization of biodiesel production from wild rapeseed (Brassica campestris), Sci. Agropecu. 3 (2012) 35–44.
[57] S. Sohail, M.W. Mumtaz, H. Mukhtar, T. Touqeer, M.K. Anjum, U. Rashid, W.A.W. A.K. Ghani, T.S.Y. Choong, Spirogyra oil-based biodiesel: response surface optimization of chemical and enzymatic transesterification and exhaust emission behavior, Catalysts 10 (2020) 1–12.
[58] T. Sangsawang, N. Rongrat, A. Yothayuth, Optimization for biodiesel production by transesterification with electric fields, Eng. J. 25 (2021) 261–268.
[59] M.D. Macías-Sánchez, A. Robles-Medina, M.J. Jiménez-Callejón, E. Hita-Peña, L. Estéban-Cerdán, P.A. González-Moreno, E. Navarro-López, E. Molina-Grima, Optimization of biodiesel production from wet microalgal biomass by direct transesterification using the surface response methodology, Renew. Energy 129 (2018) 141–149.
[60] M.D. Macías-Sánchez, A. Robles-Medina, E. Hita-Peña, M.J. Jiménez-Callejón, L. Estéban-Cerdán, P.A. González-Moreno, E. Molina-Grima, Biodiesel production from wet microalgal biomass by direct transesterification, Fuel 150 (2015) 14–20.
[61] V.C. Akubude, K.N. Nwaigwe, E. Dintwa, Production of biodiesel from microalgae via nanocatalyzed transesterification process: a review, Mater. Sci. Energy Technol. 2 (2019) 216–225.
[62] M.J. Anderson, P.J. Whitcomb, Optimizing Processes Using Response Surface Methods for Design of Experiments Second Edition RSM Simplified, 2016.
[63] N.H. Zabaruddin, L.C. Abdullah, N.H. Mohamed, T.S.Y. Choong, Optimization using response surface methodology (RSM) for biodiesel synthesis catalyzed by radiation-induced kenaf catalyst in packed-bed reactor, Processes 8 (2020) 1–18.
[64] A. Adhvaryu, S.Z. Erhan, J.M. Perez, Wax appearance temperatures of vegetable oils determined by differential scanning Calorimetry: effect of triacylglycerol structure and its modification, Thermochim. Acta 395 (2002) 191–200.
[65] N.H. Jayadas, K.P. Nair, Coconut oil as base oil for industrial lubricants-evaluation and modification of thermal, oxidative and low temperature properties, Tribol. Int. 39 (2006) 873–878.
[66] Y. Tang, J.N. Rosenberg, M.J. Betenbaugh, F. Wang, Optimization of one-step in situ transesterification method for accurate quantification of epa in nannochloropsis gaditana, Appl. Sci. 6 (2016).
[67] E.H. Peña, A.R. Medina, M.J.J. Callejón, M.D.M. Sánchez, L.E. Cerdán, P.A. G. Moreno, E.M. Grima, Extraction of free fatty acids from wet Nannochloropsis gaditana biomass for biodiesel production, Renew. Energy 75 (2015) 366–373.

[68] Q. Hu, W. Xiang, S. Dai, T. Li, F. Yang, Q. Jia, G. Wang, H. Wu, The influence of cultivation period on growth and biodiesel properties of microalga Nannochloropsis gaditana 1049, Bioresour. Technol. 192 (2015) 157–164.
[69] N. Nogueira, F.J.A. Nascimento, C. Cunha, N. Cordeiro, Nannochloropsis gaditana grown outdoors in annular photobioreactors: operation strategies, Algal Res. 48 (2020) 101913.
[70] S. Torres, G. Acien, F. García-Cuadra, R. Navia, Direct transesterification of microalgae biomass and biodiesel refining with vacuum distillation, Algal Res. 28 (2017) 30–38.
[71] Y. Zhang, S. Niu, C. Lu, Z. Gong, X. Hu, Catalytic performance of NaAlO2/γ-Al2O3 as heterogeneous nanocatalyst for biodiesel production: optimization using response surface methodology, Energy Convers. Manag. 203 (2020) 112263.
[72] B. Bazooyar, A. Ghorbani, A. Shariati, Physical properties of methyl esters made from alkali-based transesterification and conventional diesel fuel, Energy Sources, Part A Recovery, Util. Environ. Eff. 37 (2015) 468–476.
[73] R. Foroutan, H. Esmaeili, S.M. Mousavi, S.A. Hashemi, G. Yeganeh, The physical properties of biodiesel-diesel fuel produced via transesterification process from different oil sources, Phys. Chem. Res. 7 (2019) 415–424.
[74] K.O. Nwanya, P.A.C. Okoye, V.I.E. Ajiwe, Biodiesel potentials of chlorella vulgaris oil, Niger. Res. J. Chem. Sci. 9 (2021).
[75] O.S. Onyinyechi, D.T. Obinna, Comparative Assessment of Biodiesel Produced from Microalgae, Used Vegetable Oil and Fossils, vol. 8, 2020, pp. 1–10.
[76] F.R.M. Batista, K.W. Lucchesi, N.D.D. Carareto, M.C.D. Costa, A.J.A. Meirelles, Properties of microalgae oil from the species chlorella protothecoides and its ethylic biodiesel, Braz. J. Chem. Eng. 35 (2018) 1383–1394.
[77] S.S.M. Mostafa, N.S. El-Gendy, Evaluation of fuel properties for microalgae Spirulina platensis biodiesel and its blends with Egyptian petro-diesel, Arab. J. Chem. 10 (2017) S2040–S2050.
[78] M.B. Dantas, M.M. Conceição, Fernandes Jr., Thermal and kinetic study of corn biodiesel obtained by the methanol and ethanol routes, J. Therm. Anal. Calorim. 87 (2007) 835–839.
[79] P. Chand, C.V. Reddy, J.G. Venkat, T. Wang, D. Grewell, Thermogravimetric quantification of biodiesel produced via alkali catalyzed transesterification of soybean oil, Energy Fuel. 23 (2009) 989–992.

Publicación III

Elsevier 2024

Claudia Sanjurjo, Rivera N, Rodríguez E, Fernández-González A, Battez AH. Biodiesel derived from the microalgae *Nannochloropsis gaditana* and *Haematococcus pluvialis*: Physicochemical and tribological properties. Journal of Molecular Liquids 2024;408:125391. https://doi.org/10.1016/j.molliq.2024.125391.

Journal of Molecular Liquids 408 (2024) 125391

Contents lists available at ScienceDirect

Journal of Molecular Liquids

journal homepage: www.elsevier.com/locate/molliq

Biodiesel derived from the microalgae *Nannochloropsis gaditana* and *Haematococcus pluvialis*: Physicochemical and tribological properties

C. Sanjurjo [a], N. Rivera [b], E. Rodríguez [a], A. Fernández-González [c], A. Hernández Battez [a,*]

[a] Department of Construction and Manufacturing Engineering, University of Oviedo, Pedro Puig Adam S/n, 33203, Gijón, Spain
[b] Department of Marine Science and Technology, University of Oviedo, Blasco de Garay, S/n, 33203 Gijón, Spain
[c] Department of Physical and Analytical Chemistry, University of Oviedo, Julián Clavería 8, 33006, Oviedo, Spain

ARTICLE INFO

Keywords:
Viscosity
Pour point
Thermal degradation
Coefficient of friction
Wear

ABSTRACT

The physicochemical and tribological propertie of two biodiesels derived from *Nannochloropsis gaditana* and *Haematococcus pluvialis* microalgae were evaluated, and the impact of their fatty acid methyl esters (FAMEs) on the aforementioned properties was also evaluated. The *H. pluvialis* biodiesel exhibited reduced friction and wear compared to the *N. gaditana* counterpart, attributed to its lower degree of unsaturation and higher content of chain length of 17–18, which enhances the adsorption of stronger and thicker tribofilms. Additionally, the higher ratio of monounsaturated to total saturated FAME content contributed to this outcome. The content of polyunsaturated fatty acids decreased the viscosity and increased the end thermal degradation temperature.

1. Introduction

As a consequence of population growth, the demand for energy used in transportation has notably increased. This increase has led to a sharp depletion of fossil fuel reserves, with significant environmental implications. The burning of petroleum-based energy sources contributes climate change due to the emissions of greenhouse gases, as well as various organic compounds [1,2]. In addition, the decrease of fossil fuel reserves has stimulated a notable global demand for biofuels. Among these, biodiesel stands out as a promising solution, effectively addressing key environmental concerns while aligning with growing fuel demand and energy conservation priorities [3].

Biodiesel has several advantages over fossil fuels, such as renewability, biodegradability, non-toxic, excellent lubricating properties, which reduces engine wear, and contributes to the reduction of greenhouse gas emissions, which is critical to prevent climate change [4]. Furthermore, it has a high flash point and improved cetane number, which enhances its safety and improves fuel efficiency [5]. The term "biodiesel" is understood to encompass all mono-alkyl esters of long-chain fatty acids (FA) that can be obtained from a variety of vegetable oils, animal fats, and waste oil resources. Depending on the feedstock, biodiesel can be classified into four generations (Fig. 1). The first generation is derived from edible crops (castor, sunflower, rapeseed, soy or palm oil), while the second generation encompasses all vegetable sources from non-edible crops (*Jatropha curcas*, cotton seeds, *Jojoba*, Neem, etc.) that require arable land for their growth, as well as waste oils [6]. The third generation includes organisms such as microalgae (*Chlorella vulgaris, Spirulina platensis, Nannochloris* sp., etc.), macroalgae, bacteria, and fungi [7]. The fourth generation would be obtained from genetically modified microalgae. The utilization of arable land by both the first and second generations contributes to deforestation and ecosystem degradation, as well as to the challenge of global food shortages [8]. This is due to the fact that the land is occupied by these generations, who utilize it for agricultural purposes. However, the use of microalgae is emerging as a potential alternative, as these microorganisms can be cultivated without using arable land and can provide wastewater treatment [7]. In addition to facilitating the removal of PO^{3-} and NO^{3-} from wastewaters, they also play an active role in environmental CO_2 fixation [9]. Due to their ability to synthesize bioactive compounds such as proteins, fatty acids, carotenoids, etc., these microorganisms are widely used to obtain a variety of products in the cosmetic, food and pharmaceutical industries. Common applications include the production of fertilizers, pigments, food supplements, cosmetic actives, and others [10]. However, the high cost of microalgae biomass production cannot guarantee a sustainable economy. For this reason, several authors have highlighted the need to implement circular economy strategies in order to utilize all valuable components and thus make microalgae biorefinery a more profitable industry [11,12].

* Corresponding author.
E-mail address: aehernandez@uniovi.es (A. Hernández Battez).

https://doi.org/10.1016/j.molliq.2024.125391
Received 7 May 2024; Received in revised form 21 June 2024; Accepted 28 June 2024
Available online 29 June 2024

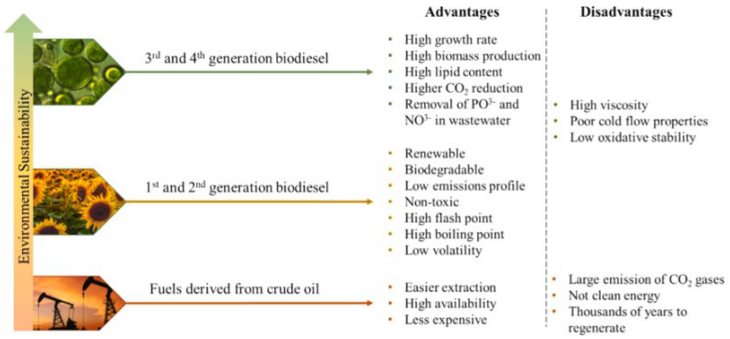

Fig. 1. Advantages and disadvantages of each generation of biodiesel [13].

The most common method for producing biodiesel is through the transesterification reaction. This process involves the reaction of triglycerides present in the oil with an alcohol, typically methanol, to produce fatty acid methyl esters (FAMEs) [1]. The molecular structure of fatty acids typically comprises carbon chains ranging from 4 to 26 atoms, and it may include one or more double bonds (DB) [14]. The carbon chain length and number of DBs (unsaturation) have a strong influence on the biodiesel properties [3]. Lubricity is one of the properties of interest, which plays a key role in the longevity of machinery protecting moving surfaces from wear and minimizing friction in automotive components, which reduces the consumption of energy and the CO_2 emissions [15]. In the context of automotive engines, fuel inlet temperatures can exceed 60 °C, which can subsequently impact the lubricity of the fuel [5]. In response to these considerations, a novel concept known as "green tribology" has emerged. This interdisciplinary field of tribology is guided by twelve principles that advocate the use of biodegradable lubricants to improve sustainability [16]. The investigation of the wear and friction coefficient resulting of the use of any biofuel is of great value in comprehending its lubrication performance.

The heterogeneity of bio-oils extracted from microalgae is dependent on the supplier, feedstock, and production method, which presents a practical challenge. Therefore, it is crucial to establish structure–property relationships to enhance the selection process of microalgae as feedstock for biodiesel production. The objective of this study is to evaluate the physicochemical and tribological performance of two modified microalgae oils, *Haematococcus pluvialis* and *Nannochloropsis gaditana*, which have been reported to have potential as feedstock to produce biodiesel [13,17]. Nevertheless, to date, no tribological evaluations have been conducted. The objective of this study is to characterize and compare the aforementioned properties and relate them to their corresponding molecular structures. This is important when considering the increasing demand for reducing fossil fuel consumption and the need for biodiesel to perform lubricant functions.

2. Experimental details

2.1. Bio-oils and biodiesel derived from microalgae

The microalgae *H. pluvialis* and *N. gaditana* were chosen for their high lipid content. The microalgae bio-oil was extracted from the biomass by the company Neoalgae (Gijon, Spain) using a proprietary method. These microalgae are commonly utilized in the cosmetic and nutritional industries due to their high content of active compounds, including antioxidants and proteins. *H. pluvialis* is the richest natural source of the antioxidant astaxanthin, which possesses anti-inflammatory and anti-aging properties, among others [17]. Conversely, *N. gaditana* is known for its high production of biomolecules, including valuable proteins. Recent studies have employed this microalgae to develop a novel protein (UCA01) with considerable potential for use in the treatment of cancer [18].

Table 1
Fatty acids (FAs) of the bio-oils from the *H. pluvialis* and *N. gaditana* used for biodiesel production.

Fatty acid	Content (%)	
	H. pluvialis	*N. gaditana*
C11:0		0.22
C12:0		0.43
C13:0		0.13
C14:0		4.72
C14:1		1.84
C15:0		0.32
C16:0	20.38	23.88
C16:1		23.86
C17:0		0.18
C17:1	2.92	0.20
C18:0	0.85	0.31
C18:1	15.89	6.01
C18:2	29.92	2.72
C18:3	15.21	1.03
C18:4	2.50	1.23
C20:4		4.11
C20:3		0.29
C20:5	3.52	25.93
C21:0		0.36
*Unidentified	8.68	1.94
SFA (saturated fatty acids)	21.23	30.55
MUFA (monounsaturated fatty acids)	18.81	31.91
PUFA (polyunsaturated fatty acids)	59.83	37.54
Total lipid content in the bio-oil	50.04	35.00

*The fatty acids not identified are also PUFA.

These bio-oils were converted into biodiesel by a transesterification reaction. The optimal reaction conditions were identified through the use of response surface methodology (RSM) [13], and these conditions were employed in the present study. The composition of FAME in the tested biodiesel was determined using gas chromatography with flame ionization detector (GC-FID) following the UNE-EN 14,103 [19] standard after the transesterification reaction. The Clarus 690 instrument (PerkinElmer) was used for this purpose and the procedure performed is the same described by Sanjurjo et al. [13]. Table 1 displays the fatty acid composition of the bio-oils extracted from the microalgae biomass.

Table 2
Temperature-related properties of the *H. pluvialis* and *N. gaditana* derived biodiesel.

Biodiesel source	Pour point (°C)	Flash point (°C)	T_{onset} (°C)	Mass loss at T_{onset} (%)	T_{offset} (°C)	Mass loss at T_{offset} (%)
H. pluvialis	− 5.1	150	211	12	290	98.2
N. gaditana	− 7.2	140–150	208	11.24	318	96.6

2.2. Physicochemical properties of the microalgae-derived biodiesel

The density and the dynamic viscosity in the range of 20–100 °C were determined in a Stabinger SVM 3001 viscometer in accordance with the ASTM D7042 [20]. The instrument operates according to the Coutte measuring principle and is equipped with an integrated density measuring cell. The kinematic viscosity was then automatically calculated from these results in accordance with the ASTM D2270 [21].

The pour point (PP) was determined through Differential Scanning Calorimetry (DSC Mettler 822e 700) analysis. The sample was heated to 50 °C at a rate of 10 °C/min and held under isothermal conditions for 10 min. The system was then cooled to −50 °C at the same rate. A heat flux (W/g) versus temperature curve was used to obtain the maximum point of the curve [13].

The flash point (FP) of the biodiesel was determined using a modified Cleveland Open Cup Tester in accordance with the EN ISO 2592 [22] and ASTM D92 [23] standards. Thermal stability (TS) was assessed through thermogravimetric analysis (TGA) under nitrogen atmosphere using a TA Instruments DSC SDT Q600 TGA & DSC to determine the temperatures at which decomposition begins (T_{onset}) and ends (T_{offset}). The results of these measurements are given in Table 2.

2.3. Tribological tests

The frictional behavior of the biodiesel was fully investigated through rolling-sliding ball-on-disc tests using an MTM-2 tribometer (PCS Instruments) under the following conditions: entrainment speed (2500–10 mm s^{-1}, load (75 N or 1.29 GPa of maximum contact pressure), slide-to-roll ratio (SRR) of 5 % and 50 %, and temperature (40 °C, 60 °C, and 80 °C). The entrainment speed (V_S) and the slide-to-roll ratio *(SRR)* are defined by the equations (1) and (2), respectively. The tangential speeds of the ball and disc at the point of contact are represented by u_{ball} and u_{disc}, respectively. 10 mL of biodiesel was in these tests. The balls (19.05 mm diameter) and discs used in these tests are made of AISI 52100 steel, with a surface roughness Ra < 0.020 μm, and a Vickers hardness (HV_{30}) of 800–920 and 720–780, respectively.

$$Vs = u_{disc} - u_{ball} \quad (1)$$

$$SRR = 2 \bullet \frac{|(u_{disc} - u_{ball})|}{(u_{disc} + u_{ball})} \times 100\% \quad (2)$$

Reciprocating friction and wear tests were conducted on all samples using a UMT-3 tribometer (Bruker Corporation). The tribological tests were performed on AISI 52100 steel specimens consisting of a ball (6 mm diameter, Rockwell C hardness (HRC) of 58–66, and surface roughness R_a≈0.05 μm) and a disc (10 mm diameter, Vickers hardness (HV30) of 190–210, and surface roughness Ra≈0.018 μm). 25 μL of lubricant was applied to the ball-disk contact to ensure continuous lubrication throughout the test. The test conditions were as follows: frequency (15 Hz), stroke length (4 mm), 60 min, temperature (40 °C and 80 °C), and load (10 N or 1.43 GPa of maximum contact pressure). The coefficient of friction (COF) was calculated and recorded during the tribological tests. At least two tests were conducted with a fresh biodiesel sample under the same tribological conditions. Prior to the tribological test, the ball and disc surfaces were meticulously cleaned using heptane, acetone, and ethanol in an ultrasonic bath for a period of 10 min per solvent. This was followed by hot air drying.

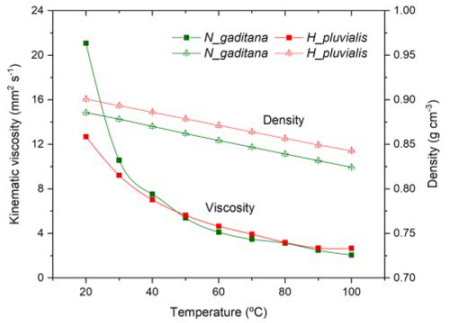

Fig. 2. Kinematic viscosity and density of the H. pluvialis and N. gaditana derived biodiesels.

2.4. Analysis of wear surface

Following the reciprocating tribological tests, the wear volume on the disk surface was measured using a confocal microscope and interferometer (Leica 3D DCM). We then identified the wear mechanism using a JEOL model 6610LV SEM scanning electron microscope operating at 15 kV acceleration voltage and 100X magnification. X-ray photoelectron spectroscopy was conducted using a Phoibos spectrometer with monochromatized K_αAl (1486.74 eV) as X-ray source. High-resolution spectra were obtained with an energy pass of 30 eV and an energy step of 0.1 eV for the carbon, nitrogen, iron, and oxygen elements. An electron flood gun was employed to compensate for the sample charge during the measurements.

3. Results and discussion

3.1. Physicochemical properties

The low pour point values shown in Table 2 for both biodiesels are due to their high content of monounsaturated fatty acids (MUFAs) as shown in Table 1. Farfan-Cabrera et al. [24] reported that the lowest PP is related to the high content of PUFAs with long chains (C13-C21) as the main FAs in the bio-oils derived from microalgae. Conversely, higher PP values are associated with the presence of high content of MUFAs as the main FAs. MUFAs are known to contain trans DB, whereas PUFAs present cis DB, which hinders crystal packing and results in lower PP values. For N. gaditana, the PP value appears to be significantly influenced by the presence of C20:5, which exhibits a high degree of packing due to its cis DB [25]. This finding suggests that pour point is influenced not only by the MUFA and PUFA content, but also by the number of DBs. Table 1 displays the concentration of each FA in the biodiesels. The number of DBs has a greater impact on the *N. gaditana* derived biodiesel than on the *H. pluvialis* counterpart, as confirmed by Diez-Valbuena et al. [26]. Their study, which employed machine learning techniques on a database of 238 biodiesel examples [27], demonstrated that double bonds have a greater influence on pour point than MUFA and PUFA.

The flash point (FP) of biodiesel is a critical factor for its storage and handling due to safety concerns. Biodiesels with high flash points are considered non-flammable. The biodiesels tested in this study, derived from *H. pluvialis* and *N. gaditana*, have similar flash point values ranging from 140-150 °C (Table 2). These FP values are comparable to those of biodiesel derived from corn, palm, and honge [28,29,30]. This suggests

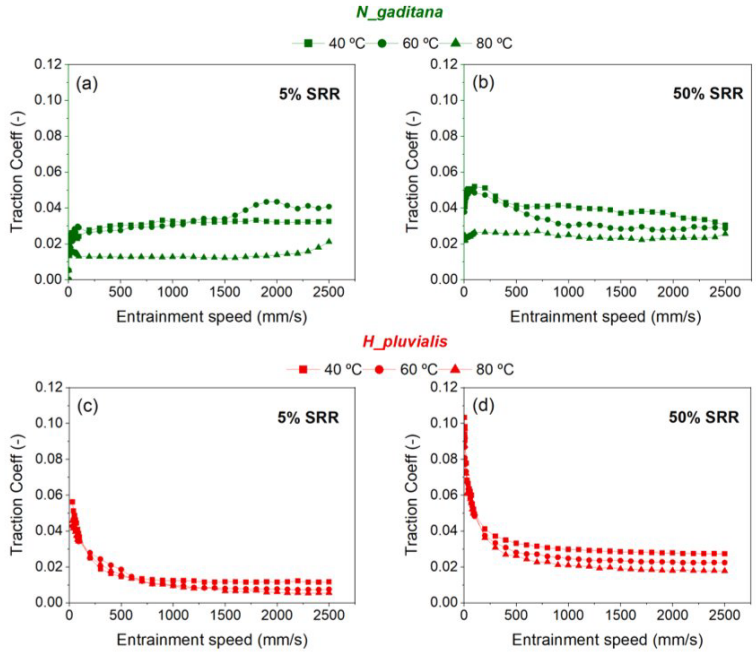

Fig. 3. Traction coefficient versus entrainment speed in rolling-sliding tests: (a) *N. gaditana* at 5% of SRR, (b) *N. gaditana* at 50% of SRR, (c) *H. pluvialis* at 5% of SRR, (d) *H. pluvialis* at 50% of SRR.

that the influence of the FAME content on this property is difficult to determine.

The oxidative stability of the oil is dependent upon the predominant FAs present. In general, high content of PUFAs results in high oxidation rates because the double bonds react readily with oxygen, resulting in free radicals formation and subsequent polymerization and further degradation [31]. The study found that the onset degradation temperatures of the tested biodiesel were similar (Table 2), but the offset temperatures differed by 6 %. The higher offset temperature in the case of the *N. gaditana* derived biodiesel can be attributed to its lower content of PUFAs.

Fig. 2 shows the density and kinematic viscosity of the two tested biodiesels. Both biodiesels meet the density requirements of the EN 14214:2013 V2 + A2 standard [32], and their viscosity exceeds the values required by the EN 14214:2013 V2 + A2 [32] and ASTM D6751-23a [33] standards. Despite this, the biodiesels can still be blended and used in various concentrations. The viscosity of the FA chain increases with its length due to a higher degree of intermolecular interactions [34]. Furthermore, the viscosity of the biodiesel is affected by the presence of MUFA and PUFA. Specifically, the presence of MUFA increases viscosity while the presence of PUFA decreases it. This fact was observed at temperatures below 30 °C, having the *N. gaditana* biodiesel a higher viscosity than its *H. pluvialis* counterpart, but this behavior may be also attributed to the higher non-lipid content or impurities of the *N. gaditana* biodiesel. However, the viscosity of both biodiesels was similar between 40–100 °C.

3.2. Tribological properties

Fig. 3 shows the results of the rolling-sliding tests conducted using both biodiesels. The coefficients of friction determined during the tests are generally between 0.01 and 0.1, which are typical values for mixed/EHL lubrication. The data indicates that friction decreased with temperature due to the reduction in viscosity of the biodiesel. Conversely, friction increased with SRR as the sliding component in the ball-disc contact increased. It is noteworthy that the biodiesel derived from *H. pluvialis* outperformed the biodiesel derived from *N. gaditana*. After the transesterification reaction with methanol, all the FAs in the bio-oils from the microalgae *H. pluvialis* and *N. gaditana* were converted into FAME with one more carbon atom. As a result, the biodiesel derived from *H. pluvialis* has an average carbon chain length of 18.88, while that from *N. gaditana* has 17.63. The average carbon chain length of the biodiesel derived from *H. pluvialis* is longer, resulting in a lower COF. This is due to the production of stronger molecular linkages and thicker adsorbed films on surfaces [24].

Fig. 4 shows the evolution of the COF during the reciprocating tests (Fig. 4a and 4b represent the test sample closer to the average COF), as well as the average value for the tests conducted with the biodiesels derived from the microalgae *H. pluvialis* and *N. gaditana*. The friction values observed in these tests are typical of the mixed lubrication regime, with the exception of the test carried out with the biodiesel derived from *N. gaditana* at 80 °C, where the COF exceeded 0.1, which is typical of boundary lubrication regime. At 40 °C, the friction remained relatively constant for both biodiesels, but the biodiesel obtained from

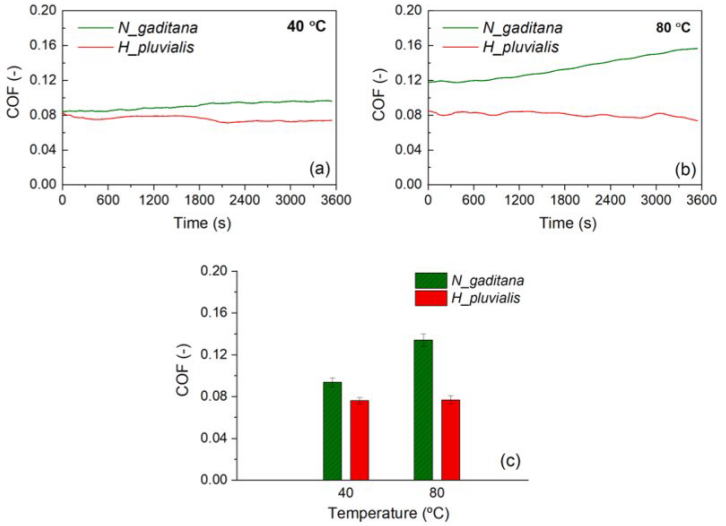

Fig. 4. Coefficient of friction from reciprocating friction and wear tests: (a) at 40 °C, (b) at 80 °C, (c) average coefficient of friction and deviation at 40 °C and 80 °C.

H. pluvialis exhibited better anti-friction behavior. At 80 °C, the *H. pluvialis* biodiesel exhibited similar antifriction behavior to that at 40 °C. In contrast, the biodiesel derived from *N. gaditana* exhibited higher friction that increased throughout the experiment. On the other hand, the use of *H. pluvialis* biodiesel resulted in lower and constant friction with increasing temperature. These results can be assigned to the adsorption of organic polar molecules on the metallic surface, which reduces friction, and to the stronger molecular linkages and thicker adsorbed tribofilms of the biodiesel derived from *H. pluvialis*. Furthermore, the *H. pluvialis* biodiesel exhibited a higher ratio of monounsaturated to total saturated FAME content (Table 1), which resulted in a superior friction modifier effect. This finding was also reported by Hamdan et al. [16].

Both biodiesels have a strong polarity due to the organic polar molecules derived from the transesterification of the fatty acids. The polarity of these biodiesels was determined by the non-polarity index (*NPI*), which is calculated using the equation (3) [35]. A low *NPI* indicates a highly polar molecule or compound (e.g. *NPI* = 50 for short synthetic esters) and a high *NPI* indicates a non-polar molecule or compound (e.g. *NPI* = 300 for polyalphaolefins) [36]. The *NPI* values for the tested biodiesel, excluding the unidentified fatty acids, were similar. The *NPI* of the biodiesel derived from *H. pluvialis* was 49.12, while the *NPI* of the biodiesel derived from *N. gaditana* was 50.15.

$$NPI = \frac{TotalnumberofCatoms \times Molecularweight}{Numberofcarboxylicgroups \times 100} \quad (3)$$

Although both biodiesels have similar polarity, their organic polar molecules can be adsorbed differently, either through physical adsorption (physisorption) or chemical adsorption (chemisorption). Physisorption occurs at ambient temperature by forming hydrogen bonds with the surface oxides of hydroxides [37] but there is usually an upper temperature limit to this process, which decrease with the increase of temperature [38]. Wang et al. [37] found that a physically adsorbed film formed by a mixture of polyalphaolefin and glycerol monooleate (GMO)

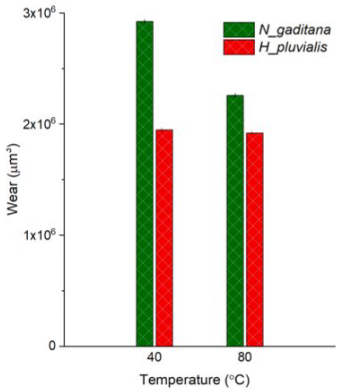

Fig. 5. Wear volume after reciprocating tests.

decreased sharply from 70 °C to 130 °C, and the low friction coefficient at low temperature was caused by the physical adsorption film of GMO, while the low friction at high temperature was caused by the chemical adsorption film. In our case, the adsorption mechanism during the reciprocating tests at 40 °C is mainly of physisorption, and this mechanism changed to chemisorption when the temperature increased to 80 °C. The differences in the friction results could be related to the strength of the chemical bonds formed by the fatty acid molecules with the surface, similar to the observations made by Simic and Kalin [39]. Adhvaryu et al. [40] also found that the length of the hydrocarbon chain and the relative distribution of unsaturation in the FA chain can affect

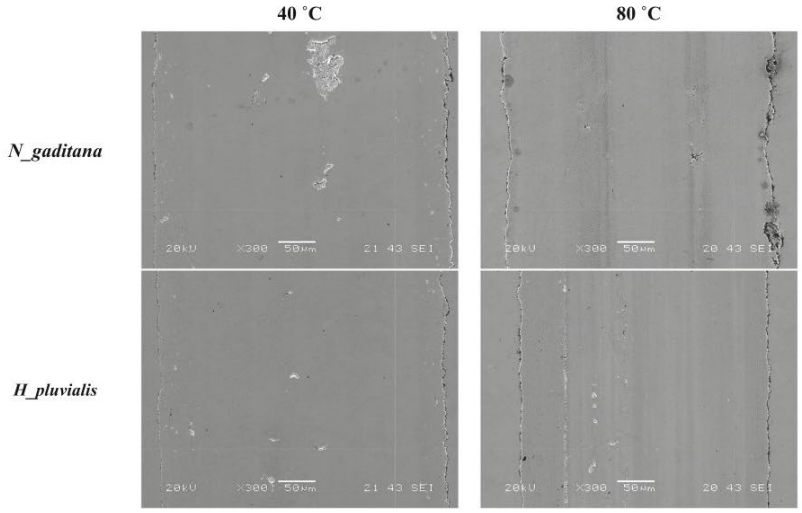

Fig. 6. SEM images of the worn surface after reciprocating tests.

adsorption on the metal surface. This study was conducted based on the calculated free energy of adsorption (ΔG_{ads}) and reported that an average chain length of 17–18 favors lower ΔG_{ads} values resulting in strong adsorption, while increasing the degree of unsaturation or the average number of double bonds per molecule results in a higher ΔG_{ads} and a weaker adsorption. In our case, the *H. pluvialis* biodiesel has a degree of unsaturation of 1.51 and its counterpart from *N. gaditana* has 1.92. This 21 % lower degree of unsaturation of the *H. pluvialis* biodiesel contributes to a lower ΔG_{ads} and therefore to a stronger adsorption. On the other hand, both biodiesels had a similar average chain length

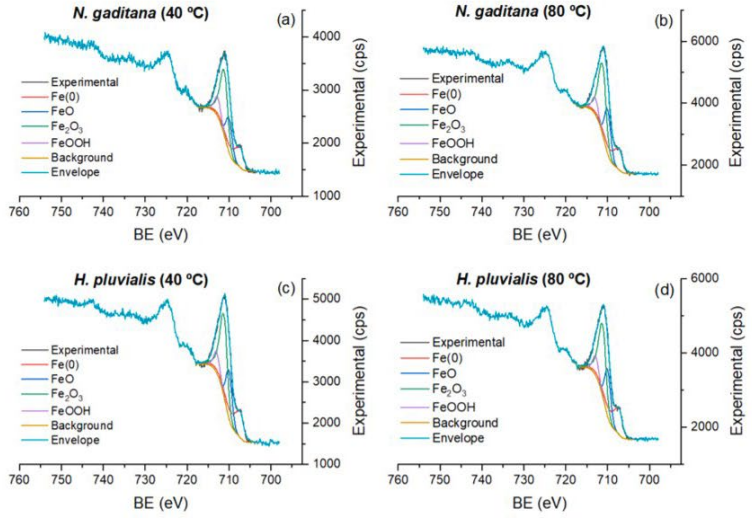

Fig. 7. Curve fitting for Fe2p3/2 high resolution spectra for both microalgae-derived biodiesel: (a) *N. gaditana* at 40 °C, (b) *N. gaditana* at 80 °C, (c) *H. pluvialis* at 40 °C, (d) *H. pluvialis* at 80 °C.

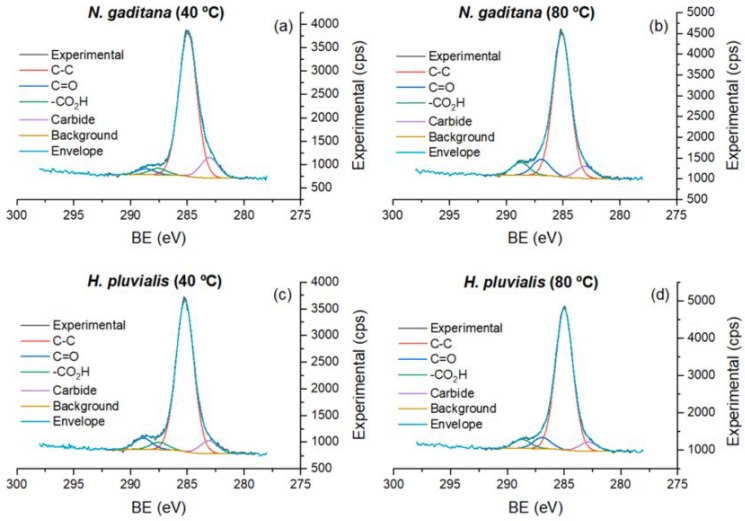

Fig. 8. Curve fitting for C1s high resolution spectra for both microalgae-derived biodiesel: (a) *N. gaditana* at 40 °C, (b) *N. gaditana* at 80 °C, (c) *H. pluvialis* at 40 °C, (d) *H. pluvialis* at 80 °C.

(16.04 for *H. pluvialis* and 16.93 for *N. gaditana*), but the content of fatty acids with a chain length of 17–18 was 67.29 % in the *H. pluvialis* and 11.68 % in the *N. gaditana* counterpart. This fact could explain the better tribological behavior of *H. pluvialis* biodiesel compared to *N. gaditana* biodiesel.

Fig. 5 displays the anti-wear performance of the tested biodiesels. It

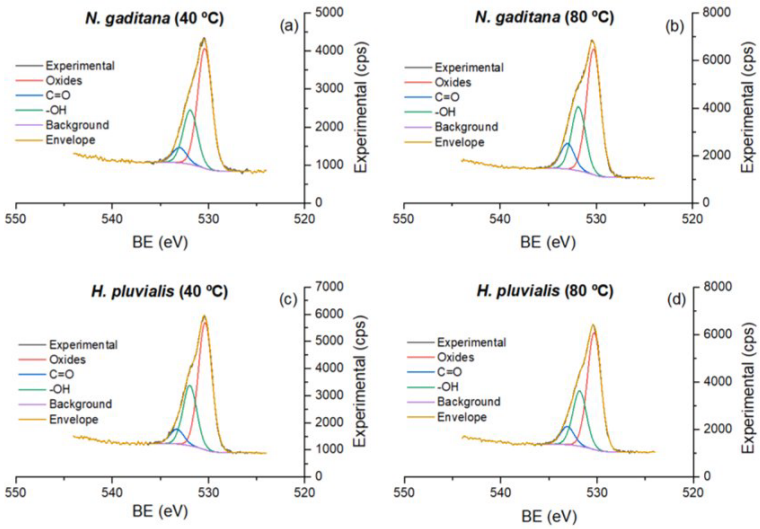

Fig. 9. Curve fitting for O1s high resolution spectra for both microalgae-derived biodiesel: (a) *N. gaditana* at 40 °C, (b) *N. gaditana* at 80 °C, (c) *H. pluvialis* at 40 °C, (d) *H. pluvialis* at 80 °C.

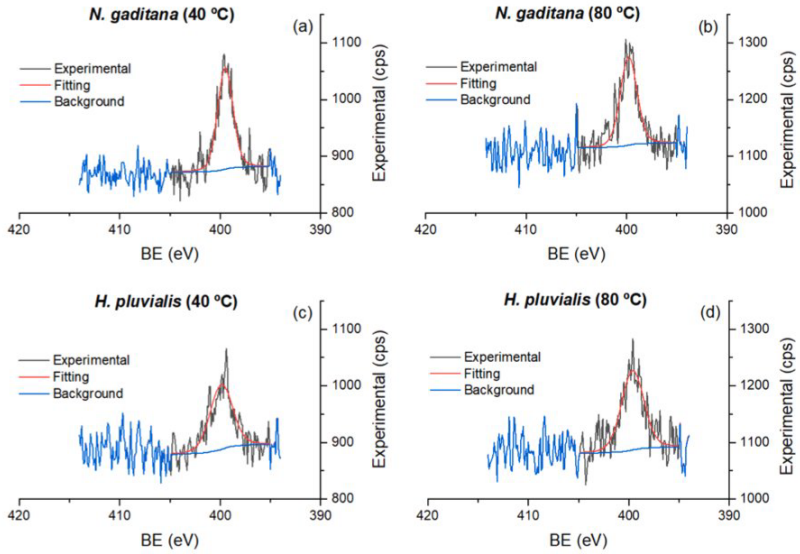

Fig. 10. Curve fitting for N1s high resolution spectra for both microalgae-derived biodiesel: (a) *N. gaditana* at 40 °C, (b) *N. gaditana* at 80 °C, (c) *H. pluvialis* at 40 °C, (d) *H. pluvialis* at 80 °C.

is clear that the biodiesel derived from *H. pluvialis* exhibited the best results at both temperatures. This little influence of test temperature on the antiwear performance was also observed with the use of glycerol monooleate as additive to a polyalphaolefin [39]. Conversely, the biodiesel from *N. gaditana* demonstrated inferior anti-wear behavior. The reduction in wear observed in the test at 80 °C with the biodiesel derived from *N. gaditana* could be related to the formation of chemisorbed films involving some degree of chemical bonding between the organic polar molecules and the metallic surface.

3.3. Surface characterization

Fig. 6 shows the SEM images of the worn surface on the disc following the reciprocating tests. The observed wear mechanisms in both cases were adhesion and plastic deformation. Pits were found on the wear surface, particularly after the test at 40 °C with the *N. gaditana*-derived biodiesel, which explains the highest wear volume.

3.4. X-ray photoelectron spectroscopy

Fig. 7 depicts the tentative curve fitting for the Fe 2p3/2 spectrum, which employs four distinct curves associated with Fe (0) (Gaussian: Lorentzian 85:15 with exponential blend k = 0.65), FeO (Gaussian), Fe_2O_3 (Gaussian:Lorentzian 55:45 with exponential blend k = 1.5), and FeOOH (Gaussian:Lorentzian 45:55). The selected curve shapes were based on Mangolini's work [41]. The results indicate that a tribo oxide film is formed, consistent with the results obtained by Xu et al. [42], although the differences among the different samples are subtle and, therefore, not statistically significant. C1s fitting is challenging, particularly with complex organic samples such as ours [43]. Nevertheless, it appears evident that *N. gaditana* at 40 °C exhibits a greater quantity of the peak with the lowest binding energy (Fig. 8), which is particularly noteworthy given that this sample also exhibits the most unfavorable friction and wear behaviors. These low positions are typically associated with compounds with a low oxidation degree. Regarding the possible assignments of the fitted positions, it should be noted that the entire fitting task is particularly challenging in samples like ours, as previously stated. Consequently, the final assignments should not be considered absolutely reliable. Nevertheless, the positions agree with those usually assigned to C–C (ca. 284.9 eV), C = O (ca. 287.6 eV), $–CO_2H$ (ca. 288.7 eV) and metal carbides (283.0 eV) [42,44].

Table 3
Molar ratios in XPS surface analysis.

	Fe	C	O	N
H. pluvialis 40 °C	1	27.3	12.2	0.4
H. pluvialis 80 °C	1	24.8	10.3	0.5
N. gaditana 40 °C	1	41.1	10.6	0.8
N. gaditana 80 °C	1	19.9	10.1	0.4

Furthermore, the O1s spectra of the four samples (Fig. 9) exhibit a striking resemblance, displaying a combination of three distinct curves at 530.3 eV, 531.9 eV, and 533.0 eV, with an approximate area ratio of 10:5:2. These features are typically attributed to metal oxides, C–O, and C = O [45,46]. In contrast, the N1s spectra (Fig. 10) exhibit a single peak between 399.5 eV and 399.9 eV. Table 3 presents the molar ratio of Fe, O, C, and N in the different samples. It is noteworthy that *N. gaditana* exhibits a higher quantity of organic matter on the surface (carbon) at 40 °C than at 80 °C. This aligns with a higher worn volume at 40 °C in comparison to 80 °C (Fig. 5). However, *H. pluvialis* maintains the organic layer in comparable proportions at both temperatures, as does the wear volume.

4. Conclusions

The microalgae utilized as a source of third-generation biodiesel

contain a diverse array of fatty acids that undergo transesterification to form different FAMEs. The composition of these FAMEs exerts a strong influence on the physicochemical and tribological behavior of the third-generation biodiesel. Consequently, the study of the structure–property relationships represents a crucial approach for the selection of micro-algae for this purpose. The microalgae *Nannochloropsis gaditana* and *Haematococcus pluvialis* were employed for biodiesel production and the resulting biodiesel samples were subjected to physicochemical and tribological characterization. The primary conclusions of this study are as follows:

- The pour point of the biodiesel derived from microalgae is influenced not only by the content of MUFA and PUFA, but also by the *cis/trans* position of the double bonds.
- Both biodiesel samples exhibited comparable flash point and oxidative stability values. However, the influence of the FAME content on the flash point is challenging to ascertain. The higher offset thermal degradation temperature of the *N. gaditana* derived biodiesel can be the result of its lower content of PUFA.
- The viscosity of the biodiesel increases with the presence of MUFA (higher at low temperature in the case of the tested biodiesel derived from *N. gaditana*) and decreases with the presence of PUFA (lower at low temperature in the case of the tested biodiesel derived from *H. pluvialis*).
- The lower degree on unsaturation and the higher content of fatty acids with a carbon chain length of 17–18 of the *H. pluvialis* biodiesel leads to a stronger adsorption on the surfaces that results in a lower COF and superior antiwear properties. The higher ratio of mono-unsaturated to total saturated FAME content in the *H. pluvialis* biodiesel also favoured this result.
- All the surfaces analyzed with XPS exhibited similar characteristics, with only subtle differences. The most notable difference was the appearance of a low-binding energy band in the C1s spectrum for *N. gaditana* at 40 °C. This may be related to its inferior tribological performance. Similarly, the presence of carbon on the surface appears to correlate with the observed wear volume behavior.

CRediT authorship contribution statement

C. Sanjurjo: Writing – original draft, Resources, Investigation, Data curation. **N. Rivera:** Resources, Investigation, Data curation. **E. Rodríguez:** Supervision, Resources, Project administration, Funding acquisition. **A. Fernández-González:** Writing – original draft, Investigation, Data curation, Conceptualization. **A. Hernández Battez:** Writing – review & editing, Supervision, Resources, Project administration, Methodology, Funding acquisition, Conceptualization.

Declaration of competing interest

The authors declare that they have no known competing financial interests or personal relationships that could have appeared to influence the work reported in this paper.

Data availability

Data will be made available on request.

Acknowledgments

This publication is part of the R&D project PID2022-136656NB-I00, funded by MICIU/AEI/10.13039/501100011033/ and by "FEDER/UE". The authors of the work wish to express their gratitude to the University Institute of Industrial Technology of Asturias (IUTA) for financing the project "OPTRANSESTERAL" [grant number SV-23-GIJON-1-05].

References

[1] F. Sundus, M.A. Fazal, H.H. Masjuki, Tribology with biodiesel: a study on enhancing biodiesel stability and its fuel properties, Renew. Sustain. Energy Rev. 70 (2017) 399–412, https://doi.org/10.1016/j.rser.2016.11.217.
[2] S. Samanta, R.R. Sahoo, Waste cooking (palm) oil as an economical source of biodiesel production for alternative green fuel and efficient lubricant, Bioenergy Res. 14 (2021) 163–174, https://doi.org/10.1007/s12155-020-10162-3.
[3] M. Sudan Reddy Dandu, K. Nanthagopal, Tribological aspects of biofuels – a review, Fuel (2019) 258, https://doi.org/10.1016/j.fuel.2019.116066.
[4] D. Kumar, A. Kumar, A. Singla, R. Dewan, Production and tribological characterization of castor based biodiesel, Mater. Today Proc. 46 (2021) 10942–10949, https://doi.org/10.1016/j.matpr.2021.02.009.
[5] M.A. Fazal, A.S.M.A. Haseeb, H.H. Masjuki, Investigation of friction and wear characteristics of palm biodiesel, Energy Convers. Manag. 67 (2013) 251–256, https://doi.org/10.1016/j.enconman.2012.12.002.
[6] W.C. Ulakpa, R.O.E. Ulakpa, M.C. Egwunyenga, T.C. Egbosiuba, Transesterification of non-edible oil and effects of process parameters on biodiesel yield, Cleaner Waste Systems 3 (2022) 100047, https://doi.org/10.1016/j.clwas.2022.100047.
[7] N.S.M. Aron, K.S. Khoo, K.W. Chew, P.L. Show, W.H. Chen, T.H.P. Nguyen, Sustainability of the four generations of biofuels – a review, Int. J. Energy Res. 44 (2020) 9266–9282, https://doi.org/10.1002/er.5557.
[8] M.A.H. Shaah, M.S. Hossain, F.A.S. Allafi, A. Alsaedi, N. Ismail, M.O.A. Kadir, et al., A review on non-edible oil as a potential feedstock for biodiesel: physicochemical properties and production technologies, RSC Adv. 11 (2021) 25018–25037, https://doi.org/10.1039/d1ra04311k.
[9] P. Xu, J. Li, J. Qian, B. Wang, J. Liu, R. Xu, P. Chen, W. Zhou, Recent advances in CO_2 fixation by microalgae and its potential contribution to carbon neutrality, Chemosphere 319 (2023) 137987, https://doi.org/10.1016/j.chemosphere.2023.137987.
[10] M.F. Bashir, M.U. Farooq, S. Khalid, Q. Ali, The role of microalgae in different biotechnology applications, Bull. Biol. All Sci. Res. 7 (2022) 25, https://doi.org/10.54112/bbasr.v2022i1.25.
[11] C. Fuentes, J.I. Gayo, V. Ndovela, E. Wood, R. Vijay, C. Anne, Towards a circular economy: a novel microalgal two-step growth approach to treat excess nutrients from digestate and to produce biomass for animal feed, Bioresour. Technol. 320 (2021) 124349, https://doi.org/10.1016/j.biortech.2020.124349.
[12] A.G. Olabi, N. Shehata, E. Taha, C. Rodriguez, R. Chinyere, C. Russell, M. A. Abdelkareem, Role of microalgae in achieving sustainable development goals and circular economy, Sci. Total Environ. 854 (2023) 158689, https://doi.org/10.1016/j.scitotenv.2022.158689.
[13] C. Sanjurjo, P. Oulego, M. Bartolomé, E. Rodríguez, R. Gonzalez, B.A. Hernández, Biodiesel production from the microalgae nannochloropsis gaditana: optimization of the transesterification reaction and physicochemical characterization, Biomass Bioenergy 185 (2024) 107240, https://doi.org/10.1016/j.biombioe.2024.107240.
[14] E. Contreras-Gallegos, F.A. Domínguez-Pacheco, C. Hernández-Aguilar, A. Bedoya, S. Alvarado, E. Marín, et al., Study of mineral-based oils with Jatropha curcas L. as bio-additive through thermal and kinematic viscosity properties, Int. J. Thermophys. (2022) 43, https://doi.org/10.1007/s10765-021-02932-8.
[15] N. Kumar, W. Varun, S. Chauhan, Analysis of tribological performance of biodiesel, Proc. IME, Part J: J. Eng. Tribol. 228 (2014) 797–807, https://doi.org/10.1177/1350650114532452.
[16] S.H. Hamdan, W.W.F. Chong, J.H. Ng, M.J. Ghazali, R.J.K. Wood, Influence of fatty acid methyl ester composition on tribological properties of vegetable oils and duck fat derived biodiesel, Tribol. Int. 113 (2017) 76–82, https://doi.org/10.1016/j.triboint.2016.12.008.
[17] G.K.S.H. Nishshanka, V.C. Liyanaarachchi, P.H.V. Nimarshana, et al., Haematococcus pluvialis: a potential feedstock for multiple-product biorefining, J. Clean. Prod. 344 (2022) 131103, https://doi.org/10.1016/j.jclepro.2022.131103.
[18] R. Carrasco, A. Escobar, C. Fajardo, I. Morano, F. Amil, G. Martinez, C. Fuentes, V. Capilla, L. Tomas, L. Soriano, P. Guarnizo, R. Vallejo, F. Fernandez, Develepment of new antiproliferative compound agains human tumor cells from the marine microalgae nannochloropsis gaditana by applied proteomics, Int. J. Mol. Sci. 22 (1) (2021) 96.
[19] UNE-EN 14103:2020. Fat and oil derivatives - Fatty Acid Methyl Esters (FAME) - Determination of ester and linolenic acid methyl ester contents.
[20] ASTM D7042-21a. Standard Test Method for Dynamic Viscosity and Density of Liquids by Stabinger Viscometer (and the Calculation of Kinematic Viscosity).
[21] ASTM D2270-10(2016). Standard Practice for Calculating Viscosity Index from Kinematic Viscosity at 40 °C and 100 °C.
[22] UNE-EN ISO 2592:2018. Petroleum and related products - Determination of flash and fire points - Cleveland open cup method (ISO 2592:2017).
[23] ASTM D92-18. Standard Test Method for Flash and Fire Points by Cleveland Open Cup Tester.
[24] L. Farfan-Cabrera, M. Franco-Morgado, A. González-Sánchez, J. Pérez-González, B. M. Marín-Santibáñez, Microalgae biomass as a new potential source of sustainable green lubricants, Molecules 27 (2022) 1205, https://doi.org/10.3390/molecules27041205.
[25] C. Bahubali, A. Gopalan. Improving biodiesel's properties. Digital Refining 2019;1-5. https://www.digitalrefining.com/article/1002283/improving-biodiesels-properties.
[26] G. Díez-Valbuena, A. García-Tuero, J. Díez, E. Rodríguez, B.A. Hernández, Prediction of the cold flow properties of biodiesel using the FAME distribution and machine learning techniques, J. Mol. Liq. 400 (2024) 124555, https://doi.org/10.1016/j.molliq.2024.124555.

[27] G. Díez Valbuena, A. García Tuero, J. Díez, E. Rodríguez-Ordóñez, B.A. Hernández, Supplementary material from: prediction of the cold flow properties of biodiesel using the FAME distribution and machine learning techniques, Zenodo (2024), https://doi.org/10.5281/zenodo.10670349.
[28] H. Aulia, F. Hidayat, T. Sriana. Characteristic study of biodiesel mixtures from used oil and diesel oil, in: IOP Conference Series: Materials Science and Engineering. Institute of Physics Publishing 2020;830:022014. Doi: 10.1088/1757-899X/830/2/022014.
[29] V. Atgur, G. Manavendra, B. Rao, I. Veza, I. Fattah, Thermal and combustion characteristics of honge, jatropha, and honge-jatropha mixed biodiesels, Environ. Prog. Sustain. Energy 43 (2023) 14199, https://doi.org/10.1002/ep.14199.
[30] B. Bazooyar, A. Ghorbani, A. Shariati, Physical properties of methyl esters made from alkali-based transesterification and conventional diesel fuel, Energy Sources, Part A: Recovery, Utilization and Environmental Effects 37 (2015) 468–476, https://doi.org/10.1080/15567036.2011.586975.
[31] R. Sherwin, Oxidation and antioxidants in fat and oil processing, J. Am. Oil Chem. Soc. 55 (1978) 809–814, https://doi.org/10.1007/BF02682653.
[32] UNE-EN 14214:2013 V2+A2. Liquid petroleum products. Fatty acid methyl esters (FAME) for use in diesel engines and heating applications. Requirements and test methods.
[33] ASTM D6751-23a. Standard Specification for Biodiesel Fuel Blendstock (B100) for Middle Distillate Fuels.
[34] G. Knothe, K. Steidley, Kinematic viscosity of biodiesel fuel components and related compounds. Influence of compound structure and comparison to petrodiesel fuel components, Fuel 84 (2005) 1059–1065, https://doi.org/10.1016/j.fuel.2005.01.016.
[35] A. Pettersson, Environmentally adapted lubricants. Properties and performance. Doctoral Thesis. Luleå University of Technology 2006:66. ISSN: 1402-1544.
[36] G. Van der Waal, The relationship between the chemical structure of ester base fluids and their influence on elastomer seals, and wear characteristics, J. Synth. Lubr. 1 (1984) 280–301, https://doi.org/10.1002/jsl.3000010404.
[37] W. Wang, et al., Friction reduction mechanism of glycerol monooleate-containing lubricants at elevated temperature - transition from physisorption to chemisorption, Sci. Prog. 104 (1) (2021), https://doi.org/10.1177/0036850421998529.
[38] L.R. Rudnick, Lubricant additives: chemistry and applications, 2nd ed., CRC, Boca Raton, 2009.
[39] R. Simic, M. Kalin, Adsorption mechanisms for fatty acids on DLC and steel studied by AFM and tribological experiments, Appl. Surf. Sci. 283 (2013) 460–470, https://doi.org/10.1016/j.apsusc.2013.06.131.
[40] A. Adhvaryu, et al., Friction behavior of some seed oils: biobased lubricant applications, Ind. Eng. Chem. Res. 45 (2006) 3735–3740, https://doi.org/10.1021/ie051259z.
[41] F. Mangolini, A. Rossi, N. Spencer, Influence of metallic and oxidized iron/steel on the reactivity of triphenyl phosphorothionate in oil solution, Tribol. Int. 44 (6) (2011) 670–683, https://doi.org/10.1016/j.triboint.2010.02.009.
[42] Y. Xu, X. Hu, K. Yuan, G. Zhu, W. Wang, Friction and wear behaviors of catalytic methyle sterified bio-oil, Tribol. Int. 71 (2014) 168–174, https://doi.org/10.1016/j.triboint.2013.11.018.
[43] T. Gengenbach, G. Major, M. Linford, C. Easton, Practical guides for X-ray photoelectron spectroscopy (XPS): interpreting the carbon 1s spectrum, J. Vac. Sci. Technol. A 39 (2021) 013204, https://doi.org/10.1116/6.0000682.
[44] Y. Xu, X. Zheng, X. Hu, K. Dearn, H. Xu, Effect of catalytic esterification on the friction and wear performance of bio-oil, Wear 311 (2014) 93–100, https://doi.org/10.1016/j.wear.2013.12.029.
[45] S. Suzuki, K. Yanagihara, K. Hirokawa, XPS study of oxides formed on the surface of high-purity iron exposed to air, Surf. Interf. Sci. 30 (2000) 372–376, https://doi.org/10.1002/1096-9918(200008)30:1<372::AID-SIA721>3.0.CO;2-R.
[46] T. Das, B. Saikia, H. Dekaboruah, M. Bordoloi, D. Neog, J. Bora, J. Lahkar, B. Narzary, S. Roy, D. Ramaiah, Blue-fluorescent and biocompatible carbon dots derived from abundant low-quality coals, J. Photochem. Photobiol. B: Bio. 195 (2019) 1–11, https://doi.org/10.1016/j.jphotobiol.2019.04.004.

Publicación IV

Springer 2024

Claudia Sanjurjo, Rodríguez E, Bartolomé M, González R, Hernández A. Optimizing the Conversion of Bio-Oil from Haematococcus pluvialis to Fatty Acid Methyl Esters. BioEnergy Research 2024. https://doi.org/10.1007/s12155-024-10794-9.

BioEnergy Research
https://doi.org/10.1007/s12155-024-10794-9

Optimizing the Conversion of Bio-Oil from *Haematococcus pluvialis* to Fatty Acid Methyl Esters

C. Sanjurjo[1] · E. Rodríguez[1] · M. Bartolomé[2] · R. González[2] · A. Hernández Battez[1]

Received: 22 March 2024 / Accepted: 1 August 2024

Abstract
Haematococcus pluvialis microalgae have emerged as a prevalent source of antioxidants in cosmetics and nutritional products. Additionally, numerous researchers have posited the potential of this microalgae to produce fatty acid methyl esters (FAME). Nevertheless, the optimization of the production of FAME from *H. pluvialis* oil has not been investigated. In this study, the transesterification reaction of *H. pluvialis* bio-oil was optimized using the response surface methodology, resulting in optimal experimental conditions for an oil to methanol ratio of 1:4.17, at a temperature of 80 °C, with a reaction time of 47 min. The resulting FAME was found to not comply with the biodiesel standard in terms of the content of polyunsaturated fatty acids (6.02%), as well as kinematic viscosity (7.02 mm^2/s). Further study is required to reduce these parameters in order to ensure biodiesel quality and compliance with the standard. Nevertheless, its high flash point value of 150 °C and its high thermal stability within the temperature range of 211–290 °C suggest the potential for utilization as a biolubricant.

Keyword Microalgae · Fatty acid methyl ester · Biofuel · Transesterification

Introduction

In recent years, society has become increasingly concerned about the depletion of fossil resources. As a result, vegetable-based products have been explored and utilized as substitutes. Microalgae are being researched as a potential alternative to conventional vegetable sources in various industries, including cosmeceuticals, nutraceuticals, and the energy industry. This is due to their ability to produce high-value products, such as carotenoids (astaxanthin, fucoxanthin), lipids, and protein, among others, when grown under stress conditions [1]. The stress conditions during culture and growth are directly influenced by factors such as salinity of the medium, light/dark cycle, type of bioreactor, temperature, dissolved oxygen concentration, agitation, and the contribution of nutrients such as carbon, nitrogen, and phosphorus [2].

✉ E. Rodríguez
eduardo@uniovi.es

[1] Department of Construction and Manufacturing Engineering, University of Oviedo, Pedro Puig Adam, S/N, 33203 Gijón, Spain

[2] Department of Marine Science and Technology, University of Oviedo, Blasco de Garay, S/N 33203, Gijón, Spain

Microalgae have several advantages as a raw material, including being a renewable resource, not requiring arable land, and being able to absorb nutrients such as phosphates and nitrates, making them suitable for cultivation in wastewater. They also have a continuous production, high growth rate, and high biomass production and are the largest supplier of O_2 on the planet. Additionally, they are great CO_2 absorbers and have a great diversity of species (> 30,000) [2]. Algal biomass can be used to synthesize various biofuels, including jet fuels, bioethanol, methane, biodiesel, and biobutanol [3]. However, the bio-oil obtained from microalgae is unstable, making its implementation at an industrial scale both difficult and expensive. Additionally, the process requires large quantities of organic solvents for oil extraction from dry biomass, and the harvesting, drying, and extraction of oil from biomass pose significant challenges [4].

Haematococcus pluvialis is a unicellular microalga belonging to the volvocalean group. It has a multilayered cellular architecture that includes a central tripartite crystalline layer and a distinct gelatinous extracellular matrix. This microalga is known to be one of the best natural sources of astaxanthin, which can reach up to 5 wt% of dry biomass [5]. Astaxanthin is a natural antioxidant carotenoid synthesized in certain microalgal species. *H. pluvialis* is a source with

Published online: 17 August 2024

high astaxanthin content, possessing antiaging, anticancer, anti-inflammatory, and immune-enhancing properties [5].

Triglycerides are molecular structures formed by linking three fatty acids (FAs) through glycerol and can reach a dry biomass content of 80 wt% [6]. These structures comprise the bio-oil and serve as the raw material for synthesizing industrial products, such as biofuels or biolubricants. The FAs of microalgae usually have 16 to 24 carbon atoms, with some containing 5 or 6 double bonds [7]. In contrast, plant crop FAs have shorter chains (8 to 20 carbon atoms) and contain a lower number of double bonds or unsaturations [8]. The molecular structure of biodegradable materials can affect the strength of the C-H bonds, which in turn affects properties such as thermal and oxidative stability. To prevent this, it is advisable to choose a raw material that is free of unsaturation or to eliminate it using complementary techniques such as epoxidation [9].

Figure 1 displays the various stages of biomass production, from cultivation to extraction of the compounds of interest, as well as the various flow lines for the utilization of the residual biomass after astaxanthin extraction. In addition to synthesizing biodiesel through transesterification reaction, other lines of interest may include producing ethanol or methane through processes such as biomethanization (or anaerobic digestion) and hydrolysis [10].

Following the extraction of astaxanthin from *H. pluvialis*, a by-product in the form of biomass residue is generated. This by-product has been identified by other authors as a potential source of value in biorefining routes [5]. The by-product rich in triglycerides, obtained after separating the astaxanthin-containing phase, can be used for biodiesel/biolubricant production. For this purpose, the transesterification reaction is commonly employed, where triglycerides react with an alcohol in the presence of a catalyst and under specific temperature conditions to yield fatty acid methyl or ethyl esters (FAMEs/FAEEs) as the main product and glycerin as a secondary product [11]. The presence of moisture has a significant impact on the reaction, as it reacts with the medium to hydrolyze the fatty acids. The resulting free fatty acids (FFA) react with the alkaline catalyst to form soap [12]. Therefore, it is important to check the moisture and FFA content of the oil prior to the transesterification reaction. When the FFA content is greater than 2–4 mg KOH/g, acid catalysts are recommended [13]. Additionally, the use of cosolvents that homogenize the system and increase the indissolubility of the alcohol with the bio-oil is crucial. Also important is the use of cosolvents that homogenize the system and increase the indissolubility of the alcohol with the bio-oil [12].

Transesterification reaction has been typically optimized using independent variables such as alcohol ratio, reaction time, reaction temperature, catalyst concentration, and stirring speed. This technique has been widely used to optimize biodiesel production and obtain the experimental conditions to reach the highest FAME yield (%) from edible crops (such as sunflower, soybean, and palm), non-edible crops that require arable land (such as Jatropha and Neem), and microalgae as *Nannochloropsis* sp., *N. gaditana*, or *C. pyrenoidosa* [14–16]. However, the application of the response surface methodology (RSM) to optimize the transesterification reaction of the bio-oil from *H. pluvialis* microalgae has not yet been explored. This microalgae strain has been reported to have great potential as a feedstock for biodiesel/biolubricant production due to its high lipid content (reported as 43%) and rapid growth rate [17, 18].

The aim of this study is to determine the optimal conditions for FAME production from *H. pluvialis* bio-oil by applying RSM to the transesterification reaction and

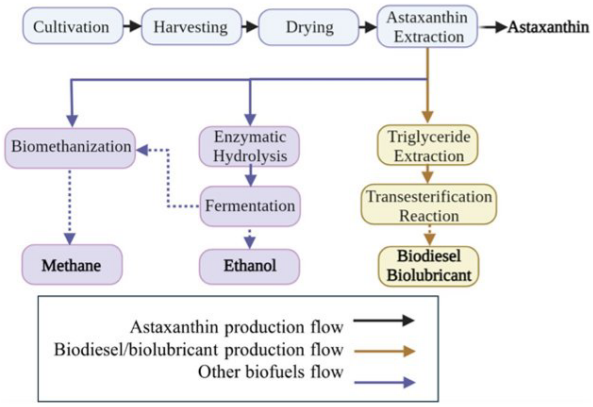

Fig. 1 Flowchart for the synthesis of various valuable products from *H. pluvialis* microalgae

determining the physicochemical properties of this modified microalgae bio-oil such as density, viscosity, flash point, pour point, thermal stability, lower and higher heating values, and fatty acid distribution (saturated fatty acids or SFAs, monounsaturated fatty acids or MUFAs, and polyunsaturated fatty acids or PUFAs).

Material and Methods

Bio-Oil Characterization

The oil derived from *H. pluvialis* was supplied by Neoalgae Micro Seaweed Products (Gijón, Spain) and was selected following an analysis of its saponifiable lipid (SL) content using the technique described by Callejón [19], wherein the SL content per unit of microalgae bio-oil (MBO) is provided following a transesterification reaction with methanol in the presence of the acid catalyst acetyl chloride. A 50% SL content was determined for the MBO. The lipid profile analysis after the transesterification reaction was conducted following the UNE-EN 14103 standard using a Clarus 690 instrument (PerkinElmer) and gas chromatography with flame ionization detector (GC-FID). The Elite-WAX column (30 m × 0.25 mm × 0.25 µm) was used with hydrogen as the carrier gas flowing at a rate of 2 mL/min. The detector was set at 250 °C, and the oven heating program consisted of the following steps: (1) holding at 60 °C for 2 min, (2) heating from 60 to 200 °C at a rate of 10 °C/min, (3) heating from 200 to 240 °C at a rate of 5 °C/min, and (4) holding at 200 °C for 7 min.

Furthermore, the total acid number (TAN) and water content were quantified using the Metrohm 848 Tritino plus (ASTM D664 standard) and the Metrohm 899 Karl Fischer, respectively, with an estimated precision of ± 0.01 mg KOH/g and ± 0.1 ppm. To determine the best route according to the characteristics of the oil, the TAN is of great importance. If its value is higher than 2 g KOH/g, it would be necessary to carry out a prior esterification with an acid catalyst.

Transesterification Reaction

Design of Experiments

The transesterification reaction was optimized using a central composite design (CCD) of a two-level factorial approach with RSM and the Design Expert 13 software. Table 1 shows the selected independent variables and parameter levels, which are coded as − 1 (minimum), 0 (center), + 1 (maximum), and ± α (extreme star points). The levels of each parameter were selected according to the bibliography consulted for previous studies, and in addition to this, they were also applied in previous research [20].

Nineteen runs were conducted, consisting of six star points, five center point replications, and eight factorial design runs.

The alcohol used in the reaction was methanol and the catalyst CH_3ONa was used at a concentration of 1.5% by the weight of oil, in accordance with the literature consulted [21]. A basic catalyst was selected after verifying that the acidity of the oil was less than 2 g KOH/g. Previous tests were also carried out with a basic KOH catalyst, obtaining better results for CH_3ONa.

To perform the reaction, 1 g of MBO was mixed with 2 mL of hexane, the corresponding amount of methanol (3–15 g) and the catalyst in a 100 mL flask. During the reaction time, the flask was in an oil bath to keep the mixture at the required temperature. A Dimroth condenser was also used to prevent loss of hexane and methanol at higher temperatures.

Finally, the output variable evaluated was the FAME yield (%), calculated according to Eq. 1. The amount of FAME converted was obtained through the analysis described in "Bio-Oil Characterization" using GC-FID and an internal standard of methyl nonadecanoate.

$$Y(\text{ FAME yield } \%) = \frac{\text{Amount transformed to FAME (g)}}{\text{Total SL amount convertible to FAME (g)}} \times 100 \quad (1)$$

Table 1 Input variables and levels for optimizing the MBO transesterification reaction

Independent variables	Factor	Variable levels				
		− 2 (− α)	− 1	0	+ 1	+ 2 (+ α)
MBO to methanol ratio (wt.)	*A*	1:3	1:6	1:9	1:12	1:15
Reaction temperature (°C)	*B*	30	50	70	90	110
Reaction time (min)	*C*	30	67.5	105	142.5	180

Table 2 Design of experiments used in this study

Standard order	Run order	Factorial input variable		
		A	B	C
11	1	0	−2	0
18	2	0	0	0
2	3	1	−1	−1
6	4	1	−1	1
10	5	2	0	0
4	6	1	1	−1
9	7	−2	0	0
13	8	0	0	−2
19	9	0	0	0
3	10	−1	1	−1
8	11	1	1	1
1	12	−1	−1	−1
17	13	0	0	0
7	14	−1	1	1
14	15	0	0	2
12	16	0	2	0
5	17	−1	−1	1
16	18	0	0	0
15	19	0	0	0

Table 2 presents the configuration of the test runs using the Design Expert software. Analysis of variance (ANOVA) was performed to determine the interaction of the response *Y* with each input variable using Design Expert 13 software. The probability value with a 95% confidence interval was used to evaluate the significance of the model.

Purification Process

To achieve the purest possible product, a multi-step purification process was followed as described in Fig. 2. Following the transesterification reaction, the product was centrifuged for 10 min at 7000 rpm (Microcen 24—CE 202) to eliminate glycerol. The resulting liquid was then washed with deionized water to remove excess methanol, traces of catalyst, and other impurities present in the original MBO. This step was repeated until the effluent reached a neutral pH. Finally, transfer the sample to a rotary evaporator set at 60 °C and 20 mbar for 20 min (Hei-Vap Core, Heidolph) to remove any traces of water, methanol, and hexane.

FAME Physicochemical Characterization

The transformation of the sample from triglyceride to FAME was confirmed through an analysis using a Fourier Transform Infrared (FTIR) spectrometer (Varian 670-IR) with an accuracy of better than 0.07 cm^{-1}, in addition to GC-FID analysis.

A high-precision Stabinger SVM 3001 rotational viscometer was employed to determine the density at 20 °C and the kinematic viscosity at 40 °C in accordance with the ASTM D7042 standard.

The pour point (PP) was determined through Differential Scanning Calorimetry (DSC Mettler 822e 700) analysis. DSC has a heat flow accuracy of better than ± 2% and a temperature accuracy of ± 1 °C. This technique can directly measure the change in enthalpy for a system during cooling. The change in enthalpy can be estimated using the sample PP [22]. The sample was heated to 50 °C at a rate of 10 °C/min and held under isothermal conditions for 10 min. The system was then cooled to − 50 °C under a nitrogen atmosphere at the same rate. The PP value can be obtained at the maximum point of the curve by using heat flux (W/g) versus temperature plots [23].

The upper and lower heating values (LHV and HHV) were determined in an IKA C4000 calorimeter according to ISO 1928.

The flash point (FP) of the FAME was determined using a modified Cleveland Open Cup Tester in accordance with

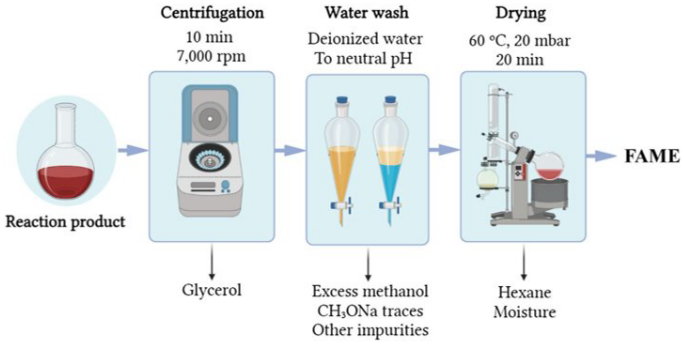

Fig. 2 FAME purification process

EN ISO 2592 and ASTM D92 standards. The modified cup was filled with 15 mL of FAME and heated in increments of 5 °C until it reached its FP.

The FAME's thermal stability (TS) was then assessed using thermogravimetric analysis (TGA) with a TA instrument that has a temperature accuracy of 0.001 °C (200 to 1300 °C). The results were analyzed using Universal Analysis 2000 software. The sample weighed 6 mg, and it was heated at a constant rate of 20 °C/min from 25 to 600 °C under a nitrogen atmosphere with a flow rate of 50 mL/min. The weight loss of the sample was plotted against time to determine the onset temperature of decomposition.

Results and Discussion

Lipid Profile and Molecular Structure

Table 3 presents the results of the lipid profile analysis, which are consistent with data reported for *H. pluvialis* by Bilbao et al. [24] and Damiani et al. [25]. Taking into account the indications of the UNE EN 14214 standard, in which fatty acids with 4 or more double bonds are considered to be PUFAs, *H. pluvialis* presents a PUFA content of 6.02%. The most abundant FAs in the sample are palmitic acid (C16:0) with 20.38%, oleic acid (C18:1) with 15%, linoleic acid (C18:2) with 29.92%, and linolenic acid (C18:3) with 15.21%. All MUFAs and SFAs were identified in the method, indicating that the unidentified peaks belong to PUFAs.

UNE EN 14214: according to the standard, fatty acids must have 4 or more double bonds to be considered a PUFA.

The acidity value of 0.08 mg KOH/g obtained for the MBO indicates the absence of FFA that could interfere with the reaction. Therefore, an esterification process with an acid catalyst was unnecessary. Additionally, the water content of the sample (1580–1820 ppm) was due to ambient moisture, and thus, a prior drying process was not required.

Figure 3b shows the plot of wave number versus transmittance, displaying the specific molecular bonds present in both MBO and FAME through the infrared spectrum. The wavelength of 1435 cm^{-1} represents the -CH_3 bonds, which, together with GC-FID, confirms the transformation taking place in the reaction. The wavelength ranges of 2800–3000 cm^{-1}, 1730–1750 cm^{-1}, and 1000–1300 cm^{-1} correspond to -C-H bonds and -C=O, -C-O esters [26]. In the range of 3000–3700 cm^{-1}, the -O–H bonds are present, which strongly relate to the thermal and oxidative stability of the sample [27]. The presence of -O–H molecules increases with the water content, making this wavelength informative since water and moisture contribute to FAME degradation. As shown, this band has a lower presence in FAME compared to MBO, indicating lower water content and better stability of the FAME.

Optimization of Transesterification Reaction by RSM

Table 4 shows the actual and predicted *Y* response obtained using the Design Expert software and the relative error between the two values.

Model Adequacy Check

Equation 2 was generated from the empirical model that correlates the coded input variables with the response *Y* through a quadratic regression.

$$Y = 55.77 - 6.94A + 2.70B - 3.9C + 0.8588AB + 2.45AC - 2.73BC + 6.96A^2 + 6.88B^2 + 0.5278C^2 \quad (2)$$

The results of the final ANOVA are presented in Table 5.

Figure 4 shows the interaction between the input variables and the response *Y* (according to Eq. 2) using a 3D surface plot. It is observed that the reaction time interacts similarly to the alcohol ratio (Fig. 4a) and the reaction temperature (Fig. 4b). *Y* does not respond to time variation, while for the other two variables, it fluctuates significantly. This statement supports the ANOVA results presented in Table 5, where the factors *AC* and *BC* had *p* values greater than 0.05, indicating that they were not significant terms.

In contrast, the relationship between alcohol ratio and temperature indicates a minimum stationary point at [0, 0, 0], with *Y* increasing towards the extremes of [−2, 2]. The highest predicted *Y* values fall within the range of [−1.5, 2] for alcohol ratio and [0, 2] for reaction temperature.

The increase in temperature results in an increase in equilibrium conversion and therefore an increase in FAME yield. Furthermore, it was identified that the effect of temperature

Table 3 Fatty acid composition of *H. pluvialis*

Fatty acid	Content (%)	Total	(%)
C16:0	20.38 ± 0.21	**Not identified**	8.68 ± 1.04
C17:1	2.92 ± 0.02	**SFA**	21.23 ± 0.21
C18:0	0.85 ± 0.01	**MUFA**	18.81 ± 0.12
C18:1	15.89 ± 0.13	**PUFA**$^{\text{UNE EN 14214}}$	6.02
C18:2	29.92 ± 0.07	**Total lipid content**	50.04
C18:3	15.21 ± 0.17		
C18:4	2.50 ± 0.02		
C20:5	3.52 ± 0.04		

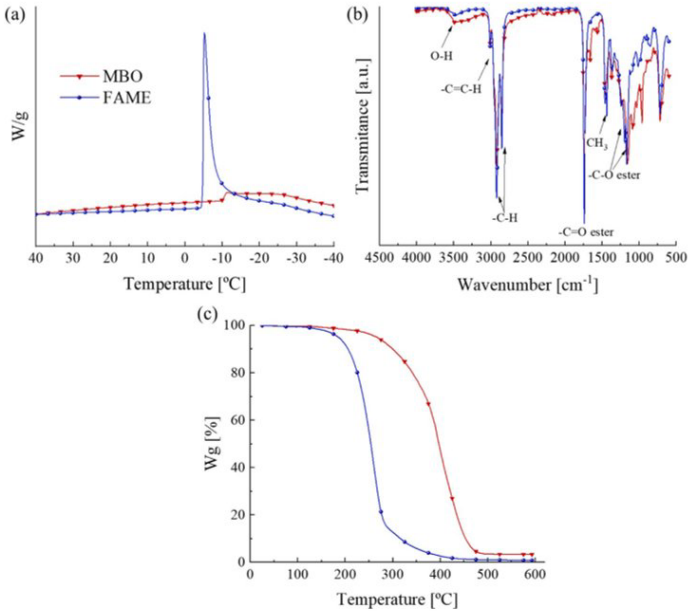

Fig. 3 **a** DSC at low temperatures, **b** FTIR spectra, and **c** TGA of the MBO and FAME.

Table 4 Actual and predicted *Y* response results obtained in this study

Factorial input variable			Responses, *Y*		
A	*B*	*C*	Actual	Predicted	
			Y (%)	*Y* (%)	Error (%)
0	−2	0	80.48	77.89	3.21
0	0	0	56.89	55.77	1.96
1	−1	−1	57.65	58.37	1.25
1	−1	1	60.94	60.91	0.04
2	0	0	67.84	69.73	2.78
1	1	−1	74.01	70.93	4.16
−2	0	0	97.23	97.49	0.27
0	0	−2	65.23	65.69	0.71
0	0	0	49.12	55.77	13.55
−1	1	−1	90.12	88.00	2.36
1	1	1	66.12	62.57	5.37
−1	−1	−1	77.47	78.87	1.81
0	0	0	56.93	55.77	2.03
−1	1	1	72.71	69.84	3.95
0	0	2	48.39	50.08	3.48
0	2	0	83.94	88.68	5.64
−1	−1	1	70.69	71.62	1.31
0	0	0	55.36	55.77	0.75
0	0	0	58.42	55.77	4.53

on the FAME yield is less pronounced when reaction times are longer. This allows for high FAME yield at low temperatures to be achieved when utilizing longer reaction times. Kumar also reported this temperature–time balance in a jatropha-algae biodiesel mixture, where the maximum conversion achieved was 96.29% for a time of 180 min and 45 °C [28].

Optimization Conditions of RSM Analysis

After selecting the empirical model that best fits the experimental dataset and studying the influence of each input variable on *Y*, the optimal conditions for producing FAME from *H. pluvialis* were determined.

The limiting criteria for obtaining optimal conditions were input parameters in range (alcohol ratio, temperature, time) and maximized output (FAME yield) [29].

The optimal conditions obtained in coded format were − 1.61 for alcohol ratio, 0.53 for temperature, and − 1.54 for reaction time. These values were decoded to obtain the actual experimental configuration, which is tabulated in Table 6. Based on Eq. 2, this configuration gives a predicted *Y* of 103.32%. The experimental tests were conducted under optimal conditions resulting in a FAME yield of 98.44%. This represents a 2.26% error relative to

Table 5 ANOVA of the fitting model for *Y*

Source	*df*	*F* value	*p* value	Remark
Model	9	24.95	< 0.0001	Significant
A—MBO to methanol ratio	1	54.19	< 0.0001	
B—reaction temperature	1	8.17	0.0188	
C—reaction time	1	17.15	0.0025	
AB	1	0.4148	0.5355	
AC	1	3.37	0.0995	
BC	1	4.18	0.0712	
A^2	1	80.62	< 0.0001	
B^2	1	78.75	< 0.0001	
C^2	1	0.4637	0.5130	
Residual	9			
Lack of fit	5	1.13	0.4664	Not significant
Model summary	R^2	R^2 (adj.)	R^2 (pred.)	Adeq. precision
	0.9614	0.9228	0.7884	17.3295

Note that the *F* and *p* values represent the significance of the model. Differences were considered significant at $p < 0.05$. An *F* value of 24.95 and a *p* value < 0.0001 indicate that both the model and its terms are significant. The adjusted R^2 of 0.9614 is also consistent with these values. Adequate precision represents the signal-to-noise ratio, so a ratio greater than 4 is desirable, which in this case is 17.3295. The predicted R^2, obtained by comparing the experimental values of *Y* with those obtained by applying Eq. 2, is also in reasonable agreement with the adjusted R^2, with a difference of less than 0.2. The model is appropriate for predicting *Y*, as shown in Table 4, where the actual and predicted values are very close, with a relative error of no more than 6%, except for one of the five replicates of the central point, which presented an error of 13.5% (outlier)

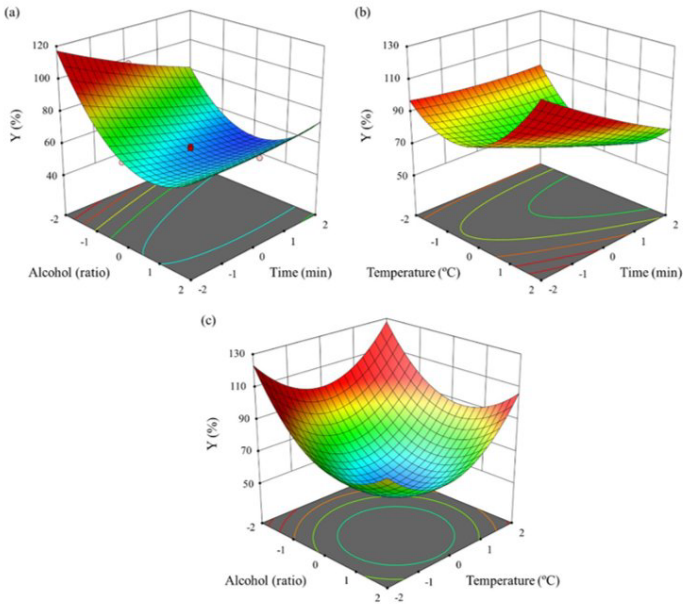

Fig. 4 Interaction between independent variables for FAME yield. **a** Alcohol ratio vs. reaction time. **b** Temperature vs. reaction time. **c** Alcohol ratio vs. reaction temperature

Table 6 Coded and real values for optimal transesterification conditions

Input variable	Coded value		Real value
MBO to methanol ratio	− 1.61		4.17
Reaction temperature (°C)	0.53		80
Reaction time (min)	− 1.54		47
Response,*Y*	**Predicted**	**Actual**	**Error (%)**
FAME yield (%)	103.32	98.44	2.26

the predicted value, which is the highest conversion rate achieved.

FAME Physicochemical Characterization

The FAME had a density value of 900 kg/m3, which is within the range of the UNE EN 14214 standard. This value is significantly higher than that reported for biodiesel from other vegetable sources, such as palm kernel or the microalgae *S. oleosa*, both of which have values of 879 kg/m^3 [30, 31]. However, higher values have been reported, such as for FAME derived from rapeseed oil, with a density value of 916 kg/m^3 [32]. The kinematic viscosity value was slightly elevated, reaching 7.02 mm2/s, 2 mm2/s above the upper limit specified by standard for biodiesel. This value is also significantly higher than that reported by other vegetable sources, which typically range from 4 to 6 mm^2/s [33, 34]. Nevertheless, the density and viscosity values of the present study have been determined to fall within the operational range for use as biolubricants, as defined by the SAE J-300 standard. Consequently, it would be of interest to investigate the tribological properties of this biofuel in future studies.

The fluid's working temperature range was determined through a comprehensive thermal analysis. The results of TGA from Fig. 3c shows that FAME has an onset thermal degradation temperature of 211 °C, which is lower than that of the MBO at 348 °C. Additionally, FAME exhibits maximum degradation above 425 °C, resulting in a quasi-complete degradation of the sample. However, the MBO residue remains as it does not fully degrade at the highest test temperature. The onset thermal degradation temperature of FAME derived from *H. pluvialis* has been determined to be higher than that reported for biodiesel derived from jatropha and rapeseed [32, 35]. In comparison with other microalgae, the FAME derived from *S. platensis* and *N. gaditana* strains have been found to exhibit higher degradation onset temperatures, with values of 300 °C and 240 °C, respectively [20, 36]. This observed difference may be attributed to the higher content of unsaturations in the case of *H. pluvialis*, in comparison to the aforementioned last two strains of microalgae, which would have a deleterious effect on its thermal stability.

During the FP measurements, the FAME sample exhibited foaming formation at 100 °C and a continuous ignition from 150 to 155 °C, which is considered the FP temperature. The foaming at 100 °C may be due to the presence of small contaminants, such as other lipids, in the microalgae FAME that break down when heated and tend to form a thin layer of foam in the presence of air [37]. The presence of foam on the surface hinders the dispersion of combustion gases, causing the foam to expand. This FP value is consistent with the typical range observed for FAME derived from vegetal sources, falling between 140 and 190 °C [31, 33].

The determination of PP was challenging for the MBO sample due to its non-pure compound nature, resulting in the absence of a characteristic peak. Instead, it exhibited a broad exothermic freezing band between − 2 and − 32 °C (Fig. 3a). In contrast, the FAME sample displayed a well-defined exothermic freezing peak with an onset temperature of − 4.6 °C and a peak temperature of − 5.1 °C. Additionally, the PP value of the FAME from *H. pluvialis* was slightly lower than that of biodiesel from other vegetable sources. Those derived from edible waste, palm kernel, honge waste cooking oil, or *S. oleosa* have PP values above 0 °C [30, 31, 38]. Lower PP values have been reported for microalgae such as *S. platensis* (− 9 °C) [36]. The reduction in PP in microalgae FAME is attributed to the different molecular characteristics of the fatty acids present in edible vegetable oils and those present in MBOs. In contrast to vegetable oils, MBOs have a higher percentage of polyunsaturated fatty acids, with a value of 6.02% in this study. The presence of cis double bonds in unsaturated compounds hinders crystal packing, resulting in lower PP values [39].

Additionally, the LHV and HHV were determined to be 38.03 and 40.38 MJ/kg, respectively. These values are close to those reported for biodiesel from vegetable sources as jatropha and honge (38.66 and 39.79 MJ/kg, respectively), which in turn are slightly lower than diesel (44.22 MJ/kg) [38].

Most of the important properties exhibited by FAME derived from *H. pluvialis* do not align with the stipulated limits set by the standard. The high viscosity and the PUFA content of 6.02% are significant limitations. It is common for microalgae to contain high levels of PUFAs, with values ranging from 20 to 75% being typical [40]. Although the presence of these structures negatively affects its oxidative stability, the presence of more than one double bond in the carbon chain lowers the viscosity by hindering molecular packing [41]. Consequently, the presence of PUFAs serves to prevent the viscosity from increasing further. Conversely, these values of density, viscosity, and working temperature fall within the operational range for use as a lubricant, in accordance with the SAE J300 Standard for the viscosity grade. Typical lubricant densities range from 700 to 950 kg/m^3, with operational temperature ranges between 20 and 90 °C for medium load applications [42].

Conclusions

This research examined the parameters that influence the conversion of bio-oil derived from the microalgae *Haematococcus pluvialis* to fatty acid methyl esters (FAMEs) through a transesterification reaction. The optimization process of this reaction was conducted using response surface methodology. An empirical model was obtained, and the optimal conditions for maximizing FAME production were determined. However, the mixture of FAMEs from *H. pluvialis* does not meet the standard requirements for classification as biodiesel. Consequently, further research is required to obtain a biodiesel of the requisite quality. Nevertheless, some of the physicochemical properties of this mixture permit its utilization as a biolubricant.

Author Contribution C. Sanjurjo: conceptualization, formal analysis, investigation, writing—original draft. E. Rodríguez: investigation, funding acquisition, project administration, writing—review and editing. M. Bartolomé: data curation, formal analysis. R. González: data curation, software. A. Hernández Battez: conceptualization, funding acquisition, investigation, project administration, writing—review and editing.

Funding Open Access funding provided thanks to the CRUE-CSIC agreement with Springer Nature. This publication is part of the R&D project PID2022-136656NB-I00, funded by MICIU/AEI/https://doi.org/10.13039/501100011033/ and by "FEDER/UE." The Foundation for the Promotion of Applied Scientific Research and Technology in Asturias (Spain) is also acknowledged for funding the contract of Claudia Sanjurjo at the University of Oviedo (Spain) [grant number SV-PA-21-AYUD/2021/50987]. The authors of the work wish to express their gratitude to the University Institute of Industrial Technology of Asturias (IUTA) for financing the project "OPTRANSESTERAL" [grant number SV-23-GIJON-1–05].

Data Availability The datasets generated during the current study are available in the ZENODO repository, https://doi.org/10.5281/zenodo.10689754.

Declarations

Competing Interests The authors declare no competing interests.

References

1. Tang DYY, Khoo KS, Chew KW, Tao Y, Ho SH, Show PL (2020) Potential utilization of bioproducts from microalgae for the quality enhancement of natural products. Bioresource Technol 304:122997. https://doi.org/10.1016/j.biortech.2020.122997
2. Farfan-Cabrera LI, Franco-Morgado M, González-Sánchez A, Pérez-González J, Marín-Santibáñez BM (2022) Microalgae biomass as a new potential source of sustainable green lubricants. Molecules 27:1205. https://doi.org/10.3390/molecules27041205
3. Polaris Market Research (2021) Algae biofuel market share, size, trends, industry analysis report, by type (jet fuel, bioethanol, methane, biodiesel, bio-butanol, green diesel, bio-gasoline, others). https://www.polarismarketresearch.com/industry-analysis/algae-biofuels-market. Accessed 17 July 2024
4. Neag E, Stupar Z, Maicaneanu SA, Roman C (2023) Advances in biodiesel production from microalgae. Energies 16:1129. https://doi.org/10.3390/en16031129
5. Nishshanka GKSH, Liyanaarachchi VC, Nimarshana PHV, Ariyadasa TU, Chang JS (2022) *Haematococcus pluvialis*: a potential feedstock for multiple-product biorefining. J Clean Prod 344:131103. https://doi.org/10.1016/j.jclepro.2022.131103
6. Ahmad A, Hassan SW, Banat F (2022) An overview of microalgae biomass as a sustainable aquaculture feed ingredient: food security and circular economy. Bioengineered 13:9521–9547. https://doi.org/10.1080/21655979.2022.2061148
7. Zulu NN, Zienkiewicz K, Vollheyde K, Feussner I (2018) Current trends to comprehend lipid metabolism in diatoms. Prog Lipid Res 70:1–16. https://doi.org/10.1016/j.plipres.2018.03.001
8. Giakoumis EG (2013) A statistical investigation of biodiesel physical and chemical properties, and their correlation with the degree of unsaturation. Renew Energy 50:858–878. https://doi.org/10.1016/j.renene.2012.07.040
9. Abolins A, Kirpluks M, Vanags E, Fridrihsone A, Cabulis U (2020) Tall oil fatty acid epoxidation using homogenous and heterogeneous phase catalysts. J Polym Environ 28:1822–1831. https://doi.org/10.1007/s10924-020-01724-9
10. Harun R, Danquah MK (2011) Enzymatic hydrolysis of microalgal biomass for bioethanol production. Chem Eng J 168:1079–1084. https://doi.org/10.1016/j.cej.2011.01.088
11. Sanjurjo C, Rodríguez E, Viesca JL, Hernández A (2023) Influence of molecular structure on the physicochemical and tribological properties of biolubricants: a review. Lubricants 11:380. https://doi.org/10.3390/lubricants11090380
12. Makareviciene V, Skorupskaite V (2019) Transesterification of microalgae for biodiesel production. In: Second and third generation of feedstocks: the evolution of biofuels. Elsevier, pp 469–510. https://doi.org/10.1016/B978-0-12-815162-4.00017-3
13. Azad AK, Sharma SC, Rasul MG (2017) Clean energy for sustainable development: comparisons and contrasts of new approaches. Elsevier, Queensland
14. Patil PD, Gude VG, Mannarswamy A, Cooke P, Munson-McGee S, Nirmalakhandan N, Lammers P, Deng S (2011) Optimization of microwave-assisted transesterification of dry algal biomass using response surface methodology. Bioresour Technol 102:1399–1405. https://doi.org/10.1016/j.biortech.2010.09.046
15. Macías-Sánchez MD, Robles-Medina A, Jiménez-Callejón MJ, Hita-Peña E, Estéban-Cerdán L, González-Moreno PA, Navarro-López E, Molina-Grima E (2018) Optimization of biodiesel production from wet microalgal biomass by direct transesterification using the surface response methodology. Renew Energy 129:141–149. https://doi.org/10.1016/j.renene.2018.06.001
16. Wan Mahmood WMA, Theodoropoulos C, Gonzalez-Miquel M (2017) Enhanced microalgal lipid extraction using bio-based

solvents for sustainable biofuel production. Green Chem 19:5723–5733. https://doi.org/10.1039/c7gc02735d
17. Otero P, Saha SK, Gushin JM, Moane S, Barron J, Murray P (2017) Identification of optimum fatty acid extraction methods for two different microalgae *Phaeodactylum tricornutum* and *Haematococcus pluvialis* for food and biodiesel applications. Anal Bioanal Chem 409:4659–4667. https://doi.org/10.1007/s00216-017-0412-9
18. Wu YH, Yang J, Hu HY, Yu Y (2013) Lipid-rich microalgal biomass production and nutrient removal by *Haematococcus pluvialis* in domestic secondary effluent. Ecol Eng 60:155–159. https://doi.org/10.1016/j.ecoleng.2013.07.066
19. Jiménez-Callejón MJ, Robles-Medina A, Macías-Sánchez MD, Hita-Peña E, Esteban-Cerdán L, González-Moreno PA, Molina-Grima E (2014) Extraction of saponifiable lipids from wet microalgal biomass for biodiesel production. Bioresource Technol 169:198–205. https://doi.org/10.1016/j.biortech.2014.06.106
20. Sanjurjo C, Oulego P, Bartolomé M, Rodríguez E, González R, Hernández A (2024) Biodiesel production from the microalgae *Nannochloropsis gaditana*: optimization of the transesterification reaction and physicochemical characterization. Biomass Bioenerg 185:107240. https://doi.org/10.1016/j.biombioe.2024.107240
21. Encinar JM, Nogales-Delgado S, Pinilla A (2021) Biolubricant production through double transesterification: reactor design for the implementation of a biorefinery based on rapeseed. Processes 9:1224. https://doi.org/10.3390/pr9071224
22. Adhvaryu A, Erhan SZ, Perez JM (2003) Wax appearance temperatures of vegetable oils determined by differential scanning calorimetry: effect of triacylglycerol structure and its modification. Thermochim Acta 395:191–200. https://doi.org/10.1016/S0040-6031(02)00180-6
23. Jayadas NH, Nair KP (2006) Coconut oil as base oil for industrial lubricants-evaluation and modification of thermal, oxidative and low temperature properties. Tribol Int 39:873–878. https://doi.org/10.1016/j.triboint.2005.06.006
24. Scodelaro Bilbao PG, Damiani C, Salvador GA, Leonardi P (2016) *Haematococcus pluvialis* as a source of fatty acids and phytosterols: potential nutritional and biological implications. J Appl Phycol 28:3283–3294. https://doi.org/10.1007/s10811-016-0899-z
25. Damiani MC, Popovich CA, Constenla D, Leonardi PI (2010) Lipid analysis in *Haematococcus pluvialis* to assess its potential use as a biodiesel feedstock. Bioresource Technol 101:3801–3807. https://doi.org/10.1016/j.biortech.2009.12.136
26. Aisien FA, Aisien ET (2023) Modeling and optimization of transesterification of rubber seed oil using sulfonated CaO derived from giant African land snail (*Achatina fulica*) catalyst by response surface methodology. Renew Energy 207:137–146. https://doi.org/10.1016/j.renene.2023.02.093
27. Mohamed Shameer P, Ramesh K (2017) FTIR assessment and investigation of synthetic antioxidant on the fuel stability of *Calophyllum inophyllum* biodiesel. Fuel 209:411–416. https://doi.org/10.1016/j.fuel.2017.08.006
28. Kumar S, Jain S, Kumar H (2017) Process parameter assessment of biodiesel production from a Jatropha–algae oil blend by response surface methodology and artificial neural network. Energ Source Part A 39:2119–2125. https://doi.org/10.1080/15567036.2017.1403514
29. Kumar S, Jain S, Kumar H (2020) Experimental study on biodiesel production parameter optimization of jatropha-algae oil mixtures and performance and emission analysis of a diesel engine coupled with a generator fueled with diesel/biodiesel blends. ACS Omega 5:17033–17041. https://doi.org/10.1021/acsomega.9b04372
30. Foroutan R, Esmaeili H, Mousavi SM, Hashemi SA, Yeganeh G (2019) The physical properties of biodiesel-diesel fuel produced via transesterification process from different oil sources. Phys Chem Res 7:415–424. https://doi.org/10.22036/pcr.2019.173224.1600
31. Suherman S, Abdullah I, Sabri M, Silitonga AS (2023) Evaluation of physicochemical properties composite biodiesel from waste cooking oil and *Schleichera oleosa* oil. Energies (Basel) 16:5771. https://doi.org/10.3390/en16155771
32. Alves CT, Peters MA, Onwudili JA (2022) Application of thermogravimetric analysis method for the characterisation of products from triglycerides during biodiesel production. J Anal Appl Pyrolysis 168:105766. https://doi.org/10.1016/j.jaap.2022.105766
33. Bazooyar B, Ghorbani A, Shariati A (2015) Physical properties of methyl esters made from alkali-based transesterification and conventional diesel fuel. Energ Source Part A 37:468–476. https://doi.org/10.1080/15567036.2011.586975
34. Alviso D, Saab E, Clevenot P, Romano SD (2020) Flash point, kinematic viscosity and refractive index: variations and correlations of biodiesel–diesel blends. J Braz Soc Mech Sci 42:347. https://doi.org/10.1007/s40430-020-02428-w
35. Jain S, Sharma MP (2012) Application of thermogravimetric analysis for thermal stability of *Jatropha curcas* biodiesel. Fuel 93:252–257. https://doi.org/10.1016/j.fuel.2011.09.002
36. Mostafa SSM, El-Gendy NS (2017) Evaluation of fuel properties for microalgae *Spirulina platensis* bio-diesel and its blends with Egyptian petro-diesel. Arab J Chem 10:S2040–S2050. https://doi.org/10.1016/j.arabjc.2013.07.034
37. Kubar AA, Ali A, Kumar S, Huo S, Ullah MW, Alabbosh KFS, Ikram M, Cheng J (2022) Dynamic foam characteristics during cultivation of *Arthrospira platensis*. Bioeng 9:257. https://doi.org/10.3390/bioengineering9060257
38. Atgur V, Manavendra G, Rao BN, Veza I, Fattah IMR (2024) Thermal and combustion characteristics of honge, jatropha, and honge-jatropha mixed biodiesels. Environ Prog Sustain Energy 43:14199. https://doi.org/10.1002/ep.14199
39. Bahubali C, Gopalan A (2019) Improving biodiesel's properties. Digital Refining Proce 1–5.https://www.digitalrefining.com/article/1002283/improving-biodiesels-properties. Accessed 17 July 2024
40. Deshmukh S, Kumar R, Bala K (2019) Microalgae biodiesel: a review on oil extraction, fatty acid composition, properties and effect on engine performance and emissions. Fuel Process Technol 191:232–247. https://doi.org/10.1016/j.fuproc.2019.03.013
41. Rodrigues J, Cardoso F, Lachter E, Estevao L, Lima E, Nascimento R (2006) Correlating chemical structure and physical properties of vegetable oil esters. J Amer Oil Chem Soc 83:353–357. https://doi.org/10.1007/s11746-006-1212-0
42. Johnson M (2008) Lubricant selection: function and composition. Tribol Lubr Technol 18–28. https://www.stle.org/images/pdf/STLE_ORG/BOK/LS/Gears/Lubricant%20Selection_Function%20and%20Composition_tlt%20article_April08.pdf. Accessed 17 July 2024